

Update of preclinical and human studies of calcium and colon cancer prevention

Martin Lipkin

Subject headings calcium/metabolism; colonic neoplasms/prevention and control; vitamin D

Many articles on the subject of colon cancer begin by noting that the disease continues to be a major cause of tumor mortality in the United States and other countries. Despite attempts at reduction, the incidence of this disease is still high in Western populations and is increasing in some Eastern countries. Chemoprevention of this disease therefore continues to be an important public health objective. Among recent chemopreventive approaches, an increased intake of calcium and vitamin D continues to be evaluated in both preclinical and clinical studies. Many experimental findings, as described below, have indicated real associations between high calcium and vitamin D intake and decreased risk for colorectal cancer.

BASIC STUDIES OF CALCIUM METABOLISM

Calcium is both an essential structural body component and a critical functional element in living cells. It is a key component for maintaining cell structure, membrane viscosity or rigidity, and the related membrane permeability is partly dependent on local calcium concentration. Calcium is also a pivotal regulator of a wide variety of cell functions in its role as a major second messenger^[1].

Among the numerous cell properties modulated by calcium, its participation in cell division and the regulation of cell proliferation and differentiation are particularly important^[2]. Low levels of intracellular ionized calcium contribute to cell proliferation, and increasing calcium concentration in cell and organ culture media decreased cell proliferation; and induced cell differentiation in rat esophageal epithelial cells^[3], murine epidermal cells^[4], mammary cells^[5,6], and colon cells^[7].

The absorption and metabolism of calcium are

carefully regulated, 1, 25-dihydroxyvitamin D₃ is an important calcium modulator that can become deficient as a consequence of inappropriate diet or inadequate exposure to sunlight. Therefore vitamin D₃ also may have a role in the regulation of cell proliferation and differentiation while modulating calcium metabolism. It has also been shown to directly inhibit the proliferation of several malignant cell lines *in vitro*^[8-10], and to induce the differentiation of human colonic cells^[11], human myeloid leukemia cells^[12], and other cell lines *in vitro*^[13,14]. A role of vitamin D as a chemopreventive agent has also been studied in rodent models^[15-19], and the tumor growth and promotional stage of chemical carcinogenesis have been inhibited by vitamin D. On the other hand, vitamin D₃ enhanced chemically-induced transformation of cultured cells *in vitro*^[20,21] and promoted skin tumor formation in mice^[22].

PRECLINICAL AND EARLY HUMAN INTERVENTION STUDIES OF EFFECTS OF INCREASED DIETARY CALCIUM

Preclinical studies

The results of direct experimental studies of calcium intake and colon cancer development are summarized in Table 1. The results of many individual studies are further described in Tables 2-5. In many preclinical experimental models, calcium effects on colon cancer development and on cellular processes associated with colon cancer have been remarkably consistent: ① decreasing and normalizing excessive proliferation of colonic epithelial cells, reducing the susceptibility of proliferating epithelial cells to accumulate abnormalities in their DNA; ② reducing the cytotoxicity of fecal water; ③ increasing the differentiation and maturation of colonic epithelial cells; and ④ decreasing the end-stage development of colon cancer itself.

In animal models (Tables 2,3), oral calcium supplementation decreased epithelial cell hyperproliferation when it was induced by several factors that stimulate tumor promotion: the administration of bile acids and fatty acids, dietary fat, a Western-style diet, and partial enteric resection. Of further importance colonic

Strang Cancer Research Laboratory at the Rockefeller University and Weill Medical College of Cornell University, New York, NY 10021, USA

Correspondence to: Martin Lipkin, Strang Cancer Research Laboratory at the Rockefeller University and Weill Medical College of Cornell University, New York, NY 10021, USA

Tel. +1-212-5342024, Fax. +1-212-8799371

Email: lipkin@rockvax.rockefeller.edu

Received 1999-09-28

carcinogenesis itself, when induced by chemical carcinogens, decreased with increasing dietary calcium intake, with almost all studies showing a decrease in the number of tumors induced, the percent of invasive carcinomas, or the number of animals with multiple tumors.

Thus, a wide variety of rodent studies (Tables 1-3 with references) demonstrated that increasing dietary calcium intake reduced colonic tumor formation: mechanisms involved included decreased epithelial cell hyperproliferation; decreased or nilthine decarboxylase activity; decreased ras mutations in colonic epithelial cells; and calcium-binding of bile acids, fatty acids and phosphate into insoluble complexes, reducing their direct irritant and hyperproliferative effects on colonic epithelial cells and reducing the cytotoxicity of fecal water.

Two recent series of studies also have evaluated the effects of calcium and vitamin D on colonic tumor development when these nutrients were fed to rodents on Western-style diets. The first group of studies utilized preclinical models of normal mice. In the colonic crypts of these normal mice hyperproliferation, hyperplasia, abnormal differentiation and maturation of colonic crypt epithelial cells, and the late-stage preneoplastic lesion of whole-colonic-crypt dysplasia developed when the mice were fed Western-style diets containing low calcium and vitamin D^[26,33,34].

The second series of studies utilized mice having targeted mutations that are relevant to human colon cancer, the targeted mutation causing adenomas and carcinomas to develop in the mice^[35,36]. Recent studies demonstrated the Western-style diets increased the development of the neoplastic colonic lesions that were initiated by those mutations; and the neoplasms together with carcinomas were decreased by: increasing calcium and vitamin D together with lowering fat content of diet^[37], or increasing dietary calcium and vitamin D alone (Yang *et al*, unpublished data).

In other organs, Western-style diets also have induced epithelial cell hyperproliferation and hyperplasia in mammary gland^[38,39], and hyperproliferation in pancreas^[40] and prostate gland^[41] in short-term studies; increasing dietary

calcium and vitamin D alone also inhibited the development of those lesions^[25].

EARLY HUMAN CLINICAL TRIALS OF CALCIUM AND COLON CANCER CHEMOPREVENTION

Prior to most of the preclinical studies noted above, a first human study was carried out^[28] which began to evaluate calcium's chemopreventive effects on the human colon. That first study, and a majority of the human studies that followed demonstrated that increased dietary calcium could decrease hyperproliferation of colonic epithelial cells in human subjects; and several studies further demonstrated calcium's binding of bile acids and fatty acids into insoluble complexes in the colon, decreasing the cytotoxicity of fecal water, the latter contributing to the decreased colonic epithelial cell hyperproliferation observed in human subjects (Tables 4,5).

The first pilot study in this human series noted above, and several other that followed, demonstrated significant reduction of excessive colonic epithelial cell proliferation, or reduced size of the proliferative compartment in colonic crypts. However, other human studies of supplemental calcium administration did not show this effect^[42]. Several of those studies were accompanied by experimental techniques that included extremely low initial baseline levels of colonic cell proliferation measured before calcium administration, very high amounts of calcium intake by subjects before calcium was given, and enemas given prior to colonic biopsies that likely perturbed the mucosa^[42]. Because early positive results were found in humans where calcium reduced colonic epithelial cell proliferation^[28], a further large randomized adenoma-recurrence clinical trial was developed and carried out, recently verifying that increased calcium intake caused a significant reduction in the development of actual tumors (recurrent adenomas) in the human colon^[32]. A further human study was recently carried out increasing dietary calcium intake through low fat dairy foods: this caused increased maturation and decreased proliferation of colonic epithelial cells following the increased dietary calcium intake^[43].

Table 1 Summary of studies on calcium and colon cancer

·Majority of epidemiologic studies suggest protective effect
· <i>In vitro</i> studies: decreased proliferation and increased differentiation and maturation of many types of epithelial cells
· <i>In vivo</i> rodent studies: numerous studies demonstrated inhibition of colonic tumor development preceded by decreased hyperproliferation, ODC and ras mutations, binding of bile and fatty acids into insoluble complexes reducing irritant and hyperproliferative effects, reduced cytotoxicity of fecal water
·Human studies: decreased hyperproliferation in most studies, increased differentiation and maturation of colonic epithelial cells, binding of bile and fatty acids into insoluble complexes, decreased cytotoxicity of fecal water
·Decreased recurrence of human adenomas

Table 2 Dietary calcium effects on epithelial cells in the colon and other organs of rodents

Cell proliferation	References*
Calcium decreased hyperproliferation Gover <i>et al</i> , 1994	
Calcium: decreased hyperproliferation when induced by doxycholic acid	Wargovich <i>et al</i> , 1983
Decreased hyperproliferation when induced by fatty acids	Wargovich <i>et al</i> , 1984
Decreased hyperproliferation when induced by cholic acid	Bird <i>et al</i> , 1986
Decreased hyperproliferation induced by partial enteric resection	Appleton <i>et al</i> , 1986
Decreased deoxycholic acid-induced hyperproliferation	Hu <i>et al</i> , 1989
Decreased MNNG-induced hyperproliferation on diet low in fat and calcium	Reshef <i>et al</i> , 1990
Decreased hyperproliferation induced by Western-style diet	Newmark <i>et al</i> , 1991
Decreased AOM-induced ODC and Tyr K	Arlow <i>et al</i> , 1989
Decreased ODC induced by bile acids	Baer <i>et al</i> , 1989
Decreased hyperproliferation when induced by Western-style diet	Richter <i>et al</i> , 1995 ^[24]
Decreased hyperproliferation in other organs when induced by Western-style diet	Xue <i>et al</i> , 1999 ^[25]

*Studies without reference numbers are found in^[23].

Table 3 Dietary calcium effects on colonic epithelial cells of rodents

Tumor development	References*
Calcium: decreased tumors induced by partial enteric resection and carcinogen	Appleton <i>et al</i> , 1987
Decreased proliferation and tumor formation induced by dietary fat and carcinogen	Pence <i>et al</i> , 1988
Decreased intestinal tumors after AMO	Skrypec <i>et al</i> , 1988
Decreased colonic tumors induced by AMO	Wargovich <i>et al</i> , 1990
Decreased the number of invasive carcinomas after MNU and cholic acid	McSherry <i>et al</i> , 1989
Decreased the number of rats with multiple tumors after DMH	Sitrin <i>et al</i> , 1991
Decreased K-ras mutations	Llor <i>et al</i> , 1990
Unchanged tumor incidence after DMH	Karkara <i>et al</i> , 1989
Unchanged tumor incidence after DMH	Kaup <i>et al</i> , 1989
Decreased late-stage precancerous lesion of whole colonic crypt dysplasia	Risio <i>et al</i> , 1996 ^[26]

*Studies without reference numbers are found in [23].

Table 4 Calcium effects on colonic cell proliferation, differentiation and cytotoxicity in human subjects

<i>In vitro</i>	References*
Decreased proliferation (2mM)	Buset <i>et al</i> , 1986
Decreased proliferation (2.4mM)	Appleton <i>et al</i> , 1988
Decreased proliferation (2mM)	Arlow <i>et al</i> , 1988
Decreased proliferation (2mM)	Buset <i>et al</i> , 1987
Decreased proliferation (2mM)	Friedman <i>et al</i> , 1989
Protected colonic cells against toxicity of bile acids and fatty acids (5mM)	Buset <i>et al</i> , 1989
Decreased growth of human colon cancer cell lines	Guo <i>et al</i> , 1990 ^[27]
Increased histone acetylation: cell differentiation (1-2mM)	Boffa <i>et al</i> , 1989

*Studies without reference numbers are found in^[23].

Table 5 Calcium effects on colonic cell proliferation, differentiation and cytotoxicity of fecal water in human subjects

<i>In vivo</i>	References*
Decreased hyperproliferation	Lipkin <i>et al</i> , 1985 ^[28]
Decreased hyperproliferation	Lipkin <i>et al</i> , 1989
Decreased hyperproliferation	Rozen <i>et al</i> , 1989
Decreased proliferation	Lynch <i>et al</i> , 1991
Decreased proliferation	Berger <i>et al</i> , 1991
Decreased proliferation	Wargovich <i>et al</i> , 1992
Decreased proliferation	Barsoum <i>et al</i> , 1992
Decreased proliferation	O'Sullivan <i>et al</i> , 1993
Decreased proliferation	Bostick <i>et al</i> , 1995
Unchanged proliferation	Gregoire <i>et al</i> , 1989
Unchanged proliferation	Cats <i>et al</i> , 1995
Decreased ODC	Lans <i>et al</i> , 1991 ^[29]
Normalized differentiation-associated lectin binding	Yang <i>et al</i> , 1991 ^[30]
Decreased cytotoxicity of fecal water	Govers <i>et al</i> , 1996 ^[31]
Increased maturation of colonic epithelial cells	Holt <i>et al</i> , 1998 ^[43]
Decreased adenoma recurrence	Baron <i>et al</i> , 1999 ^[32]

*Studies without reference numbers are found in^[23].

REFERENCES

- 1 Rasmussen H. The calcium messenger system (in 2 parts). *N Engl J Med*, 1986;314:1094-1164
- 2 Whitfield JF, Boynton AL, MacManus JP, Sikorsaka M, Tsang BK. The regulation of cell proliferation by calcium and cyclic AMP. *Mol Cell Biochem*, 1979;27:155-179
- 3 Bakcock MS, Marino MR, Gunning WT III, Stoner GD. Clonal growth and serial propagation of rat esophageal epithelial cells. *In Vitro*, 1983;19:403-415
- 4 Hennings H, Michael D, Chang C, Steinhart P, Holbrook K, Yuspa SH. Calcium regulation of growth and differentiation of mouse epidermal cells in culture. *Cell*, 1980;19:245-254
- 5 McGrath MC, Soule HD. Calcium regulation of normal mammary epithelial cell growth in culture. *In Vitro*, 1984;20:652-662
- 6 Soule HD, McGrath CM. A simplified method for passage and long term growth of human mammary epithelial cell. *In Vitro*, 1985;22:6-12
- 7 Boffa LC, Mariani MR, Newmark H, Lipkin M. Calcium as modulator of nucleosomal histones acetylation in cultured cells. *Proc Am Assoc Cancer Res*, 1989;30:8
- 8 Niendorf A, Arps H, Dietel M. Effect of 1,25 dihydroxyvitamin D3 on human colon cancer *in vitro*. *J Steroid Biochem*, 1987;27:825-828
- 9 Colston K, Colston MJ, Feldman D. 1,25 Dihydroxyvitamin D3 and malignant melanoma: the presence of receptors and inhibition of cell growth in culture. *Endocrinology*, 1981;108:1083-1086
- 10 Lointier P, Wargovich MJ, Saez S, Levin B, Wildrick DM, Boman BM. The role of vitamin D3 in the proliferation of a human colon cancer cell line *in vitro*. *Anticancer Res*, 1987;7:817-822
- 11 Higgins PJ, Tanaka Y. Cytoarchitectural response and expression of c-fos/p52 genes during enhancement of butyrate initiated differentiation of human colon carcinoma cells by 1,25 Dihydroxyvitamin D3 and its analogs. In: Lipkin M, Newmark HL, Kelloff G, eds. Calcium, vitamin D, and prevention of colon cancer. *Boca Raton: CRC Press*, 1991:305-326
- 12 Miyaura C, Abe E, Kuribayashi T, Tanaka H, Konno K, Nishii Y, Suda T. 1 α ,25 Dihydroxyvitamin D3 induced differentiation of human myeloid leukemia cells. *Biochem Biophys Res Comm*, 1981;102:937-943
- 13 Kuroki T, Chida K, Hashiba H, Hosoi J, Hosomi J, Sasaki K, Abe E, Suda T. Regulation of cell differentiation and tumor promotion by 1 α ,25 Dihydroxyvitamin D3. In: Humberman E, Barr SH, eds. *Carcinogenesis a comprehensive survey*. New York: Raven Press, 1985:275-286
- 14 Suda T, Miyaura C, Abe E, Kuroki T. Modulation of cell differentiation, immune responses and tumor promotion by vitamin D compounds. *Bone Min Res*, 1986;4:1-48
- 15 Eisman JA, Barkla DH, Tutton PJM. Suppression of *in vivo* growth of human cancer solid tumor xenografts by 1,25 dihydroxyvitamin D-3. *Cancer Res*, 1987;47:21-25
- 16 Honma Y, Hozumi M, Abe E, Konna K, Fukushima M, Hata S, Nishiji Y, Deluca HF, Suda T. 1 α ,25-Dihydroxyvitamin D-3 and 1 α -hydroxyvitamin D-3 prolong survival time of mice inoculated with myeloid leukemia cells. *Proc Natl Acad Sci USA*, 1983;80:201-204
- 17 Chida K, Hashiba H, Fukushima M, Suda T, Kuroki T. Inhibition of tumor promotion in mouse skin by 1 α ,25dihydroxyvitamin D-3. *Cancer Res*, 1985;45:5426-5430
- 18 Kawaura A, Tanida N, Sawada K, Oda M, Shimoyama T. Supplemental administration of 1 α hydroxyvitamin D-3 inhibits promotion by intrarectal instillation of lithocholic acid in N methyl N-nitrosourea induced colonic tumorigenesis in rats. *Carcinogenesis*, 1989;10:647-649
- 19 Hashiba H, Fukushima M, Chida K, Kuroki T. Systemic inhibition of tumor promoter induced ornithine decarboxylase in 1 α -hydroxyvitamin D-3 treated animals. *Cancer Res*, 1987;47:5031-5035
- 20 Kuroki T, Sasaki K, Chida K, Abe E, Suda T. 1 α ,25 Dihydroxyvitamin D-3 markedly enhances chemically induced transformation in BALB 3T3 cells. *Gann*, 1983;4:611-614
- 21 Jones CA, Callahan MF, Huberman E. Enhancement of chemical carcinogen induced cell transformation in hamster embryo cells by 1,25 dihydroxycholecalciferol, the biologically active metabolite of vitamin D-3. *Carcinogenesis*, 1984;5:1155-1159
- 22 Wood AW, Chang RL, Huang M T, Baggiolini E, Partridge JJ, Uskokovic M, Conney AH. Stimulatory effect of 1 α ,25-dihydroxyvitamin D3 on the formation of skin tumors in mice treated chronically with 7,12 dimethylbenz[α]ant hracene. *Biochem Biophys Res Comm*, 1985;130:924-931
- 23 Lipkin M, Newmark H. Calcium and the prevention of colon cancer. *J Cell Biochem*, 1995;22(Suppl):65-73
- 24 Richter F, Newmark H, Richter A, Leung D, Lipkin M. Inhibition of Western diet induced hyperproliferation and hyperplasia in mouse colon by two sources of calcium. *Carcinogenesis*, 1995;16:2685-2689
- 25 Xue L, Lipkin M, Newmark H, Wang J. Influence of dietary calcium and vitamin D on diet induced epithelial cell hyperproliferation in mice. *J Natl Can Inst*, 1999;91:176-181
- 26 Risio M, Lipkin M, Newmark H, Yang K, Rossini F, Steele V, Boone C, Kelloff G. poptosis, cell replication, and Western style diet induced tumorigenesis in mouse colon. *Cancer Res*, 1996;56:4910-4916
- 27 Guo YS, Draviam E, Townsend, CM Jr, Singh P. Differential effects of Ca²⁺ on proliferation of stomach, colonic, and pancreatic cancer lines *in vitro*. *Nutr Cancer*, 1990;14:149
- 28 Lipkin M, Newmark H. Effect of added dietary calcium on colonic epithelial cell proliferation in subjects at high risk for familial colonic cancer. *N Engl J Med*, 1985;313:1381-1384
- 29 Lans JJ, Jaszwski R, Arlow FL, Tureaud J, Luk GD, Majumdar AP. Supplemental calcium suppresses colonic mucosal ornithine decarboxylase activity in elderly patients with adenomatous polyps. *Cancer Res*, 1991;51:3416-3419
- 30 Yang K, Cohen L, Lipkin M. Lectin soybean agglutinin: measurements in colonic epithelial cells of human subjects following supplemental dietary calcium. *Cancer Lett*, 1991;56:65-69
- 31 Govers MJ, Tremont DS, Lapre JA, Kleibeuker JH, Vonk RJ, Van der Meer R. Calcium in milk products precipitates intestinal fatty acids and secondary bile acids and thus inhibits colonic cytotoxicity in humans. *Cancer Res*, 1996;56:3270-3275
- 32 Baron JA, Beach M, Mandel JS. Calcium supplements for the prevention of colorectal adenomas. *N Engl J Med*, 1999;340:101-107
- 33 Newmark H, Lipkin M, Maheshwari N. Colonic hyperplasia and hyperproliferation induced by a nutritional stress diet with four components of Western style diet. *J Natl Cancer Inst*, 1990;82:491-496
- 34 Newmark H, Lipkin M, Maheshwari N. Colonic hyperproliferation induced in rats and mice by nutritional stress diets containing four components of human Western style diet (Series 2). *Am J Clin Nutr*, 1991;54:209-214s
- 35 Fodde R, Edelmann W, Yang K, van Leeuwen C, Carlson C, Renault B, Breukel C, Alt E, Lipkin M, Khan P. A targeted chain termination mutation in the mouse Apc gene results in multiple intestinal tumors. *Proc Natl Acad Sci USA*, 1994;91:8969-8973
- 36 Yang K, Edelmann W, Fan K, Lau K, Kolli VR, Fodde R, Khan M, Kucherlapti R, Lipkin M. A mouse model of human familial adenomatous polyposis. *J Exp Zool*, 1997;277:245-254
- 37 Yang K, Edelmann W, Fan KH, Lau K, Leung D, Newmark H, Kucherlapati R, Lipkin M. Dietary influences on neoplasms in a mouse model for human familial adenomatous polyposis. *Cancer Res*, 1998;58:5713-5717
- 38 Khan N, Yang K, Newmark H, Wong G, Telang N, Rivlin R, Lipkin M. Mammary duct epithelial cell hyperproliferation and hyperplasia induced by a nutritional stress diet containing four components of a Western style diet. *Carcinogenesis*, 1994;15:2645-2648
- 39 Xue L, Newmark H, Yang K, Lipkin M. Model of mouse mammary gland hyper proliferation and hyperplasia induced by a Western style diet. *Nutr Cancer*, 1996;26:281-287
- 40 Xue L, Yang K, Newmark H, Leung D, Lipkin M. Epithelial cell hyperproliferation induced in the exocrine pancreas of mice by a Western style diet. *J Natl Can Inst*, 1996;88:1586-1590
- 41 Xue L, Yang K, Newmark H, Lipkin M. Induced hyperproliferation in epithelial cells of mouse prostate by a Western style diet. *Carcinogenesis*, 1997;18:995-999
- 42 Lipkin M, Newmark H. Chemoprevention studies: controlling effects of initial nutrient levels. *J Natl Can Inst*, 1993;85:1870-1871
- 43 Holt P, Atallasoy E, Gelman J, Guss J, Moss S, Newmark H, Fan K, Yang K, Lipkin M. Modulation of abnormal colonic epithelial cell proliferation and differentiation by low fat dairy foods. *JAMA*, 1998;280:1074-1079

Edited by MA Jing-Yun
Proofread by MIAO Qi-Hong

A DNA delivery system containing listeriolysin O results in enhanced hepatocyte-directed gene expression

Cherie M. Walton, Catherine H. Wu and George Y. Wu

Subject headings DNA; gene expression; listeriolysin O; hepatocytes

Abstract

AIM To determine whether incorporation of the pH-dependent bacterial toxin listeriolysin O (LLO) into the DNA carrier system could increase the endosomal escape of internalized DNA and result gene expression.

METHODS A multi-component delivery system was prepared consisting of asialoglycoprotein (ASG), poly L-lysine (PL), and LLO. Two marker genes, luciferase and β -galactosidase in plasmids were complexed and administered *in vitro* to Huh7[ASG receptor (+)] and SK Hep1 [ASG receptor (-)] cells. Purity, hemolytic activity, gene expression, specificity, and toxicity were evaluated.

RESULTS An LLO-containing conjugate retained cell-targeting specificity and membranolytic activity. In ASG receptor (+) cells, luciferase gene expression was enhanced by more than 7-fold over that of conjugates without the incorporation of listeriolysin O. No significant expression occurred in ASG receptor (-) cells. Enhancement of β -galactosidase gene expression was less, but still significantly increased over controls. There was no detectable toxicity at concentrations shown to be effective in transfection studies.

CONCLUSIONS ASOR-PL can be coupled to LLO using disulfide bonds, and successfully target and increase the gene expression of foreign DNA.

INTRODUCTION

We have previously demonstrated targeted delivery of DNA to the liver via the recognition of asialoglycoprotein-polylysine (PL) containing conjugates by the hepatic asialoglycoprotein (ASG) receptors^[1,2]. Binding of the ASG-PL-DNA complexes to the ASG receptors resulted in internalization of the ligand-receptor complex into the cells via receptor-mediated endocytosis. However, a problem with using receptor-mediated endocytosis as a gene delivery system is that once the specific ligand-DNA complex is internalized, it must escape the endosome before delivery to the lysosome in order to avoid intracellular degradation. The endocytosis pathway is somewhat "leaky", which allows for the escape of some DNA without additional membrane disruption. However, most of the delivered genetic material remains trapped in the endosome and is degraded by lysosomal proteases. This may account for low transfection efficiency and transient expression^[3].

To address this problem we sought to use the natural properties of a bacterial toxin to enable targeted DNA to escape from endosomal vesicles. Listeriolysin O (LLO) is a pH dependent, thiol-activated, membranolytic protein secreted by the bacteria *Listeria monocytogenes*. LLO is necessary for the pathogenicity of *L. monocytogenes*. Ingested bacteria are taken up by host cells, primarily by macrophages, into phagolysosomes. However, the organism secretes LLO in the phagolysosome, where upon acidification, the LLO undergoes a conformational change, resulting in rupture of the vesicle. Escape of the bacteria from the vesicle occurs before contact with lysosomal enzymes allowing for further replication in the cytosol^[4,5].

In the following report, we demonstrate that the incorporation of LLO into the ASG-PL carrier system results in increased gene expression while retaining cell type specificity.

MATERIALS AND METHODS

Synthesis of asialoorosomucoid (ASOR)-PL-LLO conjugates

ASOR and polylysine were chemically conjugated

Department of Medicine, Division of Gastroenterology-Hepatology, University of Connecticut Health Center, Farmington, CT

Correspondence to: George Y. Wu, M.D., Ph.D., Department of Medicine, Division of Gastroenterology-Hepatology, University of Connecticut Health Center, Farmington, CT 06030, USA

Tel.(860)679-3878, Fax.(860)679-3159

Email.Wu@nso.uchc.edu

Received 1999-08-17

using a water soluble carbodiimide as described previously^[6,7]. In brief, ASOR, prepared by desialylation of orosomucoid from pooled human serum^[6], was mixed with PL, MW=38500 (Sigma Chemical Co.), in a 1:1 weight ratio. The reactants were coupled by addition of 1-ethyl-3-(3-dimethylaminopropyl)-carbodiimide (Pierce Chemical Co.) and purified by cation exchange chromatography. LLO was purified using a CH₂ spiral concentrator (Amicon) and DEAE Sephacel column (Pharmacia Fine Chemicals)^[18]. The cleavable cross linker N-succinimidyl 3-(2-pyridyldithio) propionate, SPDP, (Pierce Chemical Co.) was added to both ASOR-PL and LLO proteins according to the Pierce protocol. One milligram of both proteins was incubated with 25mM SPDP in dimethylsulfoxide for 30 minutes at room temperature. Free SPDP was separated from linked by application to a PD-10 desalting column (Pharmacia Fine Chemicals) and elution with water. The concentration of SPDP linked to the proteins was determined by measuring the release of 2-thione after reduction with 100mM DTT and reading the absorbance at 343 nm. The LLO-SPDP was activated for coupling by reduction with 12mg DTT in 100mM NaCl, 100mM Na acetate pH 4.5. Free DTT was removed by application to a PD-10 desalting column and elution with water.

Preparation of ASOR-PL-DNA complexes

The reporter genes used in these experiments were either CMV luciferase (CMV luc) or β -galactosidase (β -gal) plasmid DNA. The ratio of conjugate needed to bind a specific amount of DNA was determined by adding increasing amount of ASOR-PL-SPDP to 1 mg of CMV luc or β -gal plasmid DNA in 0.15 M saline. These samples were run on 1% agarose gels, and the point of DNA retardation was visualized by staining with ethidium bromide and observation with UV. This ratio was used in subsequent experiments. One milligram of the SPDP linked ASOR-PL and CMV luc or β -gal plasmid DNA in the proper proportion were incubated for 30min at room temperature in 0.15M saline. The ASOR-PL-SPDP-DNA complex was added to DTT reduced LLO-SPDP in a 2:1 molar ratio. The conjugate was incubated overnight at 4°C and filtered through a 0.2 μ m Nalgene syringe filter.

Characterization of protein-DNA complexes

The conjugate was characterized by Western blotting with polyclonal antibodies to LLO (Immune Response Corporation). One milligram of LLO and the final conjugate either with or without DTT (100 mM) reduction were run on a 7.5% SDS-PAGE gel. The proteins were transferred to a nylon membrane (Amersham), quenched for one hour in 5% dry milk dissolved in 10mM Tris, 150mM NaCl

and 0.5% Tween-20, and probed in the same buffer with a polyclonal antibody to LLO. Detection of the antigen-antibody complex was determined by exposure to anti-rabbit IgG horseradish peroxidase (Sigma) and developed with 3',3'-diaminobenzidine and hydrogen peroxide (Sigma)^[9].

To determine if the DNA remained bound conjugates under experimental conditions, agarose gels were run. One microgram of DNA bound to conjugate was run in a 1% agarose gel and visualized with ethidium bromide and UV.

Hemolytic activity

Hemolytic activity was determined by the adding the conjugate to one milliliter of PBS, pH 5.5, and 5 mM DTT plus 6×10^8 human red blood cells. Samples were incubated for 30 minutes at 37 °C and quantified by absorbance at 541 nm on a spectrophotometer. One hemolytic unit (HU) is the amount of LLO needed to release hemoglobin from 50% of the red blood cells^[10].

Targeted gene expression

Conjugates containing 1 μ g of CMV luc or β -gal DNA were added to Huh7 (ASG receptor positive) or SK Hep1 (ASG receptor negative) cells in 1 mL of DMEM containing 2 mM CaCl₂ and incubated for 4 h at 37 °C. Then FBS was added to a final concentration of 10% and cells were further incubated for 48 h. ASOR-PL-DNA, ASOR-PL-DNA plus free LLO, and ASOR-PL-LLO-DNA plus a 200-fold excess ASOR were used as controls. Gene expression was measured by luciferase detection using the luciferin substrate (Promega), and detection of activity using a luminometer. Luciferase expression results were standardized by measuring protein concentrations according to the Bradford assay^[9].

Cells incubated with β -gal were washed with PBS pH 7.4, fixed with 4% paraformaldehyde, and stained with X-gal (20 μ g/L in dimethylformamide) for 30 minutes at 37 °C. Cells were observed with light microscopy and positive (blue stained) cells were counted.

Toxicity studies

Huh7 and SK Hep1 cells were incubated with ASOR-PL-DNA, free LLO, ASOR-PL-LLO-DNA or ASOR-PL-LLO-DNA in the presence of a 200-fold excess of ASOR in Dulbecco's minimal essential media (DMEM)+2 mM CaCl₂ for 4 h at 37 °C. Fetal bovine serum (FBS) in a final concentration of 10% was added, and the cells were further incubated for 24 and 48 hrs at 37 °C. Cell viability was determined by trypan blue exclusion^[11].

RESULTS

The molar ratio of SPDP linked to ASOR-PL and

LLO, determined by the release of 2-thione after reduction, was found to be 1:1. The ratio of ASOR-PL-SPD P needed to retard migration of DNA in agarose gels was 114:1 moles. ASOR- PL-LLO-DNA complexes were analyzed on a Western blot with a polyclonal antibody to LLO. As shown in Figure 1, purified LLO migrated at a position expected for M_r 58000, lane 2. Molecular weight markers are shown in lane 1. ASOR-PL alone, as expected, did not bind to the antibody indicating that the ASOR-PL conjugate itself was not capable of non-specific binding with the anti-LLO antibody, lane 3. However, after coupling to LLO, the conjugate did react with anti-LLO antibody, and this conjugate was found not to migrate into the gel, lane 4. No contaminating bands were visualized. Chemical reduction of the complex with DTT resulted in a free band migrating at the position of LLO, lane 5. An agarose gel of the conjugate revealed no migrating bands, indicating that DNA remained bound (data not shown).

The results of hemolytic assays are shown in Table 1. LLO alone, as expected, was highly hemolytic at pH 5.5, but only minimally active at pH 7.4 when concentrations were low. However, at high concentrations, greater than 0.5 $\mu\text{g/mL}$, the pH had little effect. Hemolytic assays demonstrated that hemolytic activity of the conjugate was concentration dependent. Similar to LLO alone, the highest activity occurred at pH 5.5. At pH 7.4, the conjugate did not cause appreciable hemolysis. This suggested the conjugation procedure does not appreciably alter the hemolytic characteristics of the LLO, and that at physiological pH, the conjugate has no active LLO.

Figure 2, panel A, shows that prototype ASOR-PL-DNA complexes introduced into Huh7 [ASG receptor positive] cells produced approximately 5000 light units, lane 1. However, compared to the prototype, ASOR-PL-LLO-DNA complexes produced luciferase activity 7 times higher, lane 2. This enhancement was decreased by 60% with the addition of free ASOR to compete with the complex for ASG receptors, lane 3. The addition of free (not conjugated) LLO to ASOR-PL complexes in exactly the same molar concentration as provided by the ASOR-PL-LLO conjugate did not enhance luciferase gene expression, lane 4. This indicates that the observed enhancement of transfection could not be due to the effects of any free LLO. DNA alone had no significant gene expression, lane 5. In SK Hep1 [ASG receptor negative] cells there was no significant gene expression with prototype, lane 1, or ASOR-PL-LLO-DNA complexes, lane 2. Of course, controls consisting of addition of LLO to prototype ASOR-PL complexes, and DNA alone in this cell line alone had no detectable levels of luciferase expression, lanes 3 and 4, respectively.

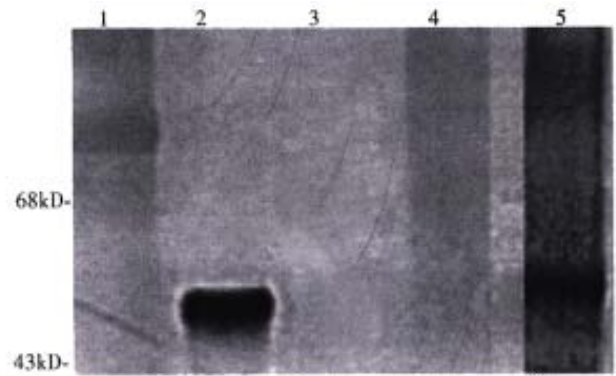


Figure 1 A Western blot of purified conjugates. One milligram of LLO and the final conjugate either with or without DDT (100mM) reduction were run on a 7.5% SDS-PAGE gel. The proteins were transferred to anylon membrane, quenched, and probed with a polyclonal antibody to LLO. Detection of the antigen-antibody complex was determined by exposure to anti-rabbit IgG horseradish peroxidase and developed with 3',3'-diaminobenzidine and hydrogen peroxide as described in Materials and Methods. Molecular weight markers, lane 1; LLO alone, lane 2; ASOR-PL, lane 3; ASOR-PL-LLO-DNA, lane 4; ASOR-PL-LLO-DNA+100mM DTT, lane 5.

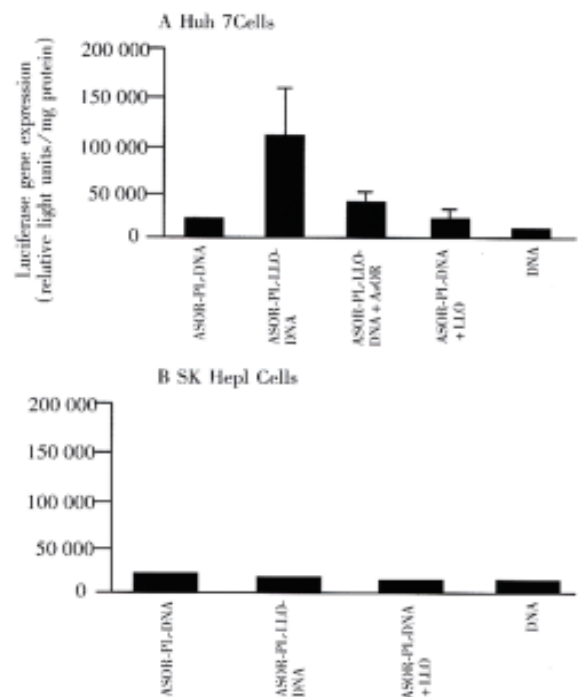


Figure 2 Targeted luciferase gene expression. Conjugates containing 1 μg of CMV luc were added to Huh7 (ASG receptor positive) or SK Hep1 cells (ASG receptor negative) and incubated for 48h as described in Materials and Methods. Gene expression was measured by luciferase detection using the luciferin substrate, and detection of activity using a luminometer. Luciferase expression results were standardized by measuring protein concentrations according to the Bradford assay. Panel A, Huh7 cells: ASOR-PL-DNA, lane 1; ASOR-PL-LLO-DNA, lane 2; ASOR-PL-LLO-DNA+200-fold molar excess of ASOR, lane 3; ASOR-PL-DNA+LLO, lane 4; DNA alone, lane 5. Panel B, SK Hep1 cells: ASOR-PL-DNA, lane 1; ASOR-PL-LLO-DNA, lane 2; ASOR-PL-DNA+LLO, lane 3; DNA alone, lane 4.

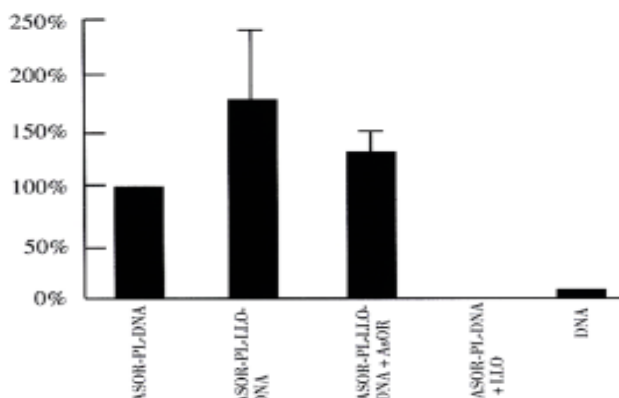


Figure 3 Targeted β -galactosidase gene expression. Conjugates containing 1 μ g of β -gal DNA were added to Huh7 (ASG receptor positive) or SK Hep1 cells (ASG receptor negative) and incubated for 48h. Cells incubated with β -gal were washed with PBS pH 7.4, fixed with 4% paraformaldehyde and stained with X-gal as described in Materials and Methods. Cells were observed with light microscopy and positive (blue stained) cells were counted. ASOR-PL-DNA, lane 1; ASOR-PL-LLO-DNA, lane 2; ASOR-PL-LLO-DNA+ASOR, lane 3; ASOR-PL-DNA+LLO, lane 4; DNA alone, lane 5.

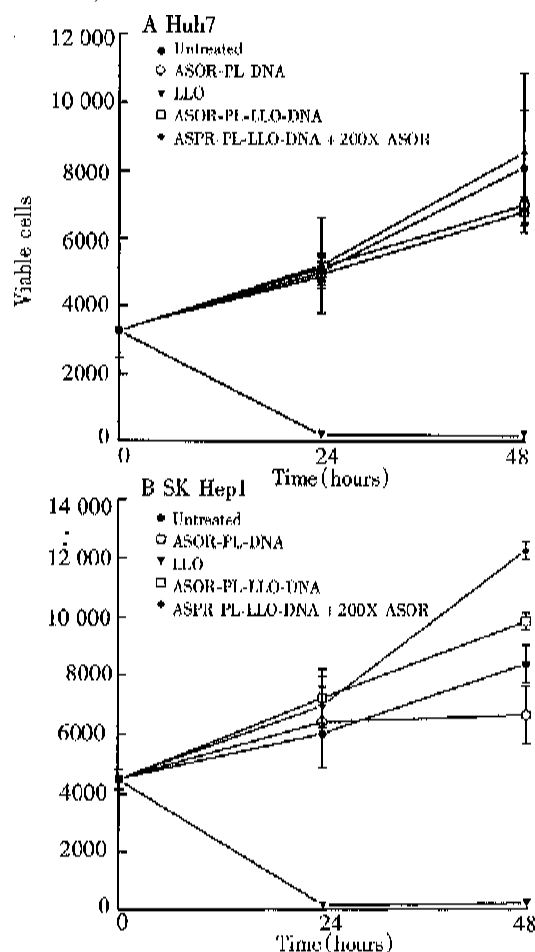


Figure 4 Toxicity of complexes. Huh7 (ASG receptor positive) and SK Hep1 (ASG receptor negative) cells were incubated with ASOR-PL-DNA, free LLO, ASOR-PL-LLO-DNA or ASOR-PL-LLO-DNA in the presence of a 200-fold excess of ASOR as described in Materials and Methods. Cell viability was determined by trypan blue exclusion. Panel A, Huh7 cells; Panel B SK Hep1 cells.

Table 1 Hemolytic activity* of ASOR-PL-LLO and LLO alone

LLO (μ g)	LLO		ASOR-PL-LLO-DNA	
	pH 5.5	pH 7.4	pH 5.5	pH 7.4
0.005	1.000	0.024	0	0
0.010	1.380	0.051	0	0
0.050	1.680	0.074	0.010	0
0.100	1.900	1.280	0.021	0
0.500	1.900	1.730	0.349	0
1.000	2.100	1.900	0.947	0.013
2.000	2.100	2.100	1.900	0.020

*A⁵⁴¹ where 100% hemolysis a value of 2.100.

Figure 3 shows the results of studies of Huh7 cells transfected with a gene for β -galactosidase. The ASOR-PL-LLO-DNA complex containing β -gal DNA increased gene expression 185% over prototype ASOR-PL complexes (complex lacking LLO), lane 2. The enhancement was inhibited by 30% with addition of a 200-fold excess ASOR, lane 3. ASOR-PL-DNA plus free LLO, and DNA alone had no significant gene expression, lanes 4 and 5, respectively.

In order to determine whether the LLO-containing conjugate was toxic, cell viability studies were performed and the results are shown in Figure 4. Huh7 and SK Hep1 cells, panels A and B respectively, treated with ASOR-PL-DNA, ASOR-PL-LLO-DNA with or without an excess of ASOR proliferated at the same rate as control (untreated) cells. However, LLO alone in the same concentration as present in the ASOR-PL-LLO-DNA rapidly decreased viable cell numbers. Thus, the concentration of complexes used for expression studies were found not to be toxic to either Huh7 or SK Hep1 cells.

DISCUSSION

Many approaches have been developed to solve the problem of low transfection efficiency and transient expression of gene delivery systems. Partial hepatectomy, chloroquine administration, and viruses or viral peptides have shown to be useful in increasing the duration of expression^[6,12-16]. The current report is the first demonstration that the natural escape strategies of the bacterial toxin LLO can be useful as a potential component of a targetable DNA delivery system to increase efficiency^[4,5].

LLO is a thiol-containing protein^[5]. Experiments on direct bonding to ASOR-PL-SPDP resulted in low efficiency (data not shown). In subsequent experiments LLO was also treated with SPDP to increase the number of potential cross linking residues. Subsequent reduction with DTT resulted in successful conjugation.

The conjugated LLO had lower hemolytic activity compared to equal amounts of free LLO.

This was in spite of the fact that DTT is added to samples to activate the thiol groups. This reduction would also cleave coupled LLO from the conjugate. The lower molar activity of the released LLO may have been due to the addition of SPDP, or to interference from ASOR or DNA that was independent of thiol reduction. Nevertheless, the hemolytic activity of the conjugate was pH dependent as seen with native LLO. This is important as one of the theoretical advantages for the use of LLO was the lack of activity at physiological pH, and restored activity in the acidic environment of the endosome. Toxicity due to extracellular activity would be minimized.

In summary, the above experiments show that ASOR-PL can be coupled to LLO using disulfide bonds, and successfully target and increase the gene expression of foreign DNA. The increase in expression was blocked with the addition of a large molar excess of ASOR, and was present only in ASG receptor positive cells, indicating retention of hepatocyte specificity.

ACKNOWLEDGMENTS The technical assistance of Ying Zhang, and the secretarial assistance of Martha Schwartz are gratefully acknowledged. This work was supported in part by a grant from the National Institutes of Health, DK -42182 (GYW), the Immune Response Corporation (GHW), and the Herman Lopata Chair for Hepatitis Research.

REFERENCES

- 1 Wu GY, Wu CH. Receptor mediated in vitro gene transformation by a soluble DNA carrier system. *J Biol Chem*, 1987;262:4429-4432
- 2 Wu GY, Wu CH. Receptor mediated gene delivery and expression in vivo. *J Biol Chem*, 1988;263:14621-14624
- 3 Cotten M, Baker A, Saltik M, Lehmann H, Panzenbock B, Chiocca S. Receptor mediated gene delivery. In: Blum HE, ed. *Molecular diagnosis and gene therapy*. Boston MA: Kluwer Academic Publishers, 1996:80-91
- 4 Geoffrey C, Gaillard JL, Alouf FE, Berche P. Purification, characterization and toxicity of the sulfhydryl activated hemolysin listeriolysin O from *Listeria monocytogenes*. *Infect Immun*, 1987;55:1641-1646
- 5 Vasquez Boland JA, Dominguez L, Rodriguez-Ferri EF, Suarez G. Purification and characterization of two *Listeria ivanovi* cytotoxins, a sphingomyelinase C and a thiol activated toxin (ivanolysin O). *Infect Immun*, 1989;57:3928-3935
- 6 Wu GY, Zhan P, Sze LL, Rosenberg AR, Wu CH. Incorporation of adenovirus into a ligand based DNA carrier system results in retention of original receptor specificity and enhances targeted gene expression. *J Biol Chem*, 1994;269:11542-11546
- 7 McKee TD, DeRome ME, Wu GY, Findeis MA. Preparation of asialoorosomucoid polylysine conjugates. *Bioconj Chem*, 1994;5:306-311
- 8 Walton CM, Wu CH, Wu GY. A method for purification of listeriolysin O from a hypersecretor strain of *Listeria monocytogenes*. *Prot Express Purif*, 1999;15:243-245
- 9 Harlowe E, Lane D (eds). *Antibodies, a laboratory manual*. Cold Spring Harbor Laboratories, 1988
- 10 Cossart P, Vicente MF, Mengaud J, Baquero F, Perez Diaz JC, Berche P. Listeriolysin O is essential for virulence of *Listeria monocytogenes*: direct evidence obtained by gene complementation. *Infect Immun*, 1989;57:3629-3636
- 11 Garvey JS, Cremer NE, Sussendorf DN (eds). *Methods in immunology*. 3rd ed. Reading MA: WA Benjamin, Inc, 1997:449
- 12 Wu CH, Wilson JM, Wu GY. Targeted genes: delivery and persistent expression of a foreign gene driven by mammalian regulatory elements in vivo. *J Biol Chem*, 1989;264:16985-16987
- 13 Roy Chowdhury N, Hays RM, Bommineni VR, Franki N, Roy Chowdhury J, Wu CH, Wu GY. Microtubular disruption prolongs the expression of human bilirubinuridinediphosphoglucuronate glucuronyl transferase1 gene transferred into Gunn rats. *J Biol Chem*, 1996;271:2341-2346
- 14 Feng M, Jackson WH Jr, Goldman CK, Rancourt C, Wang M, Dusing SK, Siegal G, Curiel DT. Stable in vivo gene transduction via a novel adenoviral/retroviral chimeric vector. *Nat Biotech*, 1997;15:866-870
- 15 Schlegel R, Wade M. Biologically active peptides of the vesicular stomatitis virus glycoprotein. *J Virol*, 1985;53:319-323
- 16 Wagner E, Plank C, Zatloukal K, Cotton M, Birnstiel ML. Influenza virus hemagglutinin HA 2 N terminal fusogenic peptides augment gene transfer by transferring polylysine DNA complexes: toward a synthetic virus like gene transfer vehicle. *Proc Natl Acad Sci USA*, 1992;89:7934-7938

Edited by MA Jing-Yun
Proofread by MIAO Qi-Hong

Characterization of six tumor suppressor genes and microsatellite instability in hepatocellular carcinoma in southern African blacks

C. Martins, M.A. Kedda, M.C. Kew*

Subject headings carcinoma, hepatocellular; southern African blacks; cumulative LOH; tumor suppressor genes; microsatellite genomic instability; liver neoplasms

Abstract

AIM To analyse cumulative loss of heterozygosity (LOH) of chromosomal regions and tumor suppressor genes in hepatocellular carcinomas (HCCs) from 20 southern African blacks.

METHODS *p53*, *RB1*, *BRCA1*, *BRCA2*, *WT1* and *E-cadherin* genes were analysed for LOH, and *p53* gene was also analysed for the codon 249 mutation, in tumor and adjacent non-tumorous liver tissues using molecular techniques and 10 polymorphic microsatellite markers.

RESULTS *p53* codon 249 mutation was found in 25% of the subjects, as was expected, because many patients were from Mozambique, a country with high aflatoxin B₁ exposure. LOH was found at the *RB1*, *BRCA2* and *WT1* loci in 20%(4/20) of the HCCs, supporting a possible role of these genes in HCC. No LOH was evident in any of the remaining genes. Reports of mutations of *p53* and *RB1* genes in combination, described in other populations, were not confirmed in this study. Change in microsatellite repeat number was noted at 9 / 10 microsatellite loci in different HCCs, and changes at two or more loci were detected in 15%(3/20) of subjects.

CONCLUSION We propose that microsatellite/genomic instability may play a role in the pathogenesis of a subset of HCCs in black Africans.

INTRODUCTION

The evolution of cancer is thought to occur from the stepwise accumulation of genetic aberrations in the same cell. These include loss of function of tumor suppressor genes, activation of proto-oncogenes, faulty DNA mismatch repair, and the integration of viral DNA^[1,2]. Hepatocellular carcinoma (HCC) is a leading cause of death in both Africa and the Far East, resulting in at least 310000 deaths worldwide each year^[3]. HCC is multifactorial in aetiology and its pathogenesis is complex. The major risk factors involved in the development of the tumor are chronic HBV and HCV infections, cirrhosis and aflatoxin B₁ (AFB) exposure^[4,5].

Heavy dietary AFB intake is thought to cause a guanine (G) to thymine (T) transversion at the third base of codon 249 of the *p53* gene, and for this reason clustering of this point mutation occurs in HCCs from Africa and China^[6-8]. In addition, other mutations in, or deletions of, the *p53* gene (on chromosome 17p13.1) are found with relatively high frequency in human HCCs in other countries. The functional loss of this tumor suppressor gene, as well as its abnormal expression, have been proposed to play a significant role in HCC development^[9] or at least in the development of a subset of HCCs. The majority of *p53* alterations reported to date have loss of one allele accompanied by mutations of the second allele^[10]. Abnormalities of the *p53* gene, such as gene mutation, deletion, or the nuclear accumulation of mutant *p53* protein have also been found to correlate with increased allelic loss at the Breast Cancer Susceptibility Gene 1 (*BRCA1*) locus (17q21). This gene is thought to encode a transcription factor which acts as a tumor suppressor^[11]. LOH of the *BRCA1* gene in HCC was reported in a Korean study^[12]. The Breast Cancer Susceptibility Gene 2 (*BRCA2*) (13q12-13) product is thought to be a tumor suppressor^[13] involved in cellular proliferation and differentiation^[14], and may be involved in the development of HCC^[15]. LOH at the *BRCA2* locus has been reported in HCC^[15,16] and it has been suggested that mutations of the *BRCA2* gene may be involved in hepatocarcinogenesis^[15]. The retinoblastoma (*RB1*) gene (13q14.2) product (pRB) functions as a cell cycle regulator^[17], and its

MRC/CANSA/University Molecular Hepatology Research Unit, Department of Medicine, University of the Witwatersrand Medical School, 7 York Road, Parktown 2193, Johannesburg, South Africa. Supported in part by grants/bursaries from the University of the Witwatersrand, and the Foundation for Research Development, Pretoria, South Africa.

Correspondence to: Professor M.C. Kew, Department of Medicine, Medical School, 7 York Road, Parktown, 2193, Johannesburg, South Africa.

Tel. +27(0)11 488 3626, Fax. +27(0)11 643 4318

Email:014anna@chiron.wits.ac.za

Received 1999-08-10

absence leads to unrestricted cell growth. Although there is no definite evidence that mutations of the RB gene are involved in HCC, LOH of the RB1 gene has been documented in human HCCs^[18,12]. LOH of WT1 and 11p13 have been reported in human HCCs^[12,16]. WT1 appears to be involved in proliferation, differentiation and apoptosis^[19,20]. The product of the E-cadherin (Uvomorulin) gene (16q221) is the primary adhesion molecule in epithelium^[21]. Loss of function of E-cadherin may lead to decreased cell-cell adhesion^[22], cellular phenotypic changes, and the development of invasive properties^[23]. In HCC, multicentric development and the formation of intrahepatic metastases is common^[24]. LOH on chromosome 16q has been previously reported to be important in the initiation or progression of HCC^[25,26].

Polymerase chain reaction (PCR) amplification of microsatellites (sequences uniformly distributed throughout the human genome) provides a simple and effective method of rapidly detecting loss of heterozygosity/microsatellite instability (LOH/MI)^[27]. Microsatellite instability is defined as the loss or gain of microsatellite repeats at 2 or more loci and is detected by the presence of extra bands or band shifts between tumor and non-tumorous tissue DNA.

In this study, we examined the G-T transversion at codon 249 of the *p53* gene, LOH of the *p53*, RB1, BRCA1, BRCA2, WT1 and E-cadherin genes, and microsatellite instability at 10 loci flanking these genes, in HCC and adjacent non-tumorous liver, from 20 southern African blacks.

MATERIALS AND METHODS

Subjects

The subjects included 20 southern African black men, aged between 20 and 40 years. HCC tissue and matched non-tumorous liver were obtained at necropsy or during surgical resection. DNA was extracted from the tissues using a modified "salting-out" procedure^[28].

HBV markers

The HBV status of the subjects was determined previously using commercially available kits to detect HBV markers in serum (Abbott Labs, Chicago, IL, USA).

LOH and microsatellite instability

Microsatellite instability (MI) and loss of heterozygosity (LOH) studies were carried out by PCR and gel electrophoresis using polymorphic repeat markers (Table 1).

PCR products of the polymorphic loci *p53*, D17S846 and RB1.20 were resolved on 4%

composite agarose gels, while radioactively labeled PCR products of the remaining loci were resolved on polyacrylamide gels, and viewed by autoradiography. Band mobility shifts between tumor and matched non-tumorous liver DNA were scored as a change in allele repeat number. LOH was characterized by the disappearance of one band or a considerable (≥40%) decrease in band intensity in heterozygotes, whilst microsatellite instability was determined by expansion and/or contraction of microsatellite sequences.

PCR for LOH and MI

A standard PCR protocol (primers, Table 1) was followed for the *p53*, WT1, D13S137, RB(1.20), D13S120, D13S127, D17S855, and D17S846 loci. Each PCR reaction consisted, at final volume, of 100ng DNA, 1U *Taq* DNA polymerase (Promega, Madison, USA), 1×buffer, 1 mM each dATP, dTTP, dGTP, 0.1 mM dCTP, 0.025 μCi α³²P dCTP, and 50 pmol of each primer; in a total volume of 50 μL, amplification for 30 cycles of denaturation at 94 °C for 30 s, annealing 55 °C for 30 s, extension at 72 °C for 1min, and a final cycle of 72 °C for 10 minutes.

The PCR reaction for the D16S301 and D16S260 loci (primers, Table 1) consisted, at final volume, of 100ng DNA, 1U *Taq*-DNA Polymerase, 1×buffer, 0.1 % gelatin, 1 mM each dGTP, dATP, dTTP, 0.1 mM dCTP, and 0.025 μCi α³²P dCTP, 50 pmol of each primer; in a total volume of 25 μL, amplification for 25 cycles of denaturation at 94 °C for 1 min, annealing at 55 °C for 2 min, extension at 72 °C for 2.5 min, and a final cycle of 72 °C for 10 minutes.

p53 codon 249 mutation

The *p53* codon 249 mutation was detected by PCR-RFLP using primer sequences F3 and R3 (Table 1), and confirmed by sequence analysis. The PCR reaction consisted of, at final volume^[6], 100 ng DNA, 2.5U of *Taq*-DNA polymerase (Promega), 1×buffer, 1mM MgCl₂, 0.8 mM each of dCTP, dATP, dGTP, dTTP, and 50 pmol of each primer; in a total volume of 50 μL, amplification for 30 cycles of denaturation at 94 °C for 15 s, annealing at 56 °C for 15 s, and extension at 72 °C for 30 s. The 110 bp PCR product was sized on ethidium bromide stained agarose gels against a 100 bp DNA ladder (Promega). AG to T transversion at the third base of codon 249 was detected by the presence or absence of a *Hae*III restriction site^[6]. All samples shown by digestion to have the codon 249 mutation were sequenced in both directions both upstream and downstream in separate reactions, to confirm the presence of the mutation.

Table 1 PCR primers

Gene/Locus	Primer	Primer sequence	Amplicon	Amplicon length
<i>p53</i>	<i>p53F3</i> <i>p53R3</i>	5'GTTGGCTCTGACTGT-ACCAC 5'CTGGAGTCTTCCAGT-GTGAT	exon 7 spanning codon 249 ^[6]	110bp
<i>p53</i>	<i>p53ivs1a</i> <i>p53ivs1b</i>	5'GCACTTTCCTCAACTCTACA 5'AACAGCTCCTTTAATGGCAG	ALU sequence within intron 1 of <i>p53</i> gene ^[43]	200bp-300bp
D13S120 (BRCA2)	1353L 1353R	5'ATGACCTAGAAATGATACTGGC 5'CAGACACCACAACACACATT	(AC) ₇₃ repeat at D13S120 ^[44]	112bp-136bp
D17S846 (BRCA1)	FF RF	5'TGCATACCTGTACTACTTCAG 5'TCCTTTGTTGCAGATTCTTC	(GGAA) ₂₅ repeat at D17S846 ^[45]	250bp-300bp
D17S855 (BRCA1)	FS RS	5'GGATGGCCTTTTAGAAAGTGG 5'ACACAGACTTGTCTACTGCC	AC repeat at D17S855 ^[46]	145bp
WT1	400 401	5'AATGAGACTTACTGGGTGAGG 5'TTACACAGTAATTTCAAGCAACGG	AC repeat within 3' untranslated sequence of WT33 ^[47]	100bp-200bp
RB1	B57 B103	5'TGTATCGGCTAGCCTATCTC 5'AATTAACAAGGTGTGGTGGT	[CTTT(T)] _n (n=14-26) repeat within intron 20 of RB gene ^[48,49]	400bp-600bp
D13S127 (BRCA2/RB1)	1341L 1341R	5'CAGATATGTACTCATGCACATG 5'AAACAAATGAGTTGGCTGT	(AC) ₃₅ repeat at D13S127 ^[44]	130bp-142bp
D13S137 (RB1)	F R	5'TTTCCTCATCTTTCCCAATTG 5'CAGGAGGGATGGACTCACTTC	(GT) ₂₂ repeat at D13S137 ^[50]	±135bp
E-cadherin	E-cadF1 E-cadF1	5'GATCCTAAGGACAAATGTAGATGCTCT 5'AGCCACTTCCCAGAACTTGGCTTCC	D16S301 locus polymorphic AC region ^[51]	146bp
E-cadherin	E-cadF2 E-cadR2	5'GGTTGAGATGCTGACATGC 5'CAGGGTGGCTGTTATAATG	D16S260 locus polymorphic AC repeat region ^[52]	±234bp

Note: WT1: Wilm's tumor gene; RB1: Retinoblastoma gene; BRCA1: Breast cancer susceptibility gene 1; BRCA2: Breast cancer susceptibility gene 2; bp: base pairs.

Sequencing

All sequencing was carried out using the Sequenase PCR Product Sequencing Kit (United States Biochemical Corp., Cleveland, Ohio), according to the manufacturer's instructions.

RESULTS

HBV status

Seven patients were currently infected with HBV (5 of these were HBsAg-positive; HBeAg-negative; the HBeAg status of the remaining 2 was unknown), and 6 were previously infected (anti-HBc and anti-HBs-positive). The HBV status of the remaining patients was not known (Table 2).

LOH/MI analyses

LOH was noted for the WT1 (1/13 subjects), RB (1.20) (1/10 subjects), D13S120 (1/20 subjects) and D13S127 (2/14 subjects) loci (Table 2).

The D13S137 and D13S127 loci flank the RB1 gene, while the RB (1.20) repeat sequence is within intron 20 of the same gene. LOH at the D13S127 locus suggests loss of at least a portion of the RB1 gene as shown in 2/14 informative subjects. LOH at RB (1.20) indicated loss of the RB1 gene in a

further 1/10 informative subjects. The RB1 gene was thus lost in 3/18 informative subjects (Table 2). LOH at the D13S120 and D13S127 loci flanking the BRCA2 gene was shown in 2/20 informative subjects (Table 2). No LOH was found for any of the remaining loci (Table 2).

Microsatellite/genomic instability (or a gain/loss of microsatellite repeats) was found in 15% (3/20) of subjects.

p53 gene codon 249 analysis

The *p53* codon 249 mutation was detected in 25% of the subjects using PCR-RFLP analysis, and confirmed by sequencing. The *p53* codon 249 mutation was detected in the tumor tissue of 3 subjects, in the non-tumorous liver of 1 subject, and in both the tumor and non-tumorous liver tissue of 1 subject (Table 2).

Sequencing gel electrophoresis of the *p53* gene product revealed a gel artifact, in all subjects with wild-type chromosomes, previously described by Kapelner *et al* (1994).

All tumors were at an advanced stage. No attempt was made to correlate the presence of LOH or microsatellite instability with clinical or other features.

Table 2 LOH, SSCP and sequence analysis

Subject number	VNTRs										p53 codon 249		HBV status
	p53	WT1	RB1		BRCA2		BRCA1		E-cadherin		T	NT	
	(ALU)	(AC)	D13S137 (GT) ₂₂	RB1.20 [CTTT(T)] _n	D13S120 (AC) ₇₃	D13S127 (AC) ₃₅	D17S855 (AC)	D17S846 (GGAA) ₂₅	D16S301 (AC)	D16S260 (AC)			
1	NI	NI	-	-	-	NI	-	-	-	NI	-/-	-/-	HBsAg+; HBeAg-
2	-	-	-	-	-	NI	-	-	-	NI	-/-	-/-	HBsAg+
3	-	-	-	-	-	-	-	-	NI	-	+/-	-/-	HBsAg+; HBeAg-
4	-	-	-	NI	-	-	?	NI	-	-	-/-	-/-	anti-HBc+; anti-HBs+
6	-	?	?	?	-	NI	?	-	?	-	+/-	-/-	HBsAg+; HBeAg-
7	?	?	?	?	-	-	?	?	-	-	-/-	-/-	anti-HBs+; anti-HBc+
8	↑	△	NI	+	↓	↓	△	△	↑	-	+/-	-/-	anti-HBs+; anti-HBc+
14	-	NI	?	NI	-	+	-	?	?	NI	-/-	-/-	anti-HBs+; anti-HBc+
16	?	?	△	?	+	+	?	?	△	↑	-/-	-/-	HBsAg+
18	↑	+	?	?	↑	-	?	?	?	↑	-/-	-/-	HBsAg+; HBeAg-
24	NI	-	NI	-	-	-	-	-	NI	-	-/-	+/-	anti-HBs+; anti-HBc+
39	-	NI	-	?	-	-	-	NI	?	-	-/-	-/-	HBsAg+; HBeAg-
40	NI	-	?	-	-	NI	-	-	?	-	-/-	-/-	anti-HBs+; anti-HBc+
48	NI	-	-	-	-	-	-	-	?	?	-/-	-/-	?
50	NI	-	-	NI	-	-	-	NI	-	NI	-/-	-/-	?
51	NI	-	?	NI	-	NI	-	-	-	-	-/-	-/-	?
52	NI	-	NI	-	-	NI	-	-	-	-	+/-	-/-	?
53	-	-	-	-	-	-	-	-	NI	-	-/-	-/-	?
54	-	?	-	-	-	-	-	-	-	NI	-/-	-/-	?
56	NI	-	-	NI	-	-	-	NI	NI	NI	-/-	-/-	?

Note: LOH: loss of heterozygosity; -: HBV status-negative for particular antigen/antibody, mutation studies-mutation absent; LOH studies: no LOH; →p53 codon 249 mutation analysis: G→T transversion absent; +: HBV status-positive for particular antigen/ antibody, mutation studies-mutation present, →LOH studies: LOH, →p53 codon 249 mutation analysis: G→T transversion present;

?: results not obtained because of unsuccessful PCR or HBV status unknown; △: a change in repeat number between tumor (T) and non-tumorous liver (NT) in both chromosomes; ↑ / ↓ : an increase/decrease in repeat number between tumor (T) and non-tumorous liver (NT) in one chromosome; NI: not informative; VNTRs: Variable number of tandem repeat sequences; HBV: Hepatitis B virus; WT1: Wilm's tumor gene; RB1: Retinoblastoma gene; BRCA1: Breast cancer susceptibility gene 1; BRCA2: Breast cancer susceptibility gene 2; HBsAg: hepatitis B virus S antigen; HBeAg: hepatitis B virus E antigen; anti-HBs: antibody to hepatitis B virus S antigen; anti-HBc: antibody to hepatitis B virus C antigen

DISCUSSION

LOH of the *p53* gene has been reported with relatively high frequency in HCCs from Japan (29%-69%)^[29,30], and also from southern Africa (60%), and Taiwan (39.3%)^[6,31]. No LOH was detected for *p53* in this study, although inactivation/reduction of *p53* gene expression or of its product by means other than LOH may have occurred in our population. In a study by Walker *et al* (1991), *p53* allele loss occurred only in HBV-negative tumors. It thus appeared as if a mechanism other than loss of one *p53* allele and mutation of the second allele was operating in HBV-positive tumors, thereby eliminating fully functional *p53* protein. The obvious mechanism would be the formation of complexes between wild-type *p53* protein and viral protein/s leading to the loss of function of wild-type *p53* protein. Such associations have been well documented in the literature^[32]. In our study most samples were HBV positive and a mechanism such as that mentioned above, rather than *p53* gene inactivation by physical mutation and LOH, may have been operating in our tumors to eliminate the function of the *p53* protein. Alternatively, should

both alleles of the *p53* gene be mutated in ways other than LOH in our samples, such as point mutations and small deletions (<50bp)^[18], these would not have been detected by the techniques employed in this study.

The *p53* codon 249 mutation was detected in 25% (5/20) subjects. This was expected as the subjects were southern African blacks, some of whom came from Mozambique and other areas where aflatoxin exposure is prevalent. The *p53* codon 249 mutation was found in both tumor and non-tumorous liver tissues of one subject. This could have been caused by contamination of the non-tumorous liver with tumor tissue. In another subject the mutation was detected in the non-tumorous liver only. The presence of this mutation has been documented in non-tumorous liver and not in the corresponding tumor tissues^[33], where it was proposed that normal liver subjected to prolonged aflatoxin exposure could gradually accumulate high levels of AGT mutations, whereas the mutation would not necessarily arise in neoplastic populations that were cloned from single progenitor cells resistant to aflatoxin. Unfortunately, insufficient

tissue was available in these two patients for histopathological examination, so we cannot exclude microscopic contamination as a cause of this finding in the two subjects. Two patients with a codon 249 G \rightarrow T transversion were HBsAg positive, 2 subjects were anti-HBs/anti-HBc positive and the HBV status of 1 subject was unknown. This concur red with previous studies where mutations at codon 249 were not found in non-HB V-related HCCs^[34], and is in agreement with previous work which suggests that both aflatoxin exposure and HBV infection are required for this mutation to occur^[29,33].

A gel artefact generated by formation of a mini hairpin secondary structure in the codon 249 region of the *p53* gene in 34 wild type chromosomes, lead to a "missing" G at the third base of codon 249 in the sequence of the sense strand^[35]. In a study by Kapelner *et al* (1994), as with our samples, Hae-III digest confirmed the presence of the recognition sequence GGCC. However, since there has been no other report of this "G deletion" in such a commonly sequenced region, Kapelner *et al* (1994) suggested that this artifact may not occur often.

LOH appears to have occurred in 4 subjects at the RB1 (3/18 or 17%), BRCA2 (2/20 or 10%) and WT1 (1/13 or 8%) loci (2 of these subjects had LOH at both the RB1 and BRCA2 genes). Although reduction to homozygosity has been apparent in certain individuals, and has consistently been scored as LOH, 'band disappearance' may also be caused by a gain/loss in microsatellite repeats. We think, however, that this is unlikely to be the case in so many individuals.

LOH of the retinoblastoma gene has been documented in 33% of HCCs from Korea^[12], 16%-73% of HCCs from Japan^[18,30] and 27% of HCCs from Australia^[36]. One copy of the RB1 gene was lost in 17% (3/18) of HCCs in this study. Although our sample is small, this frequency differs from the higher percentages found thus far. This may reflect population differences, LOH of the RB1 gene may play a role in a small subset of southern African HCCs. Coincident mutation of the *p53* and RB1 genes has been observed in 25%^[18], and 12.9%^[37] of advanced HCCs in Japan and Australia respectively^[36]. Mutations and LOH in these genes is most frequently observed in advanced stage HCCs, like those investigated here. However, no coincident mutation of these genes was detected in this study.

LOH of the BRCA2 gene has been reported in 3% of Japanese HCCs^[15], and in 40% of HCCs from the USA^[16]. In this study one copy of the BRCA2 gene was lost in 10% (2/20) HCCs. This

finding supports the notion that BRCA2 may function as a tumor suppressor gene in the liver^[15], and that it may in some way be involved in the progression of a small number of HCCs. To our knowledge, LOH of the BRCA1 gene has been reported only once, in a study in which 11.5% (3/6) of HCCs showed LOH at this locus^[12]. No LOH was found for this gene in our sample population. LOH at 11p13, the region containing the WT1 gene, as well as LOH of the gene itself has been reported in 4%-7% HCCs^[12,16]. Our result of 8% (1/13) LOH agrees with these findings. LOH of the region where the E-cadherin gene is located (16q22) has been reported in 64%-91% of Chinese and Japanese HCCs^[25,26]. No LOH was found for this gene in our study. Although all the HCCs used in this study were in advanced stages, it was not established whether they were highly undifferentiated. There may be retention of *E-cadherin* expression in these samples and no loss of intercellular adhesiveness.

We cannot say whether HBV played any role in the chromosome losses reported here^[37]. Cumulative LOH is thought to reflect the sequential development of HCC progression.

LOH of a number of tumor suppressor genes may be important in the advancement of HCC^[37]. Frequent loss of tumor suppressor genes has been reported in Korean HCCs, where 86% HCCs had LOH of 1 gene, and 59% had LOH of 2-4 genes^[12]. Piao *et al* (1997), investigated 10 tumor suppressor genes (-VHL, APC, EXT1, WT1, RB1, *p53*, BRCA1, nm23, DPC4, DCC). The genes most often lost were *p53* (66%), RB1 (33%), EXT1 (33%), and APC (20%). The genes found to be lost most often in our study were RB1 (17%) and BRCA2 (10%). However, as the total LOH of the *p53*, RB1, BRCA1, BRCA2, WT1 and *E-cadherin* genes in this study was 20% (4/20), we conclude that LOH of tumor suppressor genes is infrequent in our HCCs.

Microsatellite/genomic instability is reflected in the expansion/contraction of microsatellite sequences, and is thought to be a product of replication errors^[38]. Microsatellite instability has been considered to be insignificant in HCC development by some authors, while others believe that it may be significant^[39]. To our knowledge, this is the first time microsatellite instability has been looked at in HCCs from a southern African black population. It is important to note that there are differences in allele frequency between our southern African Negroid population and the Asian, European and Australian populations, characterized previously at the WT1, D13S137, D13S120,

D13S127, D17S855, D16S301, and D16S260 loci (paper in preparation). Microsatellite instability has been documented in 40% of HCCs from the USA^[39], and in 41% of HCCs at two or more loci in a French study^[40]. In a Korean study microsatellite instability was detected in 4/10 (40%) HCCs, where each subject showed instability at two or more loci^[39]. Of the 9 markers used in their study, 3 showed genetic instability in one or more subjects. In our study 3/20 (15%) HCCs showed instability at two or more loci. Of the 10 loci investigated, 9 showed genetic instability in one or more subjects. Cumulative microsatellite instability indicates advanced HCC. One of these subjects also had the codon 249 mutation in the *p53* gene. We were not able to determine whether joint changes at the loci were necessary for tumor development, or whether they represented independent events in tumor initiation and/or progression. Microsatellite/genomic instability is believed to occur at random and may reflect alteration of the entire genome of the cancer cell^[41]. The order of these changes is most likely insignificant. Their cumulative effect however, may be important^[42]. We propose that microsatellite/genomic instability may play a role only in a small subset of HCC in our population.

In conclusion, our observations support a possible role of *p53*, WT1 and BRCA2 genes in the pathogenesis of HCC, and that microsatellite instability appears to be an important factor contributing to HCC development in a subset of our HCCs.

REFERENCES

- 1 Yee CJ, Roodi N, Verrier CS, Parl FF. Microsatellite instability and loss of heterozygosity in breast cancer. *Cancer Res*, 1994;54:1641-1644
- 2 Fujimoto Y, Kohgo Y. Alteration of genomic structure and/or expression of cancer associated genes in hepatocellular carcinoma. Abstract in English, article in Japanese. *Rinsho Byori*, 1998;46:9-14
- 3 Parkin DM, Stjernsward J, Muir C. Estimates of the worldwide frequency of twelve major cancers. *Bull WHO*, 1984;62:163-182
- 4 Harris CC. Hepatocellular carcinogenesis: recent advances and speculations. *Cancer Cells*, 1990;2:146-148
- 5 Saito I, Miyamura T, Ohbayashi A, Harada H, Katayama T, Kikuchi S, Watanabe Y, Koi S, Onji M, Ohta Y, Choo QL, Houghton M, Kuo G. Hepatitis C virus infection is associated with the development of hepatocellular carcinoma. *Proc Natl Acad Sci USA*, 1990;87:6547-6549
- 6 Bressac B, Kew M, Wands J, Ozturk M. Selective G to T mutations of *p53* gene in hepatocellular carcinoma from southern Africa. *Nature*, 1991;350:429-431
- 7 Hsu IC, Metcalf RA, Sun T, Welsh JA, Wang NJ, Harris CC. Mutational hotspot in the *p53* gene in human hepatocellular carcinomas. *Nature*, 1991;350:427-428
- 8 Scorsone KA, Zhou YZ, Butel JS, Slagle BL. *p53* mutations cluster at codon 249 in hepatitis B virus-positive hepatocellular carcinomas from China. *Cancer Res*, 1992;52:1635-1638
- 9 Bressac B, Galvin KM, Liang TJ, Isselbacher KJ, Wands JR, Ozturk M. Abnormal structure and expression of *p53* gene in human hepatocellular carcinoma. *Proc Natl Acad Sci USA*, 1990;87:1973-1977
- 10 Nigro JM, Baker SJ, Preisinger AC, Jessup JM, Hostetter R, Cleary K, Bigner S, Davidson N, Baylin S, Devilee P, Glover T, Collins F, Weston A, Modali R, Harris C, Vogelstein B. Mutations in the *p53* gene occur in diverse human tumor types. *Nature*, 1989;342:705-708
- 11 Smith SA, Easton DF, Evans DGR, Ponder BAJ. Allele losses in the region 17q12-21 in familial breast and ovarian cancer involve the wild-type chromosome. *Nature Genet*, 1992;2:128-131
- 12 Piao Z, Kim H, Jeon B, Lee WJ, Park C. Relationships between loss of heterozygosity of tumor suppressor genes and histologic differentiation in hepatocellular carcinoma. *Cancer*, 1997;80:865-872
- 13 Gudmundsson J, Johannesdottir G, Bergthorsson JT, Arason A, Ingvarsson S, Egilsson V. Different tumor types from BRCA2 carriers show wild-type chromosome deletions on 13q12-13. *Cancer Res*, 1995;55:4830-4832
- 14 Rajan JV, Marquis ST, Gardner HP, Chodosh LA. Developmental expression of BRCA2 colocalizes with BRCA1 and is associated with proliferation and differentiation in multiple tissues. *Dev Biol*, 1997;184:385-401
- 15 Katagiri T, Nakamura Y, Miki Y. Mutations in the BRCA2 gene in hepatocellular carcinomas. *Cancer Res*, 1996;56:4575-4577
- 16 Wang HP, Rogler CE. Deletion in human chromosome arms 11p and 13q in primary hepatocellular carcinomas. *Cytogenet Cell Genet*, 1988;48:72-78
- 17 Hsia CC, Di Bisceglie AM, Kleiner DE Jr., Farshid M, Tabor E. RB tumor suppressor gene expression in hepatocellular carcinomas from patients infected with the hepatitis B virus. *J Med Virol*, 1994;44:67-73
- 18 Murakami Y, Hayashi K, Hirohashi S, Sekiya T. Aberrations of the tumor suppressor *p53* and retinoblastoma genes in human hepatocellular carcinomas. *Cancer Res*, 1991;51:5520-5525
- 19 Evans RM, Hollenberg SM. Zinc fingers: guilt by association. *Cell*, 1988;52:1-3
- 20 Menke AL, Shvarts A, Riteco N, Van Ham RCA, Van Der Eb AJ, Jochemsen AG. Wilms' tumor 1-Kts isoforms induce *p53* independent apoptosis that can be partially rescued by expression of the epidermal growth factor receptor or the insulin receptor. *Cancer Res*, 1997;57:1353-1363
- 21 Shimoyama Y, Hirohashi S, Hirano S, Noguchi M, Shimosato Y, Takeichi M, Abe O. Cadherin cell adhesion molecules in human epithelial tissues and carcinomas. *Cancer Res*, 1989;49:2128-2133
- 22 Takeichi M. Cadherins: a molecular family important in selective cell cell adhesion. *Ann Rev Biochem*, 1990;59:237-252
- 23 Behrens J, Mareel MM, Van Roy FM, Birchmeier B. Dissecting tumor cell invasion: epithelial cells acquire invasive properties after the loss of uvomorulin-mediated cell-cell adhesion. *J Cell Biol*, 1989;108:2434-2447
- 24 Nagao T, Inoue S, Yoshimi F, Sodeyama M, Omori Y, Mizuta T, Kawano N, Morioka Y. Postoperative recurrence of hepatocellular carcinoma. *Ann Surg*, 1990;211:28-33
- 25 Slagle BL, Zhou YZ, Birchmeier W, Scorsone KA. Deletion of the E-cadherin gene in hepatitis B virus-positive Chinese hepatocellular carcinomas. *Hepatology*, 1993;18:757-762
- 26 Tsuda H, Zhang W, Shimosato Y, Yokota J, Terada M, Sugimura T, Miyamura T, Hirohashi S. Allele loss on chromosome 16 associated with progression of human hepatocellular carcinoma. *Proc Natl Acad Sci USA*, 1990;87:6791-6794
- 27 Weissbach J, Gyapay G, Dib C, Vignal A, Morissette J, Millasseau P, Vaysseix G, Lathrop M. A second-generation linkage map of the human genome. *Nature*, 1992;359:794-801
- 28 Miller S, Dykes D, Polesky H. A simple salting out procedure for extracting DNA from human nucleated cells. *Nuc Acids Res*, 1988;16:1215
- 29 Oda T, Tsuda H, Scarpa A, Sakamoto M, Hirohashi S. *p53* gene mutation spectrum in hepatocellular carcinoma. *Cancer Res*, 1992;52:6358-6364
- 30 Fujimoto Y, Hampton LL, Wirth PJ, Wang NJ, Xie JP, Thorngeston SS. Alterations of tumor suppressor genes and allelic losses in human hepatocellular carcinomas in China. *Cancer Res*, 1994;54:281-285
- 31 Slagle BL, Zhou YZ, Butel JS. Hepatitis B virus integration event in human chromosome 17p near the *p53* gene identifies the region of the chromosome commonly deleted in virus positive hepatocellular carcinomas. *Cancer Res*, 1991;51:49-54
- 32 Wang XW, Forrester K, Yeh H, Feitelson MA, Gu JR, Harris CC. Hepatitis B virus X protein inhibits *p53* sequence-specific DNA binding, transcriptional activity, and association with transcription factor ERCC3. *Proc Natl Acad Sci USA*, 1994;91:2230-2234
- 33 Kirby GM, Batist G, Fotouhi Ardakani N, Nakazawa H, Yamasaki H, Kew M, Cameron RG, Alaoui-Jamali MA. Allele-specific PCR analysis of *p53* codon 249 AGT transversion in liver tissues from patients with viral hepatitis. *Int J Cancer*, 1996;68:21-25

- 34 Hollstein M, Sidransky D, Vogelstein B, Harris CC. *p53* mutations in human cancers. *Science*, 1991;253:49-53
- 35 Kapelner SN, Turner RT, Sarkar G, Bolander ME. Deletion mutation can be an unsuspected gel artifact. *Biotechniques*, 1994;17:64-66
- 36 Walker GJ, Hayward NK, Falvey S, Graham W, Cooksley WGE. Loss of somatic heterozygosity in hepatocellular carcinoma. *Cancer Res*, 1991;51:4367-4370
- 37 Yumoto Y, Hanafusa T, Hada H, Morita T, Ooguchi S, Shinji N, Mitani T, Hamaya K, Koide N, Tsuji T. Loss of heterozygosity and analysis of mutation of *p53* in hepatocellular carcinoma. *J Gastroenterol Hepatol*, 1995;10:179-185
- 38 Gao X, Zacharek A, Salkowski A, Grignon DJ, Sakr W, Porter AT, Honn KV. Loss of heterozygosity of the *BRCA1* and other loci on chromosome 17q in human prostate cancer. *Cancer Res*, 1995;55:1002-1005
- 39 Kazachkov Y, Yoffe B, Khaoustov VI, Solomon H, Klintmalm GB, Tabor E. Microsatellite instability in human hepatocellular carcinoma: relationship to *p53* abnormalities. *Liver*, 1998;18:156-161
- 40 Salvucci M, Lemoine A, Azoulay D, Sebah M, Bismuth H, Reyns M, May E, Debuire B. Frequent microsatellite instability in post hepatitis B viral cirrhosis. *Oncogene*, 1999;13:2681-2685
- 41 Li C, Larsson C, Futreal A, Lancaster J, Phelan C, Aspenblad U, Sundelin B, Liu Y, Ekman P, Auer G, Bergerheim USR. Identification of two distinct deleted regions on chromosome 13 in prostate cancer. *Oncogene*, 1998;16:481-487
- 42 Butel JS, Lee TH, Slagle BL. Is the DNA repair system involved in hepatitis B-virus mediated hepatocellular carcinogenesis. *Trends Microbiol*, 1996;4:119-124
- 43 Futreal PA, Barrett JC, Wiseman RW. An *ALU* polymorphism intragenic to the *TP53* gene. *Nuc Acids Res*, 1991;19:6977
- 44 Bowcock A, Osborne Lawrence S, Barnes R, Chakravarti A, Washinton S, Dunn C. Microsatellite polymorphism linkage map of human chromosome 13q. *Genomics*, 1993;15:376-386
- 45 Fletjer WL, Kukowska-latallo JF, Kiouisis S, Chandrasakharappa SC, King SE, Chamberlain JS. Tetranucleotide repeat polymorphism at D17S846 maps within 40kb of GAS at 17q12.22. *Hum Molec Genet*, 1993;2:1
- 46 Anderson LA, Friedman L, Osborne Lawrence S, Lynch E, Weissenbach J, Bowcock A, King MC. High density genetic map of the *BRCA1* region of chromosome 17q12 q21. *Genomics*, 1993;17:618-623
- 47 Haber DA, Buckler AJ, Glaser T, Call KM, Pelletier J, Sohn RL, Douglass EC, Housman DE. An internal deletion within an 11p13 Zinc finger gene contributes to the development of Wilm's tumor. *Cell*, 1990;61:1257-1269
- 48 Henson JW, Schnitker BL, Correa KM, von Deimling A, Fassbender F, Xu HJ, Benedict WF, Yandell DW, Louis DN. The retinoblastoma gene is involved in malignant progression of astrocytomas. *Ann Neurol*, 1994;36:714-721
- 49 Yandell DW, Dryja TP. Detection of DNA sequence polymorphisms by enzymatic amplification and direct genomic sequencing. *Am J Hum Genet*, 1989;45:547-555
- 50 Petrukhin KE, Speer MC, Cayanis E, Bonaldo MF, Tantravahi U, Soares MB, Fischer SG, Warburton D, Gilliam C, Ott J. A microsatellite genetic linkage map of human chromosome 13. *Genomics*, 1993;15:76-85
- 51 Thompson AD, Shen Y, Holman K, Sutherland GR, Callen DF, Richards RI. Isolation and characterization of (AC)_n microsatellite genetic markers from human chromosome 16. *Genomics*, 1992;13:402-408
- 52 Weber JL, Kwitek AE, May PE. Dinucleotide repeat polymorphisms at the D16S260, D16S261, D16S265, D16S266, and D16S267 loci. *Nuc Acids Res*, 1990;18:4034

Edited by MA Jing-Yun

Protective effect of Irsogladine on monochloramine induced gastric mucosal lesions in rats: a comparative study with rebamipide

H Yamamoto, M Umeda, H Mizoguchi, S Kato and K Takeuchi

Subject headings irsogladine; rebamipide; monochloramine; gastric mucosal lesions; rats; comparative study

Abstract

AIM To examine the effect of irsogladine, a novel antiulcer drug, on the mucosal ulcerogenic response to monochloramine (NH_2Cl) in rat stomach, in comparison with rebamipide, another antiulcer drug with cytoprotective activity.

METHODS AND RESULTS Oral administration of NH_2Cl (120 mM) produced severe hemorrhagic lesions in unanesthetized rat stomachs. Both irsogladine (1 mg/kg-10 mg/kg, po) and rebamipide (30 mg/kg-100 mg/kg, po) dose-dependently prevented the development of these lesions in response to NH_2Cl , the effect of irsogladine was significant at 3 mg/kg or greater, and that of rebamipide only at 100 mg/kg. The protective effect of irsogladine on NH_2Cl -induced gastric lesions was significantly reduced by N^G -nitro-L-arginine methyl ester (L-NAME) but not by indomethacin, while that of rebamipide was significantly mitigated by indomethacin but not by L-NAME. Topical application of NH_2Cl (20mM) caused a marked reduction of potential difference (PD) in *ex-vivo* stomachs. This PD reduction was not affected by mucosal application of irsogladine, but significantly prevented by rebamipide. The mucosal exposure to NH_4OH (120 mM) also caused a marked PD reduction in the ischemic stomach (bleeding from the carotid artery),

resulting in gastric lesions. These ulcerogenic and PD responses caused by NH_4OH plus ischemia were also significantly mitigated by rebamipide, in an indomethacin-sensitive manner, while irsogladine potently prevented such lesions without affecting the PD response, in a L-NAME-sensitive manner.

CONCLUSION These results suggest that ① NH_2Cl generated either exogenously or endogenously damages the gastric mucosa, ② both irsogladine and rebamipide protect the stomach against injury caused by NH_2Cl , and ③ the mechanism underlying the protective action of irsogladine is partly mediated by endogenous nitric oxide, while that of rebamipide is in part mediated by endogenous prostaglandins.

INTRODUCTION

Helicobacter pylori, recognized as the major cause of gastritis and peptic ulcer diseases^[1-3] has a high activity of urease, resulting in a high concentration of ammonia (NH_4OH) in the stomach of infected patients^[3]. Since *H. pylori* associated chronic active gastritis is characterized by an invasion of neutrophils in the gastric mucosa^[1,2,4] and since neutrophils utilize the H_2O_2 -myeloperoxidase-halide system to generate an oxidant capable of destroying a variety of mammalian cell targets as well as microorganisms^[5,6], it is assumed that neutrophil-derived hypochlorous acid (HClO) interacts with NH_4OH to generate cytotoxic monochloramine (NH_2Cl)^[7,8]. Indeed, it has been shown that NH_2Cl plays a role in the pathogenesis of NH_4OH -induced gastric lesions in rats^[9,10]. We have also reported previously that both endogenous and exogenous NH_2Cl damaged the gastric mucosa at much lower concentrations than NH_4OH ^[11,12].

Irsogladine, a novel antiulcer drug [2,4-diamino-6-(2,5-dichlorophenyl)-s-triazine maleate], has been shown to not only prevent gastric mucosal lesions in a wide variety of experimental models but show the healing promoting action of gastric ulcers as well, without any suppression of gastric secretion^[13-15]. These

Department of Pharmacology and Experimental Therapeutics, Kyoto Pharmaceutical University, Misasagi, Yamashina, Kyoto 607-8414, Japan

Hedeichiro Yamamoto, male born on 1975-07-10 in Osaka City, Japan, graduated from Kyoto Pharmaceutical University in 1998, now a graduated student of Kyoto Pharmaceutical University, majoring in gastrointestinal pharmacology and physiology and having 6 papers published.

This work was supported in part by a grant from Nippon Shinyaku Co. Ltd.

Correspondence to: Shinichi Kato, Ph.D., Department of Pharmacology and Experimental Therapeutics, Kyoto Pharmaceutical University, Misasagi, Yamashina, Kyoto 607-8414, Japan
Tel. +81-75-595-4680, Fax. +81-75-595-4774
Email: skato@mb.kyoto-phu.ac.jp

Received 1999-08-31

effects of irsogladine may be accounted for by cytoprotective activity, yet the detailed mechanism is not fully understood. Thus, it is of interest to test whether this agent has any prophylactic action against NH_2Cl -induced gastric lesions.

In the present study, we examined the effects of irsogladine on the mucosal ulcerogenic response induced by NH_2Cl , either administered exogenously or occurring endogenously, and compared those with the effects of another cytoprotective drug, rebamipide. We also investigated the underlying mechanism of their protection, especially in relation to endogenous prostaglandins (PGs) and nitric oxide (NO).

MATERIALS AND METHODS

Animals

Male Sprague-Dawley rats (200 g-240 g in weight, Nippon Charles River, Shizuoka, Japan) were used in all experiments. The animals, kept in separate cages with raised mesh bottoms, were deprived of food but allowed free access to tap water for 18 hours prior to the experiments. Studies were carried out using four to eight rats under either conscious or anesthetized conditions induced by urethane (1.25 g/kg, ip). All experimental procedures described here were approved by the Experimental Animal Research Committee of the Kyoto Pharmaceutical University.

General procedures

The experiments were classified into roughly two studies: one was to investigate the effects of irsogladine and rebamipide on gastric ulcerogenic response to exogenously administered NH_2Cl in unanesthetized rats, and the other was to investigate their effects on gastric ulcerogenic response to NH_4OH in anesthetized rats subjected to ischemia. In the latter situation, it is assumed that NH_2Cl is generated endogenously from interaction of NH_4OH with neutrophil-derived $\text{HClO}^{[10]}$.

Induction of gastric lesions induced by NH_2Cl

The effects of irsogladine and rebamipide on gastric mucosal ulcerogenic response induced by exogenous NH_2Cl . The animals were administered 1 ml of NH_2Cl (120 mM)-po by esophageal intubation. The solution of NH_2Cl was prepared by mixing NH_4OH (240 mM) and HClO (240 mM) in a test tube, immediately before the administration. The animals were sacrificed 1 hour after the administration of NH_2Cl , and the stomachs were removed, inflated by injecting 8 mL of 2% formalin and immersed in 2% formalin for 10 min to fix the gastric wall, and opened along the greater curvature. The area (mm^2) of hemorrhagic lesions was measured under a dissecting microscope with a square grid ($\times 10$).

The person measuring the lesions did not know the treatment given to the animals. These procedures were used in all the subsequent studies for evaluating macroscopical lesions. Irsogladine (1, 3 and 10 mg/kg) and rebamipide (30 and 100 mg/kg) were administered po 30 min before NH_2Cl treatment. In some cases, indomethacin (10 mg/kg, sc) or L-NAME (10 mg/kg, iv) was given 60 min or 40 min before NH_2Cl treatment.

Measurement of transmucosal potential difference

Transmucosal potential difference (PD) was measured in chambered stomachs of anesthetized rats as previously described^[15]. Briefly, a rat stomach was mounted on an *ex-vivo* chamber (area exposed 3.14 cm^2) and perfused at a flow rate of 1 mL/min with saline (154 mM-NaCl). PD was determined using two agar bridges, one positioned in the chamber and the other in the abdominal cavity, and monitored continuously on a recorder (U-228, Tokai-Irika, Tokyo, Japan). Approximately 1 h after PD was stabilized, the perfusion system was interrupted and the solution in the chamber was withdrawn, and the mucosa was exposed to 1 mL carboxymethyl cellulose (CMC) solution (control group), 20 min later followed by 1 mL NH_2Cl (20 mM, the final concentration is 10 mM) for 10 min. After application of NH_2Cl , the mucosa was rinsed with saline, another 2 mL saline was instilled, and the perfusion system was resumed. Irsogladine (3 mg/kg) or rebamipide (100 mg/kg) was applied to the chamber for 30 min in place of CMC solution, starting 20 min before NH_2Cl treatment. In a separate experiment, the animals were subjected to ischemia by bleeding from the carotid artery (1 mL/100 g body weight), then the mucosa was exposed to 1 mL of CMC, 20 min later followed by 1 mL of NH_4OH (120 mM, the final concentration is 60 mM) for 1 hour. At the end of the experiment, the mucosa was excised, and the area (mm^2) of hemorrhagic lesions was measured as described as above. Irsogladine (3 mg/kg) or rebamipide (100 mg/kg) was applied to the chamber 10 min before the onset of ischemia plus NH_4OH treatment. Control animals received CMC as the vehicle. In some cases, indomethacin (10 mg/kg) was given sc 30 min before rebamipide, while L-NAME (10 mg/kg) was given iv 10 min before irsogladine treatment.

Preparation of drugs

Drugs used in this study were urethane (Tokyo Kasei, Tokyo, Japan), irsogladine (Nihon-Shinyaku Co., Kyoto, Japan), rebamipide (Otsuka Pharmaceutical Co., Tokushima, Japan), indomethacin and L-NAME (Sigma Chemicals, St. Louis, MO, USA). Indomethacin was suspended in

saline with a drop of Tween 80 (Wako, Osaka, Japan), while L-NAME was dissolved in saline. Other drugs were suspended with 0.5% CMC solution. Each drug was prepared immediately before use and administered *po* in a volume of 0.5 mL/100 g body weight or *iv* in a volume of 0.1 mL/100 g body weight or applied topically to the chamber in a volume of 1 mL/stomach.

Statistics

Data are presented as the means \pm SE from 4 to 8 rats per group. Statistically analyses were performed using two-tailed Student's *t* test or Dunnett's multiple comparison test, and $P < 0.05$ values were regarded as significant.

RESULTS

Effects of irsogladine on gastric ulcerogenic response to NH₂Cl

Intragastric administration of NH₂Cl caused severe band-like hemorrhagic lesions in the gastric mucosa, the lesion score being $138.0 \text{ mm}^2 \pm 19.0 \text{ mm}^2$. Pretreatment of the animals with irsogladine (1, 3 and 10 mg/kg, *po*) significantly reduced the severity of gastric lesions in response to NH₂Cl in a dose-dependent manner. The degree of inhibition was 35.1%, 86.3% and 83.3%, respectively (Figure 1). Rebamipide (30 and 100 mg/kg, *po*) also lowered the severity of gastric lesions induced by NH₂Cl, but the degree of inhibition at 100 mg/kg was 59.3%, which was less than that observed by irsogladine at 3 mg/kg.

Effects of L-NAME and indomethacin on protective action of irsogladine against NH₂Cl-induced gastric lesions

The severity of gastric lesions induced by NH₂Cl was not affected by prior administration of either indomethacin (5 mg/kg, *sc*) or L-NAME (10 mg/kg, *iv*), the lesion score being $146.8 \text{ mm}^2 \pm 9.8 \text{ mm}^2$ or $135.6 \text{ mm}^2 \pm 7.0 \text{ mm}^2$, respectively (Figure 2). However, the protective action of irsogladine (3 mg/kg, *po*) against NH₂Cl-induced gastric lesions was significantly mitigated by prior administration of L-NAME but not indomethacin; the lesion score in the presence of L-NAME was $72.8 \text{ mm}^2 \pm 9.1 \text{ mm}^2$, which was significantly greater than that observed in the absence of L-NAME ($19.8 \text{ mm}^2 \pm 3.1 \text{ mm}^2$). By contrast, indomethacin but not L-NAME significantly antagonized the protective action of rebamipide (100 mg/kg, *po*) against these lesions.

Effects of irsogladine on mucosal PD response induced by NH₂Cl

Normal stomachs mounted on the chamber and perfused with saline generated a stable PD of -30 to -38 mV (mucosa negative), and the values

remained relatively unchanged during a 2-hour test period. Mucosal exposure to NH₂Cl (10 mM) caused a marked reduction of PD to $60.0\% \pm 6.2\%$ of basal values within 10 min, and the PD remained low for 1 hour thereafter (Figure 3). The PD reduction in response to NH₂Cl was not affected by prior exposure of the mucosa to irsogladine (3 mg/kg). However, the reduced PD response to NH₂Cl was significantly mitigated when the mucosa was pre-exposed to rebamipide (100 mg/kg) for 30 min; the PD reduced to $57.7\% \pm 3.1\%$ of basal values 10 min later, which was significantly less as compared with that ($60.0\% \pm 6.2\%$ of basal values) in control rats.

Effects of irsogladine on mucosal ulcerogenic and PD responses induced by NH₄OH under ischemic conditions

To confirm the protective action of irsogladine and rebamipide on NH₂Cl-induced gastric toxicity, we tested the effects of these drugs on the mucosal ulcerogenic and PD responses induced by endogenously generated NH₂Cl by application of a low concentration of NH₄OH (60 mM) in the ischemic stomach^[9]. As shown in Figure 4, topical application of NH₄OH at 60 mM produced a persistent reduction of PD in the stomach made ischemic by bleeding; the PD was reduced to $42.6\% \pm 6.2\%$ of basal values within 10 min and remained low thereafter. This concentration of NH₄OH did not have any effect on PD in normal stomachs without subjecting to ischemia (not shown). The reduced PD response to NH₄OH plus ischemia was not affected by prior exposure of the mucosa to irsogladine (3 mg/kg), in the absence or presence of L-NAME. By contrast, rebamipide (100 mg/kg)-pre-exposed to the mucosa significantly attenuated the PD reduction in response to NH₄OH plus ischemia. In these animals the recovery of PD was also significantly expedited, and the PD almost completely normalized within 60 min after NH₄OH plus ischemia. In addition, the preventive effect of rebamipide on the PD response to NH₄OH plus ischemia was also significantly antagonized in the presence of indomethacin.

On the other hand, the mucosal exposure to NH₄OH in the ischemic stomachs resulted in severe hemorrhagic lesions within 1 hour, the lesion score being $53.6 \text{ mm}^2 \pm 12.2 \text{ mm}^2$ (Figure 5). The development of gastric lesions induced by NH₄OH plus ischemia was significantly prevented by irsogladine (3 mg/kg) as well as rebamipide (100 mg/kg), the inhibition being 79.5% and 82.3%, respectively. The protective effect of irsogladine or rebamipide against NH₄OH plus ischemia-induced gastric lesions was significantly antagonized by L-NAME or indomethacin, respectively.

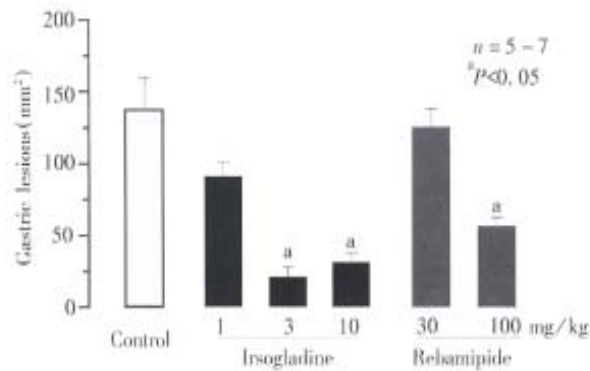


Figure 1 Effects of irsogladine and rebamipide on gastric lesions induced by NH_2Cl in rats. The animals were given NH_2Cl (120 mM; 5 mL/kg) po, and sacrificed 1 hour later. Irsogladine (1 mg/kg-10 mg/kg) or rebamipide (30, 100 mg/kg) was given po 30 min before administration of NH_2Cl . Data are presented as the mean \pm SE from 5-7 rats. *Statistically significant difference from control ($P < 0.05$).

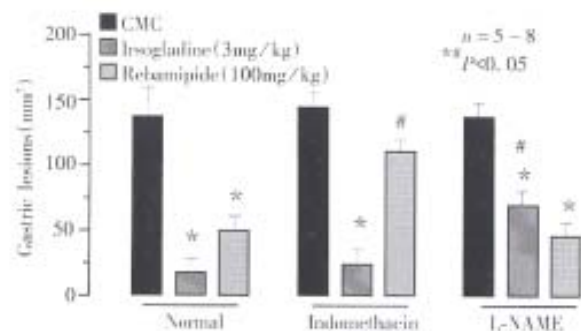


Figure 2 Effects of indomethacin and L-NAME on the mucosal protective action of irsogladine and rebamipide against NH_2Cl -induced gastric lesions in rats. The animals were administered po with 1 mL of NH_2Cl (120 mM), and sacrificed 1 hour later. Irsogladine (3 mg/kg) or rebamipide (100 mg/kg) was given po 30 min before NH_2Cl treatment. Indomethacin (5 mg/kg, sc) or L-NAME (10 mg/kg, iv) was given 30 or 10 min before the above agents. Data are presented as the mean \pm SE from 5-8 rats. Statistically significant difference at $P < 0.05$; *from the corresponding control (CMC); #from the corresponding value in normal group.

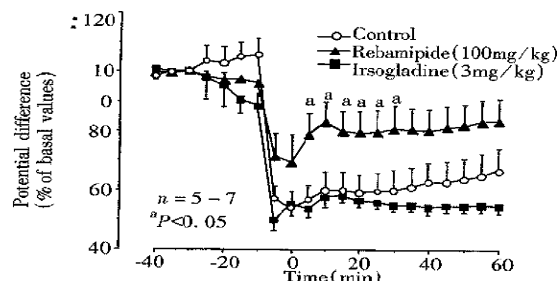


Figure 3 Effects of irsogladine and rebamipide on changes in transmucosal PD in response to NH_2Cl in anesthetized rat stomachs. The stomach was mounted on an ex-vivo chamber, and NH_2Cl (20 mM; 1 mL) was applied topically to the stomach for 10 min. Irsogladine (3 mg/kg) or rebamipide (100 mg/kg) was applied to the chamber for 30 min, starting 20 min before exposure to NH_2Cl . Data are presented as the mean \pm SE of value determined every 5 min from 5-7 rats. *Statistically significant difference from control, $P < 0.05$.

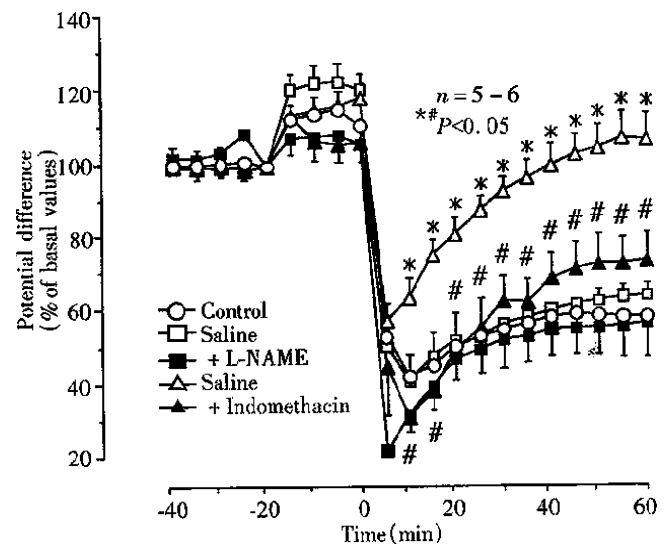


Figure 4 Effects of irsogladine and rebamipide on changes in transmucosal PD in response to NH_4OH in rat stomachs under ischemic conditions. The stomach mounted on a ex-vivo chamber was subjected to ischemia by bleeding from the carotid artery (1 mL/100 g body wt), and then exposed to NH_4OH (120 mM; 1 mL) for 1 h thereafter. Irsogladine (3 mg/kg) or rebamipide (100 mg/kg) was applied to the chamber 20 min before the onset of ischemia and NH_4OH treatment. Indomethacin (5 mg/kg, sc) or L-NAME (10 mg/kg, iv) was given 30 or 10 min before the above agents. Data are presented as the mean \pm SE of values determined every 5 min from 5-6 rats. Statistically significant difference at $P < 0.05$; *from control; #from vehicle.

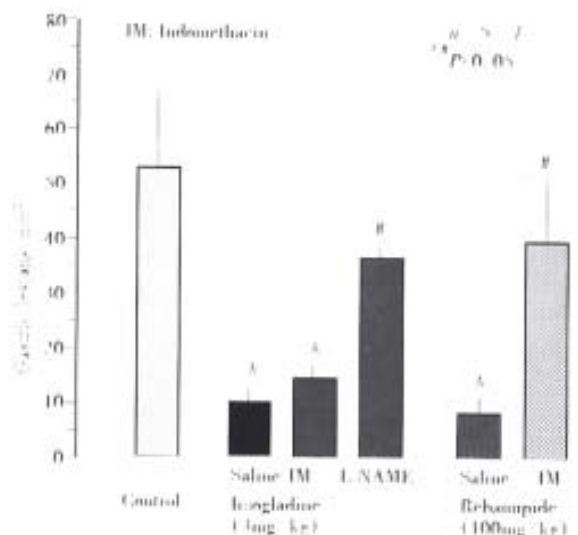


Figure 5 Effects of irsogladine and rebamipide on gastric mucosal lesions induced by NH_4OH in anesthetized rat stomachs under ischemic conditions. The stomach mounted on an ex-vivo chamber was subjected to ischemia by bleeding from the carotid artery (1 mL/100 g body weight), and then exposed to NH_4OH (120 mM) for 1 h thereafter. Irsogladine (3 mg/kg) or rebamipide (100 mg/kg) was applied to the chamber 20 min before the onset of ischemia and NH_4OH treatment. Indomethacin (5 mg/kg, sc) or L-NAME (10 mg/kg, iv) was given 30 or 10 min before the above agents. Data are presented as the mean \pm SE from 4-6 rats. Statistically significant difference at $P < 0.05$; *from control; #from vehicle.

DISCUSSION

The present study demonstrated that irsogladine, a novel antiulcer drug, conferred a protection against gastric damage induced in rat stomachs by NH_2Cl , either given exogenously or occurred endogenously. We also found that rebamipide, another antiulcer drug, showed similar protection against such damage, although the effect was less potent than that of irsogladine. In addition, the present results suggest that the mechanisms underlying their protection are different; the protective action of irsogladine is partly mediated by endogenous NO, while that of rebamipide is accounted for by endogenous PGs as well as a radical scavenging action.

H. pylori has a high urease enzyme activity, resulting in an abnormally high concentration of ammonia (NH_4OH) in the stomach of infected patients^[3]. It is also known that NH_4OH interacts with neutrophil-derived HClO to generate cytotoxic NH_2Cl , a powerful oxidant capable of destroying a variety of micro-organisms as well as mammalian cell targets^[4,7]. Murakami *et al.*^[17] demonstrated in rats that NH_4OH -induced gastric mucosal lesions were significantly inhibited by taurine, a scavenger of HClO , suggesting a pathogenic role of NH_2Cl in the development of such lesions. We also found previously that the mixture of low concentration of NH_4OH and HClO , which did not have any gastric mucosal toxicity by each alone, caused severe lesions in the rat gastric mucosa under unanesthetized conditions^[11,12]. In addition, we reported that the gastric lesions induced by endogenously generated NH_2Cl by a low concentration of NH_4OH plus ischemia were totally prevented by taurine in anesthetized *ex-vivo* stomachs^[11,12]. It is known that ischemia activates xanthine oxidase, which is responsible for the production of reactive oxygen metabolites such as H_2O_2 , and that the generation of HClO by neutrophils is dependent on the quantity of H_2O_2 produced^[4,5]. It may therefore be assumed that NH_4OH even at low concentrations produces NH_2Cl by interaction with HClO in the ischemic stomach, resulting in damage to the mucosa.

The gastric lesions induced by oral administration of NH_2Cl were significantly prevented by irsogladine as well as rebamipide in a dose-dependent manner, although the effect of irsogladine was more potent than that of rebamipide. Similar results were obtained by these drugs against gastric lesions induced by NH_4OH plus ischemia, where NH_2Cl is assumed to be generated endogenously from interaction of NH_4OH with neutrophil-derived HClO ^[10]. These results clearly showed that both irsogladine and rebamipide conferred a protection against damage induced by

NH_2Cl , either administered exogenously or occurring endogenously. However, the mechanisms underlying gastric protection seemed to be different between these two drugs. The protective action of irsogladine was significantly attenuated by pretreatment with L-NAME but not indomethacin, while that of rebamipide was attenuated by indomethacin but not L-NAME. These results suggest that the protective action of irsogladine and rebamipide may be mediated by endogenous NO and PGs, respectively. Moreover, these drugs caused different effects on the PD response induced by NH_2Cl or NH_4OH plus ischemia. Rebamipide significantly prevented the PD reduction in response to these treatments while irsogladine had no effect on such PD responses. It is considered that gastric PD is one of the indicators for the integrity of the gastric mucosa, including the development of mucosal injury as well as the recovery from injury^[18,19]. From the present results, it is suggested that irsogladine does not inhibit the onset of injury caused by NH_2Cl but prevents the ultimate generation of gastric damage, probably by preventing the later extension of injury, while rebamipide reduced the gastric ulcerogenic response by inhibiting the initial irritating action of NH_2Cl on the mucosa.

The local release of NO regulates the gastric mucosal microcirculation and maintains the mucosal integrity in collaboration with PGs and sensory neurons^[20,21]. At present, the mechanism by which irsogladine stimulates the release of NO in the gastric mucosa remains unknown. We previously reported that mucosal application of NO donor prevented the development of gastric lesions induced by NH_2Cl without any influence on the PD responses^[11,12]. These data are in agreement with the present findings that irsogladine reduced the severity of NH_2Cl -induced gastric lesions but had no effect on the reduced PD response. On the other hand, it has been shown that rebamipide protects the gastric mucosa from various necrotizing agents by increasing PG biosynthesis in the mucosa and scavenging free radicals^[22-24]. Exogenous PGE_2 has also been shown to inhibit gastric lesions in response to NH_2Cl or NH_4OH plus ischemia^[11]. These data support the present observation that rebamipide protected the stomach against NH_2Cl -induced damage, in an indomethacin-sensitive manner. It should also be noted in the present study that rebamipide prevented the PD reduction in response to NH_2Cl or NH_4OH plus ischemia. Since taurine, a scavenger of HClO , markedly suppressed the PD reduction caused by NH_2Cl ^[11,12], it is likely that rebamipide may prevent gastric ulcerogenic and PD responses to NH_2Cl through a radical scavenging

action, in addition to mediation by endogenous PGs.

In conclusion, the present results taken together suggest that NH_2Cl generated either endogenously or exogenously, damages the gastric mucosa at a low concentration. Gastric mucosal lesions caused by NH_2Cl was prevented by both irsogladine and rebamipide, although the former action was more potent than the latter. Although the exact mechanisms underlying gastroprotection afforded by irsogladine and rebamipide remain unknown, it is assumed that their mechanisms are different; the effect of irsogladine is mediated at least partly by endogenous NO, while that of rebamipide is attributable to endogenous PGs as well as its radical scavenging action. Since an important feature of *H. pylori* infection is neutrophil infiltration in the gastric mucosa^[1,2], it is possible that NH_2Cl is formed in the inflamed gastric mucosa, where neutrophil and *H. pylori* are located in juxtaposition. Thus, the present study also suggests that irsogladine may have therapeutic potential in the prevention and/or treatment of gastric mucosal damage related to *H. pylori*.

REFERENCES

- Marshall BJ, Warren JR. Unidentified curved bacilli on gastric epithelium in active chronic gastritis. *Lancet*, 1983;1:1273-1275
- Graham DY. Campylobacter pylori and peptic ulcer disease. *Gastroenterology*, 1989;96(Suppl):615-625
- Marshall BJ, Langton SR. Urea hydrolysis of patients with Campylobacter pyloridis infection. *Lancet*, 1983;1:965-966
- Whitehead R, Truelove SC, Gear MWL. The histological diagnosis of chronic gastritis in fibrotic gastroscopy biopsy specimens. *J Clin Pathol*, 1972;25:1-11
- Badwey JA, Karnovsky ML. Active oxygen species and the functions of phagocytic leukocytes. *Ann Rev Biochem*, 1980;46:695-726
- Klevanoff SJ. Oxygen metabolism and the toxic properties of phagocytes. *Ann Intern Med*, 1980;93:480-489
- Grisham MB, Jefferson MM, Thomas EL. Chlorination of endogenous amines by isolated neutrophil. Ammonia-dependent bactericidal, cytotoxic, and cytolytic activities of the chloramines. *J Biol Chem*, 1984;259:10404-10413
- Grisham MB, Hernandez LA, Granger DN. Xanthine oxidase and neutrophil infiltration in intestinal ischemia. *Am J Physiol*, 1986; 251:G567-G574
- Murakami M, Asagoe K, Dekigai H, Kusaka S, Saita H, Kita T. Products of neutrophil metabolism increase ammonia induced gastric mucosal damage. *Dig Dis Sci*, 1995;40:268-273
- Dekigai H, Murakami M, Kita T. Mechanism of *Helicobacter pylori* associated gastric mucosal injury. *Dig Dis Sci*, 1995;40:1332-1339
- Nishiwaki H, Kato S, Takeuchi K. Irritant action of monochloramine in rat gastric mucosa. *Gen Pharmacol*, 1997;29:713-718
- Kato S, Nishiwaki H, Kanaka A, Takeuchi K. Mucosal ulcerogenic action of monochloramine in rat stomachs. *Dig Dis Sci*, 1977;42: 2156-2161
- Ueda F, Aratani S, Mimura K, Kimura K, Nomura A, Enomoto H. Effect of 2,4 diamino 6 (2,5-dichlorophenyl) s triazine maleate (MN-1695) on gastric ulcers and gastric secretion in experimental animals. *Arzneimittelforschung*, 1984;34P:474-477
- Ueda F, Aratani S, Mimura K, Kimura K, Nomura A, Enomoto H. Effect of 2,4²diamino 6 (2,5-dichlorophenyl) s triazine maleate (MN-1695) on gastric mucosal damage induced by various necrotizing agents in rats. *Arzneimittelforschung*, 1984;34:478-484
- Okabe S, Takeuchi K, Ishihara Y, Kunimi H. Effect of 2,4 diamino 6 (2,5 dichlorophenyl) s triazine maleate (MN-1695) on gastric secretion and on experimental gastric ulcers in rats. *Pharmacometrics*, 1984;24:683-689
- Takeuchi K, Ishihara Y, Okada M, Niida H, Okabe S. A continuous monitoring of mucosal integrity and secretory activity in rat stomach. A preparation using a lucite chamber. *Jpn J Pharmacol*, 1989;49:235-244
- Murakami M, Saita H, Teramoto S, Dekigai H, Asagoe K, Kusaka S, Kita T. Gastric ammonia has a potent ulcerogenic action on the rat stomach. *Gastroenterology*, 1993;105:1710-1715
- Ivy KJ, Den Besteubm L, Glifton JA. Effect of bile salts on ionic movement across the human gastric mucosa. *Gastroenterology*, 1970;59:683-690
- Svanes K, Ito S, Takeuchi K, Silen W. Restitution of the surface epithelium of the in vitro frog gastric mucosa after damage with hyperosmolar sodium chloride; morphologic and physiologic characteristic. *Gastroenterology*, 1982;82:1409-1426
- Whittle BJR, Lopez Belmonte J, Moncada S. Regulation of gastric mucosal integrity by endogenous nitric oxide; interactions with prostanoids and sensory neuropeptides in the rat. *Br J Pharmacol*, 1990;99:607-611
- Tepperman BL, Whittle BJR. Endogenous nitric oxide and sensory neuropeptides interact in the modulation of the rat gastric microcirculation. *Br J Pharmacol*, 1992;105:171-175
- Ishihara K, Komuro Y, Nishiyama N, Yamasaki K, Hotta K. Effect of rebamipide on mucus secretion by endogenous prostaglandin-independent mechanism in rat gastric mucosa. *Arzneimittelforschung*, 1992;42:1462-1466
- Yamasaki K, Kanbe T, Chijiwa T, Ishihara H, Morita S. Gastric mucosal protection by OPC-12759, a novel antiulcer compound in the rat. *Eur J Pharmacol*, 1987;142:23-29
- Yoshikawa T, Naito Y, Tanigawa T, Kondo M. Free radical scavenging activity of the novel anti ulcer agent rebamipide studied by electron spin resonance. *Arzneimittelforschung*, 1993;43:363-366

Edited by MA Jing-Yun

Proofread by MIAO Qi-Hong

Hepatocellular carcinoma in central Sydney: a 10 year review of patients seen in a medical oncology department

Desmond Yip¹, Michael Findlay², Michael Boyer¹ and Martin H. Tattersall³

Subject headings carcinoma, hepatocellular; liver neoplasms; survival/rate; Australia

Abstract

AIM To report a single Australian oncology unit's experience with the management of patients with hepatocellular carcinoma (HCC), in the context of a literature review of the current management issues.

METHODS Retrospective case record review of 76 patients with diagnosis of HCC referred to the unit between 1984 and 1995.

RESULTS Sixty-three patients had adequate records for analysis. Thirty-six (56%) were migrants with half from Southeast Asia. Twenty-four patients had a documented viral aetiology. Nine (14%) of 51 patients with pathological confirmation of HCC had normal alpha-fetoprotein levels. Median survival of the 20 patients managed palliatively was 5 weeks compared to 16 weeks for the cohort overall. Surgery in 16 patients rendered all initially disease free with a median survival of 88 weeks. Chemoembolisation induced tumor responses in 5 of the 11 patients so treated. Systemic chemotherapy and tamoxifen treatment caused tumor response in two of 12 and one of 25 respectively.

CONCLUSION Prolonged survival of patients with HCC depends on early detection of small tumors suitable for surgical resection. Other active treatments are palliative in intent and have limited success. In addition to tumor response and survival duration, the toxicities of

therapies and the overall quality of life of patients need to be considered as important outcomes. Viral hepatitis prevention and screening of individuals at risk are strategies that are important for HCC management in communities where the disease is endemic.

INTRODUCTION

Hepatocellular carcinoma (HCC) is the fourth most common cause of death from malignancy in the world and the third most common in men^[1]. High risk areas such as Asia and Africa are associated with endemic hepatitis B and C infections. In Australia HCC is still a relatively uncommon cancer as it is in most developed nations. In the state of New South Wales the incidence was 2.6 per 100 000 for males and 1.1 per 100 000 for females from 1985 to 1989. The incidence is significantly higher in male and female migrants from China, Taiwan and Vietnam^[2].

We reviewed all cases of HCC that were seen in the Department of Medical Oncology at Royal Prince Alfred Hospital a tertiary centre situated in central Sydney between January 1984 to December 1995. Patient demographics, presenting symptoms, disease stage, prognostic indicators as well as treatment and outcomes were determined.

METHOD

Using the Clinical Reporting System (CRS) database in the Department of Medical Oncology, the names of 76 patients with the diagnosis of HCC were obtained. The departmental files and the medical records were then examined and information collected using a proforma. Parameters collected included sex, age, nationality, clinical and pathological status, presenting symptoms, ECOG (Eastern Cooperative Oncology Group) performance status at time of initial contact, presence or absence of cirrhosis, documentation of possible etiological factors and alpha-fetoprotein (AFP) levels. Tumor response to therapy was recorded using WHO response criteria. Partial response was defined as a greater than 50% reduction in the sum of the products of the longest tumor dimension and its widest perpendicular, in

¹Department of Medical Oncology, Royal Prince Alfred Hospital, Camperdown, NSW, Australia

²Wellington Cancer Centre Private Bag 7902, Wellington, New Zealand
Email: michael.findlay@wnhealth.co.nz

³University of Sydney, Camperdown NSW, Australia
Dr. Desmond Yip, male, born on 1966-01-28 in Sydney, Australia. Graduated from Sydney University in 1989, trained in medical oncology, now working in clinical research with an interest in gastrointestinal malignancies and novel therapies. Currently a clinical research fellow, Department of Medical Oncology, Guy's Hospital, London, United Kingdom.

Correspondence to: Dr. Michael Findlay, Wellington Regional Oncology Unit, Wellington Hospital, Private Bag 7902, Wellington, New Zealand

Tel. +64-4 385 5999, Fax. +64-4 385 5984

Email: woncmf@wnhealth.co.nz

Received 1998-08-10

the absence of new lesions. Where disease was not measurable, changes in AFP level were monitored. Complete response was defined as no tumor evident on imaging plus normalisation of AFP if this was measured. Progressive disease was defined as 25% increase in measurable tumor size or sustained increase in AFP.

Survival time was measured from the date of diagnosis to the date of death determined where possible from the hospital records, contact with local doctors and computer search of the New South Wales Cancer Registry databases.

RESULTS

Seventy-six patients with a diagnosis of HCC were seen in the Department during this period. Of these, sixty-three patients had records that contained sufficient information for analysis.

Demographics

The mean age of the patients was 50 years (range 27-77) with 43 males and 20 females. Fifty-six percent of the patients were born overseas with over half of these born in Southeast Asia (Table 1).

Clinical characteristics

Of 57 patients where data on symptoms were available, thirteen (23%) patients were asymptomatic at the time of diagnosis. Three had an ECOG performance status of 4 (totally bedbound) and six a score of 3 (spending more than 50% of waking hours in bed). The most common presenting symptom was pain in 33 (58%) followed by weight loss in 27 (47%) and abdominal distension in 17 (30%). Sixteen (28%) patients presented with jaundice. The median duration of symptoms before presentation was two months, ranging from immediately prior to presentation up to 50 weeks.

The most common documented aetiological factor for hepatocellular carcinoma in this series was hepatitis B infection in 21 (33%) patients. Five patients had hepatitis C infection, and three of these were co-infected with both hepatitis B and C. Routine testing for hepatitis C at Royal Prince Alfred Hospital only became available from mid 1989 and retrospective testing was not done in the cohort, which may explain the relatively low infection rate in this series. Five (22%) of the 23 patients with viral hepatitis were Australian born. Of the three patients who had cirrhosis secondary to hemochromatosis all had alcohol as a cofactor. Alcohol was a cofactor in 5 (19%) of the 26 Australian born patients and five (14%) of the overseas born patients. Twenty-three patients had no apparent causative factor. One patient had a past history of low grade lymphoma and another hydatid liver disease. These causative factors are listed in Table 2.

Pathological confirmation of diagnosis was

obtained in 51 patients (81%) mainly by fine needle aspiration biopsy. In the remainder, a clinical diagnosis was based on radiological appearance on CT scan or hepatic angiogram and a raised serum AFP level. There were nine patients (14%) with pathological confirmation of HCC who had normal AFP levels at presentation. The initial levels ranged from 0 to 36000 IU. Thirty-five (69%) of the 51 patients where information was available had clinical, pathological or radiological evidence of cirrhosis at initial presentation. Thirty-four patients (of 56 evaluable) had multifocal tumors on imaging or pathology and six had regional node enlargement. Ten of 61 patients (16%) had distant metastases with the sites being lung in (7) and bone (4).

Treatment

Twenty (30%) patients received no anti-tumor treatment and were managed with supportive care. Six of these patients presented with ECOG performance status 3 or 4. The median survival of this group was five weeks from the time of diagnosis.

The remaining 43 patients received some form of anti-tumor therapy. The median time from diagnosis to initiation of treatment was 15 days (range 0 days to 5.2 years). Seventeen patients received two types of therapy and four patients received three or four different treatments.

Surgery was performed in 16 (25%) patients, either in the form of a lobectomy or hemihepatectomy. Three of these patients had surgery after chemoembolization. Two patients had repeat resections for relapse 5 and 39 months after curative resection. No patients in the series received allograft transplantation as their first therapeutic intervention. All patients who underwent surgery were rendered clinically disease free afterwards. Their median survival was 88 weeks (range 5- 354 weeks) from diagnosis or surgery with the median time to relapse being 43 weeks (range 4-182). Two patients are still alive at one year and two years after surgery.

Chemoembolization of the HCC by the selective injection of cisplatin and Lipiodol into the hepatic artery was carried out in 11 (17%) patients. In three patients this was done prior to surgery in an attempt to reduce the vascularity and size of the tumor. One of these patients received alcohol injection into the tumor as well and proceeded to an orthotopic liver transplantation. The other two patients had initial marked falls in the AFP to almost within normal range but these had risen to beyond pretreatment levels prior to surgery. Six patients (55%) had a 50% reduction in AFP with the median time to progression being 25 weeks (excluding the transplanted patient from the calculation of the duration of response). Median

survival from chemoembolization was 48.5 weeks.

Twelve (19%) patients were treated with systemic chemotherapy. Three were given anthracycline treatment alone (2 adriamycin, 1 epirubicin), while others received various combinations of cisplatin, adriamycin, 5-fluorouracil (5FU), etoposide and mitomycin C. Two patients received more than one regimen of chemotherapy. Only two patients had objective tumor responses to chemotherapy. Another two had stable disease. The median time to tumor progression was 26 weeks.

Tamoxifen was administered to 25 (40%) patients, with only one showing evidence of AFP response. The time to progression was 44 weeks. Two other patients had stable disease.

Table 3 summarises the response rates, response duration and overall survival of the groups of patients according to the treatments received. The median survival of the group as a whole was 16 weeks with the mean being 50 weeks.

Table 1 Countries of birth of cohort

Country of Birth	No.
Australia	26
Egypt	3
Europe	11
India	1
Pacific Islands	1
Southeast Asia	20
Unknown	1
Total	63

Table 2 Breakdown of established aetiological factors in cohort

Alcohol	10
Chronic autoimmune hepatitis	3
Hepatitis B	21
Hepatitis C	5
Hepatitis B+C	3
Haemochromatosis	3
Unknown	23
Total	63

Table 3 Summary of treatments received for hepatocellular carcinoma

Treatment	Number of patients (%)	Number responding (%)	Median time to progression (weeks)
Observation	20 (30)		
Surgery	16 (25)	16 (100)	43
Chemoembolization	11 (17)	6 (54)	25
Systemic chemotherapy	12 (19)	2 (27)	26
Tamoxifen	25 (40)	1 (4)	44

DISCUSSION

Despite a variety of therapeutic strategies HCC remains a significant cause of cancer death worldwide. The mainstay of treatment is resection of the disease. This is facilitated by early detection of tumors and by liver transplantation when poor hepatic function would otherwise prevent resection.

Other treatments, largely directed at palliation such as chemotherapy (\pm embolization), percutaneous ethanol injection, radiation and hormone therapy are modest in their effects however they may play a role in conjunction with surgery. Equally or more important strategies are prevention of predisposing illnesses (e.g., hepatitis B) or modification of the cirrhotic pre-malignant field defect.

Hepatic resection is generally only feasible in patients with focal lesions and with adequate underlying hepatic function^[3]. Because of tumor stage at presentation and the presence of cirrhosis, the proportion of patients suitable for surgery is generally small. The role of orthotopic hepatic transplantation is still controversial. There have been concerns about the perioperative mortality and the frequency of tumor recurrence in the transplanted liver, but transplantation offers some chance of cure of both the tumor and the cirrhosis. A recent series^[4] of 48 patients with small tumors (single <5 cm or no more than three <3 cm) and cirrhosis undergoing transplantation, reported overall survival and disease free survival at four years to be 75% and 83% respectively. Ninety-four percent of these patients had underlying viral hepatitis.

Percutaneous ethanol injection of these tumors has usually been restricted to non-surgical candidates and one series from Italy has shown encouraging survival figures where ethanol injection was used instead of surgery^[5]. This approach may provide a treatment for patients with no access to resection services or those with poor liver reserve, who are not otherwise able to have a liver transplant. Other forms of imaging-directed destruction such as cryotherapy, laser and thermotherapy may have similar potential.

As is the published experience, we found the response rate with systemic chemotherapy low and of short duration. Doxorubicin, remains the most widely used agent but being liver metabolized it may result in unpredictable toxicity in those with hepatic disease. When used as a single agent it generally has a response rate below 20%^[6]. Epirubicin, idarubicin and mitoxantrone all have activity comparable to doxorubicin. Single agent activities of other intravenously administered cytotoxics such as cisplatin, 5-fluorouracil, etoposide and mitomycin C are all in the range of 0%-15%^[6]. The Eastern Cooperative Oncology Group^[7] has evaluated 432 patients in four sequential trials of varying combinations of 5-FU, streptozotocin, semustine, doxorubicin, zinostatin, amsa crine and cisplatin. The median survival of the group as a whole with systemic chemotherapy was 14 weeks with a one-year survival of only 15%. The best median survival of 24 weeks was obtained with the combination of 5-FU and semustine. Although any

of these agents may cause greater response rates if given intra-arterially with or without embolization, most reports of trials of chemotherapy, both single agent and combinations have small patient numbers and none shows a convincing superiority to be considered standard treatment^[7,8].

Chemoembolization consists of a relatively selective embolization of the tumor blood supply with agents such as cisplatin and Lipiodol. While theoretically attractive, the technique may result in hepatic decompensation because the cirrhotic liver is more dependent on blood from the hepatic artery than the portal vein. For this reason embolization techniques are suitable for a small group of patients. In the Group D'Etude de Traitement du Carcinome Hepatocellulaire^[9] randomised trial of chemoembolisation versus conservative management in 96 selected patients from 24 centres, there was no significant survival difference detected after accounting for differences in baseline and prognostic characteristics. Small survival differences however would not be detected by a study of this size. Half of the patients in the treatment group had reduction in AFP levels. These observations are in keeping with the findings in our study. Hepatic decompensation however was seen in 70% of patients having chemoembolization. Another multicentre randomised study^[10] of Lipiodol/cisplatin chemoembolization in 73 patients also reported no survival difference. Transarterial embolization without chemotherapy in a single institutional study has also demonstrated no survival advantage versus supportive care^[11]. In these circumstances, a more appropriate endpoint may be symptom control, analgesic requirements and quality of life rather than survival. Symptomatic rather than asymptomatic patients may be more appropriate candidates for chemotherapy.

Oestrogen receptors have been detected in normal liver tissue and in HCC with the levels tending to be higher in the neoplastic tissue. This provides the rationale of using the anti-oestrogen tamoxifen. Seven randomized trials of tamoxifen versus placebo in advanced HCC have been reported^[12-18]. Three^[12-14] which had under 38 patients each reported improved survival in the tamoxifen treated arms. An additional two randomized trials investigating chemotherapy and tamoxifen found no improvement in response or survival when tamoxifen was added to doxorubicin^[19] or intra-arterial cisplatin and 5FU^[15]. An overview of the published randomised trials of tamoxifen versus active or no active treatment in HCC between 1978 and 1995 suggested a moderate benefit with a 2.2 odds ratio for 1 year survival^[20]. However the largest randomized study so far involving 496 patients has recently been presented and showed no survival benefit of

tamoxifen compared to supportive care^[19].

Antiandrogen therapy has also been tried in HCC on the basis that it is a male predominant disease, it can be induced by androgen therapy and that the receptors are expressed in high levels in the tumors. A European Organisation for Research and Treatment of Cancer (EORTC) multicentre trial^[21] compared antiandrogen therapy with a luteinising hormone-releasing hormone (LHRH) agonist either goserelin or triptoreline, with a pure antiandrogen nilutamide alone or in combination against placebo in 244 patients with advanced HCC. No significant difference however was found in any of the groups.

A recent study reports an apparent reduction in the incidence of new primary HCCs in patients administered polyprenic acid, an acyclic retinoid, after resection for HCC. This strategy targets the pre-malignant field defect that leads to HCC^[22].

Radiation therapy has been more usually applied in the form of radioactive ligands injected into the hepatic artery than as external radiation. A preliminary report of a randomized trial from Hong Kong has shown that ¹³¹I labelled lipiodol injected post-resection improves the time to tumor recurrence^[23]. Similarly data from pilot studies suggest post-transplant/resection - chemotherapy may improve outcome, although randomized trials are still underway^[24].

Viral hepatitis is a significant causative factor for HCC in our cohort especially in those born overseas, being present in over one-third. In the migrant population high hepatitis B endemicity accounts for the high prevalence rate. In hepatitis B associated cirrhosis the cumulative incidence of hepatocellular carcinoma has been found to be 59% over a six-year period^[25]. With hepatitis C associated cirrhosis, a Japanese prospective study^[26] has reported that 75% of patients will develop HCC by 15 years. Preventative measures such as hepatitis B vaccination in endemic disease populations is obviously an important and effective strategy. A recent study from Taiwan has reported that a national hepatitis B vaccination program has reduced the annual HCC incidence in children of aged 6-14 years from 0.7 to 0.36 per 100 000 ($P < 0.01$), with a similar effect on population mortality^[27]. Treatment of viral related chronic active hepatitis with interferon alpha may not only prevent development of cirrhosis but also reduce the frequency of subsequent HCC^[28].

Alcohol was also an important risk factor in the Australian born patients in our series. In a larger published series of HCC^[29] from western Sydney it was found to be an association in 46% of the Australian patients and only 13% of those born overseas.

Screening of high risk populations for HCC by a combination of serum AFP determination and

imaging with high resolution real time ultrasound can detect HCC at an early stage which might be amenable to curative resection. AFP however can be normal in patients with asymptomatic small tumors. The reliability of ultrasound is operator dependent and many studies have been in Japanese patients who have generally a thinner body habitus which may make imaging easier than in Westerners. Studies suggest that treatment of these early lesions may produce a true survival benefit although there have been no randomized trials reporting mortality reduction from screening^[30]. This strategy can only be considered an option in high risk populations, rather than on a general population basis.

CONCLUSION

Hepatocellular carcinoma is becoming a greater problem in developed countries such as Australia with the wave of immigration from countries affected by endemic viral hepatitis. Treatment modalities are unsatisfactory once the tumor has spread and become inoperable. Public health measures need to focus on the targeting of risk factors and surveillance of at risk subgroups.

REFERENCES

- Pisani P, Parkin DM, Bray FI, Ferlay J. Estimates of the world-wide mortality from twenty five major cancers in 1990. *Int J Cancer*, 1999;83:18-29
- McCredie M, Coates M, Duque-Portugal. Common cancers in migrants to New South Wales 1972-1990. Cancer Epidemiology Research Unit. NSW Central Cancer Registry, 1993
- Farmer DG, Rosove MH, Shaked A, Busuttil RW. Current treatment modalities for hepatocellular carcinoma. *Ann Surg*, 1993; 219:236-247
- Mazzaferro V, Regalia E, Doci R, Andreola S, Pulvirenti A, Bozzetti A, Montalto F, Ammatuna M, Morabito A, Gennari L. Liver transplantation for the treatment of small hepatocellular carcinomas in patients with cirrhosis. *N Engl J Med*, 1996;334:693-699
- Livraghi T, Giorgio A, Marin G, Salmi A, de Sio I, Bolondi L, Pompili M, Brunelo F, Lazzaroni S, Torzilli G. Hepatocellular carcinoma and cirrhosis in 746 patients: long term results of percutaneous ethanol injection. *Radiology*, 1995;197:101-108
- Ahlgren J, Wanebo H, Hill M. Hepatocellular carcinoma. In: Gastroenterological oncology. Philadelphia: J B Lippincott, 1992: 428-430
- Falkson G, Nnaan A, Schutt AJ, Ryan LM, Falkson HC. Prognostic factors for survival in hepatocellular carcinoma. *Cancer Res*, 1988; 48:7314-7318
- Farmer DG, Rosove MH, Shaked A, Busuttil RW. Current treatment modalities for hepatocellular carcinoma. *Ann Surg*, 1994; 219:236-247
- Groupe D'Etude et de Traitement du Carcinome Hepatocellulaire. A comparison of lipiodol chemoembolisation and conservative treatment for unresectable hepatocellular carcinoma. *New Eng J Med*, 1995;332:1256-1261
- Rougier P, Pelletier G, Ducreux M, Gay F, Lubinski M, Hagege H, Dao T, Van Steenberghe V, Buffet C, Adler M, Pignon JP, Roche A et al. Groupe CHC2. Unresectable hepatocellular carcinoma: lack of efficacy of lipiodol chemoembolization. Final results of a multicentre randomized trial (Abstract). *Proc Am Soc Clin Oncol*, 1997;16:279
- Bruix J, Llovet J, Castells A, Montana X, Bru C, Ayuso MC, Vilana R, Rodes J. Transarterial embolization versus symptomatic treatment in patients with advanced hepatocellular carcinoma: results of a randomized, controlled trial in a single institution. *Hepatology*, 1998; 27:1578-1583
- Farinati F, Salvagnini M, de Maria N, Fornasiero A, Chiaramonte M, Rossaro L, Naccarato R. Unresectable hepatocellular carcinoma: a prospective controlled trial with tamoxifen. *J Hepatol*, 1990;11:297-301
- Martinez Cerezo FJ, Tomas A, Donosi L, Enriquez J, Guarner C, Balanzo J, Martinez Noguera A, Vilardell F. Controlled trial of tamoxifen in patients with advanced hepatocellular carcinoma. *J Hepatol*, 1994;20:702-706
- Elba S, Giannuzzi V, Misciagna G, Manghisi O. Randomised controlled trial of tamoxifen versus placebo in inoperable hepatocellular carcinoma. *Ital J Gastroenterol*, 1994;26:66-68
- Uchino J, Une Y, Sato Y, Gondo H, Nakajima Y, Sato N. Chemohormonal therapy of unresectable hepatocellular carcinoma. *Am J Clin Oncol*, 1993;16:206-209
- Castells A, Bruix J, Bru C, Ayuso C, Roca M, Boix L, Vilana R, Rodes J. Treatment of hepatocellular carcinoma with tamoxifen: a double blind placebo-controlled trial in 120 patients. *Gastroenterology*, 1995;109:917-922
- Riestra S, Rodriguez M, Delgado M, Suarez A, Gonzalez N, de la Mata M, Diaz G, Mino Fugarolas G, Rodrigo L. Tamoxifen does not improve survival of patients with advanced hepatocellular carcinoma. *J Clin Gastroenterol*, 1998;26:200-203
- Pignata S, Izzo F, Farinati F, Palmieri G, Belli M, Manzione L, Pedicini T, D'Aprile M, Giorgio A, Russo M, Calandra M, Monfardini S, Galo C, Perrone F. Role of Tamoxifen (TM) in the treatment of hepatocellular carcinoma (HCC). Results from the CLIP-01 randomised trial (Abstract). *Proc Am Soc Clin Oncol*, 1998;17:257a
- Melia P, Johnson P, Williams R. Controlled clinical trial of doxorubicin and tamoxifen versus doxorubicin alone in hepatocellular carcinoma. *Cancer Treat Rep*, 1987;71:1213-1216
- Simonetti R, Liberati A, Angiolini C, Pagliaro L. Treatment of hepatocellular carcinoma: a systematic review of randomized controlled trials. *Ann Oncol*, 1997;8:117-136
- Grimaldi C, Bleiberg H, Gay F, Messner M, Rougier P, Kok L, Cirera L, Cervantes A, De Greve J, Paillot B, Buset M, Nitti D, Sahmoud T, Duez N, Wils J. Evaluation of antiandrogen therapy in unresectable hepatocellular carcinoma: results of a European Organization for Research and Treatment of Cancer multicentric double blind trial.
- Muto Y, Moriwaki H, Ninomiya M, Adachi S, Saito A, Takasaki KT, Tanaka T, Tsurumi K, Okuno M, Tomita E, Nakamura T, Kojima T. Prevention of second primary tumours by an acyclic retinoid, polyphenolic acid, in patients with hepatocellular carcinoma. *N Eng J Med*, 1996;334:1561-1567
- Leung WT, Lau WY, Ho S, Chan M, Lee WY, Leung N, Chan A, Yeo W, Johnson PJ. Reduction of local recurrence after adjuvant intra arterial lipiodol-iodine 131 for hepatocellular carcinoma-a planned interim analysis of a prospective randomized study. *Proc Am Soc Clin Oncol*, 1997;19:279a (abstract 988)
- Olthoff KM, Rosove MH, Shackleton CR, Imagawa DK, Farmer DG, Northcross P, Pakrasi AL, Martin P, Goldstein LI, Shaked A. Adjuvant chemotherapy improves survival after liver transplantation for hepatocellular carcinoma. *Ann Surg*, 1995;221:734-743
- Oka H, Kurioka N, Kim K, Kanno T, Kuroki T, Mizoguchi Y, Kobayashi K. Prospective study of early detection of hepatocellular carcinoma in patients with cirrhosis. *Hepatology*, 1990;12: 680-687
- Ikeda K, Saitoh S, Koida I, Arase Y, Tsubota A, Chayama K, Kumada H, Kawanishi M. A multivariate analysis of risk factors for hepatocellular carcinoma carcinogenesis: a prospective observation of 795 patients with viral and alcoholic cirrhosis. *Hepatology*, 1993;18:47-53
- Chang MH, Chen CJ, Lai MS, Hsu HM, Wu TC, Kong MS, Liang DC, Shau WY, Chen DS. Universal hepatitis B vaccination in Taiwan and the incidence of hepatocellular carcinoma in children. *N Engl J Med*, 1997;336:1855-1859
- Nishiguchi S, Kuroki T, Nakatani S, Morimoto H, Takeda T, Nakajima S, Shiomi S, Seki S, Kobayashi K, Otani S. Randomised trial of effects of interferon alpha on incidence of hepatocellular carcinoma in chronic active hepatitis C with cirrhosis. *Lancet*, 1995;346:1051-1055
- Brotodihardjo AE, Tait N, Weltman MD, Liddle C, Little JM, Farrell GC. Hepatocellular carcinoma in western Sydney. Aetiology, changes in incidence, and opportunities for better outcomes. *Med J Aust*, 1994;161:433-435
- Dusheiko GM, Hobbs KE, Dick R, Burroughs AK. Treatment of small hepatocellular carcinomas. *Lancet*, 1992;340:285-288

The expression of c-src gene in the carcinogenesis process of human cardia adenocarcinoma

WANG Xiu-Jia, YUAN Shu-Lan, XIAO Lin, WANG Xu-Hua and WANG Chao-Jun

Subject headings c-src gene; expression product; PP60^{c-src}; cardia adenocarcinoma; carcinogenesis; neoplasm metastasis; immunohistochemistry

Abstract

AIM To investigate the activation, expression of c-src gene and its role in the carcinogenic process of human cardia adenocarcinoma (CA). **METHODS** Fifty-six cases of CA, 34 cases of normal, 36 cases of proliferative epithelia adjacent to carcinoma, and 20 cases of lymph node metastases of CA were studied for PP60^{c-src}, the expression product of c-src gene immunohistochemically by using the specific monoclonal antibody, Mab327.

RESULTS The positive rates of PP60^{c-src} in the normal epithelia, proliferative epithelia, CA and lymph node metastases were 29.4% (10/34), 94.4% (34/36), 71.4% (40/56) and 60.0% (12/20), respectively, among them, the differences of the positive rates were statistically significant ($P < 0.01$). The expression levels of PP60^{c-src} in CA and proliferative epithelia were significantly higher than that in the normal epithelia ($P < 0.01$). The PP60^{c-src} positive rates in the papillary, tubular, poorly differentiated and mucous adenocarcinoma were 75.0% (6/8), 81.8% (18/22), 50.0% (10/20) and 100.0% (6/6), respectively, whereas those of tubular and mucous adenocarcinomas were significantly higher than those of papillary and poorly differentiated adenocarcinomas ($P < 0.05$), and the PP60^{c-src} expression levels of tubular and

mucous adenocarcinomas were also significantly higher than those of papillary and poorly differentiated adenocarcinomas ($P < 0.01$).

CONCLUSION The activation and expression of c-src gene are associated with the initiation and development of human CA; the protein amount of PP60^{c-src} increased during the process of carcinogenesis; and PP60^{c-src} expression is also related to lymph node metastases.

INTRODUCTION

There is a general tendency in gastric cancer that the incidence rate of cardia adenocarcinoma (CA) is increasing steadily, and cancer of the distal stomach is decreasing proportionately. The biological and epidemiological features of CA are distinct from those of the distal stomach, and the underlying cause remained unelucidated^[1-3]. PP60^{c-src} is the product of c-src gene possessing the activity of tyrosine kinase. Increased expression of c-src gene had been reported in some human sarcoma and cancers of breast^[4], esophagus^[5], stomach^[6] and colon^[7], and the activation and expression of c-src gene might be associated with the initiation and development of some cancers. Our previous study showed the activation and expression of c-src gene was associated with the development and differentiation of esophageal squamous cell carcinomas^[8], we believed that similar changes might occur in cancer of cardia, therefore, the following study was carried out.

MATERIALS AND METHODS

Sample collection and processing

All 56 cases of CA samples were collected from the CA patients surgically treated in Yanting Institute of Cancer Prevention of Sichuan Province. All tissue specimens were routinely processed, formalin-fixed and paraffin-embedded, at least 2 serial paraffin sections of 4 μ m - 6 μ m thickness were made, one was stained with hematoxylin and eosin (HE) and the other was used for PP60^{c-src} protein detection by immunohistochemical staining.

Reagents

The monoclonal antibody Mab327 (mouse IgG) was kindly given by the Molecular Pathology

Institute of Cancer Research, Cancer Center, The First University Hospital of West China University of Medical Sciences, Chengdu 610041, Sichuan Province, China

WANG Xiu-Jie, male, born on 1957-02-15 in Ziyang, Sichuan Province and graduated from West China University of Medical Sciences in 1982, now Associate Professor of Oncology, engaged in the researches of etiology and mechanisms of carcinogenesis of cancers, screening and developing anti-cancer drugs, having 20 papers published.

Project supported by the grant of West China University of Medical Sciences, No.L293015

Correspondence to: WANG Xiu-Jie, Institute of Cancer Research, Cancer Center, The First University Hospital of West China University of Medical Sciences, Chengdu 610041, Sichuan Province, China.

Tel. +86-28-5501218, Fax. +86-28-5583252

Received 1999-07-21 Accepted 1999-09-22

Department of Nagoya University, Japan; Streptavidin-Peroxidase Immunohistochemical Staining Kit (Zymed USA) was purchased from Fuzhou Maxim Biotech, Inc.

Immunohistochemical analysis of PP60^{c-src} protein

PP60^{c-src} protein was detected immunohistochemically with LSAB method according to the manufacturer's instructions with slight modification. Briefly, the tissue sections were deparaffinized and rehydrated through graded alcohols, and digested with trypsin. Then, endogenous peroxidase activity was blocked with 3% H₂O₂, and after treatment with normal serum, the sections were incubated with Mab 327 at a dilution of 1:100 overnight at 4 °C, with biotinylated second antibody 20 min, and with streptavidin peroxidase 30 min at room temperature. Subsequently, the sections were subjected to color reaction with 0.02% 3,3-diaminobenzidine tetrahydrochloride containing 0.005% H₂O₂ in PBS (pH 7.4), and were counterstained with hematoxylin lightly. In each staining run, a known PP60^{c-src} positive sample was added as positive control, and a section of the same sample was incubated with PBS instead of Mab327 as negative control.

Histopathological examination

Histopathological diagnosis for CA and related lesions were made, and the histological types of CA were examined by 2 experienced pathologists according to the given criteria^[8].

Qualitative and quantitative analysis of immunohistochemical staining of PP60^{c-src}

The immunostaining results of PP60^{c-src} were analyzed according to the known criteria^[5]. The percentages of positive PP60^{c-src} cell in CA and related lesions were assessed and scored as follows: negative (-), <25% (+), 25%-50% (++), >50% (+++); The intensity of staining in PP60^{c-src} positive cytoplasm and/or cell membrane were compared with the negative control and scored as follows: negative (-), weak (+), moderate (++) and strong (+++).

RESULTS

Histopathologic examination

Among the 56 cases of CA samples, there were 34 normal epithelia adjacent to cancer, 36 proliferative epithelia adjacent to cancer, 56 adenocarcinomas including papillary (8/56), tubular (22/56), poorly differentiated (20/56), mucous adenocarcinomas (6/56), and 20 CA with lymph node metastases.

Localization and distribution of PP60^{c-src}

Positive PP60^{c-src} protein cells showed brown staining in their cytoplasm and cell membranes, no positive staining was found in the negative controls. The intensity of staining varied with different lesions and different histologic types. Positive staining of PP60^{c-src} was localized in apex of glandular epithelial cells (Figure 1); in papillary and tubular adenocarcinomas, positive staining was distributed along the papillary margin or glandular lining, both the cytoplasm and cell membranes were positively stained but that of cell membranes were stronger than those in cytoplasm (Figure 2); the positive staining in poorly differentiated adenocarcinomas were evenly distributed in cytoplasm and cell membranes (Figure 3); and in the mucous adenocarcinomas, the positive PP60^{c-src} staining was unevenly distributed as micromasses.

PP60^{c-src} expression in CA and in the related lesions

The positive rates of PP60^{c-src} expression in CA, proliferative and normal epithelia adjacent to cancer were 71.4% (40/56), 94.4% (34/36) and 29.4% (10/34), respectively (Table 1). The positive rates of the former two were higher than that in the latter ($P<0.01$), and the positive staining intensities in CA and proliferative epithelia were also stronger than that in the normal epithelia ($P<0.01$).

PP60^{c-src} expression in different histological types

The positive rates of PP60^{c-src} in papillary, tubular, poorly differentiated and mucous adenocarcinoma were 75.0% (6/8), 81.8% (18/22), 50.0% (10/20), and 100.0% (6/6), respectively (Table 2) and the positive rates in tubular and mucous adenocarcinomas were higher than those in poorly differentiated or papillary adenocarcinomas ($P<0.05$); the percentages of high PP60^{c-src} expression (++++ in tubular and mucous adenocarcinoma were 63.6% (14/24) and 100.0% (6/6), respectively; while that in papillary and poorly differentiated ones were all low (+), there were significant differences between them ($P<0.01$).

PP60^{c-src} expression in CA with lymph node metastases

The positive rate of PP60^{c-src} expression was 60.0% (12/20) in 20 cases of metastatic lymph node (Table 1), among them, the positive ones in papillary, tubular, poorly differentiated and mucous adenocarcinomas were 2/2, 2/4, 6/12 and 2/2, respectively; the expression intensity of PP60^{c-src} in CA with lymph node metastases was the same as those without (Figure 4).

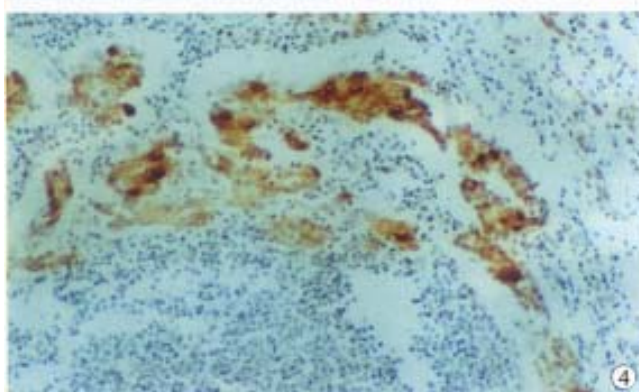
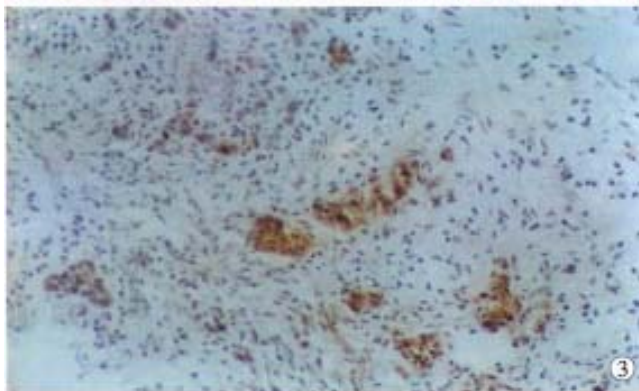
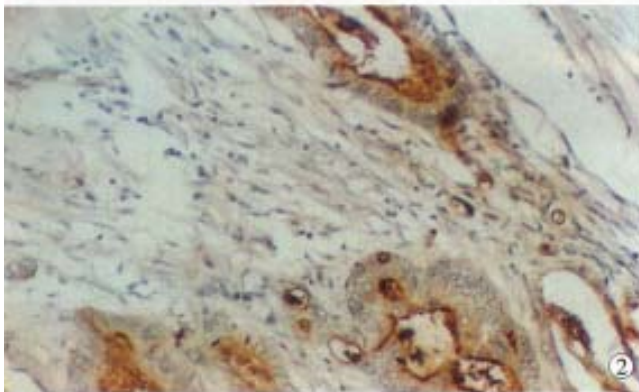
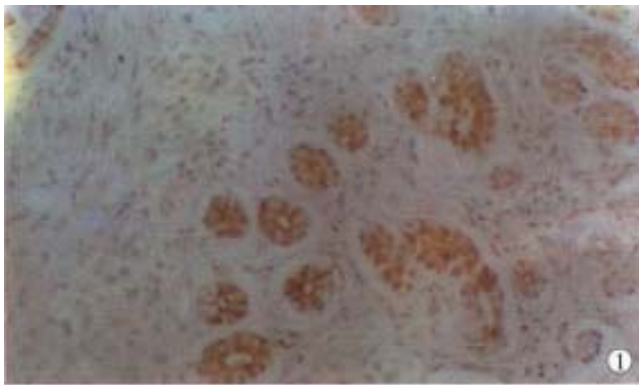


Figure 1 The expression of PP60^{c-src} in the proliferative epithelia adjacent to carcinoma. LSAB×200

Figure 2 The expression of PP60^{c-src} in tubular adenocarcinoma. LSAB×200

Figure 3 The expression of PP60^{c-src} in the poorly differentiated adenocarcinoma. LSAB×200

Figure 4 The expression of PP60^{c-src} in the lymph node metastasis of CA. LSAB×200

Table 1 The expression of PP60^{c-src} in CA and related lesions

Lesion	Case	Staining intensity			Positive rate (%)
		- (%)	+ (%)	+++ + (%)	
Normal epithelia	34	24(70.5)	10(29.4)	0(0)	10(29.4)
Proliferative epithelia	36	2 (5.6)	6(16.7)	28(77.8) ^d	34(94.4) ^b
Cardia adenocarcinoma	56	16(28.6)	20(35.7)	20(35.7) ^d	40(71.4) ^b
Lymph node metastases	20	8(40.0)	8(40.0)	4(20.0)	12(60.0)

^b $P < 0.01$, in comparison of the positive rates in different lesions ($\chi^2 = 34.19$) vs normal epithelia; ^d $P < 0.01$, in comparison of the positive intensity in different lesions ($\chi^2 = 25.08$) vs normal epithelia.

Table 2 The expression of PP60^{c-src} in CA of different histological types

Lesion	Case	Staining intensity			Positive rate (%)
		-(0/10)	+ (%)	+++ + (%)	
Papillary	8	2(25.0)	6(75.0)	0(0)	6(75.0)
Tubular	22	4(18.2)	4(18.2)	14(63.6) ^b	18(81.8) ^a
Poorly differentiated	20	10(50.0)	10(50.0)	0(0)	10(50.0)
Mucous	6	0(0)	0(0)	6(100.0) ^b	6(100.0) ^a
Total	56	16(28.6)	20(35.7)	20(35.7)	40(71.4)

^a $P < 0.05$, in comparison of the positive rates of tubular and mucous adenocarcinomas vs those of papillary and poorly differentiated adenocarcinomas ($\chi^2 = 8.11$); ^b $P < 0.01$, in comparison of the positive rates of tubular and mucous adenocarcinomas vs those of papillary and poorly differentiated adenocarcinomas ($\chi^2 = 27.56$).

DISCUSSION

PP60^{c-src} is a phosphorylated cytoplasmic protein encoded by c-src gene, having the activity of tyrosine kinase. The expression of PP60^{c-src} can be found in many normal cells, which plays important roles in the regulation of cell proliferation, differentiation and transformation^[4]. Recent studies indicated that the increase in the amount of PP60^{c-src} protein and kinase activity was associated with initiation and development of some human neoplasms, and the activation and increase of expression were one of the factors for cancer initiation^[4-8]. In this study, the expressions of PP60^{c-src} in CA, proliferative epithelia and normal epithelia were 71.4% (40/56), 94.4% (34/36) and 29.4% (10/34), respectively and the positive rates of PP60^{c-src} in CA and proliferative epithelia were much higher than that in the normal epithelia ($P < 0.01$). Jankowski *et al* analyzed the expression product of c-src gene in 15 cases of esophageal adenocarcinoma and 15 cases of Barrett's esophageal epithelia immunohistochemically, the positive rates were 20% (3/15), suggesting that the expression of c-src gene is related to the development of esophageal adenocarcinoma. Therefore, the results of this study indicated that the activation and expression of c-src gene might be associated with the initiation and development of CA. However, the high expression of PP60^{c-src} in the proliferative epithelia might be associated with the proliferation of glandular epithelial cells, occurring in the aged rats^[9]. The low PP60^{c-src} expression in some normal epithelia adjacent to cancer might be explained by the fact that there had

been PP60^{c-src} expression in the normal epithelia related to the initiation of cancer^[5-8]. On the other hand, it indicated that the activation and expression of *c-src* gene might be an early event in the carcinogenesis of CA.

Although it was well known that the activation and expression of *c-src* gene were associated with the initiation of some human neoplasms. The results obtained mainly from biochemical assay by measuring the protein amount and kinase activity of PP60^{c-src} varied with the methodology. Most of the studies reported that PP60^{c-src} protein kinase activity increased in the cancer cell lines and cancer tissues from cancers of stomach, colon, lung and kidney, etc., but compared with those of normal tissues related to cancer, no difference of PP60^{c-src} protein amount was found, the increase in PP60^{c-src} protein kinase activity could not be explained by the increase of protein expression encoded by *c-src* gene^[6,10]. In the present study, PP60^{c-src} protein was detected by using the specific monoclonal antibody Mab 327, immunohistochemically, the high level of PP60^{c-src} expressions (+ + - + +) in CA and proliferative epithelia were 35.7% and 77.8%, respectively, a low PP60^{c-src} expression (+) was found in some normal epithelia adjacent to cancer, the difference of expression intensity was significant statistically ($P < 0.01$). The results of this study suggested that the protein amount of PP60^{c-src} expression was increased in carcinogenesis of CA.

With regard to the relationship between expression product of *c-src* gene, PP60^{c-src} and the differentiation of cancer cells, there was no consensus in this aspect^[6,8,9,11]. Fanning *et al*^[1] reported a high level of *c-src* expression in well differentiated bladder cancers, and proposed that PP60^{c-src} protein and kinase activity were associated with the differentiation of epithelial cells of urinary tract and grade I-II bladder carcinomas. However, Takekura *et al*^[6] could not find the difference of PP60^{c-src} kinase activity between well and poorly differentiated gastric carcinomas. In this study, PP60^{c-src} positive rates varied in different histological types of CA; the positive rates in mucous adenocarcinomas (100.0%, 6/6) and tubular adenocarcinomas (81.8%, 18/22) were higher than those in papillary (75.0%, 6/8) and poorly differentiated types (50.0%, 10/20), the difference being significant statistically ($P < 0.05$). And the high level of expressions (++ - +++) in mucous and tubular adenocarcinomas were 100.0% (6/6) and 63.6% (14/18), respectively, only low expression (+) was found in papillary and poorly differentiated adenocarcinomas, the differences of expression level were also significant statistically

($P < 0.01$). These results suggested that the expression level of PP60^{c-src} was associated with the differentiation and histological types of CA, high PP60^{c-src} expressions in mucous and tubular adenocarcinomas might be related to their well differentiation and other biologic behaviors.

The relationship between the PP60^{c-src} expression with increase in kinase activity and metastatic colon carcinomas had been reported already^[12,13], but there was no report of detection of PP60^{c-src} protein in lymph node metastases by immunohistochemical staining. Talamonti *et al*^[12] discovered increase in PP60^{c-src} kinase activity, in the stages of polyps and primary carcinomas. Termuhlen *et al*^[13] reported that PP60^{c-src} kinase activity in hepatic metastases of colorectal carcinoma increased by 2.2 folds, and in extrahepatic metastases increased by 12.7 folds, while compared with that in normal mucosa, PP60^{c-src} kinase activity in the hepatic metastases of non-colorectal carcinomas increased only slightly. In this study, PP60^{c-src} protein was detected in the lymph node metastases of CA, the positive rate was 60.0% (12/20), the expression level of PP60^{c-src} was equal to that of the same primary adenocarcinoma. The results of this study suggested that PP60^{c-src} expression is associated with the lymph node metastases of CA, which deserved further investigation.

REFERENCES

- 1 Powell J, McConkey CC. Increasing incidence of adenocarcinoma of the gastric cardia and adjacent sites. *Br J Cancer*, 1990;62:440-443
- 2 Blot WJ, Devesa SS, Kneller RW, Fraumeni JF. Rising incidence of adenocarcinoma of the esophagus and gastric cardia. *JAMA*, 1991;265:1287-1289
- 3 Sampliner RE. Adenocarcinoma of the esophagus and gastric cardia: is there progress in the face of increasing cancer incidence. *Ann Intern Med*, 1999;130:67-69
- 4 Jacobs C, Rübsamen H. Expression of PP60 *c-src* protein kinase in adult and fetal human tissue: high activities in some sarcomas and mammary carcinomas. *Cancer Res*, 1983;43:1696-1702
- 5 Jankowski J, Coghill G, Hopwood D, Wormely KG. Oncogenes and onco suppressor genes in adenocarcinoma of the esophagus. *Gut*, 1992;33:1033-1038
- 6 Takekura N, Yasui W, Yoshida K, Tsujino T, Nakayama H, Kameda T, Yokozaki H, Nishimura Y, Ito H, Tahara E. PP60 *c-src* protein kinase activity in human gastric carcinomas. *Int J Cancer*, 1990;45:847-851
- 7 Cartwright CA, Kamps MP, Meisler AI, Pipas JM, Eckert W. PP60^{c-src} activation in human colon carcinoma. *J Clin Invest*, 1989;83:2025-2033
- 8 Wang XJ, Wang CJ, Huang GQ, Xiao HY. A study of *c-src* gene expression product PP60^{c-src} in esophageal carcinoma. *J WCUIMS*, 1995;26:197-201
- 9 Majumdar APN, Tureaud J, Relan NK, Kessel A, Dutta S, Hatfield JS, Fligiel SEG. Increased expression of PP60^{c-src} in gastric mucosa of aged rats. *J Gerontol*, 1994;49:B110-116
- 10 Cartwright CA, Meisler AI, Eckhart W. Activation of the PP60^{c-src} protein kinase is an early event in colonic carcinogenesis. *Proc Natl Acad Sci USA*, 1990;87:558-562
- 11 Fanning P, Bulovas K, Saini KS, Libertino JA, Joyce AD, Summerhayes IC. Elevated expression of PP60 *c-src* in low grade human bladder carcinomas. *Cancer Res*, 1992;52:1457-1462
- 12 Talamonti MS, Roh MS, Curley SA, Gallick GE. Increase in activity and level of PP60^{c-src} in progressive stages of human colorectal cancer. *J Clin Invest*, 1993;91:53-60
- 13 Termuhlen PM, Curley SA, Talamonti MS, Saboorian MH, Gallick GE. Site specific differences in PP60^{c-src} activity in human colorectal metastases. *J Surg Res*, 1993;54:293-298

Edited by WU Xie-Ning

Proofread by MIAO Qi-Hong

Clinical and experimental study on regional administration of phosphorus 32 glass microspheres in treating hepatic carcinoma

LIU Lu, JIANG Zao, TENG Gao-Jun, SONG Ji-Zhi, ZHANG Dong-Sheng, GUO Qing-Ming, FANG Wen, HE Shi-Cheng, GUO Jin-He

Subject headings liver neoplasms/therapy; phosphorus-32 glass microspheres (^{32}P -GMS); ^{31}P -GMS; interventional therapy

Abstract

AIM To study the therapeutical effectiveness, dosage range and toxic adverse effects of domestic phosphorus 32 glass microsphere and evaluate its clinical significance.

METHODS I. Fifty-two BALB/c tumor bearing male nude mice were allocated into treatment group ($n = 38$) and control group ($n = 14$). In the former group different doses of ^{32}P -GMS were injected into the tumor mass, while in the latter ^{31}P -GMS or no treatment was given. The experimental animals were sacrificed in batches, and then the tumors and their nearby tissues were examined by light and electron microscopy. II. Through selective catheterization of hepatic artery, ^{32}P -GMS was infused to 5 healthy domestic pigs in a dosage equivalent to the therapeutic dose for human being, and ^{31}P -GMS was infused to another 5 healthy domestic pigs. Two pigs infused with contrast medium served as whole course blank controls. One pig from each group was surrendered to euthanasia at week 1, 4, 8 and 16 respectively. The ultrastructural histopathological changes in liver tissues taken from different sites were evaluated *semiquantitatively*. III. One hundred and twenty-seven times of ^{32}P -GMS intrahepatic artery interventional therapies were performed on 93

patients with hepatic carcinoma, including 79 cases of primary hepatic carcinoma and 14 cases of secondary hepatic carcinoma. ^{32}P -GMS ($n = 30$), and group B, ^{32}P -GMS and half-dose of trans-hepatic artery embolization (TAE) ($n = 49$), and 18 patients with HCC by TAE only as control group C. Fourteen patients with secondary hepatic carcinoma were treated in the same way as group B or C.

RESULTS I. Comparing with the control group, the treatment group of tumor bearing nude mice attained the tumor inhibition rates of 59.7%-93.7% ($F = 579.62$, $P < 0.01$) at 14d. At an absorbed dose of 7320Gy, the tumor cells were completely destroyed. When the absorbed doses ranged from 1830Gy to 3660Gy, most of the tumor cells showed the evidences of injury or necrosis, but there appeared some well-differentiated tumor cells and enhanced effect of the autoimmunocytes. At an absorbed dose of 366Gy or less, some tumor cells still remained active proliferative ability. The definite anticancer effect appeared as early as 3d after intratumoral injection of ^{32}P -GMS. II. The cumulative amount of ^{32}P -GMS in the target tissue after trans-hepatic artery instillation attained more than 90% of the total dose administered. Semiquantitative analysis of ultrastructural morphology in the experimental group showed no statistical difference between the nuclear abnormality (n_{abn}) and mitochondrial variability (M_{var}) at week 1 or 2, but revealed prominent difference ($\chi^2 = 6.70-9.68$, $P < 0.01$, $\chi^2 = 65.09-115.09$, $P < 0.001$) as compared with those in the other groups. In the experimental group the n_{abn} in tissues showed no significant difference between week 8 and week 16. no apparent changes were found in the stomach, spleen, kidney and lung tissues of the experimental pigs. III. The therapeutical results of HCC patients in group A were closely approximated to those of group C, no hematological toxic side effects were noted, and the systemic reaction was mild. In some patients 2 mos-3 mos after treatment some secondary

Experimental Center of Modern Medical Sciences, Nanjing Railway Medical College, Nanjing 210009, Jiangsu Province, China
LIU Lu, M.D. female, born in 1946-10-17 in Jinan, Shandong Province, Han nationality, graduated from Nanjing Railway Medical College in 1970 and is now an Associate Professor, majoring in nuclear medicine and having more than 50 papers published at home and abroad.

Supported by the Science and Technology Commission of Jiangsu Province, No. BJ93077. Sponsored by Project No. 863 of National High-Tech Research and Development Program, No. 715-002-0200.
Correspondence to: LIU Lu, Experimental Center of Modern Medical Sciences, Nanjing Railway Medical College, Nanjing 210009, China
Tel. +86-25-3301508 Ext. 2708, Fax +86-25-3426368
Email: xue-c@263.net

Received 1999-07-14

foci appeared around the periphery of the primary lesion. In general better effectiveness was obtained in patients with small lesion. After analyzing by RIDIT method, the therapeutic result in group B was significantly better than that in group C, and secondary foci around the original lesion were rarely seen at 3mos after treatment. In group C the collateral circulation was reestablished along the periphery of primary foci and the secondary foci appeared more frequently, and were required to undergo several courses of treatment. In group B, 4 cases of HCC were treated surgically as their mass decreased in size after ^{32}P -GMS treatment. Resected specimens showed that the tumor was encapsulated by fibrotic tissue and most of the tumor cells necrosed. The 3-year survival rates were 43.3%-51.0% after A and B regimen treatment. In 14 cases of secondary HCC, the foci were well controled within one year after-treatment.

CONCLUSION When the experimental model of implanted human liver cancer cells received ^{32}P -GMS of 1830Gy-3660Gy, it produced excellent anticancer effect without any injury to the normal neighboring tissues and the prominent anticancer effect was shown within 3d after intratumoral injection. Intrahepatic arterial administration of ^{32}P -GMS at the macrocosmic absorbed dosage less than 190 Gy/dose exerted reversible sub-lethal injury to domestic pig liver tissues. It took more than 8 weeks to repair the injured liver tissue and restore its function. ^{32}P -GMS trans-hepatic artery embolization is an effective and safe regimen in treating hepatic carcinoma.

INTRODUCTION

Trans-hepatic artery embolization (TAE)^[1] is the main regimen for treating unresectable hepatic carcinoma (HCC). The experimental investigation using microsphere carriers such as colloidal microsphere, artificial cell membrane-liposome etc, in treating malignant tumors had been carried out for more than a decade with advanced development^[2]. The microspheres mainly conjugated with anticancer drugs released slowly into the cancer tissue. Up to now, a novel anticancer microsphere preparation has been evolved, i.e. incorporation of radionuclide (^{32}P or ^{90}Y) to the glass microspheres forming a nontoxic, undegradable radioactive radiation source through

regional medication, which aroused the interest and notice of investigators in this field^[3-5].

We report the results of evaluating the pharmacology, toxicology and clinical effect of ^{32}P -phosphorus-glass microspheres (^{32}P -GMS) in three parts. I. By using human liver cancer cell bearing nude mouse model to explore the experimental anti cancer effect of intratumoral injection of ^{32}P -GMS and investigate the appropriate dose range, time course and the influence on the neighboring tissues. II. By administrating ^{32}P -GMS to the whole liver or certain liver lobes of domestic pig model and observing the local irradiative reaction and systemic toxic effect on the normal liver tissue to provide the experimental basis for determining the appropriate tolerable dosage and treatment course of ^{32}P -GMS internal irradiation in normal human liver tissues. III. From 1996 to 1998, 93 patients with liver cancer received 127 times of interventional ^{32}P -GMS internal irradiation.

MATERIALS AND METHODS

Medicaments

By activation of standardized glass microspheres with nonradioactive ^{31}P (^{31}P -GMS, cold sphere) through nuclear-chemical reaction [^{31}P (n, γ) ^{32}P] transformed into radioactive ^{32}P glass microsphere (provided by nuclear Power Research Institute of China, nPIC)^[6], having the properties as follows: diameter of glass sphere 46 μm -76 μm , radioactive nuclide purity >99%, radioactivity per unit 550 MBq·g⁻¹ 3700 MBq·g⁻¹ (15 mCi·g⁻¹-100 mCi·g⁻¹), ^{32}P elution rate <0.1% within 30 days; ^{32}P physical half-life 1428 days, average β ray energy per disintegration: 0.695 MeV (maximum energy 1.711 MeV); and soft tissue penetration distance, max. 8.0 mm, averaging 3.2 mm. ^{32}P -GMS suspension was prepared by mixing ^{32}P -GMS with super-liquidized iodized oil or 50% glucose solution to the concentration of 100 mg·mL⁻¹ on oscillator.

Dosimetry

Loevinger's formula^[7] for calculating the absorbed dose of β emitter radionuclide:

$$D_{\beta\infty} = 73.8 E_{\beta} C_0 T_{\text{eff}}$$

where $D_{\beta\infty}$ the total absorbed beta particle dose (cGy), E_{β} , the average beta ray energy per disintegration (MeV), C_0 , the initial tissue concentration of radioactivity (mCi/kg) and T_{eff} , the effective half-life (days).

Based on the pharmacokinetic characteristics of regional administration of ^{32}P -GMS and the related parameters, the following formulae were established^[8]:

$$D \text{ (cGy)} = 20A \text{ (MBq)} \cdot m \text{ (kg)}^{-1}$$

$$D \text{ (cGy)} = 732A \text{ (mCi)} \cdot m \text{ (kg)}^{-1}$$

where A: the cumulative activity of radioactive nuclide, D: the total dose of absorbed β particles in tissue, m: the tissue weight.

Animal experiment

Human liver cancer cell-bearing nude mouse model and anti-cancer effect of ^{32}P -GMS Human liver cancer cell line subset (H-CS)^[9] with higher oncogenicity and liability of metastasis was implanted into the dorsal subcutaneous tissue of 52BALB/c nu/nu nude mice (male, body weight 16.8 g-21.3 g, mean 19.2 g, aged 4 weeks, derived from Shanghai Experimental Animal Center, Chinese Academy of Sciences) at the dosage of 0.1 mL-0.2 mL (1×10^7 tumor cells for each animal).

Experiment 1. Forty tumor-bearing nude mice with the tumor mass diameter of 0.7 cm-1.0 cm, different doses of ^{32}P -GMS were injected to the mass center of 32 nude mice (subgroup 1-V) in the treatment group and non-radioactive ^{31}P -GMS to mass center of 8 nude mice as the control subgroup. The animals were sacrificed on the 14th day.

Experiment 2. Twelve tumor-bearing nude mice with matched tumor size were equally allocated into treatment and control group, and ^{32}P -GMS 3.7 MBq were injected to the tumor mass at points with 0.8 cm apart from each other, the total dosage being 7.4 MBq-14.8 MBq, varied with the size of tumor. no treatment was given to the control animals. The mice in the treatment group were sacrificed in batches on day 3, 6, 13, 20, and 28 after medication and the same was done for those in control group. The tumor masses were disposed similar to Experiment 1. One mouse in both treatment and control groups died on day 19 and 22 spontaneously without any difference from the survivals in appearance. All of the tumor specimens were submitted to gross inspection, light and electron microscopy to observe the morphological and ultrastructural changes and then calculate the tumor inhibition rate. Tumor inhibition rate (at the time of execution) = (tumor weight of control-tumor weight of treatment group) / tumor weight of control group $\times 100\%$.

Experimental study on the toxicology of ^{32}P -GMS

Twelve domestic pigs (6 males, 6 females) with average body weight of 23.4 kg, were randomly divided into 3 groups: warm sphere group, ^{32}P -GMS ($n=5$), cold sphere group ^{31}P -GMS ($n=5$) and whole course blank control group ($n=2$). Under generalized anesthesia the catheter was inserted through femoral artery to the hepatic artery of the experimental animal. To the warm sphere group ^{32}P -GMS was administered at a dose equivalent to that of man, ^{31}P -GMS administered to the cold

sphere group and roentgenographic contrast medium to the blank control group. For the pigs with ^{32}P -GMS, the distribution of nuclide radioactivity was studied by SPECT. The radioactivity count rate was recorded on the body surface of hepatic, pulmonary and splenic regions of pigs for 14 consecutive days. One pig a time was surrendered to euthanasia on week 1, 2, 4, 8 and 16. The animal liver was dissected and weighed as soon as possible. From different sites of liver 8 tissue specimens were taken for light and electron microscopy. And at the same time, the major organs suspected to be involved such as lung, spleen, stomach and kidney were sampled for light microscopy. At the corresponding time point, liver biopsies were performed on the rest surviving animals for light and electron microscopy.

Venous blood specimens were taken for routine blood count, estimation of liver and renal function and for dynamic study of liver fibrosis markers, such as hyaluronic acid (HA), human procollagen III (hPCIII), collagen IV(C-IV), laminin (LN) and glycocholate (CG) by radioimmunoassay. The specimens prepared routinely were studied under H-600 electron microscopy at 8 000 folds magnification, to observe the ultrastructure and analyze morphometrically. A total of 100 hepatocyte nuclei and 100 mitochondria were observed in each sample group, and the nuclear abnormality (N_{abn}) and mitochondrial variability (M_{var}) were calculated respectively. The characteristics of abnormal nuclei were: nuclei irregular and deformed in shape; abnormal nuclear membrane, distension of the perinuclear gap; abnormal chromatin with peripheral condensation, and increase in intranuclear inclusion bodies with giant nucleolus. The abnormal mitochondria were characterized by swelling with disrupted external membrane and decrease in cristae; shrunken mitochondria, deep staining of ground matrix with decreased granules but with some vacuoles. The rates of abnormal nucleus and mitochondria variation were the percentage calculated from the number of abnormal or variation per total number of nuclei observed.

Preliminary clinical application of ^{32}P -GMS in treating hepatic carcinoma

Clinical materials Seventy-nine cases of primary hepatocellular carcinoma, male 67 and female 12 with average age of 52 years (32 years-77 years). The diagnosis was based on the evidence afforded from the results of B-mode sonography, computed tomography or angiogram and blood AFP $> 400 \mu\text{g/L}$. In some cases with negative AFP, their pathological and cytological evidence settled the diagnostic problem. The clinical types in 79 cases of HCC were single massive types (52 cases, left lobe 3, right lobe 49); multi-nodular type (24 cases); and

diffuse type (3 cases). According to Child's classification of liver function, 25 were of grade A, 40 grade B and 14 grade C. The average diameter of tumor mass was 8 cm (3 cm-15 cm), 62 cases (78.5%) showed positive hepatitis B antigen, 52 cases (65.8%) were complicated with cirrhosis, 4 cases (5.1%) portal vein embolization, 6 (7.6%) pulmonary metastasis, 7 (8.9%) peritoneal lymph node metastasis and 8 (10.1%) had family histories of gastrointestinal tumors. In 14 cases of secondary hepatic carcinoma, 6 were primary colonic tumors, 5 gastric, 1 pulmonary and 2 esophageal cancers.

Treatment regimen and grouping Superselective catheterization was performed by Seldinger's procedure to the distal end of hepatic artery proper for 127 times in 93 cases of hepatic carcinoma. No hepatic A-V fistula was found in all of the cases as confirmed by DSA, then the ^{32}P -GMS suspension prepared by occlusion of super-liquidized iodized oil 4 mL-10 mL and ^{32}P -GMS with calculated tumor tissue absorbed dose of 50Gy -100Gy and activity range from 370 MBq-470 MBq was instilled. HCC patients were allocated randomly into 3 groups. Group A: ^{32}P -GMS internal irradiation embolization therapy (30 cases); Group B: ^{32}P -GMS and half dose TAE [Adriamycin (Ad) 30 mg/m²+cis-diammine dichloroplatinum (CDDP) 50 mg/m²+iodized oil] combined therapy (49 cases); Group C: TAE (18 cases). Fourteen cases of secondary hepatic carcinoma were treated by B and C regimen. After embolization the vasculature and tumors staining disappeared on DSA.

Follow-up Before treatment the average life quantity score was 65.5 (Karnofsky score)^[10]. The results in liver and renal function, ECG, routine blood counts, blood AFP and CEA on day 10-14 after treatment were compared with the corresponding basal data. SPECT liver images were conducted in 20 cases before treatment. Distribution of nuclide radioactivity in chest and abdomen within 80 h after treatment was studied using bremsstrahlung conducted by SPECT. Plain film of liver region showed the foci of condensed iodized oil shadow within 5 days after treatment. B-mode sonogram, or computed tomogram or plain film of abdomen was taken at the scheduled time of follow-up.

Evaluation of therapeutical results According to the modified WHO^[10] criteria for tumor therapy, the effectiveness of grades A, B and C was the product of two perpendicular diameters which were decreased >50%, 50%-25% and 25%-10%, respectively, while the product decreased <10% was defined as stable. When the product was increased, it meant ineffective.

Statistical method

Chi-square test and RIDIT method were used for analyzing categorical data, *t* test and ANOVA were used for analyzing numerical data and survival rate was calculated by life-table method.

RESULTS

Changes in implanted human hepatic carcinoma

Gross inspection (Figure 1) The similar manifestation in Experiments I, II and controls was the rapid progressive growth of tumor mass, beginning from the dorsal injection points extended to the contralateral side, eventually distributed to the whole dorsa and buttocks. At the time of execution, the tumor mass presented nodular or lobular in shape with axial diameter of 2.3 cm - 4.0 cm, hard and firm in consistency on palpitation with thin intact reddish covering epiderma without ulceration. After the covered epiderma was incised, there was plenty of blood vessels on the mass surface, bleeding readily, and the section showed light reddish in color, dense in consistency, rich in vessels, and sometimes with central necrosis and focal liquification. In the treatment group the growth of tumor mass was evidently inhibited, and the inhibiting rate was directly proportional to the dosage administered and time elapsed (Tables 1, 2). About 5 days after medication, the tumor mass began with ulceration, bleeding or petechia, liquification and cystic degeneration. These changes might result in increase in tumor size, but that was qualitatively different from the growth of tumor in control group. The tumor of subgroups I and II shrank with scars or cystic degeneration. The section of tumor showed grayish white color with poor vascularity. In subgroups III-IV, most of the implanted tumors presented with ulceration, bleeding, liquification and cystic degeneration, the section of tumor showed grayish white in color with poor vascularity, too. These changes had already appeared on 3 day after medication.

Table 1 Nude mice in different absorbed dosage group the tumor weight (g) variance, SNK analysis and tumor inhibiting rate (14d)

Group	No. of Cases (n)	Tumor weight ^① ($\bar{x} \pm s$)	SNK ^②	Absorbed dose mean value (Gy)	Tumor inhibiting rate (%)	Necrosed tumor cell (%)
Control	8	6.25 \pm 0.39	A	-	-	4
I	6	0.40 \pm 0.10 ^a	B	7320	93.6	82
II	6	0.46 \pm 0.08 ^a	B	3660	92.5	78
III	8	0.94 \pm 0.10 ^a	C	1830	84.8	70
IV	6	2.17 \pm 0.26 ^a	D	366	65.3	47
V	6	2.43 \pm 0.33 ^a	E	183	59.7	40

①Variance analysis of the mean tumor weight of different doses and control group after square root correction, $F = 579.62$, $^aP < 0.01$. ②Different or same alphabets denote with or without statistical significance of mean deviations between groups respectively.

Table 2 Relationship between tumor inhibiting rate and execution time in tumor-bearing nude mice accepted ^{32}P -GMS in absorbed dose of 366Gy

Time of execution (d)	Weight of tumor (g) treatment group/control group	Tumor inhibiting rate (%)
3	1.5/2.3	34.8
6	1.7/3.2	46.9
13	2.1/5.9	64.4
20	1.6/6.7	76.1
28	1.0/6.8	85.3

Light microscopy (Figure 2) The tumor cells of control group were closely arranged in the form of trabeculae with large nuclei and prominent nucleoli. Some cells showed binuclei or giant nucleus and mitosis were readily found. Plenty of blood sinusoids and concentrated bile could be found between the intercellular space of tumor cells. Some of the tumor tissues showed fatty change or scattered focal necrosis. In the treatment group the microscopic manifestation varied with the different activities of the ^{32}P -GMS administered. In the I and II subgroups the tumor cells were loosely arranged with widely distributed coagulation necrosis. Some nuclei showed prominent shrinking degeneration. In subgroup III the tumor cells were loosely arranged and separated by thick or thin bundles of vesiculo-fibro-connective tissue forming pseudoacini, and in the nest some nuclei were broken with deeply stained scant cytoplasm. The histological characters in subgroups IV and V were that the arrangement of tumor cells transformed from dense to loose with scattered spot necrosis, blood sinuses being not found. In loosely arranged tumor cells desmosomes were fewer than those in the closely arranged tumor cells, but the degenerated necrotic cells increased. The necrosis was mainly located at the center of tumor mass and scattered among the dispersed tumor cells. In this experiment, a tumor mass with largest dose of radiation showed metaplasia in the neighboring epidermal tissues.

Electron microscopy (Figure 3) In the control group, most of the tumor cells were poorly differentiated and rapidly multiplied, with the characteristics of irregular large nuclei with deep indentation, pseudo-inclusion body formation, large and prominent nucleoli, several peripherally aggregated, nucleoli with plenty of chromatin in it. In cytoplasm mainly free polyribosome presented, while mitochondria, glycogen and rough endoplasmic reticulum were scant. In the nearby interstitial tissue infiltrated tumor cells, degenerated lymphocytes, damaged fibroblasts,

loose collagen fiber, and many vesicular inclusion bodies in the nuclei were found. The tumor cells of subgroup I revealed necrotic injury, and in the severely injured cells the nuclei lysed, cell membrane disrupted and numerous debris were found. The injured tumor cells showed condensation of nuclear chromatin, peripheral aggregation of heterochromatin in pieces, damaged organelles in cytoplasm, disappearance of mitochondrial cristae and ribosomes, appearance of many vacuoles and lipid particles. In subgroup II, many tumor cells presented histological structures similar to those in subgroup I, but with many lysosomes and mimetic secretory granules. Some were differentiated tumor cells with the characters of round nucleus with small nucleolus, evenly distributed chromatin, mainly euchromatin, mitochondria and rough endoplasmic reticula in the cytoplasm, formation of microvilli at the interface of tumor cells. The capillaries between the moderately differentiated tumor cells had thickened or loosened basal membrane with local defects, and abundant fibroblast and collagen fibers could be found in the matrix. And there was a tendency of bile canal iculi formation somewhere in the matrix. The tumor cells in subgroup III showed different morphologic appearance, some damaged mildly and others severely, but some were moderately differentiated with plenty of cytoplasmic free polyribosomes. Plasma cells scattered among the tumor cells, and some lymphocytes protruded pseudopodia when contacted with the tumor cells, no abnormality was found in the dermal cells of adjacent skin. There were residual tumor cells showing active proliferation in subgroup IV, and some normal or degenerated lymphocytes, fibroblasts and collagen fibers presented in the interstitial tissue near the tumor. In subgroup V, the histological structure was manifested in various complicated forms, and the active multiplication of tumor cells were readily seen.

Toxicological manifestation of liver tissue in domestic pigs

Absorbed dose of ^{32}P -GMS Liver tissue histological parameter of domestic pigs with intrahepatic arterial administration of ^{32}P -GMS and the absorbed dose of internal radiation in liver lobe at the time of euthanasia were estimated (Table 3). By scanning the different body surface regions of experimental pigs, the macrocosmic radioactivity counts in the target organ might attain more than 90% of total dose of ^{32}P -GMS given through the hepatic arterial catheterization. The effect of the dispersed radiation was also included in this rate.



Figure 1 ①After intratumoral injection of ^{32}P -GMS, SPECT revealed radioactive image condensed in the tumor but not in the non-target tissue. ②On the 14th day tumor in treatment group shrank prominently. ③Increased in size and plenty of blood supply in control group.

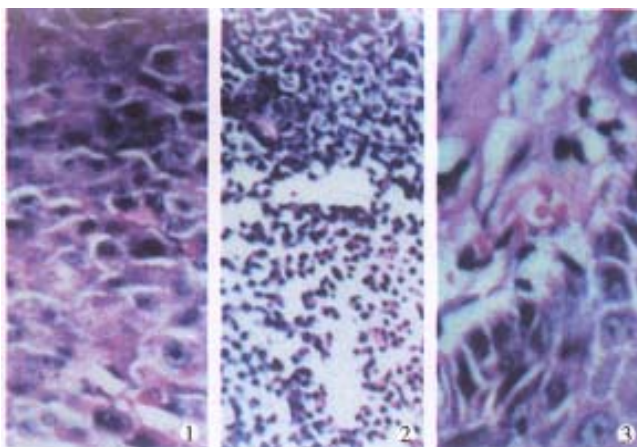


Figure 2 On the 14th day, ①Control group tumor cells densely arranged and actively growing (HE $\times 100$). ②Treatment group, tumor cells in coagulation necrosis (HE $\times 100$). ③ Treatment group, radiation injury in neighboring epidermal tissue (HE $\times 200$).

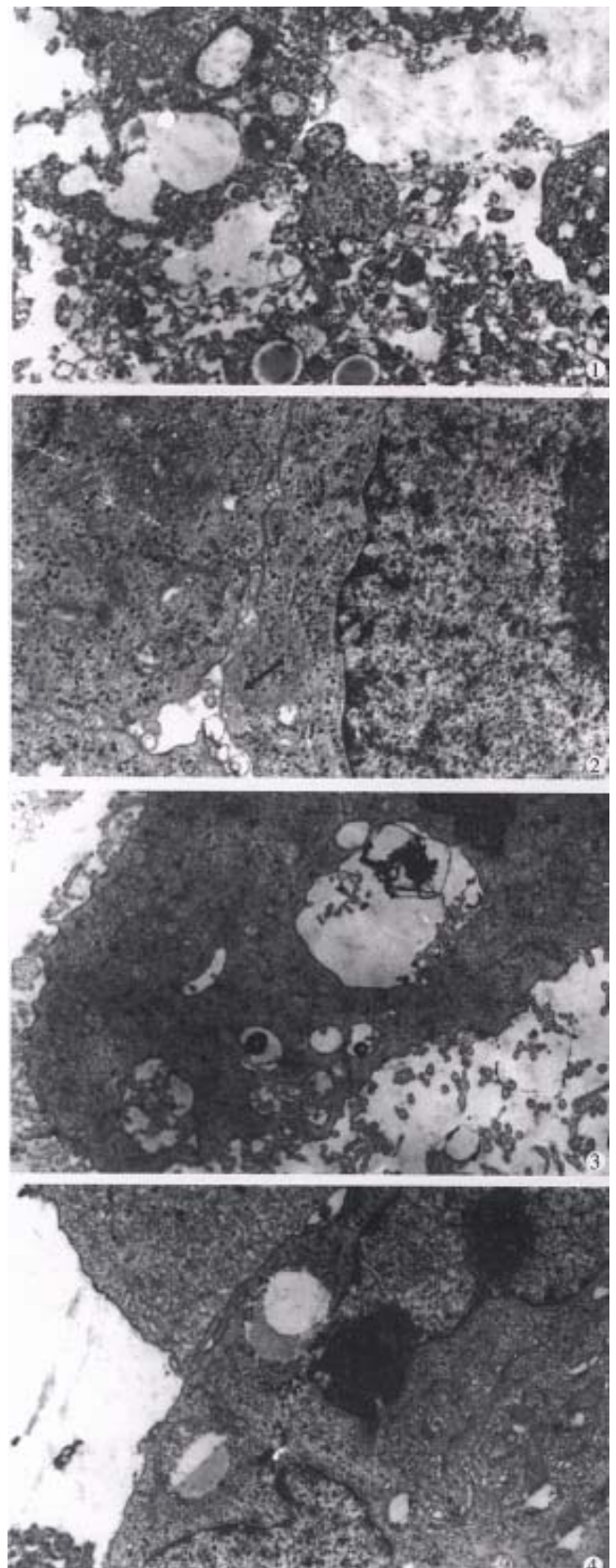


Figure 3 Results of intratumoral injection of ^{32}P -GMS demonstrated by electron microscopy: ①Necrosed tumor cells ($\times 5000$). ②Formation of bile duct-like structure among tumor cells (solid arrow) ($\times 8000$). ③Plenty of microvilli on the surface of tumor cell ($\times 7000$). ④In control group, intratumoral injection of ^{32}P -GMS showing heteromorphic tumor cell with cleavage of nucleus and scanty microvilli on surface ($\times 7000$).

Table 3 Histological liver tissue parameter and estimated value of a absorbed dose in domestic pigs with hepatic arterial administration of ^{32}P -GMS

Animal serial No.	Sex	Route of medication	Time of death (wk)	^{32}P -GMS (MPq·mg ⁻¹)		Weight (mg)	Tissue macroscopic mean absorbed dose (Gy)
				Administered activity (MBq)	Cumulated activity (MBq)		
1	F	Right hepatic artery	1	0	0	300	
2	M	Left hepatic artery	2	0	0	260	
3	F	Hepatic artery proper	4	0	0	1353	
4	M	Hepatic artery proper	8	0	0	374	
5	F	Right hepatic artery	16	0	0	1000	
6	M	Right hepatic artery	1	925	266	313	48
7	F	Left hepatic artery	2	944	465	705	190
8	M	Hepatic artery proper	4	1070	825	375	104
9	F	Left hepatic artery	8	459	529	343	136
10	M	Right hepatic artery	16	461	459	349	61 [△]
11	F	Hepatic artery proper	16	0		0	
12	M	Hepatic artery proper	16	0		0	

[△]Calculated from the estimated liver weight of 1.5kg before medication.

Serological manifestation In warm sphere group, the lactic acid dehydrogenase level attained 2 folds to the upper limit of normal in human being at the beginning, and one week later it rose to 4-6 folds. It did not decline significantly to 3-4 folds until week 4, and then it continuously declined to the initial level at week 8. As for aspartate aminotransferase (AST) or γ -glutamyl transpeptidase (γ -GT) there was an elevation in different degree, but for total protein (TP) and total bilirubin (TB) no changes were observed. These items were neither found abnormal in the cold sphere group nor in blank control one. As for the markers of pig liver fibrosis, the basal level of HA was within normal human range (2 $\mu\text{g/L}$ -100 $\mu\text{g/L}$), in the warm sphere group and rose to the peak and then declined to normal. While in the cold sphere one, it rose slightly at week 1, then restored gradually to normal. The initial level of hPCIII was 2 folds to the upper limit of normal (<120 $\mu\text{g/L}$). Within two weeks of warm sphere administration it increased to 3 folds of the normal value and recovered to initial level within 8 weeks; for the cold sphere group, hPCIII value increased slightly at week 2, then returned to the initial level at week 4. There was no abnormality of above markers in the blank control group. In the dynamic studies of G-IV, C G and LN, no apparent alterations were found in any animal group.

Light microscopy In the portal area the debris of ^{32}P -GMS (Figure 4) was found. In the warm sphere group, some hepatocytes showed granulation and eosinophil granulocytes infiltration at week 2 and week 4; slight granulation of hepatocytes and some with fatty change were found at week 8; no apparent abnormalities were found at the week 16

and during the whole course in cold sphere and blank control groups. no apparent changes were seen in the lung, spleen, stomach and kidney of all the experimental animals.

Electron microscopy (Figure 5) By electron microscopic morphometric analysis, the N_{abn} and M_{var} of the hepatocytes are shown in Table 4. One to two weeks after internal irradiation, in the warm sphere group there were alterations in nuclei and mitochondria, dilatation of rough endoplasmic reticulum, local lytic injury in endothelial lining of sinusoid, and pale faint halo at the periphery of erythrocyte. no liver tissue abnormality was found in the cold sphere group. In warm sphere one at week 4 of internal irradiation, the hepatocytes still showed some abnormal features including decreased mitochondria, distended rough endoplasmic reticulum, detached ribosome, greatly increased lysosomes and myeloid bodies, bile canaliculi disrupted showing cholestasis, and vascular endothelium was prominently damaged. Eight weeks after irradiation, the injured hepatocytes decreased. There were plenty of organelles and glycogen particles in cytoplasm, intercellular junction among the hepatocytes showed normal configuration with regularly arranged microvilli, the matrix of mitochondria condensed, rough endoplasmic reticulum distended, and fat-storing cells of collagen fibers were prominently presented in the Disse's spaces; and endothelium of blood sinus was integrated and accompanied with neutrophil granulocytes infiltration. In the liver tissue of whole liver embolization with cold spheres the nuclei of hepatocytes remained normal, but the cytoplasm revealed the changes similar to those found 4 weeks-8 weeks after internal irradiation.

The liver tissue specimens taken at 16 week of internal irradiation demonstrated that most of the hepatocytes recovered almost to normal with abundant collagen fibers in the Disse's space, while those from cold sphere group were essentially normal. The liver tissue was morphologically normal in the whole course of blank control group.

Table 4 N_{abn} and M_{var} of nucleated hepatocytes and their standard error ($P \pm SE$)

No. of week	Warm sphere group		Cold sphere group		Bland control	
	N_{abn}	M_{var}	N_{abn}	M_{var}	N_{abn}	M_{var}
1	60±4.09 ^a	80±4.00 ^a	9±2.86 ^c	5±2.18 ^c		
2	58±4.94 ^a	77±4.21 ^a	8±2.71 ^c	4±1.96 ^c		
4	38±4.85 ^b	60±4.90 ^b	5±2.18 ^c	6±2.37 ^c		
8	8±2.71 ^{cd}	12±3.25 ^{ce}	3±1.71 ^c	5±2.18 ^c		
16	4±1.96 ^{cd}	4±1.40 ^{ce}	2±1.40 ^c	2±1.96 ^c	2±1.40	2±1.40

Warm sphere group no statistical significance between week 1 and week 2, $\chi^2=0.27$, ^a $P<0.50$. In warm sphere group comparison of week 1 and week 2 with week 4, $\chi^2=6.70-9.68$, ^b $P<0.01$ and with other groups, $\chi^2=65.09-115.09$, ^c $P<0.001$. N_{abn} of week 8 compared with that of week 16, $\chi^2=1.42$, ^d $P<0.20$. M_{var} of week 8 compared with that of week 16, $\chi^2=7.68$, ^e $P<0.01$.

Clinical application

Therapeutic effectiveness (Table 5) In groups A and B, most of the HCC patients with ³²P-GMS treatment revealed prominent symptomatic improvement, relief of pain in liver region, improvement of appetite, gain of body weight, decreased tumor-size and iodized oil condensed in the form of fragments or encapsulated cumulation on the film or CT (Figure 6). No collateral circulation around the tumor body was found after ³²P-GMS treatment, but in 5 cases of group A some secondary foci neighboring the primary foci which had been controlled, appeared within 2-3 months after therapy. no such problem was found in group B. In three cases of diffused type of HCC, the foci were not controlled effectively. Of the 79 cases of HCC, the post-treated tumor size as compared with their original sizes, was decreased more than 50%, 50%-25%, 25%-10% and less than 10% in 24 (30.37%) cases, 25 (31.64%), 22 (27.84%) and 8 (10.1%), respectively. After ³²P-GMS and TAE treatment in group B, 4 received surgical resections of tumor with fair results but the other 6 with decreased tumor size refused to be operated on. Twelve of 14 cases of metastatic hepatic carcinoma after regimen B and C treatment showed decrease in size of foci, giving an effective rate of 85.71%.

Toxic or adverse effects About 2-3 days after TAE treatment in group C, some patients experienced fever of 38.5 °C and had grade IV leukocytopenia, almost all patients had nausea, vomiting and upset

or pain in liver region. Serum ALT, ALP and bilirubin were slightly elevated, the markers of liver fibrosis HA and hPCIII revealed transient elevation, restored to the pretreatment level about half month later, C-IV, LN and CG did not show any fluctuation. no abnormalities were found in renal function and ECG. As compared with group C, the above features in group A patients were rare and mild, among them 7 cases had pre treatment WBC $<2.0 \times 10^9/L$ and one patient with uremia under regimen A treatment did not present significant side effects or complications. In group B patients no grade III-IV gastrointestinal reaction and no grade IV leukocytopenia occurred after treatment (Table 6).

Living quality and survival period The median survival period of HCC patients in groups A and B was 585 days, in group C, 455 days. The 0.5, 1, 2 and 3 year survival rates in group A, B and C were 100%, 96.7%, 56.7%, 43.3%; 97.7%, 91.8%, 61.2%, 51.0% and 96.4%, 81.8%, 41.2%, 31.0%, respectively. The living quality of patients in groups A and B has improved prominently as evaluated by Karnofsky score, which rose from the basal level of 65.5 to 75.5, eventually to 80 in the recovery stage of some individual patients. A patient complicated with uremia maintained by hemodialysis survived up to 26 months after treatment, another patient committed suicide due to the cause unrelated to his illness. Two cases complicated with cancer cell embolism of portal vein survived merely 3.5 and 6.5 months and died from upper digestive tract bleeding and hepatorenal syndrome respectively.

Prognostic factors affecting the survival rate

Multifactorial analysis revealed that the following prognostic factors may affect the survival rate: accumulation of ³²P-GMS in the tumor mass, parameters of hepatic fibrosis, the clinical types, size and its magnitude of decrease after treatment and whether intrahepatic or remote metastasis was present. The therapeutic effectiveness was not fully dependent upon the different histocytological types.

Table 5 Comparison of effectiveness in different therapeutic groups

Grade of effectiveness	Group A	Group B (n)	Group C
>50%	9	15	4
50%-25%	7	18	5
25%-10%	9	13	5
<10%	5	3	4
Effective rate %	83.33	93.87	77.77

RIDIT analysis: A/C: $\alpha \neq 0.05$, no statistical difference between two groups. B/C: $\alpha=0.05$, significant difference between two groups.

Table 6 Comparison of toxic hematological reaction in different groups

Grading	Group A (n)			Group B (n)			Group C (n)		
	Hb	WBC	Plt	Hb	WBC	Plt	Hb	WBC	Plt
0	10	12	12	18	15	16	2	4	2
I	12	16	10	22	24	23	5	2	4
II	8	2	8	7	8	9	6	6	6
III				2	2	1	3	4	3
IV							2	2	3

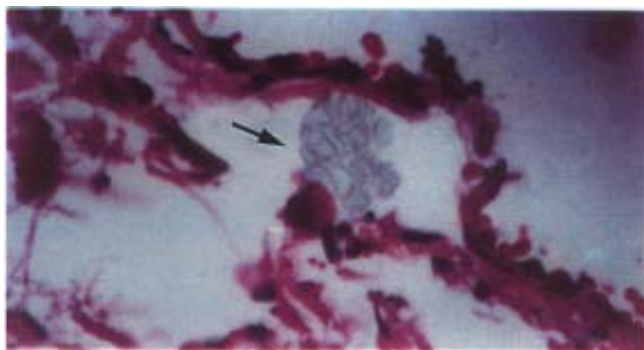


Figure 4 Pig no.10 by intrahepatic artery instillation of ^{32}P -GMS after 16wk, showing the glass fragments (solid arrow shows) in the portal area, the distorted venule in the lower part of the picture is the artifact due to compression of interlobular venule by the glass microsphere during preparing slide. HE stain $\times 400$

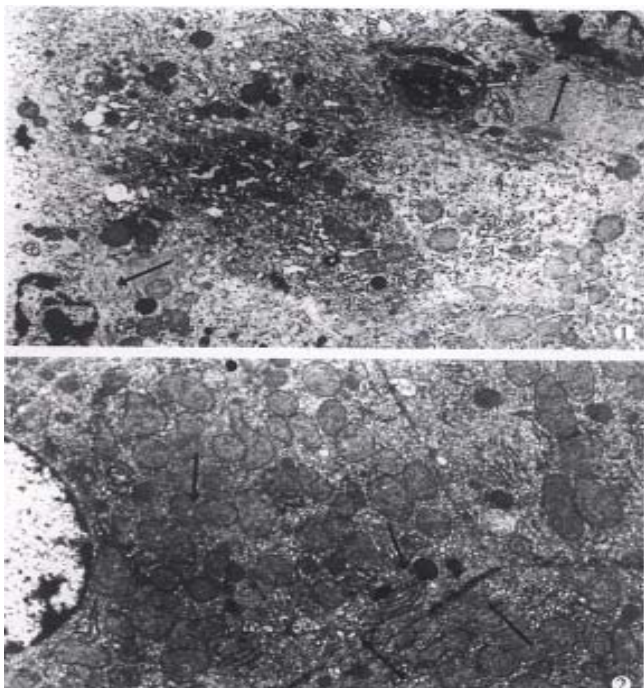


Figure 5 ①First week of internal irradiation irregularly distorted nuclei of hepatocytes, aggregation of heterochromatin at the periphery of nuclei, distension of perinuclear gap (solid arrow); decreased number of mitochondria in cytoplasm with heavy or light stained substance; dilatation of rough endoplasmic reticulum, depleted glycogen, and increased lysosomes and vacuoles. $\times 10\,000$ ②16wk of internal irradiation: normal configuration of hepatocytes, plenty of plasma mitochondria with normal cristae (curved arrow), no distention of the rough endoplasmic reticulum pool (small arrow), nor mal cellular junction (solid arrow). $\times 6000$



Figure 6 ①Case 1. Hepatic carcinoma, massive type, apparently decreased in size two months after ^{32}P -GMS treatment (solid arrow). ②Case 2. Multiple metastatic hepatic tumor apparently decreased in size of left lobe focus after ^{32}P -GMS treatment (solid arrow).

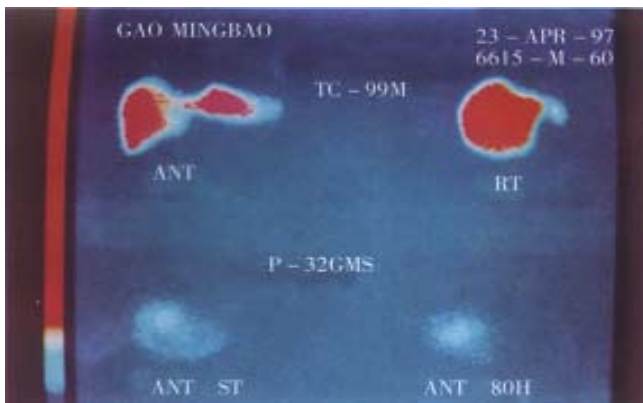


Figure 7 SPECT imaging before and after ^{32}P -GMS internal irradiation in patients with relapsed HCC (interlobular) after operation. Upper picture demonstrates interlobular colloidal image (anterio-posterior and light lateral position). Lower picture shows 80h after ^{32}P -GMS treatment, most of ^{32}P -GMS cumulated in the foci, no extrahepatic organ imaging was found.

DISCUSSION

As the experiment demonstrated that the local internal irradiation of ^{32}P -GMS surely had the cytotoxic effect on tumor cells and exerted a potent inhibitive effect on the growth of tumor even at the third day of medication. The β -ray generated from ^{32}P -GMS exerted injurious effect on tumor tissue with very complicated mechanism: ①After the tumor cells absorbed the α -ray energy, it directly affected the ionization and excitation of biological active macromolecules or broke its chemical bonds and destroyed the molecular structure. Since the active biological macromolecules were the main component of cell membrane, organelle and nucleus, defects in these structures apparently would reflect the impairment of their function. ②The indirect effect of α -ray irradiation was to conduct ionization and irradiation of the water molecule in intracellular environment and to generate many kinds of free radicals and superoxides such as O_2 , H_2O_2 etc. having very active chemical property with high oxidative toxicity. These irradiative products injured or destroyed the biological macromolecules^[12]. ③ β -ray acted on the cell DNA to induce the cell-death related gene expression, hence to accelerate the apoptosis of cancer cells^[13]. When the cancer cells received massive dose of irradiation, the metabolic activity ceased immediately, the cell structure disrupted and lysed, resulting in cell death at metaphase; when the cancer cells received irradiation at a certain dosage, and fulfilled several times of multiplication, they would lose the ability of proliferation leading to proliferative death^[14]. In addition, β -ray irradiation had the effect on occluding capillary vessels and inducing the hyperplasia of connective

tissue in tumor resulting in structural derangement and promotion of the injury and necrosis of tumor cells.

On the 14th day of local injection of ^{32}P -GMS to the tumor, the tumor cell death rate was 43%-82% in different treatment groups, but 4% in control group. The anticancer effect of ^{32}P -GMS was directly proportional to the dose administered. In a particular time period, the rate of tumor cell death exceeded its rate of proliferation, then the tumor decreased in size; on the contrary, the death rate of tumor cell did not exceed their rate of growth, the tumor growth might be somewhat inhibited in a certain extent too. In the specimens of different treatment groups, the tumor cells might exhibit as survived, denatured or necrosed (in early or typical changes). This reflected essentially the whole course of tumor cell progression from denaturing to cell death after irradiation. The ultrastructural changes demonstrated that under the effect of high-dose irradiation, the tumor tissues received a lethal radiation energy in a short period, resulting in nonexistence of tumor cells which had a high ability to synthesize endogenous protein. In subgroup I, two tumor masses ne crossed thoroughly the skin neighboring to one of them showing metaplasia. Whether this was the result of radiation injury evolving to malignant change and degeneration or not should be further investigated. Under the appropriate dose of irradiation (subgroup II and III), besides most of the tumor cells necrosed, the tendency of deriving to nearly normal histological picture evolved, such as plenty of microvilli on the cell surface, genesis of bile canaliculi-like structure, etc. These demonstrated that the ^{32}P -GMS has the ability of killing the actively proliferative tumor cells and promoted the normalization of regenerative cells. These were similar to the effect of irradiation in trace amount which might stimulate and enhance the local metabolism of inflammatory tissues, accelerate the death of injured cells and promote the growth of normal tissue, but this was not found in control group. It is also observed that the synergistic effect of immunocytes, cytolytic phenomena and its inhibition on the dispersion of tumor cells were enhanced in the tumor cells or nearby tissues. It denoted that the anticancer effect of ^{32}P -GMS was directly proportional to the time course of medication, based on the principle of after effect and cumulative effect of radioactive nuclide therapy. After intratumoral injection of ^{32}P -GMS, it was not dispersed or displayed to the non-targeting tissue as confirmed by SPECT imaging. In comparison with intratumoral injection of ethyl alcohol^[15] or acetic acid^[16,17], ^{32}P -GMS needs no repeated injection, with minimal side reaction^[18].

Intratumoral injection of ^{32}P -GMS was the best choice in treating the unresectable tumor or some metastasized lesion as well as those unsuitable for intra-arterial interventional therapy, it was also suitable for solid malignant tumors which could be reached anywhere on the human body.

We have got sufficient data from the dynamic study on the ultrastructural morphometric analysis of liver tissues taken from warm sphere, cold sphere and control groups. According to the injury of normal liver after internal irradiation and its repairing process, it was allocated into 4 periods: ① acute reactive period (within 2 weeks), ② subacute reactive period (2-4 weeks), ③ prerecovery period (4-8 weeks), ④ recovery period (8-16 weeks). In the acute period of warm sphere group, there was decreased proteosynthetic function and alteration of energy metabolism, decreased synthetic ability of ATP. The faint halo around the erythrocytes in the blood sinus as shown under electron microscopy probably was the super liquidized iodized oil. The disruption of sinusoidal endothelium was closely related to the route of medication. No apparent injury of hepatic tissue was found in the control group. This suggested that the serial changes in ultrastructure which was seen in the warm sphere group might be the result of radiation injury. The sinusoidal endothelium was most prominently disrupted. All these changes represented the synergistic action of internal irradiation and embolization. At the prerecovery period, the abnormal nuclei of hepatocytes were scarcely seen, but the cytoplasmic organelles recovered more slowly than the nuclei. Cell injury was resulting in increase in myeloid bodies in the cytoplasm, which indicated the liver tissue evolved into self-repairing stage. The hepatocytes appeared essentially normal in the recovery period. Electron microscopy revealed prominent collagen fibers in the Disse's space in some of the liver specimens, whether it indicated the tendency of early liver fibrosis or not should be further studied.

Recent evidences^[19] showed the C-IV increases prominently in the early stage of liver fibrosis, LN is closely related to the genesis of liver fibrosis, and CG is the important marker for estimating the severity of biliary cirrhosis, but the serum C-IV, LN and CG all fell into the human normal range in the whole course of the experimental animals. Therefore, the presence of collagen fibers in the Disse's space was probably of transient local changes. The transient changes in HA value were similar to those of hPCIII, and the liver injury induced serum HA elevation was positively proportional to the severity of illness, and the serum hPCIII level was closely related to the extent of fibrosis. When the function of hepatocyte was

damaged, hPCIII might be released to circulation and often used as the guidance for selection of therapeutic medicine^[20]. Therefore, the transient changes in domestic pig serum HA and hPCIII values were the impairment of liver function resulted from ^{32}P -GMS administration. It was reported^[21] that intra-hepatic arterial administration of cold spheres to the dosage equivalent to 12 folds of the human tolerable dose merely induced the clinical permissible intrahepatic changes and did not follow with portal fibrosis or hepatic cirrhosis after 90 days observation. The experiment demonstrated that the cold sphere slightly injured the hepatocytes, probably being the embolization of the nutritional artery rather than irradiation. In this experiment, through hepatic artery medication, no non-target organs developed in all of the domestic pigs. No prominent ultrastructural changes were found in the hepatic lobe during the whole course in the control animals. The experiment demonstrates that intrahepatic change of clinically permissible extent might be induced in the liver tissue of domestic pigs that received ^{32}P -GMS in the macrocosmic average absorbed dosage of 48Gy-190Gy. These changes were reversible sublethal injury^[14] and essentially recovered within 8 weeks. In the observation of 120 days there was no evidence of portal fibrosis. This is the evidence that superselective intrahepatic medication may yield a high energy region and without serious injury to the nearby non-medicated tissues or organs.

Hepatic artery embolization is the important measure in treating hepatic carcinoma^[22,23]. Investigating an ideal embolizing agent is the substantial project in interventional therapy of tumor. The ideal internal radioactive nuclide should serve as a spotted source of radiation with high energy reserve and the carrier having high orientating rate, lasting longer in the target tissue, and the loaded nuclide was not easy in detaching or leaking to circulation. ^{32}P -GMS, administrated through the hepatic artery, wedged in the terminals of this artery with its mixed iodized oil which was not absorbable could occlude the arterial capillary. In addition to the radiation obliteration of blood vessels induced by internal irradiation, the collateral circulation was not readily generated in the foci. All of the above mentioned advantages will benefit to boosting therapeutic efficiency. Therefore ^{32}P -GMS is an appropriate internal radioactive embolizing agent with medium or long duration. It has been confirmed in the clinical investigation, the tumor in liver showed angiogenesis at the microcirculatory level and might trap microspheres 3-4 folds to that of normal liver tissue^[24-26]. Instillation of therapeutic dose of radionuclide to the nutritional arteries of tumor, particularly condensed in the tumor tissue, may exert potent cytotoxic effect to

fulfill the purpose of therapy. It has been reported^[27-29] that Yttrium-90-GMS (^{90}Y -GMS) used in intrahepatic arterial embolization got fair result, and the absorbed dosage attained 50Gy-100Gy in the tumor may have radical effectiveness^[29]. Nevertheless ^{90}Y -has the disadvantages of short half-life, inconvenienced in clinical application, and ^{90}Y -GMS having smaller diameter, and higher hepato-pulmonary shunting index than that of ^{32}P -GMS^[30]. As reported that intratumoral injection of ^{90}Y -GMS in 33 cases of hepatic carcinoma, the bremsstrahlung radiation conducted by SPECT showed 21.4% had development in lung, and 14.3% in intestine. In our study ^{32}P -GMS in therapeutic dosage through superselective hepatic arterial regional instillation, particularly condensed in the tumor tissue including the central and peripheral portions, forming a high energy region and it is worth noting that extra-hepatic development was not found (Figure 7). Therefore transhepatic artery administration of anticancer agent is the first choice in regional medication to treat hepatic tumor. If the hepatic artery is severely distorted or fails in catheterization, intraparenchymal injection of ^{32}P -GMS should be considered instead.

The therapeutical results of TAE were inconsistent in different histocytological type of HCC^[31]. The clear cell type was most sensitive, the small cell and poorly or undifferentiated type was moderately sensitive. Based on the radio-biology, cell sensitivity to nuclide beam depended upon the functional status of the cell proper. The cytotoxic effect and durability of ^{32}P -GMS was superior to the other anticancer chemicals. The therapeutic results depended upon the clinical classification rather than histocytological types.

The results of clinical observation revealed that the clinical classification and the specific features of angiogram might be the basis for evaluating the therapeutical effectiveness and predicting the prognosis. The clinical materials suggested that the regimen B is superior to regimen A and C in the respect of decreasing tumor size and prolonging the survival period. The follow-up results demonstrated that the excellent effect was evolved in the cases with small tumors, plenty of blood supply, intact capsule and heavily aggregated ^{32}P -GMS in the tumor as revealed by SPECT. Analysis of the clinical classification showed that in average survival time of the 3 clinical types of HCC solitary mass type was longer than the multiple and diffuse type. The patients with apparent decrease in AFP level were consistently accompanied with decrease in tumor size and necrosis in the tumor. In case of these features relapsed and elevation of AFP or complicated with intrahepatic or remote metastasis, all these would result in poor prognosis.

Strategy of therapy: for those hepatic

carcinoma with intact capsule and diameter below 6cm treated by the regimen A for 1 or 2 courses could get satisfactory result, and for those with occult metastatic foci, the secondary foci would be present besides the controlled original lesion several months later. It is of significance to use ^{32}P -GMS and TAE in combination resulting in apparent synergetic effect (regimen B), which not only enhanced the anticancer and embolic effects but also lessened the side effects, and could completely cure the small liver cancer, eliminated the need of operation (Figure 8), diminished the number of medication with mild liver injury and low relapse rate. After undergoing regimen B treatment, some cases of unresectable tumor acquired the possibility of being resected (Figures 9, 10). The dosage of ^{32}P -GMS should be decided by the specialists majoring in nuclear medicine and interventional therapy. The optimal schedule was to give two courses of medicine at an interval of 2 months, and as the tumor size decreased, the residual lesion should be resected as soon as possible in order to improve the survivability. There were few viable cancer cells in the 4 resected specimens on pathological examination after the regimen B treatment. Hepatic carcinoma readily invaded the portal vein with cancer cell emboli. It is apparent in such case that intrahepatic artery medication should be complemented with other measures as minimal invasive embolectomy which will be an intelligent choice. For the metastatic abdominal lymph nodes intratumoral injection of ^{32}P -colloids under the guidance of CT is also a helpful measure. It is emphasized that we should choose reasonable regimen, strict manipulation, superselective catheterization, well controlled speed in medication to avoid regurgitation of nuclide to the non-target blood vessel, and lessen the complication, particularly depending on the individualized situation. The hepatic arterio-venous fistula should be considered as the contraindication for medication via catheterization.

In conclusion, ^{32}P -GMS which possesses the anticancer effect through interventional medication may block the blood supply to tumor and evenly distribute the highly concentrated anticancer medicines in the tumor to exert the radioactive cytotoxic effect with the advantage of low local radiation reaction and no apparent systemic toxic effect. ^{32}P -GMS is an effective measure for the comprehensive treatment of hepatic cancer. Owing to the moderate half-life of ^{32}P , the dosage of ^{32}P -GMS required to attain the same absorbed radioactivity is approximately one-fourth or one-third of ^{90}Y -GMS dosage^[8]. Therefore it will satisfy the clinical requirement in reducing the risk of radiation to the handlers, simplifying the medical care and lowering the expenses. Thus, a hopeful prospective therapeutic weapon will be developed and popularized in the near future.

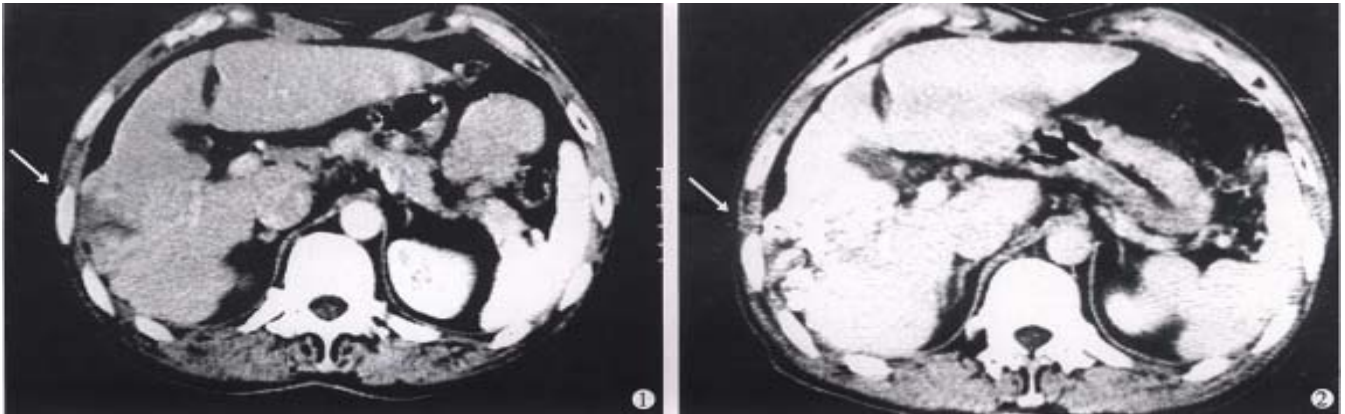


Figure 8 Male, aged 60, hospital no.202929, clinical diagnosis: right lobe medium sized hepatic carcinoma (4cm×5cm), treated by regimen A and B with an interval of 2 months. AFP from 103μg/L restored to normal range, tumor size decreased >50%, CT: 1, on pre-treatment showing a low density region in right lobe (arrow), 2, on post-treatment iodized oil distributed in fragments or encapsulated forms (arrow). Body weight gained more than 5kg and no subjective symptoms on 36 months follow-up.

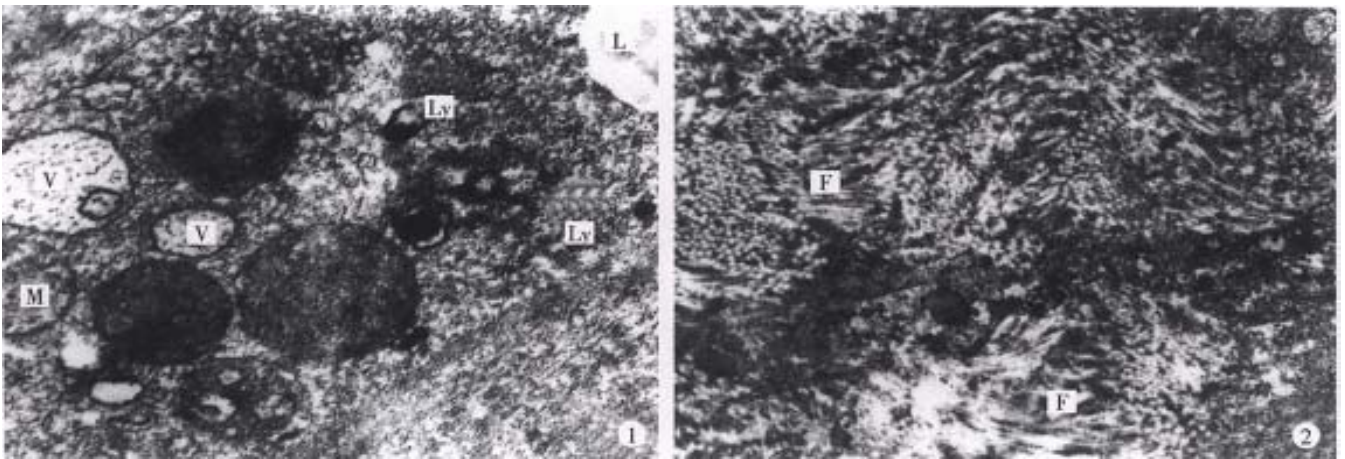


Figure 9 Male, aged 55, hospital no.202295, clinical diagnosis: left lobe medium sized hepatic carcinoma (5cm×6cm) near the hepatic hilus, treated by TAE and regimen B, with interval of 2 months, and left hepatic lobectomy was performed 6 months later. The tumor (4cm×4cm) was with hard consistency, and encapsulated fibrotic degeneration. Most of the cancer cells showed necrosis under light microscopy. Some cancer cells in the cholecystic wall were alive (may be due to the blood supply from cholecystic artery). The electron microscopy showed: 1, cancer cells degenerated and necrosed; in cytoplasm some vacuolized mitochondria (M), irregular sized vacuoles (V) and lysosome (Ly) and lipid droplet (L) were seen. The rest structures were not clear (×30000). 2, Prominent fibro-connective tissue hyperplasia (F) in the tumor tissue (×10000) was found. Patient gained body weight and no subjective upset on follow up until 12 months after operation.

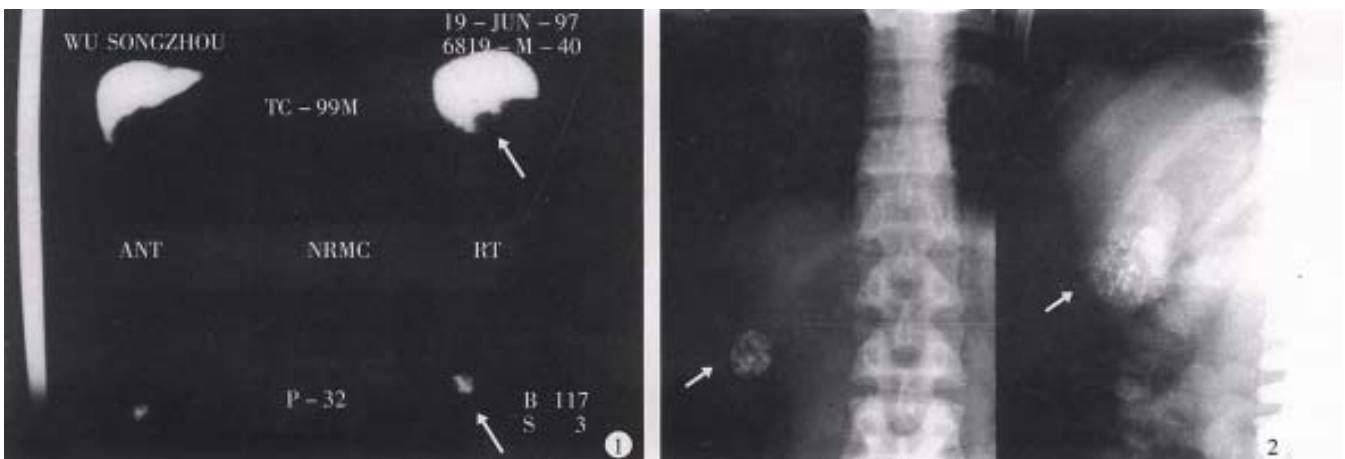


Figure 10 Male, aged 41, hospital no.207089, clinical diagnosis: uremia, right hepatic small carcinoma (4cm×3cm), with AFP>400μg/L treated by regimen A for 2 courses with interval of 3 months, resulted in AFP restored to normal level and decreased tumor size over 50%. 1, Colloidal SPECT imaging showed the space occupying lesion in the right liver lobe (as shown by arrow). 2, Comparing the tumor size before and after treatment of plain film (as arrow shown), the patient died from renal failure 26 months after operation.

REFERENCES

- 1 Tang YX, Jiang YD, Zhang Y, Li YJ, Nie Y, Zang H, Zhang XZ, Qiao WA, Lan FS. Observation on the therapeutic results of interventional irradiation in mid and late stage hepatic carcinoma. *Linchuang Yixue Yingxiang Zazhi*, 1997;8:224-225
- 2 Zhang YH, Wu YB. Advances of anticancer target preparation. *Zhongguo Yaoxue Zazhi*, 1992;27:389-393
- 3 Kobayashi H, Hidaka H, Kajiya Y, Tanoue P, Inoue H, Ikeda K, Nakajo M, Shinohara S. Treatment of hepatocellular carcinoma by transarterial injection of anticancer agents in iodized oil suspension or of radioactive iodized oil solution. *Acta Radiol Diag*, 1986;27:139-147
- 4 Herba MJ, Illescas FF, Thirlwell MP, Boos GJ, Rosenthal L, Atri M, Bret PM. Hepatic malignancies: improved treatment with intraarterial Y90. *Radiology*, 1988;169:311-314
- 5 Houle S, Yip TCK, Shepherd FA, Rotstein LE, Sniderman KW, Theis E, Cawthorn RH, Richmond Cox K. Hepatocellular carcinoma: pilot trial of treatment with Y 90 microspheres. *Radiology*, 1989;172:857-860
- 6 Sun WH, Zhang LZ, Li ML. Research on radiotherapy of ³²P glass microsphere. *Hedongli Gongcheng*, 1990;11:75-78
- 7 Loveinger R, Holt JG, Hine GJ. Internally administered radio isotopes. In: Hine GJ, Brownell GL, eds. Radiation Dosimetry. New York: Academic Press, 1956:801-873
- 8 Liu L, Sun WH, Wu FP, Han DQ, Teng GJ, Fan J. An experimental study of treatment of liver cancer by locally administration with phosphate ³²P glass microspheres & estimation of tissue absorbed dose. *Nanjing Tiedao Yixueyuan Xuebao*, 1997;16:223-226
- 9 Bao JZ, Wang Y, Zhan RZ, Wu MC. Clonal analysis of a hepatocarcinoma cell line: an experimental model of tumor heterogeneity. *Zhongliu Fangzhi Yanjiu*, 1995;22:65-67
- 10 Common statistic form and method in the diagnosis and treatment of tumor. In standards for diagnosis and treatment of common malignant tumor in China, Section 9, edited by Dept Medical Administration, Ministry of Public Health, PRC. Beijing: Beijing Med Univ & China Union Med College Joint Press, 1991:10-15
- 11 Yang SQ, eds. Health statistics. 3rd edition. Beijing: The Public Health Press, 1993:43-181
- 12 Editorial board of practical oncology. Practical Oncology. Vol. 1. Beijing: People's Medical Press, 1997:406-413
- 13 Zheng DX. Advance in apoptosis research. *Zhonghua Binglixue Zazhi*, 1996;25:50-53
- 14 Liu XC, Han KC. Hygienic protection and safety transportation of radioactive materials. Beijing: *Zhongguo Tiedao Chubanshe*, 1990:55-66
- 15 Ohto M, Karasawa E, Tsuchiya Y, Kimura K, Saisho H, Ono T, Okuda K. Ultrasonically guided percutaneous contrast medium injection and aspiration biopsy using a real time puncture transducer. *Radiology*, 1980;136:171-176
- 16 Ohnishi K, Ohyama N, Ito S, Fujiwara K. Small hepatocellular carcinoma: treatment with US guided intratumoral injection of acetic acid. *Radiology*, 1994;193:747-752
- 17 Zhao YF, Wen QS, Jia ZS. Local acetic acid injection in the treatment of transplanted tumor in mice. *Shijie Huaren Xiaohua Zazhi*, 1999;7:43-45
- 18 Liu L, Fan J, Zhang J, Du MH, Wu FP, Teng GJ. Experimental treatment carcinoma in a mouse model by local injection of phosphorus ³² glass microspheres. *J Vasc Interv Rad*, 1998;9:166
- 19 Ueno T, Inuzuka S, Torimura T, Oohira H, Ko H, Obata K, Sata M, Yoshida H, Tanikawa K. Significance of serum type IV collagen levels in various liver diseases. *Scand J Gastroenterol*, 1992;27:513-520
- 20 Axel MG, Wolfgang T, Anne N, Karl Heinz PK. Serum concentrations of laminin and aminoterminal propeptide of type III procollagen in relation to the portal venous pressure of fibrotic liver diseases. *Clin Chim*, 1986;161:249-258
- 21 Wollner I, Knutsen C, Smith P, Prieskorn D, Chrisp C, Andrews J, Juni J, Warber S, Klevering J, Crudup J, Ensminger W. Effects of hepatic arterial yttrium-90 glass microspheres in dogs. *Cancer*, 1988;61:1336-1344
- 22 Wang DZ, Sun WH, Zheng GY, Li ML, Wen YM. A study about the anticancer effect and the clinical application of the phosphate ³² glass microspheres (P32 GMS) by local arterial infusion. I. The ultrastructural study after internal radiation of P ³²GMS in cancer cells. *Huaxi Kouqiang Yixue Zazhi*, 1991;9:7-10
- 23 Chen XL, Wu YT, Yan LN, Li L, Tan TZ, Sun WH, Li ML, Jia QB, Du JP, Shen WL. Treatment of liver cancer with ³²P glass microsphere-an experimental study. *Puwai Jichuyulinchuang Zazhi*, 1996;3:68-70
- 24 Blanchard RJ, Grotenhuis I, Lafave JW, Perry JF. Blood supply to hepatic V2 carcinoma implants as measured by radioactive microspheres. *Proc Soc Exp Biol Med*, 1965;118:465-468
- 25 Sundqvist K, Hafstrom I, Perrson B. Measurements of total and regional blood flow and organ blood flow using Tc-99m labeled microspheres. *Eur Surg Res*, 1978;10:433-443
- 26 Gyves JW, Ziessman HA, Ensminger WD, Thrall JH, Niederhuber JE, Keyes JW, Walker S. Definition of hepatic tumor microcirculation by single photon emission computerized tomography (SPECT). *J Nuc Med*, 1984;25:972-977
- 27 Yan ZP, Lin G, Zhao HY, Dong YH. An experimental study and clinical pilot trials on yttrium 90 glass microspheres through the hepatic artery for treatment of primary liver cancer. *Cancer*, 1993;72:3210-3215
- 28 Andrews JC, Walker SC, Ackermann RJ, Cotton LA, Ensminger WD, Shapiro B. Hepatic radioembolization with yttrium-90 containing glass microspheres: preliminary results and clinical follow-up. *J Nucl Med*, 1994;35:1637-1644
- 29 Shepherd FA, Rotstein LE, Houle S, Yip TCK, Paul K, Sniderman KW. A phase I dose escalation trial of yttrium-90 microspheres in the treatment of primary hepatocellular carcinoma. *Cancer*, 1992;70:2250-2254
- 30 Tian JH, Xu BX, Zhang JM, Dong BW, Liang P, Wang XD. Ultrasound guided internal radiotherapy using yttrium 90 glass microspheres for liver malignancies. *J Nucl Med*, 1996;37:958-963
- 31 Wang YP, Zhang JS, Gao YA. Therapeutic efficacy of transcatheter arterial embolization of primary hepatocellular carcinoma: discrepancy in different histopathological types of HCC. *Zhonghua Fangshexue Zazhi*, 1997;31:586-588

Edited by WU Xie-Ning and MA Jing-Yun
Proofread by MIAO Qi-Hong

Portal vein embolization by fine needle ethanol injection: experimental and clinical studies

LU Ming-De, CHEN Jun-Wei, XIE Xiao-Yan, LIANG Li-Jian, HUANG Jie-Fu

Subject headings liver neoplasms/therapy; portal vein embolization; ethanol injection; carcinoma, hepatocellular/therapy

Abstract

AIM To improve the technique of intraportal embolization (PVE) therapy, a new embolic method, was devised and the safety, effectiveness and feasibility were evaluated.

METHODS PVE with intraportal ethanol injection via a fine needle was performed in 28 normal dogs, 22 SD rats, and 24 cirrhotic SD rats. After PVE, portography, histological and functional alteration of the liver were evaluated in dogs and rats, and the changes in portal hemodynamics as well as hepatic anatomy were observed in rats. In the clinical study, PVE by ethanol injection was performed in 61 patients with hepatocellular carcinoma under the guidance of portoechography with intraportal injection of CO₂. The effect of PVE was evaluated by ultrasonography and laparotomy.

RESULTS The effectiveness and toxicity were dependent on the dose of ethanol. In the dogs, 0.25mg/kg of ethanol caused incomplete embolization with least liver damage, while 1.0mg/kg induced complete embolization with a high mortality of 57.1% (4/7) due to respiratory arrest. The dose of 0.5mg/kg resulted in complete embolization with slight toxicity to the liver. In the rats, the survival rate was 100% in normal group but 40.9% in cirrhotic models after ethanol injection by dose of 0.05mg/100g. PVE for cirrhotic rats with 0.03mg/100g of ethanol induced satisfactory embolization with

significant hypertrophy in nonembolized lobes, and only slight damage to the hepatic parenchyma, and transient alteration in liver function, portal pressure and portal flow. In the clinical study, 12 cases with reverse portal flow were excluded judged by portoechography. Satisfactory embolization was gained in 90.2% (55/61) of the remaining patients determined by ultrasonography and surgery. All cases ran an uneventful postembolization course with no aberrant embolization.

CONCLUSION PVE with intraportal ethanol injection of appropriate dosage via a fine needle is safe and effective and has several advantages comparing with transcatheter method. Portoechography is a mandatory approach for the prevention of aberrant embolization.

INTRODUCTION

Hepatocellular carcinoma (HCC) is one of the most common malignancies in China. The resection rate is less than 30% since most patients are associated with cirrhosis and poor liver function. Furthermore, there are tumor emboli in the portal vein which limits surgical resection. Portal vein embolization (PVE) has been performed to increase the safety and resectability of hepatectomy by improving the functional reserve of the liver^[1-3], and prevent cancerous dissemination via portal vein^[4] and enhance the therapeutic efficacy of transcatheter arterial chemoembolization (TACE)^[5]. However, conventional PVE requires catheterization under both sonographic and fluoroscopic guidance, and selective embolization is not easy. To improve the technique, we developed a method of intraportal ethanol injection via a fine needle under the guidance of portoechography. This study is mainly to investigate the safety, effectiveness and feasibility of this technique and a series of experimental and clinical studies were carried out.

MATERIALS AND METHODS

PVE in dogs with normal liver

Twenty-eight mongrel dogs of both sexes weighing 7.5kg-15.0kg were provided from the Laboratory Animal Center of our university. Under

Department of Hepatobiliary Surgery, the First Affiliated Hospital, Sun Yat-Sen University of Medical Sciences, Guangzhou 510080, Guangdong Province, China

Dr LU Ming-De, male, born on 1951-03-25 in Hunan Province, graduated from Sun Yat-Sen University and earned Doctoral Degree (DMSc) from Kyushu University (Japan), Professor and Director of Department of Surgery, majoring in hepatobiliary surgery, having 95 papers published.

Supported by grants from the National Science Foundation of China, No.393706697 and Science and Technology Commission, Guangdong Province, China, No.970066.

Correspondence to: Dr Lu Ming-De, Department of Hepatobiliary Surgery, the First Affiliated Hospital, Sun Yat-Sen University of Medical Sciences, Guangzhou 510080, China

Tel. +86-20-87755766 Ext. 8599, Fax. +86-20-87765183

Received 1999-07-11 Accepted 1999-09-22

intraperitoneal anesthesia with sodium pentobarbital 30 mg/kg, laparotomy was performed and the left portal branches were exposed. Puncture of the origin of the portal branches supplying the left central and lateral lobes was done with a 22-gauge needle. Then 95% ethanol was injected at a dose of 0.25 mL/kg (group A, $n=7$), 0.5 mL/kg (group B, $n=11$) and 1.0 mL/kg (group C, $n=7$) at a rate of 3 mL/min.

One or two dogs in each group underwent relaparotomy 30 or 60 min after injection and a 6 Fr catheter was placed in the portal trunk. The liver together with the portal trunk was taken out. Portography with the mixture of Urografin (Schering AG, Germany) and Lipiodol (Guerbet, France) via the catheter was performed. Then the intrahepatic portal system was dissected to confirm the site of the thrombus. The same procedures were carried out at day 1 and 3, as well as of week 1, 2 or 4 in groups A and B and week 2 or 4 in group C after ethanol embolization. Tissue samples from embolic and nonembolic liver lobes were examined histologically at the same time.

PVE in rats with normal and cirrhotic liver

Sprague-Dawley (SD) rats with a body weight between 200 g–250 g were used in this experiment. Initially, twenty normal rats had liver resected under anesthesia, and the right, middle, left lobes and the whole liver of each rat were weighed. The mean weight ratios of right, middle and left lobes to the whole liver were 40.5%, 36.5% and 23.0%, respectively.

The cirrhotic model of rat was reproduced by subcutaneously injection of 60% CCl_4 with a dose of 0.3 mL/100 g once every 4 days. Throughout the period, the rats were fed with ordinary food and 5% ethanol drinking water. Histological examination confirmed the development of cirrhosis at 60 days after initial administration of CCl_4 .

In order to test ethanol tolerance of the normal and cirrhotic rats, laparotomy was performed in both normal ($n=10$) and cirrhotic rats ($n=22$) under intraperitoneal anesthesia with pentobarbital. After exposure of the hepatic hilum, portal vein was punctured with a 3-gauge needle and inject a dose of 0.05 mL/100 g of absolute ethanol. All rats in the normal group were alive but only 9 of 22 (40.9%) in the cirrhotic group survived 4 days after the injection.

Based on the technique and the results described above, embolization of the portal branches of left and central lobes (the embolized tissue accounted for 77% of the whole liver) was employed for 22 normal rats (NE group) with a dose of 0.05 mL/100 g of absolute ethanol. The portal branch of middle lobe (accounted for 36.5% of the

liver) was embolized in 24 cirrhotic rats (ME group) with a dose of 0.03 mL/100 g. The same amount of normal saline was injected into portal vein in 10 normal rats (NC group) and 10 cirrhotic rats (MC group).

At day 1, 3, 7 and 14 after PVE, the following examinations were carried out: X-ray portography, the weight ratio of hepatic lobes, liver function tests (ALT, TBIL, ALP, ALB, A/G), liver histology, portal blood flow and portal pressure measured by MRF-1200 electromagnetic flowmetry (Nikon, Japan).

PVE in patients with HCC under the guidance of portoechography

PVE was undertaken under local anesthesia. A portal branch supplied the tumor bearing segment was punctured percutaneously under the guidance of Aloka SSD 650 or 1200 ultrasound system and 3.5 MHz linear puncture probe. In order to identify the precision of the puncture and whether or not a retrograde blood flow was present, portoechography was initially introduced with injection of 5 mL carbondioxide (CO_2). If the diffusion of CO_2 was beyond the ipsilateral lobe of the liver, PVE was abandoned in case of aberrant embolization; otherwise PVE was performed with intraportal injection of 95% ethanol. The dose of ethanol ranged from 4 mL to 10 mL depending on the level the portal branch to be blocked.

From February 1993 to February 1993, portoechography was performed in 73 patients with HCC. But was quit in 12 cases due to CO_2 diffusing into both lobes of the liver. Sixty-one patients (55 males and 6 females) with an average age of 52.5 years received PVE. Forty-nine patients had cirrhosis without jaundice, ascites or serious liver function had damage^[6]. The tumors ranged from 3 cm to 12 cm in diameter, located at right lobe in 58 and left lobe in 15. All 61 patients underwent surgery 3–5 days after PVE including hepatectomy in 37 patients.

RESULTS

Canine experiment

One dog in group B died of wound infection on day 5. Four of 7 dogs in group C died of respiratory arrest on the day of the injection.

Intrahepatic portography and dissection of the portal system showed the injected portal branches were patent at 30 min and 60 min after embolization. Thrombosis was developed on day 1. In group A, portal vein embolization occurred at one segment of the liver in six dogs and failure of embolization in one dog. In groups B and C, embolization occurred at both left and central lobes in most dogs. In one dog of group B, the orifice of the branch of the

quadrate lobes was approximate to the branch of left lobe, and overembolization involving the quadrate lobes occurred. No thrombus was detected at the non-injected branches in any other dogs.

Macroscopically, the embolized lobes were swollen and congested but without any evidence of necrosis. Dark red thrombus had developed within the ethanol-injected portal branches on day 1 or 3, which were organized one week after PVE. Microscopically, focal inflammation of the intima was found in the affected portal branches. Small foci of coagulation necrosis prominently surrounding Glisson cap sule were detected at the embolized lobes and the normal structure of the lobules was preserved. The necrotic area was less than 10% of the effected lobes. Transient elevation of white blood cell and alanine aminotransferase (ALT) occurred at day 1 but returned to the baseline values within one week. The level of total bilirubin, albumin and γ -globulin did not significantly change after PVE.

Rat experiment

The survival rate after PVE was 95.8% in both NE and ME group. Postoperative portography demonstrated filling defects at injection sites and dissection of the portal system indicated the corresponding portal branches were embolized. The weight of the embolized hepatic lobes decreased gradually as the weight of non-embolized lobes increased with the time after PVE (Figure 1). On day 14, the weight of nonembolized lobes was significantly greater than the baseline value in both NE group ($5.25 \text{ g} \pm 0.38 \text{ g}$ vs $1.86 \text{ g} \pm 0.42 \text{ g}$, $P < 0.01$) and ME group ($9.58 \text{ g} \pm 1.10 \text{ g}$ vs $5.13 \text{ g} \pm 0.53 \text{ g}$, $P < 0.01$) and ratio of the nonembolized lobes to the whole liver significantly increased from 23% to 68.8% in NE group and from 63.5% to 86.8% in ME group.

Histological findings on day 1 or 2 were similar to that in the experiment of normal dogs. With respect to the ratio of total necrosis area to embolized area, ME group (30%-40%) was more severe than NE group (10%-20%). One week after PVE, organization or calcification of thrombi with partial recanalization as well as hyperplasia of fibrotic tissue in the embolized lobes was noted. Hepatocytes of the non-embolized lobes became hypertrophied and proliferative, which were more remarkable in ME group than in NE group.

The hemodynamic study demonstrated that ME group had significantly higher portal blood flow and portal pressure than NE group before PVE. On day 1 after PVE, portal blood flow and portal pressure declined slightly in both groups, then increased to a limited degree and returned to the baseline values at week 1 after PVE (Figures 2 and 3).

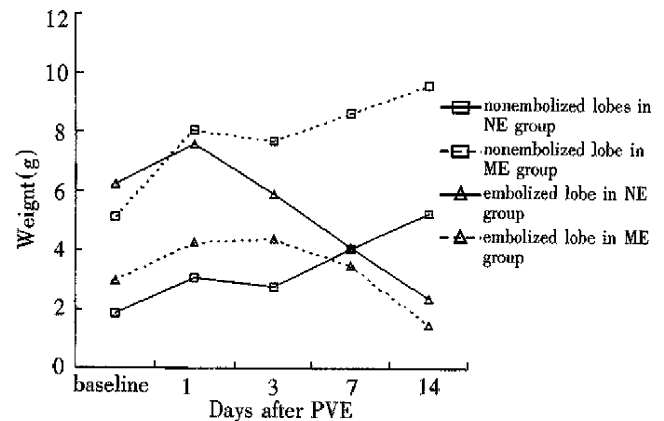


Figure 1 Changes in weight of hepatic lobes after PVE with fine needle technique.

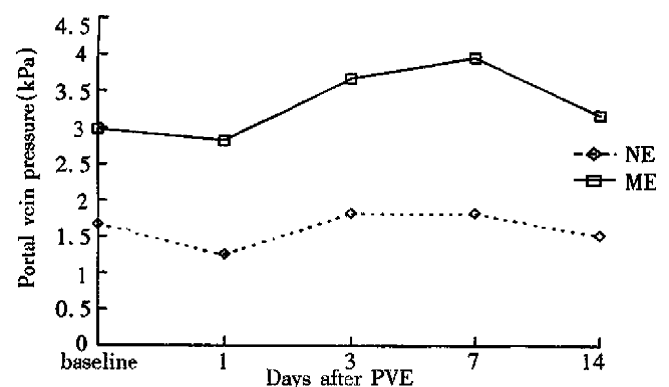


Figure 2 Changes in portal vein pressure after PVE.

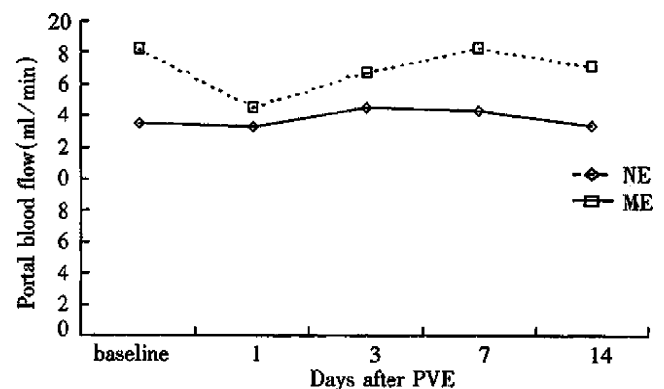


Figure 3 Changes in portal blood flow after PVE.

The serum ALT, TBIL and ALP were elevated. After PVE, they began to fall on day 3 and returned to the pre-PVE level. The albumin and A/G ratio did not significantly change in both groups after PVE.

Clinical study

The punctures were confirmed to be proper by portoechography in all cases. By CO_2 injection, a regional liver parenchyma was enhanced as high-echo pattern and developed a hyperechoic ring surrounding the tumors as our previous observation^[7]. The echo within the tumors

remained unchanged in 64 patients, but enhanced in 9 patients which represented portal blood stream within the tumors.

Enhancement of the hepatic parenchyma was localized to the area supplied by the injected branches or confined in the same lobe in 61 patients and subsequent PVE was performed. PVE was abandoned in 12 cases due to CO₂ diffusing into both lobes of the liver.

Ultrasonography did not reveal any abnormality in the injected portal branches on the day of PVE. Forty-eight hours after PVE, embolization was found in 55/61 patients (90.2%), exhibiting substantial hypoechoes within the lumen of portal vein. Of 37 patients who underwent hepatectomy afterwards the specimen inspection confirmed the injected portal veins were occluded by thrombosis. Embolization failed to develop in six patients, who were the initial cases of PVE, due to inadequate amount of ethanol (4 mL - 5 mL) injected.

Forty-five patients (73.8%) complained of abdominal pain at the right upper quadrant, sweating, transient low-grade fever or decreased pulse rate during ethanol injection. Acute ischemic cholecystitis was encountered in one patient, for which the needle may be displaced accidentally during the injection, resulting in vascular occlusion of the gallbladder. Accidental embolization by reflux ethanol was not found in all patients and the liver function tests did not show significant change following PVE.

DISCUSSION

Comparing with transcatheter PVE, the advantages of PVE with fine needle are obvious: easy to achieve selective embolization, simple in manipulation, inexpensive and radiation free. However, at least two questions have to be answered which are prerequisite for conducting this procedure. The first question is about the safety of this procedure and the second is how to avoid a possible reflux of the ethanol to other portal branches. Furthermore, the feasibility of this technique should be convinced clinically.

Absolute ethanol is an effective embolizer in PVE. However, its toxic effect should not be neglected. In the present study, the dose of 0.25 mg/kg had little toxic effect but failed to induce complete embolization. While the dose of 1.0 mg/kg caused complete embolization but resulted in severe liver dysfunction and even respiratory arrest. Satisfactory embolization could be obtained at a dose of 0.5 mg/kg in normal dogs with mild toxicity to the liver parenchyma and only transient changes in the liver function. In transcatheter PVE with ethanol injection while the

portal was occluded to blood flow, a rapid vascular obliteration and immediate embolization with entire necrosis at the affected region occurred^[8]. On the contrary, since the portal vein was not occluded during ethanol injection in our technique, most of the ethanol might be diluted by the slow blood stream rather than flushed up to the liver parenchyma. The thrombosis was resulted from agglutinations, coagulation of plasma proteins and local pylephlebitis, and the thrombosis development was relatively slow. Thus, the damage to the liver tissue was relatively mild. Such a mechanism may be more favorable for the patients with HCC and underlying cirrhosis. The local overembolization in one dog in our study was probably due to an extension of the thrombus after the injection. This complication could be prevented by carefully selecting a point for puncture that is not too close to the confluence of the portal branches.

Since 80% of the patients with HCC are associated with cirrhosis, it is necessary to investigate the effect of PVE on cirrhotic liver for a better orientation on its clinical application. The present study indicated the cirrhotic rats were less tolerant to ethanol than the normal rats, so the dose of ethanol used for PVE should be strictly controlled. On the other hand, once PVE was undertaken with a tolerant dose, the changes in histology, liver function and portal hemodynamics in cirrhotic rats were not more severe and persistent than those of normal rats. It indicated that an uneventful postoperative course could also be achieved in cirrhotic rats with an appropriate dose of ethanol.

In both normal and cirrhotic liver, the weight of nonembolic lobe was increased with hypertrophy and proliferation in the nonembolized lobe in the current study. Increase in mitotic index, DNA synthesis and the number and function of mitochondrial in these lobes has been reported^[9,10]. The hypertrophy may be contributed to the increase of nourishing factors carried by portal blood flow to the nonembolized lobes. This mechanism may play an important role in the surgery for cirrhotic patients as the improvement of functional reserve on the nonembolized lobe, hence the resectibility of HCC increased and the risk of postoperative liver failure reduced.

The features of portal circulation in the liver with HCC and cirrhosis were considered when our approach was planned for clinical use. Portal flow reflux may occur due to the circulatory disturbances within the tumor, portal branch compressed by huge mass, serious cirrhosis, portal hypertension and arteriovenous shunts. According to our previous portoecography and color Doppler study on patients with HCC, the incidence of portal vein

reflux was about 10%-30%^[11]. Since the injected portal branches were not be occluded during ethanol injection, accidental embolization could occur as the embolic agent might be carried to other branches by the reverse flow. In order to avoid the accidental embolization, it is important to obtain the information of portal hemodynamics individually prior to the procedure. Matsuda and Yabuuchi first reported a method of contrast-enhanced ultrasonography with arterial infusion of CO₂ microbubbles for assessment of the nature of liver tumor^[12]. Because the ultrasonic impedance of CO₂ gas is much different from that of the liver and the gas can be rapidly washed out off the liver. It possesses excellent contrast effect without hepatic injury. This technique has been demonstrated as high sensitivity and specificity in clinical use^[13,14]. Furthermore, the CO₂ was directly injected into the destined portal branches, such portoechography could truly reveal the hemodynamics status of the portal branch^[7]. In addition, it can be conveniently applied during the procedure of PVE. In the present study, reflux of portal stream was detected by portoechography in 12/73 patients and subsequent embolization was ceased for those patients. No accidental aberrant embolization occurred in the patients with CO₂ confined at ipsilateral half of the liver, substantiating the usefulness of portoechography in our procedure.

The present study demonstrated that intraportal ethanol injection via fine needle was able to produce complete portal vein embolization with mild liver injury in both normal and cirrhotic liver in animal and patients with HCC. Portoechography was a mandatory approach for the prevention of aberrant embolization in patients with HCC.

REFERENCES

- 1 Shimamura T, Nakajima Y, Une Y, Namieno T, Ogasawara K, Yamashita K, Haneda T, Nakanishi K, Kimura J, Matsushita M, Sato N, Uchino J. Efficacy and safety of preoperative percutaneous transhepatic portal embolization with absolute ethanol: a clinical study. *Surgery*, 1997;12:135-141
- 2 Nagino M, Nimura Y, Kamiya J, Kondo S, Uesaka K, Kin Y, Kutsuna Y, Hayakawa N, Yamamoto H. Right or left trisegment portal vein embolization before hepatic trisegmentectomy for hilar bile duct carcinoma. *Surgery*, 1995;117:677-681
- 3 Kawasaki S, Makuuchi M, Kakazu T, Miyagawa S, Takayama T, Kosuge T, Sugihara K, Moriya Y. Resection for multiple metastatic liver tumors after portal embolization. *Surgery*, 1994;115:674-677
- 4 Kinoshita H, Sakai K, Hirohashi K, Igawa S, Yamasaki O, Kubo S. Preoperative portal vein embolization for hepatocellular carcinoma. *World J Surg*, 1986;10:803-808
- 5 Fujio N, Sakai K, Kinoshita H, Hirohashi K, Kubo S, Iwasa R, Lee KC. Results of treatment of patients with hepatocellular carcinoma with severe cirrhosis of the liver. *World J Surg*, 1989;13:211-218
- 6 Liang LJ, Lu MD, Ye WJ, Huang YF. Two stage resection for advanced hepatocellular carcinoma. *Zhonghua Zhongliu Xue Zazhi*, 1992;14:449-451
- 7 Lu MD, Liang LJ, Xie XY, Li DM, Li MD, Xie YY, Peng BG. Hepatic angio echography and its clinical application. *Zhonghua Chaosheng Yingxiangxue Zazhi*, 1993;2:154-156
- 8 Ogasawara K, Uchino J, Une Y, Fujioka Y. Selective portal vein embolization with absolute ethanol induces hepatic hypertrophy and makes more extensive hepatectomy possible. *Hepatology*, 1996;23:338-345
- 9 Lee KC, Kinoshita H, Hirohashi K, Kubo S, Iwasa R. Extension of surgical indications for hepatocellular carcinoma by portal vein embolization. *World J Surg*, 1993;17:109-115
- 10 Harada H, Imamura H, Miyagawa S, Kawasaki S. Fate of the human liver after hemihepatic portal vein embolization cell kinetic and morphometric study. *Hepatology*, 1997;1162-1170
- 11 Lu MD, Xie YY, Liang LJ, Huang JF, Cao XH. Portal hemodynamics in hepatocellular carcinoma: observation by angioechography and color Doppler. *Zhonghua Chaosheng Yixue Zazhi*, 1994;10(6):24-27
- 12 Matsuda Y, Yabuuchi I. Hepatic tumors: US contrast enhancement with CO₂ microbubbles. *Radiology*, 1986;161:701-705
- 13 Kudo M, Tomita S, Tochio H, Kashida H, Hirasa M, Todo A. Hepatic focal nodular hyperplasia: specific findings at dynamic contrast enhanced US with carbon dioxide microbubbles. *Radiology*, 1991;179:377-382
- 14 Takasaki K, Saito A, Nakagawa M. Significance of angioechography for diagnosis of small intrahepatic metastasis. *Kanzuo*, 1988;29: 917-920

Edited by WU Xie-Ning

Proofread by MIAO Qi-Hong

Study on the anticarcinogenic effect and acute toxicity of liver-targeting mitoxantrone nanoparticles

ZHANG Zhi-Rong, HE Qin, LIAO Gong-Tie and BAI Shao-Huai

Subject headings mitoxantrone-nanospheres toxicity; neoplasm transplantation; nude mice

Abstract

AIM To study the anticarcinogenic effect and acute toxicity of liver targeting mitoxantrone-nanospheres.

METHODS The anticarcinogenic effect of mitoxantrone-polybutyl cyanoacrylate-nanoparticles (DHAQ-PBCA-NP) was investigated by using heterotopic and orthotopic transplantation models of human hepatocellular carcinoma (HCC) in nude mice and was compared with mitoxantrone (DHAQ) and doxorubicin (ADR). The acute toxicity of DHAQ-PBCA-NP lyophilized injection in mice was also studied.

RESULTS The tumor inhibition rates of ADR, DHAQ, DHAQ-PBCA-NP to orthotopically transplanted HCC were 60.07%, 67.49% and 99.44%, respectively, but regard to heterotopically transplanted HCC, these were 80.03%, 86.18 % and 92.90%, which were concordant with the results acquired by mitosis counting and proliferating cell nuclear antigen (PCNA). After iv administration to mice with DHAQ-PBCA-NP, the LD₅₀ was 16.9mg/kg±3.9mg/kg, no obvious local irritation was observed and there was no significant damage to the structure of liver cells, and that of the heart, spleen and kidneys.

CONCLUSION The effect of DHAQ-PBCA-NP was significantly higher than that of DHAQ and ADR in the anti-orthotopically transplanted HCC and the acute toxicity was relatively low.

School of Pharmacy, West China University of Medical Sciences, Chengdu 610041, Sichuan Province, P.R. China
Dr. ZHANG Zhi-Rong, male, 43 years old, graduated from West China University of Medical Sciences (WCUMS) as a Ph.D. in 1993. Professor of pharmaceuticals, Dean of the School of Pharmacy of WCUMS, member of Chinese Pharmacopoeia Commission, council member of Chinese Pharmaceutical Association (CPA), member of Society of Pharmaceutics of CPA, specializes in targeted delivery system and has more than 80 papers and 6 books published. Supported by the National Natural Sciences Foundation of China, No.39270786.

Correspondence to: Dr. ZHANG Zhi-Rong, School of Pharmacy, West China University of Medical Sciences, Chengdu, 610041, China. Tel.+86-28-5501566, Fax.+86-28-5583252

Received 1999-08-10

INTRODUCTION

DHAQ is a new synthetic antitumor agent, effective in many cancers, especially in hepatic cancer, a principal cancer of high incidence and mortality^[1]. Nanoparticles (NP) is a new drug carrier^[3] showing a distinguished liver targeting ability, therefore, NP loading with antihepatic cancer drug could improve the effect of original drug. The DHAQ-PBCA-NP used in this study has been proved to have remarkable liver-targeting effect. In this paper, the anticarcinogenic effect, acute toxicity and local irritation of DHAQ-PBCA-NP were studied and compared with those of ADR and DHAQ injection.

MATERIALS AND METHODS

Materials

DHAQ was obtained from Organic Chemistry Department, School of Pharmacy, West China University of Medical Sciences. DHAQ-PBCA-NP was self-made with a content of DHAQ 0.15 mg/mL diameter 55.82 nm ± 12.46 nm (*n* = 505) and drug loading 51.03%. The lyophilized ADR injection was provided by TuoBin Pharmaceutical Factory and DHAQ injection provided by Hua Da Pharmaceutical Factory with a content of DHAQ 2 mg/2 mL.

BALB/C-nu/nude mice, Kunming mice and the heterotopic and orthotopic transplantation models of HCC in nude mice were all supplied by our Laboratory Animal Center. Animal tumor cells LTNM₄ (86 generation) was obtained from Liver Cancer Laboratory, Zhongshan Hospital, Shanghai Medical University.

Methods

Tumor inhibition test of DHAQ-PBCA-NP Twenty nude mice were randomly divided into physiological saline group (0.1 mL/10 g), ADR group (20 µg/10 g), DHAQ group (20 µg/10 g) and DHAQ-PBCA-NP (15 µg/10 g) group. The drug was given intravenously to each mouse 36 h after the transplantation of HCC, then given continuously once every three days for four times. On the 14th day after the last injection, the diameter of the armpit tumors of nude mice in the physiological saline group was found over 10 mm, and one mouse died. The mice were killed, and the livers as well as the tumors were taken out, weighed and the rate of

tumor inhibition (TRI) was calculated by the following formula:

$$RTI\% = \frac{\text{The average tumor weight of control group} - \text{average tumor weight of experimental group}}{\text{The average tumor weight of control group}} \times 100\%$$

Microscopic observations and nuclear division count of tumor The hepatic cancer of nude mice taken from control group and experimental group was sectioned into ultra-slices and observed under microscope.

Calculation of positive rate of the tumor PCNA The tumor of each groups was sampled, fixed in formalin and embedded in paraffin wax, then anti-proliferating cell nuclear antigen (PCNA) monoclonal antibody PC10 was used to show the proliferating cells by highly sensitive method of ABPAP, the number of tumor cells were counted and positive rate was calculated^[4].

Acute toxicity One hundred and eight Kunming mice were randomly divided into DHAQ-PBCA-NP group, PBCA-NP group and DHAQ group. Each group was given 6 different dosages with the maximum dose 75.0 mg/kg, 1150 mg/kg and 25.2 mg/kg, respectively. The mice were observed for 21 d and the death rate of each group was recorded.

Pathologic examination Nine of 10 Kunming mice were given DHAQ -PBCA-NP intravenously in the dosage of 15 mg/kg and were killed after 5 min, 10 min, 15 min, 20 min, 30 min, 1 h, 24 h, 38 h and 72 h, respectively, another one was injected normal saline at the dosage of 0.1 mL/10 g. Tissue samples of the heart, liver, spleen, lung and kidney were fixed in formalin and embedded with paraffin wax for routine section, HE stain and observed under microscope. The liver tissue was fixed by glutaraldehyde, dehydrated with acetone gradually, embedded with 618 to make ultrathin section, then stained by uranium acetate and lead citrate and examined under transmission electron microscope.

Local irritation testing Ten Kunming mice were given DHAQ-PBCA -NP intravenously at a dosage of 0.1 mL/kg and the changes at the tail were observed for 1-7 days.

RESULTS

Tumor inhibition rate

The tumors obtained from the liver and armpit in each group were photographed (Figures 1-3). The tumor and tumor inhibition rate are listed in Tables 1 and 2, respectively. No significant difference was noted among the anti-HCC effect of DHAQ-PBCA-NP, DHAQ and ADR, but in the anti-orthotopically transplanted HCC, the effect by DHAQ-PBCA-NP was much higher than that by DHAQ or ADR.

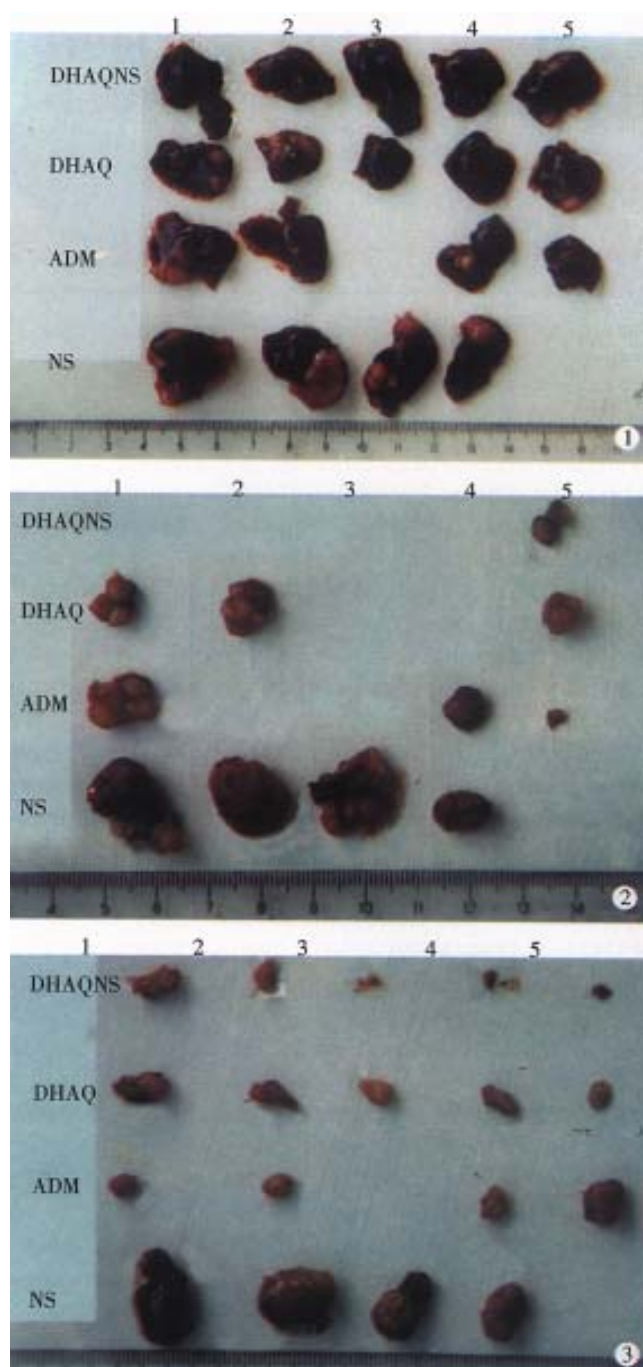


Figure 1 The liver in nude mice taken from armpit.

Figure 2 Tumor taken from liver.

Figure 3 Tumor taken from armpit.

Microscope observations of the tumor

The tumor cell proliferation in control group was very active. The tumor cell karyokinesis in DHAQ-PBCA-NP, DHAQ and ADR groups was less than that of control group (508/HP), especially in the DHAQ-PBCA-NP group, only 0-3/PH, and most were in the metaphase.

Tumor cell proliferative activity analysis The PCNA positive percentage of nude mice tumor in each

group was shown in Table 3, the killing activity of DHAQ-PBCA-NP was significantly stronger than that of DHAQ and ADR ($P<0.05$) on nude mice transplanted with HCC, and the activity of DHAQ was almost equal to the of ADR ($P>0.05$).

Table 1 Weight (g) of tumor taken from four different groups

Group	Liver tumor	Armpit tumor
DHAQ-PBCA-NP		
1	0.000	0.215
2	0.000	0.060
3	0.000	0.005
4	0.000	0.015
5	0.030	0.015
ADR		
1	0.820	0.100
2	0.000	0.050
3	0.675	0.137
4	0.210	0.410
DHAQ		
1	0.585	0.270
2	0.650	0.120
3	0.000	0.065
4	0.000	0.082
5	0.500	0.066
0.9% NS		
1	1.320	1.160
2	1.530	1.026
3	1.000	0.635
4	0.420	0.670

Table 2 Rate of tumor inhibition (RTI, %) of each group of nude mice

Drug	RTI (orthotopic)	RTI (heterotopic)
DHAQ	67.49 ^a	86.18 ^d
ADR	60.07 ^b	80.03 ^e
DHAQ-PBCA-0.9%NS	99.44 ^c	92.90 ^f

c vs b, a $P<0.05$; f vs d, e $P>0.05$; b vs a $P>0.05$.

Table 3 The cell proliferative activity of tumor of each nude mice

	DHAQ-PBCA-NP					DHAQ					ADR				0.9%NS			
	1	2	3	4	5	1	2	3	4	5	1	2	3	4	1	2	3	4
PCNA(%)	7	2	1	3	2	7	9	7	6	9	7	9	10	82	10	95	10	90
$\bar{x}\pm s$ (%)	0	0	0	0	5	0	0	0	0	0	0	0	0	0	0	0	0	0
	31.0 \pm 23.0 ^a					76 \pm 13.4 ^b					85.5 \pm 12.7 ^c				96.3 \pm 4.8			

a vs b, c $P<0.05$; b vs c $P<0.05$.

LD₅₀ and toxicity parameters The LD₅₀ was calculated by Karber method based on the mice death rate of each dosage group (Table 4).

The absolute lethal dose of DHAQ-PBCA-NP and DHAQ in mice was 75.0 mg/kg and 25.2 mg/kg, respectively whereas the minimal lethal dose was 6.5 and 4.8 mg/kg, respectively, the maximum tolerance dose was 4.5 mg/kg and 3.0 mg/kg, the earliest time of death was 7 d and 4 d, the latest time of death was 21 d and 16 d and the average time of death was 9.7 d \pm 8.8 d and 7.5 d \pm 4.2 d, respectively.

Table 4 The LD₅₀ of DHAQ-PBCA-NP, DHAQ and PBCA-NP i.v. in mice

Group	n	LD ₅₀ (mg/kg, $P=0.95$)*		
		7d	14d	21d
DHAQ	60	12.8 \pm 1.9	8.2 \pm 1.7	6.1 \pm 1.0
DHAQ-NP	60	309.9 \pm 26.2	301.0 \pm 28.3	299.0 \pm 24.2
DHAQ-PBCA-NP	60	16.9 \pm 3.9	12.3 \pm 2.7	10.1 \pm 1.9

*Dosage calculated as DHAQ.

Results of pathologic examination

There were no apparent pathological changes in the heart, liver, spleen, lung and kidney. Under the transmission electron microscope, the liver cells were structurally intact and arranged normally, only part of the mitochondria cristae were sparse and swollen (Figure 4A), but the cells returned to normal in 24 h (Figure 4B).

Local irritation

The tail veins of the mice were stained blue 1-7 days after i.v. DHAQ-PBCA-NP. Except one which appeared red and swollen slightly, the stained blue disappeared completely 4 days later, which demonstrated no irritation by DHAQ-PBCA-NP injection.

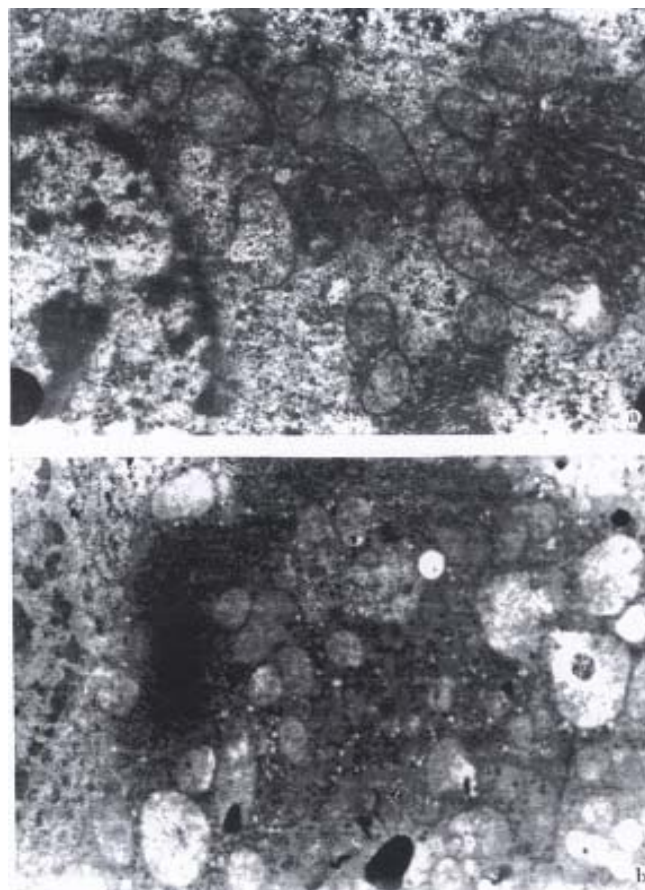


Figure 4 The mouse liver cell at 20 min (A) and 24 h (B) after i.v.15mg/kg DHAQ-PBCA-NP. TEM \times 800

DISCUSSION

The effect of DHAQ-PBCA-NP on the anti-heterotopically transplanted HCC was almost the same as that of DHAQ and ADR, which implied that it was more eligible to use the model of orthotopic transplantation than to use the heterotopic one.

The cell proliferative activity could be used for assessing the efficacy of chemotherapy. PCNA was an antigen existed largely at the junction of G₁ phase and S phase in the process of tumor cell proliferation, PC10 was the monoclonal antibody of PCNA. In order to investigate inhibiting effect of various drugs on tumor cell proliferation, a highly sensitive method of ABPAP was used for expression of PCNA by PC10 in this study, and the results were satisfactory. Furthermore, the DHAQ-PBCA-NP

injection had no adverse effect on the structure of heart, spleen, lung and kidney only some mild and reversible changes on the mitochondria of the hepatocytes implicating preparation of DHAQ-PBCA-NP was more effective and much less toxic than DHAQ.

REFERENCES

- 1 Gu GW, Lu SZ. Hepatocarcinoma pathological epidemiology. *Foreign Med Sci-Physiol, Pathol Clin Fascicle*, 1991;11:91-93
- 2 Ma YP, Zheng S. The anticancer drug mitoxantrone. *World Pharm-Synthet Drug, Biochem Drug Pharmac Fascicle*, 1986;7:324-327
- 3 Couvreur P, Kante B, Roland M, Guito P, Bauduin P, Speiser P. Polycyanoacrylate nanocapsules as potential lysosomotropic carriers: preparation, morphological and sorptive properties. *J Pharm Pharmacol*, 1979;31:331-336
- 4 Garcia RL, Coltrera MD, Gown AM. Analysis of proliferative grade using antiPCNA/cyclin monoclonal antibodies in fixed embedded tissues. *Am J Pathol*, 1989;134:733-739

Edited by WU Xie-Ning

Proofread by MIAO Qi-Hong

Study of the mechanisms of acupuncture and moxibustion treatment for ulcerative colitis rats in view of the gene expression of cytokines

WU Huan-Gan, ZHOU Li-Bin, PAN Ying-Ying, HUANG Cheng, CHEN Han-Ping, SHI Zheng and HUA Xue-Gui

Subject headings colitis, ulcerative/therapy; acupuncture and moxibustion therapy; gene expression; cytokines; interleukin-1 β ; interleukin-6

Abstract

AIM To observe the effect of acupuncture and moxibustion on the expression of IL-1 β and IL-6 mRNA in ulcerative colitis rats.

METHODS The SD rat ulcerative colitis model was created by immunological method associated with local stimulation. Colonic mucosa was prepared from human fresh surgical colonic specimens, homogenized by adding appropriate amount of normal saline and centrifuged at 3000r/min. The supernatant was collected for measurement of protein concentration and then mixed with Freund adjuvant. This antigen fluid was first injected into the plantae of the model group rats, and then into their plantae, dorsa, inguina and abdominal cavities (no Freund adjuvant for the last injection) again on the 10th, 17th, 24th and 31st day. When a certain titer of serum anti-colonic anti body was reached, 2% formalin and antigen fluid (no Freund adjuvant) were administered separately by enema. The ulcerative colitis rat model was thus set up. The animals were randomly divided into four groups: model control group (MC, $n = 8$), electro-acupuncture group (EA, $n = 8$), herbs-partition moxibustion group (HPM 8), normal control group (NC, $n = 8$). HPM: Moxa cones made of refined mugwort floss were placed on the

medicinal pad (medicinal pad dispensing: Radix Aconiti praeparata, cortex Cinnamomi, etc) for Qihai (RN 6) and Tianshu (S T 25, bilateral) and ignited. Two moxa cones were used for each acupoint once a day and 14 times in all. EA: Tianshu (bilateral) and Qihai were stimulated by the intermittent pulse with 2Hz frequency, 4mA intensity for 20 minutes once a day and 14 times in all. After treatment, rats of all four groups were killed simultaneously. The spleen was separated and the distal colon was dissected. Total tissue RNA was isolated by the guanidinium thiocyanate phenol-chloroform extraction method. RT-PCR technique was used to study the expression of IL-1 β and IL-6 mRNA. **RESULTS** IL-1 β and IL-6 mRNAs were not detected in the spleen and colonic mucosa of the NC rats, whereas they were significantly expressed in that of the MC rats. IL-1 β and IL-6 mRNAs were markedly lower in the EA and HPM rats than that in MC rats. There was no significant difference between the levels of IL-1 β and IL-6 mRNAs in the EA and HPM rats. The expressions of IL-1 β and IL-6 mRNAs were nearly the same in the spleen and colon of all groups. **CONCLUSION** Acupuncture and moxibustion greatly inhibited the expression of IL-1 β and IL-6 mRNA in the experimental ulcerative colitis rats.

INTRODUCTION

Ulcerative colitis (UC) is a nonspecific inflammatory bowel disorder of unknown etiology but associated with immunological abnormalities^[1]. The cytokines, involved in the regulation of the immune response, play important roles in the pathogenesis of UC. Especially the interleukin-1 β (IL-1 β) and interleukin -6 (IL-6), inflammatory mediators released by lymphocytes, monocytes and macro phages, are intricately linked with the initiation and propagation of the inflammatory reaction in UC^[2]. Both clinical and experimental researches indicated that acupuncture and moxibustion had good therapeutic effects on UC.

Shanghai Institute of Acupuncture-Moxibustion and Meridians, Shanghai 200030, China

Dr. WU Huan-Gan, male, born on 1956-11-21 in Xianju County, Zhejiang Province, graduated from Zhejiang College of Traditional Chinese Medicine, with Master Degree in 1990, and from Shanghai University of Traditional Chinese Medicine with Doctoral Degree in 1993; now professor, director, majoring the research of acupuncture-moxibustion immunity, having 26 papers published.

Supported by the National Natural Science Foundation of China, No.39670899.

Correspondence to: Prof. WU Huan-Gan, Shanghai Institute of Acupuncture-Moxibustion and Meridians, 650 South Wan Ping Road, Shanghai 200030, China

Tel.+86-21-64395972

Received 1999-05-23

The mechanism of such effects may be related to its immunoregulation, but the role of cytokines in it has not been reported. In this study, a UC rat model was established by immunological method to observe the effect of acupuncture and moxibustion on the expression of IL-1 β and IL-6 mRNA in spleen and colonic mucosa of model rats, in order to clarify the possible mechanism of acupuncture and moxibustion on UC.

MATERIALS AND METHODS

Material

Male SD rats weighing, 140g \pm 20g, were provided by The Experimental Animal Center of Shanghai University of TCM. The rats were randomly divided into the model group ($n=24$) and normal control group (NC, $n=8$). We consulted the Methodology of Pharmacy and created the rat model by immunological method associated with local stimulation (refer to the Abstract). These models were randomly subdivided into three groups after being created: model control group (MC, $n=8$), electro-acupuncture group (EA, $n=8$) and herbs-partition moxibustion group (HPM, $n=8$). The points Qihai (CV6) and bilateral Tianshu (ST25) were located on analogy of person's points. HPM: Moxa cones made of refined mug wort floss were placed on the medicinal pad (medicinal pad dispensing: *Radix Aconiti praeparata*, *cortex Cinnamomi*, etc) for Qihai (RN 6) and Tianshu (ST 25, bilateral) and ignited. Two moxa cones were used for each acupoint once a day and 14 times in all. EA: Tianshu (bilateral) and Qihai were stimulated by the intermittent pulse with 2Hz frequency, 4mA intensity for 20 minutes once a day and 14 times in all. After treatment, all rats of the four groups were killed simultaneously. The spleen was separated and the distal colon 6cm long was dissected and reserved in liquid nitrogen.

Method

According to the reference^[3], total tissue RNA was isolated by the guanidinium thiocyanate phenol chloroform extraction method. The concentration of sample RNA was measured with ultraviolet spectrophotometer OD260; the integrity of RNA was identified by agarose (sepharose) gel (10g/L) electrophoresis.

Two μ g total RNA was reverse transcribed to cDNA, 20 μ L reverse transcription reaction system (Promega), which comprised 10 \times reverse transcription buffer solution 2 μ L, 25 mmol/L MgCl₂ 4 μ L, 4 \times dNTPs (10mmol/L for each) 2 μ L, RNAase inhibitor 0.5 μ L (20U), AMV reverse transcriptase 0.65 μ L (15U), oligomer (dT)₁₅ and primer 1 μ L (0.5 μ g); added DEPC up to 20 μ L, well mixed, placed in 42 $^{\circ}$ C water for 40 minutes,

heated in 95 $^{\circ}$ C water for 5 minutes to deactivate reverse transcriptase, and then preserved at -20 $^{\circ}$ C.

According to the reference^[4], the primer was synthesized in the oncogene laboratory of the Cell Institute of the Chinese Academy of Sciences. The sequence of IL-1 β was ATAGCAGCTTTTCGACAGTGAG (sense chain), GTCAACT ATGTCCC-GACCATT (antisense chain) 748bp; IL-6, TTCCCTACTTTCACAAGTC (sense chain), CTAGGTTTGCCGAGTAGA (antisense chain) 567bp; glyceraldehyde dehydrogenase (GAPDH) triphosphate, TGAAGGTCGGTGTCAACGGATTTGTC (sense chain), CAGTAGGCCATGAGGTCCACCAC (antisense chain) 983bp. GAPDH as house keeping gene monitors the consumption of RNA and eliminates the errors among samples.

The total 50 μ L PCR reaction system consisted of 10 \times amplification buffer solution 5 μ L, 4 \times dNTPs (2.5 mmol/L for each) 4 μ L, primers of sense chain and antisense chain 50 pmol for each, 2 μ L reverse transcriptase product, Taq-DNA polymerase 2.5U, and added ddH₂O up to 50 μ L, to mix them together. After 10 second centrifugation, 50 μ L liquid paraffin was added and placed in PCR Gene Amp Machine (Pharmacia). The amplification condition: IL-1 β : 94 $^{\circ}$ C pre-denature 4min, 94 $^{\circ}$ C 30s, 50 $^{\circ}$ C 45s, 72 $^{\circ}$ C 90s for 30 cycles; IL-6 and GAPDH: 94 $^{\circ}$ C pre-denature 4min, 94 $^{\circ}$ C 1min, 52 $^{\circ}$ C 1min, 72 $^{\circ}$ C 1min for 30 cycles.

Ten μ L PCR product was added to 6 \times electrophoresis buffer solution 2 μ L, and underwent agarose gel (1.5 g/L, containing Ethidium bromide 0.5mg/L) electrophoresis at 100V for 1 hour and photographed under ultraviolet lamp.

RESULTS

Total RNA extraction

The ratios of OD260/OD280 of the total RNA samples were between 1.70-2.00 and two bands, 18s and 28s, were shown in electrophoresis, indicating that the total RNA was not polluted and degraded.

IL-1 β and IL-6 mRNA in spleen and colon mucosa (Figure 1)

IL-1 β and IL-6 mRNA expressions of spleen and colon mucosa were observed in model control group, electro-acupuncture group and herbs-partition moxibustion group, but the degrees of expression in EA or HPM were lower than that in MC. There was no significant difference between EA and HPM, but the degree of expression in HPM as a whole tended to be less. The expressions of spleen and colon mucosa in all groups were nearly the same. Neither IL-1 β nor IL-6 mRNA expression of spleen and colon mucosa could be observed in the normal control group.

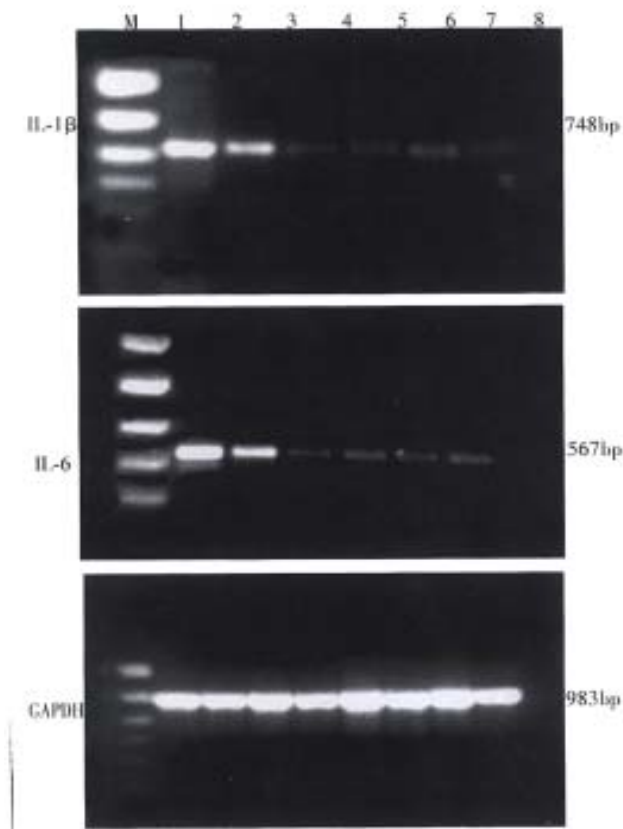


Figure 1 The effect of acupuncture and moxibustion on IL-1 β and IL-6 mRNA expression in spleen and colonic mucosa of ulcerative colitis rats.

M: Sign of PCR (Hua Mei), 1543, 994, 694, 515, 377 and 237bp from up to down respectively. 1, 3, 5 and 7 are mRNA of colonic mucosa in MC, EA, HPM and NC groups respectively; 2, 4, 6 and 8 are mRNA of spleen in MC, EA, HPM and NC groups respectively.

DISCUSSION

The pathogenesis of UC may involve in both local and systemic immunological abnormalities. Cytokines now have attracted special attention by virtue of their participation in the intestinal inflammation and immune reactions. IL-1 β and IL-6, as important inflammatory factors and immune regulators, play a fundamental role in the pathogenesis of UC. Many studies showed increased IL-1 β and IL-6 levels in the colonic mucosa and peripheral blood of patients with UC, and indicated that IL-6 was possibly correlated with the severity of the manifestations in UC patients^[5,6]. IL-1 β and IL-6, produced mainly by activated phagocytes and lymphocytes, show a wide variety of biological functions. They can influence secretion of other cytokines and inflammatory mediators in an autocrine or paracrine fashion, induce expression of surface immune molecules of antigen-presenting cells to serve as an activation factor and differentiation factor on T cells and B cells, mediate

immunoglobulin secretion, activate the complements, killer cells and phagocytes, and enhance tissue injury mediated by cellular and humoral immune reactions. In addition, IL-1 β and IL-6 can promote the expression of adhesion molecules on endothelial-leukocyte and are regarded as a chemoattractant of circulating neutrophils to migrate in to the inflamed site, thus causing a series of long lasting intestinal inflammatory reaction and tissue injury^[7-9].

This study demonstrated that IL-1 β and IL-6 were undetectable in the spleen and colonic mucosa of the normal control rats, whereas they were significantly expressed in that of the model control rats. Lymphocytes and monocytes/macrophages in the rats were activated by persistent stimulation of exogenous antigens which might contribute to the expression of cytokines. The amount of IL-1 β and IL-6 mRNA was nearly the same between the spleen and colon in different groups, suggesting that immunocytes in the spleen and colon responded to the antigen in a similar way and interacted through the pathway of cytokines. In our study the markedly decreased expressions of IL-1 β and IL-6 mRNA in EA and HPM suggested that acupuncture and moxibustion could inhibit the expression of inflammatory cytokines in UC model rats, regulate the immunological abnormalities, reduce immunocyte response to inflammation, and then contribute to the elimination of inflammation and repair of tissue.

The pathogenesis of UC may be due to an imbalance between inflammatory cytokines on one hand and anti-inflammatory immune factors such as IL-4, IL-1ra, IL-10, etc on the other. Our results suggest that in addition to inhibit the expression of inflammatory cytokines, acupuncture and moxibustion can activate the anti-inflammatory factors, but further studies are needed.

REFERENCES

- 1 Kusugami K, Fukatsu A, Tanimoto M, Shinoda M, Haruta J, Kuroiwa A. Elevation of interleukin 6 in inflammatory bowel disease in macrophage and epithelial cell dependent. *Dig Dis Sci*, 1995;40:949-959
- 2 Hyams JS, Fitzgerald JE, Treem WR, Wyzga N, Kreutzer DL. Relationship of functional and antigenic interleukin 6 to disease activity in inflammatory bowel disease. *Gastroenterology*, 1993;104:1285-1292
- 3 Chomczynski P, Sacchi N. Single step method of RNA isolation by acid guanidinium thiocyanate phenol chloroform extraction. *Anal Biochem*, 1987;162:156-159
- 4 Murphy PG, Grondin J, Altares M, Richardson PM. Induction of interleukin 6 in axotomized sensory neurons. *J Neurosci*, 1995;15:5130-5138
- 5 Mitsuyama K, Toyonaga A, Sasaki E, Ishida O, Ikeda H, Tsuruta O. Soluble interleukin 6 receptors in inflammatory bowel disease: relation to circulating interleukin 6. *Gut*, 1995;36:45-49
- 6 Stevens C, Walz G, Singaram C, Lipman ML, Zanker B, Muggia A. Tumor necrosis factor- α , interleukin 1 β , and interleukin 6 expression in inflammatory bowel disease. *Dig Dis Sci*, 1992;37:818-826
- 7 Hogaboam CM, Snider DP, Collins SM. Cytokine modulation of T lymphocyte activation by intestinal smooth muscle cells. *Gastroenterology*, 1997;112:1986-1997
- 8 Nassif A, Longo WE, Mazuski JE, Vemava AM, Kaminski DL. Role of cytokines and platelet activating factor in inflammatory bowel disease. *Dis Colon Rectum*, 1996;39:217-223
- 9 Schreiber S, Raedler A, Stenson WF, MacDermott RP. The role of the mucosal immune system in inflammatory bowel disease. *Gastroenterol Clin North Am*, 1992;21:451-502

Edited by LU Han-Ming

Proofread by MA Jing-Yun

Review

Intestinal stasis associated bowel inflammation

Shunichiro Komatsu¹, Yuji Nimura¹ and D. Neil Granger²

Subject headings intestinal stasis; bowel inflammation; endothelial cell intercellular adhesion molecule-1

INTRODUCTION

Anatomical structures that create reservoirs for stagnant intestinal contents are a characteristic feature of common inflammatory disorders such as diverticulitis and appendicitis. Intestinal diverticula, surgically constructed blind loops and pouches, obstructing carcinomas of the colon, and Hirschsprung's disease are accompanied by chronic inflammatory changes in the intestine, and are occasionally associated with mucosal ulceration followed by massive bleeding. These diseases are etiologically associated with disorders characterized by intestinal stasis and/or an altered fecal stream, resulting from "cul de sac" structures (blind loop or pouch) in the intestinal tract, bowel obstruction or impaired motility. Furthermore, some of these chronic inflammatory conditions appear to exhibit similar pathological features, such as ischemic colitis. Although these inflammatory changes have been described individually, often as case reports, relatively little attention has been devoted to the overall clinical impact of these diseases and to understanding the pathophysiology of disease initiation and progression. Studies in our laboratory and by others have provided novel insights into the molecular and cellular basis for the intense inflammatory responses that are associated with intestinal stasis. This review summarizes the findings of these studies and provides a unifying theory to explain the inflammatory responses that result from intestinal stasis.

CLINICOPATHOLOGICAL FEATURES

Whereas most intestinal (duodenal, jejunal, Meckel's, and colonic) diverticula remain asymptomatic, gastrointestinal bleeding is the most common complication, associated with mucosal ulceration^[1-4]. Meckel's diverticulum, located on the antimesenteric border of the ileum, is the most common congenital anomaly of the gastrointestinal tract. Although ulcer formation in Meckel's diverticulum is generally thought to result from ectopic gastric tissue, all of the cases cannot be explained by acid production from the functioning gastric mucosa^[2]. The diagnosis of gastrointestinal bleeding due to diverticula of the small bowel is difficult, because neither the symptoms nor physical finding are specific and endoscopic observation is hampered by the length of the intestine. Surgical resection of the involved segment of the intestine is the treatment of choice for the diverticula identified as a source of gastrointestinal hemorrhage^[1].

The terms "blind pouch" or "blind loop syndrome" represent the complications resulting from a stagnant intestine that are usually created by a side-to-side anastomosis with or without bowel resection, respectively. In cases of this syndrome, diarrhea and occult intestinal bleeding are usually found as well as symptoms resulting from malabsorption^[5-9]. Shallow and longitudinal ulcerations are occasionally observed in the resected blind intestine, similar to those of ischemic enteritis^[5,6]. Bacterial overgrowth in the blind loop has been presented in experimental models of animals^[8,9]. While this syndrome is now rare because the safety of an end-to-end anastomosis has been established, the pathological features of this condition may provide important insights concerning the linkage between intestinal stasis and the resulting inflammatory response.

Restorative proctocolectomy with ileal pouch anal anastomosis has become the surgical treatment of choice for both ulcerative colitis and familial adenomatous polyposis. In spite of the excellent functional results and improved quality of life with this procedure, major concerns persist regarding the risks for and consequences of ileal pouchitis, a long term complication that is recognized with increasing frequency. Pouchitis is a nonspecific inflammation of an ileal reservoir that typically results in

¹First Department of Surgery, Nagoya University School of Medicine, Nagoya, Japan

²Department of Molecular & Cellular Physiology, Louisiana State University Health Sciences Center, Shreveport, LA, USA

Supported by Grant-in Aid for Scientific Research (C), 11671230, by the Ministry of Education, Science, Sports and Culture of Japan.

Correspondence to: Shunichiro Komatsu, MD, First Department of Surgery, Nagoya University School of Medicine, 65 Tsurumai-cho, Showa-ku, Nagoya City 466-8550, Japan

Tel. +81-52-744-2220, Fax. +81-52-744-2230

Email. skomat@atnet.ne.jp

Received 1999-09-22

increased bowel frequency, decreased stool consistency, diminished continence, low-grade fever, malaise, and arthralgias. Oral treatment with antibiotics, such as metronidazole, is an effective therapy for active pouchitis^[10-12].

The term “obstructive colitis” was originally used to define the ulcerative inflammatory lesions that occur proximal to the colonic lesion and which is partially or potentially obstructive rather than completely obstructed^[13-16]. Complications include peritonitis, perforation, and breakdown of anastomoses made through involved segments of the colon that may appear externally normal at surgery^[13,15]. The inflammatory response associated with colonic obstruction exhibits a variety of pathological features, including ischemic^[13-16], acute necrotizing^[17], or pseudomembranous colitis^[18], resulting in confusion about the definition of this disease^[14]. The area of colitis is usually mildly dilated with moderate thickening of the wall. Thus, it is characteristically distinguished from marked distension of the bowel that is associated with thinning of the wall and transmural necrosis caused by an increased intraluminal pressure, followed by acutely developing arrest of the intramural circulation^[13].

Enterocolitis associated with Hirschsprung’s disease, which can induce perforation and/or systemic sepsis, remains a major source of morbidity and mortality, both before and after definitive surgical treatment^[19-22]. The risk of postoperative enterocolitis is significantly increased by mechanical factors related to anastomotic stricture and intestinal obstruction^[21,22], possibly eliciting a delayed intestinal transit. Crypt abscess, intraluminal fibrinopurulent debris, or mucosal ulceration are histologically observed^[19,20]. The etiology of enterocolitis is uncertain; ischemic and bacterial causes and recently, rotavirus infections, have been suggested^[23,24].

While much attention has been devoted to defining the relationship between enteric bacteria and the pathogenesis of inflammatory bowel disease (IBD), it remains unclear whether intestinal stasis, resulting in overgrowth of enteric bacteria, contributes to the development of IBD. However, there are several interesting published observations that suggest the linkage between intestinal stasis and the pathogenesis of IBD. A previous study showed evidence that the recurrence of Crohn’s disease in the neoterminal ileum after curative ileal resection is dependent on intestinal transit^[25]. Although ulcerative colitis (UC) has been described as a continuous inflammatory process starting from the rectum, isolated inflammatory changes can be

observed in the periappendicial area of a number of patients with left-sided UC^[26,27]. In recent epidemiological studies, the risk of progression of UC was significantly lower after previous appendectomy^[28,29].

Although peptic ulcers (gastric or duodenal) have been extensively studied, the mechanisms underlying the ulcerative inflammatory changes in the stagnant intestine, where acid from the stomach has already been neutralized, remains poorly characterized. Many of the features of the disease suggest an ischemic origin, which cannot be explained by atherosclerotic obstruction of the feeding arteries. Microvascular dysfunction, due to hypoperfusion following raised intraluminal pressure, has been assumed to account for the mucosal ischemia^[13]. Contribution of enteric bacteria has also been suggested, based on the observation that treatment with oral antibiotics can often relieve clinical symptoms induced by these diseases^[10-12,30,31].

INTESTINAL STASIS AND ENDOTHELIAL CELL ADHESION MOLECULES

Leukocyte-endothelial cell adhesion is now recognized to represent an early and rate-limiting step in the leukocyte infiltration and accompanying tissue injury associated with acute or chronic inflammation. There is also evidence that adherent and activated leukocytes produce microvascular dysfunction by occluding microvessels, damaging endothelial cells and increasing vascular protein leakage^[32,33]. Leukocyte-endothelial cell adhesive interactions, such as rolling, firm adhesion, and transendothelial migration, represent a highly coordinated process that is governed by a number of factors, including the expression of specific adhesion glycoproteins, physical forces generated within the microcirculation, and inflammatory mediators released by a variety of activated cells^[32-37]. The pivotal role of endothelial cell adhesion molecules (CAMs) in regulating leukocyte recruitment has been demonstrated in different models of gastrointestinal and liver inflammation using either blocking monoclonal antibodies directed against specific CAMs or mice that are genetically deficient in one or more endothelial CAMs^[34,35]. The $\alpha 2$ subfamily of integrins (CD18) are expressed on leukocytes and these integrins firmly bind to glycoproteins of the immunoglobulin superfamily, such as intercellular adhesion molecule-1 (ICAM-1) and ICAM₂, which are expressed on vascular endothelium. ICAM-1 is constitutively expressed on the surface of endothelial cells and this expression can be enhanced by endotoxin or cytokines^[36,37].

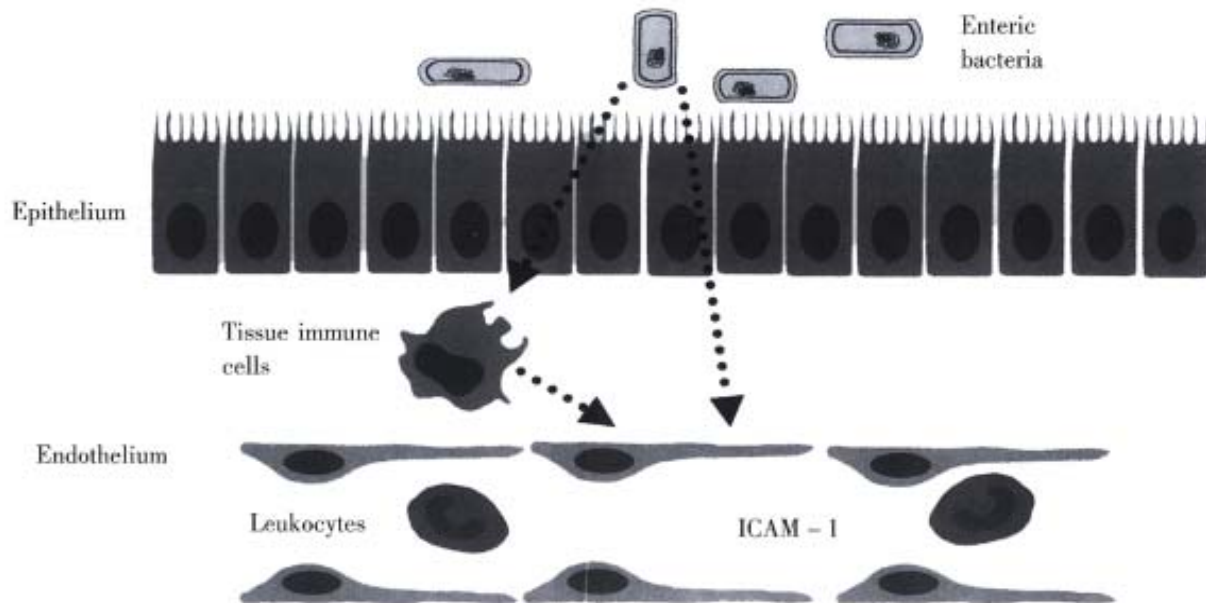


Figure 1 Mechanism underlying the influence of enteric bacteria on ICAM-1 expression on endothelial cells of the intestinal vasculature. Intestinal stasis likely causes an increased production of bacterial factors that promote ICAM-1 expression and consequently enhance the recruitment and activation of leukocytes in the intestine.

Our previous study, which employed surgical procedures to improve cecal stool flow in the rats^[38], represented the first attempt to address the issue of how intestinal stasis results in an inflammatory response. The findings of this study indicate that intestinal stasis is associated with an increased expression of ICAM-1 on endothelial cells and granulocyte infiltration. This study also suggested that it be the bacterial load of a stagnant intestine that determines the activation of mechanisms leading to infiltration of inflammatory cells, based on the responses noted in animals receiving oral antibiotics. This view is supported by a previous study, in which pretreatment with metronidazole inhibited the leukocyte-endothelial cell adhesion in rat mesenteric venules elicited by indomethacin or leukotriene B₄^[39].

A definitive explanation concerning how enteric bacteria enhance ICAM-1 expression on endothelial cells in the stagnant intestine is not readily available. However, our recent work on germfree mice demonstrated that the expression of ICAM-1, but not other endothelial CAMs such as ICAM-2, vascular cell adhesion molecule-1 (VCAM-1), or E-selectin, is altered by germfree conditions^[40]. The ICAM-1 specificity of this response argues against a role for systemic levels of bacterial endotoxin or tumor necrosis factor- α released from macrophages, which are powerful stimuli for VCAM-1 and E-selectin as well as ICAM-1^[34], as mediators of the response. There is a growing body of evidence, derived from germ free

animals, that enteric microflora contribute to the basal level of activation of the immune system, such as antibody-forming potential, phagocytosis, T-cell population and responsiveness to cytokines^[41-47]. As illustrated in Figure 1, some unique factor that is normally released from enteric bacteria promotes the increased constitutive expression of ICAM-1 in the intestinal microvasculature. Events associated with an altered enteric microflora, such as intestinal stasis or an altered fecal stream, are likely to affect the amount of this bacteria-derived factor that regulates ICAM-1 expression. In doing so, the enteric bacteria can exert a profound influence on the trafficking of leukocytes in the intestinal microcirculation. As intestinal stasis and overgrowth of enteric bacteria are associated with increased ICAM-1 expression, subsequently affecting leukocyte-endothelial cell adhesion, it is tempting to speculate that the ischemic and inflammatory changes observed in the several disorders associated with intestinal stasis may have share a common underlying mechanism that largely explains the ulcerative inflammatory lesions.

REFERENCES

- 1 Miller LS, Friedman LS. Less frequent causes of lower gastrointestinal bleeding. *Gastroenterol Clin North Am*, 1994;23:21-52
- 2 Kusumoto H, Yoshida M, Takahashi I, Anai H, Maehara Y, Sugimachi K. Complications and diagnosis of Meckel's diverticulum in 776 patients. *Am J Surg*, 1992;164:382-383
- 3 Donald JW. Major complications of small bowel diverticula. *Ann Surg*, 1979;190:183-188
- 4 de Bree E, Grammatikakis J, Christodoulakis M, Tsiftsis D. The clinical significance of acquired jejunoileal diverticula. *Am J*

- Gastroenterol*, 1998;93:2523-2528
- 5 Clawson DK. Side to side intestinal anastomosis complicated by ulceration, dilatation and anemia. *Surgery*, 1953;34:254-257
 - 6 Adachi Y, Matsushima T, Mori M, Sugimachi K, Oiwa T. Blind loop syndrome: multiple ileal ulcers following side to side anastomosis. *Pathology*, 1993;25:402-404
 - 7 Woelfel GF, Campbell DN, Penn I, Reichen J, Warren GH. Inflammatory polyposis in an ileal blind loop. *Gastroenterology*, 1983;84(5 Pt 1):1020-1024
 - 8 Justus PG, Fernandez A, Martin JL, King CE, Toskes PP, Mathias JR. Altered myoelectric activity in the experimental blind loop syndrome. *J Clin Invest*, 1983;72:1064-1071
 - 9 Welkos SL, Toskes PP, Baer H. Importance of anaerobic bacteria in the cobalamin malabsorption of the experimental rat blind loop syndrome. *Gastroenterology*, 1981;80:313-320
 - 10 Hurst RD, Molinari M, Chung TP, Rubin M, Michelassi F. Prospective study of the incidence, timing and treatment of pouchitis in 104 consecutive patients after restorative proctocolectomy. *Arch Surg*, 1996;131:497-502
 - 11 Sandborn WJ, McLeod R, Jewell DP. Medical therapy for induction and maintenance of remission in pouchitis: a systematic review. *Inflamm Bowel Dis*, 1999;5:33-39
 - 12 Kuhbacher T, Schreiber S, Runkel N. Pouchitis: pathophysiology and treatment. *Int J Col Dis*, 1998;13:196-207
 - 13 Toner M, Condell D, O'Briain DS. Obstructive colitis: ulceroinflammatory lesions occurring proximal to colonic obstruction. *Am J Surg Pathol*, 1990;14:719-728
 - 14 Levine TS, Price AB. Obstructive enterocolitis: a clinico pathological discussion. *Histopathology*, 1994;25:57-64
 - 15 Reeders JW, Rosenbusch G, Tytgat GN. Ischaemic colitis associated with carcinoma of the colon. *Eur J Radiol*, 1982;2:41-47
 - 16 Feldman PS. Ulcerative disease of the colon proximal to partially obstructive lesions: report of two cases and review of the literature. *Dis Col Rec*, 1975;18:601-612
 - 17 Hurwitz A, Khafif A. Acute necrotizing colitis associated with colonic carcinoma. *Surg Gynecol Obstet*, 1960;111:749-753
 - 18 Goulston SJ, McGovern VJ. Pseudomembranous colitis. *Gut*, 1965;6:207-212
 - 19 Elhalaby EA, Teitelbaum DH, Coran AG, Heidelberger KP. Enterocolitis associated with Hirschsprung's disease: a clinical histopathological correlative study. *J Pediatr Surg*, 1995;30:1023-1026
 - 20 Teitelbaum DH, Caniano DA, Qualman SJ. The pathophysiology of Hirschsprung's associated enterocolitis: importance of histologic correlates. *J Pediatr Surg*, 1989;24:1271-1277
 - 21 Hackam DJ, Filler RM, Pearl RH. Enterocolitis after the surgical treatment of Hirschsprung's disease: risk factors and financial impact. *J Pediatr Surg*, 1998;33:830-833
 - 22 Teitelbaum DH, Qualman SJ, Caniano DA. Hirschsprung's disease. Identification of risk factors for enterocolitis. *Ann Surg*, 1988;207:240-244
 - 23 Imamura A, Puri P, O'Briain DS, Reen DJ. Mucosal immune defence mechanisms in enterocolitis complicating Hirschsprung's disease. *Gut*, 1992;33:801-806
 - 24 Wilson-Storey D, Scobie WG, McGenity KG. Microbiological studies of the enterocolitis of Hirschsprung's disease. *Arch Dis Child*, 1990;65:1338-1339
 - 25 Rutgeerts P, Geboes K, Peeters M, Hiele M, Penninckx F, Aerts R. Effect of faecal stream diversion on recurrence of Crohn's disease in the neoterminal ileum. *Lancet*, 1991;338:771-774
 - 26 D'Haens G, Geboes K, Peeters M, Baert F, Ectors N, Rutgeerts P. Patchy cecal inflammation associated with distal ulcerative colitis: a prospective endoscopic study. *Am J Gastroenterol*, 1997;92:1275-1279
 - 27 Cohen T, Pfeffer RB, Valensi Q. "Ulcerative appendicitis" occurring as a skip lesion in chronic ulcerative colitis; report of a case. *Am J Gastroenterol*, 1974;62:151-155
 - 28 Russel MG, Dorant E, Brummer RJ, van de Kruijs MA, Muris JW, Bergers JM. Appendectomy and the risk of developing ulcerative colitis or Crohn's disease: results of a large case control study. *Gastroenterology*, 1997;113:377-382
 - 29 Rutgeerts P, D'Haens G, Hiele M, Geboes K, Vantrappen G. Appendectomy protects against ulcerative colitis. *Gastroenterology*, 1994;106:1251-1253
 - 30 Bready S, Armstrong GR, Nairn R, Gornall P, Currie ABM, Buick RG. Pseudomembranous colitis: a lethal complication of Hirschsprung's disease unrelated to antibiotic usage. *J Pediatr Surg*, 1987;22:257-259
 - 31 Leung FW, Drenick EJ, Stanley TM. Intestinal bypass complications involving the excluded small bowel segment. *Am J Gastroenterol*, 1982;77:67-72
 - 32 Granger DN, Kubes P. The microcirculation and inflammation: modulation of leukocyte-endothelial cell adhesion. *J Leuko Biol*, 1994;55:662-675
 - 33 Granger DN, Grisham MB, Kvietys PR. Mechanisms of microvascular injury. In: Physiology of the gastrointestinal tract, edited by Johnson LR. Third edition. New York: Raven Press, 1994:1693-1722
 - 34 Panes J, Granger DN. Leukocyte endothelial cell interactions: molecular mechanisms and implications in gastrointestinal disease. *Gastroenterology*, 1998;114:1066-1090
 - 35 Granger DN. Cell adhesion and migration. II. Leukocyte endothelial cell adhesion in the digestive system. *Am J Physiol*, 1997;273(5 Pt 1):G982-986
 - 36 Anderson DC. The role of $\beta 2$ integrins and intercellular adhesion molecule type 1 in inflammation. In: Physiology and pathophysiology of leukocyte adhesion, edited by D.N. Granger and G.W. Schmid-Sch-bein. New York: Oxford University Press, 1995:3-42
 - 37 Springer TA. Traffic signals for lymphocyte recirculation and leukocyte emigration: the multistep paradigm. *Cell*, 1994;76:301-314
 - 38 Komatsu S, Panes J, Grisham MB, Russell JM, Mori N, Granger DN. Effects of intestinal stasis on intercellular adhesion molecule 1 expression in the rat: role of enteric bacteria. *Gastroenterology*, 1997;112:1971-1978
 - 39 Arndt H, Palitzsch KD, Grisham MB, Granger DN. Metronidazole inhibits leukocyte endothelial cell adhesion in rat mesenteric venules. *Gastroenterology*, 1994;106:1271-1276
 - 40 Komatsu S, Berg RD, Russell JM, Nimura Y, Granger DN. Enteric microflora contribute to constitutive ICAM-1 expression: studies on germfree mice. *Gastroenterology*, 1999;116:A897
 - 41 Granholm T, Froysa B, Lundstorm C, Wahab A, Midtvedt T, Soder O. Cytokine responsiveness in germfree and conventional NMRI mice. *Cytokine*, 1992;4:545-550
 - 42 Morland B, Midtvedt T. Phagocytosis, peritoneal influx, and enzyme activities in peritoneal macrophages from germfree, conventional and ex germfree mice. *Infect Immun*, 1984;44:750-752
 - 43 Starling JR, Balish E. Lysosomal enzyme activity in pulmonary alveolar macrophages from conventional, germfree, monoassociated and conventionalized rats. *J Reticuloendothel Soc*, 1981;30:497-505
 - 44 Sellon RK, Tonkonogy S, Schultz M, Dieleman LA, Grenther W, Balish E. Resident enteric bacteria are necessary for development of spontaneous colitis and immune system activation in interleukin 10 deficient mice. *Infect Immun*, 1998;66:5224-5231
 - 45 Gautreaux MD, Deitch EA, Berg RD. T lymphocytes in host defense against bacterial translocation from the gastrointestinal tract. *Infect Immun*, 1994;62:2874-2884
 - 46 Shroff KE, Meslin K, Cebra JJ. Commensal enteric bacteria engender a self-limiting humoral mucosal immune response while permanently colonizing the gut. *Infect Immun*, 1995;63:3904-3913
 - 47 Umesaki Y, Setoyama H, Matsumoto S, Okada Y. Expansion of alpha beta T cell receptor bearing intestinal intraepithelial lymphocytes after microbial colonization in germ free mice and its independence from thymus. *Immunology*, 1993;79:32-37

Edited by WU Xie-Ning

Proofread by MIAO Qi-Hong

Brief Reports

Preparation and purification of F(ab')₂ fragment from anti hepatoma mouse IgG₁ mAb

LIU Cheng-Gang¹, ZHU Mei-Cai¹ and CHEN Zhi-Nan²

Subject headings antibody, monoclonal; F(ab')₂ fragment; papain digestion; liver neoplasms; ion-exchange chromatography

INTRODUCTION

Since the advent of hybridoma technology^[1], monoclonal antibodies have been widely used in basic studies and clinical application. F(ab')₂ is a bivalent antibody fragment which is currently used for both diagnosis and treatment^[2], and better than the original mAbs, because it does not retain complement binding function due to lack of Fc regions and reduced interaction with non-specific proteins and the smaller molecular weight than the mAbs, furthermore, it can be digested by pepsin or papain and purified by size exclusion chromatography^[4], ion-exchange chromatography^[6] or hydrophobic interaction^[7]. However, these methods are time-consuming, and cannot attain sufficient purity and recovery of F(ab')₂ fragment. Development of efficient procedures for F(ab')₂ preparation is an urgent necessity.

In the present paper, we described a method for preparation of F(ab')₂ fragment from papain digest of mouse IgG₁ mAb Hab18 and then purified by FPLC using DEAE-Sepharose-FF gel. The results showed this method was suitable for large-scale preparation and purification of F(ab')₂ fragments.

MATERIALS AND METHODS

Materials

Mouse mAb Hab18 belonged to the IgG₁ subclass

was used, and the specific antigen was human hepatoma. It was produced by our laboratory; papain was purchased from Sigma.

Methods

Papain digestion MAb HAB18 was purified from the ascitic fluid which was centrifuged at 1000 r/min for 20 min to remove cells, and the supernatant was dialyzed against 10 mmol/L phosphate buffer (PB), pH 5.5, and then placed at column of SP-cellulose FPLC, the fraction containing IgG₁ HAB18 was precipitated by adding ammonium sulfate to give 50% saturation, followed by centrifugation at 5000 r/min for 10 min after standing for 2 h. The precipitate was dissolved in PBS (10 mmol/L sodium phosphate, pH 7.4, 150 mmol/L NaCl) to 20 g/L, and dialyzed overnight against 0.1 mol/L sodium acetate, pH 5.5.

MAb digestion was carried out by the method of Parham *et al*^[8] with some modification. Briefly, papain was dissolved in 0.1 mol/L sodium acetate, pH 5.5 with 3 mmol/L EDTA, 1 mmol/L DTT (Sigma) and then incubated for 30 min at 37 °C. Activated papain was freed from excess DTT by gel filtration of the Sephadex G-25 (Pharmacia). The papain was determined by measuring absorbance at 280 nm and adjusted to 2 g/L. Preactivated papain was added to mAb HAB18 at a ratio of 1:20 (w/w) and the mixture was incubated at 37 °C for 2h. The reaction ceased by addition of 30 mmol/L iodoacetamide (Fluca) and the products analyzed by SDS-PAGE in the absence of β-mercaptoethanol.

Chromatographic purification The papain digest was dialyzed against 10 mmol/L Tris-HCl, pH 8.0 and applied to a column of DEAE-Sepharose-FF (2 cm×18 cm, Pharmacia) connected to FPLC which was equilibrated and then washed in the same buffer until the absorbance at 280 nm reached a background value of 0.01. The column was then eluted with a linear gradient from 0 mmol/L - 100 mmol/L NaCl in the same buffer. Fractions were collected and assayed for absorbance at 280 nm and analyzed by SDS-PAGE.

¹Center of Clinical Molecular Biology, General Hospital of Air Force, Beijing 100036, China

²Department of Pathology, the Fourth Military Medical University, Xi'an 710032, Shaanxi Province, China

LIU Cheng-Gang, female, born in 1971-06-09 in Weichang, Hebei Province, graduated from the Fourth Military Medical University in 1989, now technologist of molecular biology, majoring hepatoma targeting drug and molecular biology, having 4 papers published. Project supported by the National "863" Fund of China, No.863-102-12(01).

Correspondence to: LIU Cheng-Gang, Center of Clinical Molecular Biology, General Hospital of Air Force, Fu Cheng Road 30, Beijing 100036, China

Tel. +86-10-66928154

Received 1999-07-11

Analytical studies The purity of F(ab')₂ fraction was detected by SDS-PAGE which was performed in a 10% gel under reduction or non-reduction conditions according to the method of Laemmli^[9]. Proteins were treated with loading buffer in the absence or presence of β -mercaptoethanol at 100°C for 5min and stained with Coomassie Brilliant Blue R-250.

Antigen binding activities of F(ab')₂ were measured by indirect immunofluorescence. Viable hepatoma cells were fixed on the plates. F(ab')₂ fraction was diluted with PBS to 1 mg/L, and series of two-fold dilutions were prepared and added to plates which were incubated for 60 min at 37 °C, washed with BPS, and added fluorochrome-conjugated rabbit anti-mouse F(ab')₂ antibody (Sigma) then incubated for 30 min at 37 °C and examined under an immunofluorescence microscope.

Concentrations of F(ab')₂ and mAb were estimated using an extinction coefficient at 280nm and at 260 nm, protein concentration (g/L) = 1.45 × OD₂₈₀ - 0.74 × OD₂₆₀.

RESULTS

Papain digestion

The ascitic fluid from which the mAb was purified by SP-FPLC, the product of the papain digestion for 2 h and the purified F(ab')₂ were applied to SDS-PAGE under non-reduction and reduction conditions, the results indicated about 95% of the antibody were degraded to F(ab')₂ fragment after 2 h incubation. The digest contained F(ab')₂, F(ab'), and Fc fragments as well as intact IgG and other contaminating proteins. A band with M_r 160000 was corresponding to IgG under non-reduction condition before the reaction, and a band of M_r 160 000 was considered to be F(ab')₂ after digestion. Under reduction condition, IgG showed two bands of M_r 50 000 and M_r 28 000, which corresponded to heavy (H) and light (L) chains, respectively. In contrast, the H and L chains of F(ab')₂ were about M_r 30 000 and M_r 28 000 (Figure 1).

Chromatographic purification

The papain digest was separated by FPLC using DEAE-Sepharose-FF column. As shown in Figure 2, the strength of interaction with DEAE was papain < (ab')₂ < Fab' < IgG < Fc. Papain flow through the column, F(ab')₂, F(ab'), IgG, Fc and other protein bound to the column and purified F(ab')₂ fragment was obtained after elution with 50mmol/L NaCl. According to the SDS-PAGE result, the fragment was separated entirely with intact IgG, Fc, papain and other proteins.

Analytical studies

The collected F(ab')₂ pool from the DEAE column was applied to SDS-PAGE and then examined by thin-layer chromatography scanning. The results showed that the purity of F(ab')₂ fragment was more than 95%.

The immunoactivity of initial mAb and the F(ab')₂ obtained after digestion were determined using indirect immunofluorescence. After proteolytic digestion and chromatographic purification, the minimal detective concentration F(ab')₂ was 0.125 μg/mL, corresponding to 90% of their initial mAb activity.

The total protein digested by papain was 100mg. The quantity of the F(ab')₂ obtained from the DEAE-FPLC was 53mg, and the purity greater than 95 %, due to the molecular size of F(ab')₂ fragment is 68% of the intact IgG, thus, the actual yield of F(ab')₂ was about 78% of theoretical yield.

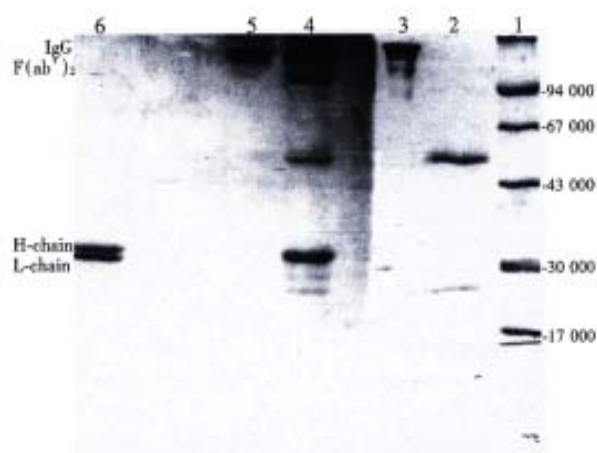


Figure1 Photograph of SDS-PAGE gel of anti-hepatoma IgG₁ mAb HAB18 before and after digestion and purification. Lane 1, molecular weight standards; lane 2-3, reduced and non-reduced mAb HAB18; lane 4, papain digest of HAB18; lane 5-6, purified F(ab')₂ fragment under non-reduction and reduction conditions.

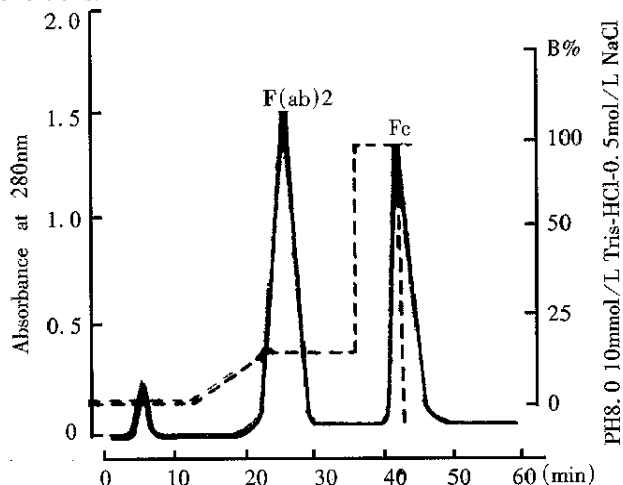


Figure2 Purification of F(ab')₂ fragment from papain digest of mAb HAB18 by FPLC using DEAE-Sepharose-FF column.

DISCUSSION

Classical preparation of $F(ab')_2$ fragments from mouse IgG mAbs used to be digested by pepsin, however, Lamoyi *et al*^[3,4] reported that the sensitivity to pepsin varied in different mouse IgG subclass, it was $IgG_3 > IgG_{2a} > IgG_{2b} > IgG_1$, pepsin had little effect on most mouse IgG₁ proteins. Parham *et al*^[6,8] used preactivatedthiol-free papain to cleave IgG₁ mAbs to $F(ab')_2$ and Fc fragments efficiently, but it needed 18h- 25h for digestion. The method described here was modified according to the reference^[8], the study showed that 2h was sufficient, more than 95 % of mAb was cleaved successfully to $F(ab')_2$ fragment using papain digest ion. Under the conditions described above, 3 anti-hepatoma IgG₁ mAbs had been so far tried and the same results obtained. The relative amounts of $F(ab')_2$ produced might vary with changes in the conditions of digestion, duration and concentration^[8], so we suggested that the conditions of digestion for each monoclonal antibody pre paration be assessed by experience. In addition, it was critical to inactivate the papain, for we observed in our experiment that it might retain activity and led to degradation of $F(ab')_2$ to Fab and smaller fragments.

There have been some papers reporting the purification of $F(ab')_2$ fragments by gel filtration^[2] or ion-exchange chromatography^[3,6]. However, $F(ab')_2$ cannot be purified to homogeneity by single-step chromatography. Koichi^[7] reported a purification scheme for $F(ab')_2$ fragment, using hydrophobic interaction, and ammonium sulfate was used in protein precipitation and purification. However, this technique might reduce significantly the antibody activity^[10]. In the present paper, we described the use of FPLC using DEAE-Sepharose-FF to the purification of $F(ab')_2$ fragment of mouse IgG₁ MA b. The advantage of the method described here was not only could be completed within on

single-step, but also the fraction containing $F(ab')_2$ fragment was homogeneous (Figure 1), which had been separated entirely from papain, intact IgG and Fc fragment, though $F(ab')_2$ sometimes contain a little of $F(ab')$, for many purpose it was no need for further purification. To be more important, the recovered $F(ab')_2$ retained 90% of their initial mAb activity.

By using the procedures above a purification cycle was only 60 min, and $F(ab')_2$ fragment obtained from each cycle could reach the level of preparation scale. Because of these advantages, they could be a simple and rapid process. This method was quite useful in immunological diagnosis and therapy with antibody fragment.

REFERENCES

- 1 Kohler G, Milstein C. Continuous cultures of fused cells secreting antibody of predefined specificity. *Nature*, 1975;256:495-497
- 2 Goding JW. Monoclonal antibodies: principles and practice. 2nd Edn. London: Academic Press, 1986:125-133
- 3 Lamoyi E, Nisonoff A. Preparation of $F(ab')_2$ fragments from mouse IgG of various subclasses. *J Immunol Methods*, 1983;56:235-243
- 4 Parham P. On the fragmentation of monoclonal IgG1, Ig G2 a and IgG 2b from BALB/c mice. *J Immunol*, 1983;131:2895-2902
- 5 Yurov GK, Neugodova GL, Verkhovsky OA, Naroditsky BS. Thiophilic adsorption: rapid purification of $F(ab')_2$ and Fc fragments of IgG1 antibodies from murine ascitic fluid. *J Immunol Methods*, 1994;177:29-33
- 6 Clezardin P, McGregor JL, Manach M, Boukerche H, Dochavanne M. One step procedure for the rapid isolation of mouse monoclonal antibodies and their antigen binding fragments by fast protein liquid chromatography on a Mono Q anion exchange column. *J Chromatography*, 1985;319:67-77
- 7 Morimoto K, Inouye K. Single step purification of $F(ab')_2$ fragments of mouse monoclonal antibodies (immunoglobulins G 1) by hydrophobic interaction high performance liquid chromatography using TSK gel phenyl 5PW. *J Biochem Biophys Methods*, 1992;24:107-117
- 8 Parham P, Androlewicz MJ, Brodsky FM, Holmes NJ, Ways JP. Monoclonal antibodies: purification, fragmentation and application to structural and functional studies of Class I MHC antigens. *J Immunol Methods*, 1982;53:133-173
- 9 Laemmli UK. Cleavage of structural proteins during the assembly of the head of bacteriophage T4. *Nature*, 1970;227:680-685
- 10 Bruck C, Portetelle D, Glineur C, Bollen A. One step purification of mouse monoclonal antibodies from ascitic fluid by DEAE affinity blue chromatography. *J Immunol Methods*, 1982;53:313-319

Edited by WU Xie-Ning

Proofread by MIAO Qi-Hong

Measurement of liver volume and its clinical significance in cirrhotic portal hypertensive patients

ZHU Ji-Ye, LENG Xi-Sheng, DONG Nan, QI Gui-Ying and DU Ru-Yu

Subject headings liver volume; hypertension, portal; liver cirrhosis; prognosis

INTRODUCTION

Accurate assessment of hepatic reserve function in cirrhotic portal hypertensive patients is important for selection of surgical procedure and evaluation of prognosis. The measurement of liver volume has been applied in clinic as widely as Child's class^[1,2]. Limited by technical condition, measurement of liver volume *in vivo* has seldom been reported in China. Using double helix-spiral CT (Elscent CT Twin), the liver volume of 25 cirrhotic patients and 30 patients in controls was assessed, and a correlation analysis was made between the liver volume and preoperative natural shunting rate, portal vein flow, portal pressure and prognosis of cirrhotic patients.

MATERIALS AND METHODS

Patients

Twenty-five patients with post-hepatitis cirrhotic portal hypertension were included in this study (16 males and 9 females, aged 24-66 years, averaging 44.2 years \pm 10.7 years, 1.58 m-1.76 m in height and 47.5 kg-70.5 kg in weight). All patients were HBsAg or HCV-antigen positive with no cardiac disease and hepatic space-occupying lesion.

Thirty patients with chronic cholelithiasis with no hepatic disease served as controls (13 males and 17 females, averaging 45.1 years \pm 14.0 years, 1.58 m-1.82 m in height and 48 kg - 85 kg in weight). All patients were HBsAg negative with no cardiac disease.

Methods

Measurement of liver volume The upper abdomen was scanned by double helix-spiral CT (Elscent CT Twin). The liver volume was measured by 3-dimensional shaded surface display software^[3].

Measurement of natural portal-systemic shunting rate

Department of Surgery, People's Hospital of Beijing Medical University, Beijing 100044, China
Dr. ZHU Ji-Ye, associate professor of surgery, male, born on July 30, 1963 and graduated from Beijing Medical University, being engaged in study on the therapy of portal hypertension.
Tel. +86-10-68314422 Ext.3500
Received 1999-04-08

^{99m}Tc-MIBI 750 mBq (20 mCi) was given intrarectally to cirrhotic portal hypertensive patients who lied supine under the detector of Technica 438H/560 γ camera to image heart, liver and spleen. The region of interest (ROI) with equal area was set up over the surface of heart and liver, portal-systemic shunting index (SI) = ROI (heart)/ROI (heart) + ROI (liver).

Measurement of portal flow and portal pressure

During breath holding after inspiration, the bore and average/maximal blood flow rate of portal vein were measured from 2-dimensional real-time ultrasonographic image with AC USON 128P/10 color Doppler ultrasound system. The portal flow was measured according to the formula (flow volume = sectional area \times flow rate). Portal pressure was measured by gastroepiploic venous centesis.

RESULTS

According to double helix-spiral CT, the average liver volume in the control group was 1070.68 cm³ \pm 227.52 cm³, and was positively correlated with height, the correlation coefficient (γ = 0.42, P < 0.05) was not correlated with that (γ = 0.17, P > 0.05) of body weight.

According to double helix-spiral CT, the average liver volume of portal hypertensive patients was 797.02 cm³ \pm 135.11 cm³, which was significantly smaller than that in the controls (P < 0.05).

The liver volume of cirrhotic portal hypertensive patients was correlative with Child's class, the liver volume and liver volume/height of patients who were Child B were significantly greater than that of patients who were Child C (P < 0.05). There was no significant correlation between liver volume and natural portal-systemic shunting index (SI) (correlation coefficient γ = -0.27, P > 0.05) and portal flow (correlation coefficient γ = 0.17, P > 0.05) (Table 1).

Among the 24 cirrhotic portal hypertensive patients who received H-graft portal-caval shunt (the bore of the artificial vessel was 8 mm), the morbidity of postoperative encephalopathy and the one-year mortality in patients with their liver volume lower than 750 cm³ were found to be higher than those in patients with their liver volume higher than 750 cm³. Significant difference was found in the morbidity of postoperative encephalopathy (Table 2).

Table 1 Comparison of liver volume in different hepatic function class ($\bar{x}\pm s$)

Hepatic function class	Case(n)	Liver volume (cm ³)	Liver volume/height (cm ³ /m)
Child A class	2	1133.0	645.6
Child B class	13	888.2 \pm 92.6 ^a	533.1 \pm 50.1 ^a
Child C class	10	672.4 \pm 91.1	393.8 \pm 48.2

^aCompared with Child C class, $P<0.05$.

Table 2 Morbidity of post-shunting encephalopathy and post-shunting mortality in patients with different liver volume

	Case (n)	Encephalopathy (n)	Morbidity of encephalopathy	One-year death	Mortality
Liver volume>750cm ³	13	1	7.7% ^a	1	7.7%
Liver volume<750cm ³	11	4	36.4%	1	9.1%

^aCompared with liver volume<750 cm³ group, $P<0.05$.

DISCUSSION

Liver cirrhotic portal hypertension is a disease with considerable individual difference. The complicated liver function and other factors will influence portal pressure and the operational results. How to evaluate patients' tolerance to operation, how to select optimal operation for patients and how to predict the prognosis are challenges to surgeons. Age, nutritional condition and hepatic function class (Child's class) have often been regarded as the criteria. Liver volume and amount of liver cells, which is an important index of the hepatic function, were overlooked, while the volume and weight of liver have been regarded as the factors as important as Child's class^[3,4].

Liver is an irregular wedge-shaped organ, critical deformity is present during the course of cirrhosis, which has brought certain difficulty to the measurement of liver volume and its weight *in vivo*. With the help of double helix-spiral CT (Elscent CT Twin), scanning could be completed during the course of breath holding, thus reduced the error. Liver volume was measured by 3-dimensional integral software accurately. The result showed that liver volume in adult had a positive and linear correlation with height, but no close correlation with body weight, this will guide the selection of donor and receptor for liver transplantation. The liver volume of cirrhotic portal hypertensive patients decreased by 25.6% as against controls. The liver volume of patients in Child C class decreased obviously in contrast with patients in Child B class, indicating that hepatic reserve function was correlative with liver volume. If patients were divided into two groups according to liver volume of 750 cm³, the morbidity of postoperative encephalopathy in patients who received portal-caval shunt with their liver volume

less than 750 cm³, was 4.5 times that of patients with their liver volume higher than 750 cm³. Owing to the poor hepatic reserve function, patients with lower liver volume were prone to encephalopathy, therefore it was not adequate to perform shunt operation on patients whose liver volume was too low. It played a role in objective evaluation of patients' tolerance to operation and selection of operational procedure^[5,6]. Our study showed that although the extent of liver atrophy was negatively correlated with portal pressure, correlation coefficient was small. Statistical analysis showed no significant difference, and portal flow was not closely correlated with liver volume. These suggest that there are many factors that influence portal pressure, natural portal-systemic shunting index and portal flow. Liver volume is probably just one of them. At the same time, the relationship between liver volume and portal pressure, portal flow and portal-systemic shunting rate needs to be further studied.

REFERENCES

- Galambos JT. Evaluation of patients with portal hypertension. *Am J Surg*, 1990;160:14-18
- Zoli M, Cordiani MR, Marchesini G, Iervese T, Bonazzi C, Bianchi G, Pisi E. Prognostic indicators in compensated cirrhosis. *Am J Gastroenterol*, 1991;86:1508-1513
- Ogasawara K, Une Y, Nakajima Y, Fukumoto T, Sane S. The significance of measuring liver volume using computed tomographic images before and after hepatectomy. *Surg Today*, 1995;25:43-48
- Ros PR, Eirahman MM, Barrda R, Somers G. Three dimensional imaging of liver masses: preliminary experience. *Appl Radiol*, 1990;19:28
- Adler M, Van Laethem J, Gilbert A, Gelin M, Bourgeois N, Vereerstraeten P, Cremer M. Factors influencing survival at one year in patients with nonbiliary hepatic parenchymal cirrhosis. *Dig Dis Sci*, 1990;35:1-5
- Albers, Hartmann H, Bircher J, Creutzfeldt W. Superiority of the Child Pugh classification to quantitative liver function tests for assessing prognosis of liver cirrhosis. *Scand J Gastroenterol*, 1989; 24:269-276

Localization of keratin mRNA and collagen I mRNA in gastric cancer by in situ hybridization and hybridization electron microscopy

SU Chang-Qing¹, QIU Hong¹ and Zhang Yan²

Subject headings keratin; collagen; *in situ* hybridization; nucleic acid; stomach neoplasms; mRNA

INTRODUCTION

Immunohistochemistry and immune electron microscopy were used to determine the keratin and collagen I polypeptides expressed in gastric mucosa and gastric cancer. We found that the canceration of gastric epithelia and the infiltration and metastasis of gastric cancer are closely related with cellular skeleton and extracellular matrix^[1]. The *in situ* hybridization (ISH) technique, developed by Gall and Pardue in 1969^[2,3], has become an essential tool for detecting the localization of synthesis and abundance of RNA transcripts on tissue sections. With a K₆ (M_r 56000) keratin cDNA probe and a collagen I α_1 -chain cDNA probe, the cDNA-mRNA ISH technique was used to study changes of keratin mRNA and collagen I mRNA expression in gastric mucosa and gastric cancer.

MATERIALS AND METHODS

Tissue preparation

Tissue samples of 58 cases of gastric cancer and 40 cases of gastric mucosa were obtained from fresh surgical specimens at the Cancer Center of PLA, Nanjing 81 Hospital, Nanjing, China. The samples for light microscopic ISH were immediately fixed in 100mL/L buffered formalin. The samples for ultrastructural ISH were fixed in PG fixative solution.

Probe preparation

Biotinylated probes of K₆ keratin cDNA and collagen I α_1 -chain cDNA were prepared from the Pst I fragments cloned at plasmid PBR322 (Amersham). The probe preparation was essentially carried out according to the methods of Obara *et al*^[4,5] by randomly primed *in vitro* transcription, with the use of biotin-11-dUTP (BRL).

Light microscopic ISH

Formalin-fixed, paraffin-embedded tissue sections were cut and mounted on glass slides that had been treated to inactivate RNase and coated with 0.05% polylysine (Sigma). All hybridization procedures were tested according to Plummer *et al*^[3] and Mandry *et al*^[6].

The sections were deparaffinized in xylene, washed in alcohol, and then air-dried. After washed in PBS, the sections were treated with 3 mg/L proteinase K (Sigma) in 10 mmol/L Tris-HCl, pH 7.4, 2mmol/L CaCl₂ for 10 min at 37 °C, and washed in PBS containing 0.2% glycine followed by fixation in 4% paraformaldehyde for 5min at 37 °C, and then dehydrated and air-dried. All sections were covered with prehybridization buffer (50% formamide, 2×SSC, 2×Denhardt's solution, 10% dextran sulfate, 500mg/L herring sperm DNA, 500mg/L yeast tRNA) for 60min at room temperature. The labeled probes were diluted to the concentration of 0.5 mg/L in the same buffer, heat-denatured at 100 °C for 5min. Each section was overlaid with this hybridization solution, covered with a coverslip, and then incubated overnight for 24 hours at 44 °C in moist chamber. Posthybridization washing was either with 50% formamide in 2×SSC or with 1mmol/L-EDTA in PBS. Blocking solution containing 3% BSA and 1mmol/L EDTA in 0.1mol/L, pH 7.4, TBS was used to reduce background staining, 10min at room temperature, followed by a brief washing in distilled water. Tissues were reacted with 1:20 streptavidin-peroxidase (Maxim) in the blocking solution for 60min at 37 °C, washed thoroughly with 2×SSC and 0.1mol/L, pH 7.4, TBS, and revealed by the addition of hydrogen peroxide and AEC, finally counterstained with hematoxylin.

The positive staining was classified into four grades: (-) no positive grains, (+/-) a few tiny

¹Central Laboratory of Nanjing 81 Hospital, Nanjing 210002, Jiangsu Province, China

²Department of Radiation Oncology, Nanjing Second Hospital, Nanjing 210003, Jiangsu Province, China

SU Chang-Qing, male, born on 1964-01-27 in Tonghua, Jilin Province, graduated from Anhui Medical University as a postgraduate in 1990, Ph.D. of molecular biology, majoring in mechanism of tumor infiltration and metastasis, having more than 50 papers published.

Project supported by the Military Youth Science Fund of China, No. 94008

Correspondence to: Dr. SU Chang-Qing, Central Laboratory of Nanjing 81 Hospital, Nanjing 210002, China

Tel. +86-25-6648090 Ext.241

Email.sucq@jlonline.com

Received 1999-04-28

grains in the cells, (+) many positive grains gathered to coarse grains, (++) thick grains in the cells gathered to slices.

Ultrastructural ISH

The positive cases demonstrated by light microscopic ISH on paraffin sections were chosen to be used for ultrastructural ISH, including 22 cases of gastric mucosa and 49 cases of gastric cancer. The prepared samples fixed in PG fixative solution were washed in PBS containing 5% sucrose, cut into 30µm-50µm thick oscillating sections and mounted on slides. The ultrastructural ISH steps, including enzymatic digestion, denaturation, hybridization, and detection probe, were carried out the same as in light microscopic ISH, with the exceptions of probe concentration of 0.1mg/L and streptavidin-peroxidase working titer of 1:100.

After the hybridization signals had been revealed, the sections were gently separated from slides and carefully folded to tissue blocks, followed by postfixation in 1% osmium tetroxide. The following procedures, including dehydration, embedded in Epon-812, ultrathin section making and staining with lead citrate and uranyl acetate, were executed according to the conventional steps of diagnostic electron microscopy. Finally, the hybridization signals were observed under H-300 transmission electron microscope.

Negative controls

Negative controls included the sections digested previously with RNase A (Sigma) and the sections incubated in prehybridization solution without probes, all of which had undergone the simultaneous ISH processes.

RESULTS

Distribution of keratin mRNA

Under light microscopy, different extent of hybridization signals was found in 22 of 40 cases of gastric mucosa, and positive grains were found in 49 of 58 cases of gastric cancer. The gastric epithelial cells positive for keratin mRNA were scattered in mucosal glands, especially in the bases of glands. The hybridization grains were tiny and dense in cytoplasm. Keratin mRNA in cancer cells increased, the quantity and distribution of positive grains were related to the histological type and differentiation of cancer cells. In well-differentiated cancer, the grains in cancer cells were thick and coarse, while in poorly-differentiated cancer, the positive grains distributed in all cytoplasm matrix and always gathered to form slices (Figure 1).

Ultrastructurally, 8 cases showed positive reaction in 22 cases of gastric mucosa, and 21 cases

positive signals were found in 21 of 49 cases of gastric cancer. The positive grains in the epithelia were tiny and distributed in cytoplasm, especially more around nuclei (Figure 2). In cancer cells, keratin mRNA positive grains increased and appeared in two forms, one was tiny grains gathered in certain sites of cytoplasm and distributed irregularly, most of which came out in poorly-differentiated cancer cells; the other was coarse grains scattered evenly in cytoplasm, which mostly emerged in well differentiated cancer cells (Figure 3). The sections of cancer tissue, through the treatment of RNase A before ISH, had few tiny grains in cytoplasm of cancer cells.

Expression of collagen I mRNA

Collagen I mRNA positive reaction was localized in the cytoplasm of mesenchymal cells, like fibroblasts in mucosal and cancer stroma. The reaction in mucosal mesenchymal cells showed dense black staining. In the stroma of well-differentiated cancer, the positive cells distributed around or in the cancer nests dispersively, most cells had coarse and thick grains and some cells only had a few tiny grains (Figure 4). In poorly-differentiated cancer, collagen I mRNA reaction distributed irregularly in fibroblasts was dense and looked like the form of dust.

Comparison of mRNA expression in gastric mucosa and gastric cancer is shown in Table 1.

Table 1 Comparison of keratin mRNA and collagen I mRNA expression

Staining grade	Keratin mRNA		Collagen I mRNA	
	Mucosa	Cancer ^a	Mucosa	Cancer
-	18	9	19	25
+/-	10	23	12	18
+	7	12	5	9
++	5	14	4	6
Total	40	58	40	58

^aP<0.05 vs mucosa group.

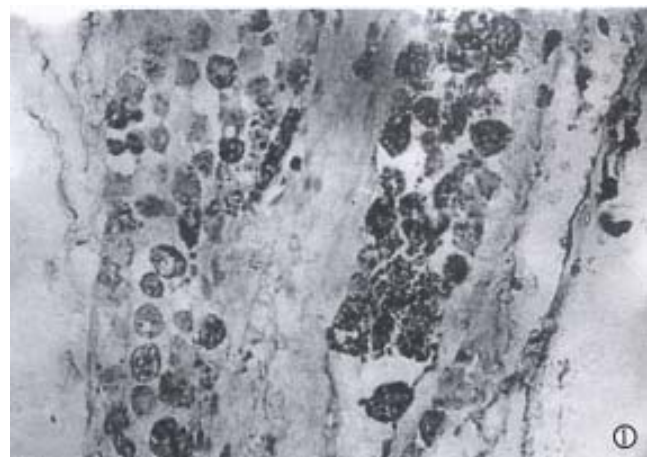


Figure 1 Poorly-differentiated carcinoma, keratin mRNA positive grains increased and distributed in cytoplasm. ×400

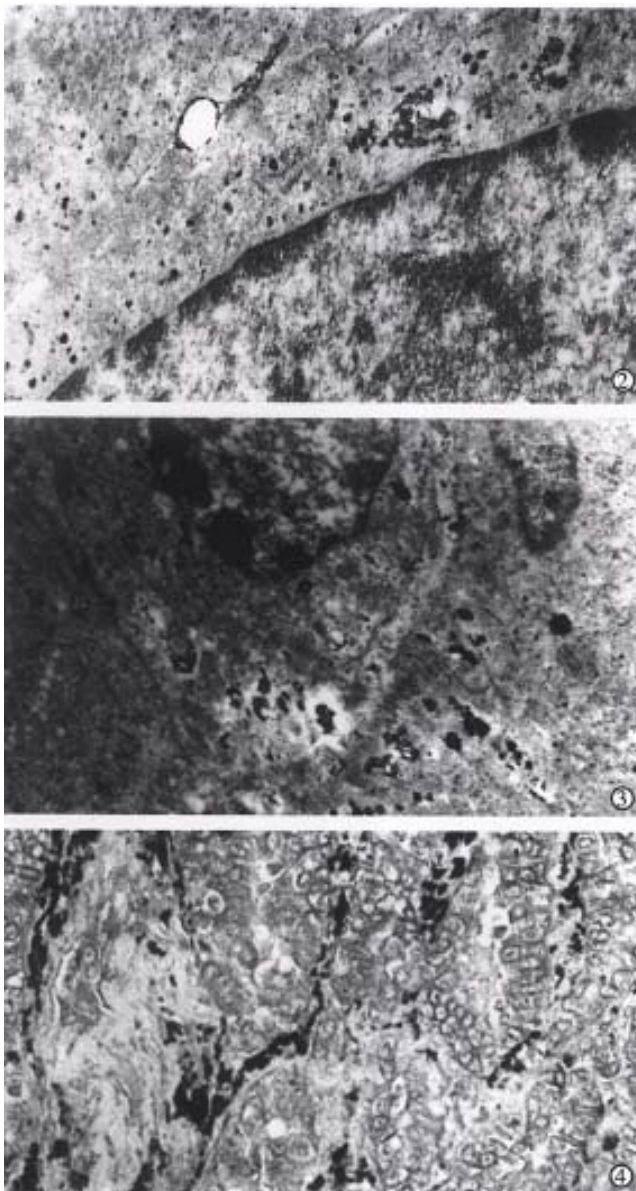


Figure 2 Normal gastric mucosa: the positive grains for keratin mRNA in the epithelial cell were tiny and distributed around nucleus. $\times 15000$

Figure 3 Well-differentiated adenocarcinoma: coarse grains for keratin mRNA increased and scattered evenly in cancer cell cytoplasm. $\times 1500$

Figure 4 Well-differentiated adenocarcinoma: collagen I mRNA positive grains appeared in mesenchymal cells. $\times 200$

DISCUSSION

In the past experiments, immunohistochemistry was used to localize cellular skeleton and extracellular matrix at gene product levels. But it is unable to differentiate active production of proteins on site from proteins stored in passive cells^[4]. A valuable alternative is the detection of mRNAs by ISH which can identify specific cell types actively transcribing specific genes. With the use of K₆ keratin cDNA probe and collagen I α_1 -chain cDNA probe, the detection of specific mRNAs by ISH was applied to

the study of their changes in gastric mucosa and gastric cancer. On paraffin sections, the expression of keratin mRNA and collagen I mRNA in target cells was directly observed, and on ultrathin sections, keratin mRNA positive reaction was observed under electron microscope. But on sections that had been treated with RNase A before ISH and hybridized without probes, no obviously positive reaction grains were found. The results demonstrated that the hybridization signals originated from RNA. The technique of pre-embedding hybridization and tissue section posthybridization treatment, is a new pre-embedding method for ultrastructural ISH. Although pre-embedding technique has the disadvantages of loss of ultrastructural membrane detail and potential loss of label during the embedding procedure, it is sufficient to localize mRNA ultrastructurally and to study the transcription and expression of genes.

The keratin, characteristic of epithelial cells, represents a complex family of 19 different components with molecular weights varying from $M_r 4000$ to $M_r 67000$. Because individual keratin is synthesized from different mRNA, the transcript level of specific keratin reflects changes in the expression of the genes, cDNA probes for various keratin mRNAs from various species have been produced. With K₆ keratin cDNA probe, which has been shown to be complementary to the mRNA for the $M_r 56000$ keratin and to share significant homology with the mRNA for $M_r 58000$ keratin^[4], the positive hybridization signals appeared clear in gastric mucosa and gastric cancer. The hybridization grains in epithelia were tiny and distributed around nuclei, and the grains in cancer cells increased ($P < 0.05$), often gathered to coarse grains or slices, and distributed heterogeneously, especially in poorly-differentiated cancer cells. The results, unanimous with that of immunohistochemistry^[1], demonstrated further that the increase of keratin in cancer cells is due to its active synthesis in cancer cells. This ability to synthesize cellular skeleton protein is related to the active reproduction and strong motility. The positive rate of keratin mRNA by ISH in gastric mucosa and cancer was lower than that of keratin by immunohistochemistry^[1], due to loss of hybridization information during the sample treatment and weakness of gene expression in some cells.

Collagen I, one of extracellular matrix components, mainly arises from mesenchymal cells. A few investigators, with immunohistochemistry and ISH, described that epithelial tissue and cancer cells, such as hepatocytes and hepatocarcinoma cells, can produce collagen I^[7]. With the use of

collagen I cDNA probe, we found that collagen I mRNA was expressed only in mesenchymal cells. Further study will prove whether this is related to the difference of probes or not. In gastric cancer stroma, the hybridization grains were thick and dense in mesenchymal cells which were distributed around or in the cancer nests. The active synthesis of collagen I plays an important role in the formation of fibrous capsule around cancer nests and in the inhibition of cancer cell infiltration and metastasis. During the process of cell canceration and cancer infiltration and metastasis, some changes will occur in extracellular matrix including collagen I, possibly due to the changes of synthesis and degradation of these components [1,8]. In our current study, the expression of collagen I in cancer stroma had no obvious changes compared with that in gastric mucosa ($P>0.05$), so that we believe that the degradation yielded by cancer cells is an essential factor in the changes of extracellular matrix. This degradation is of great importance to the infiltration and metastasis of cancer cells.

Finally, the changes in the biological characteristics of gastric cancer are due to the effect of cellular skeleton and extracellular matrix. The increase of keratin synthesis and the ability of extracellular matrix degradation in cancer cells are the key mechanism of cancer infiltration and

metastasis. The ISH technique has been proven to be a powerful tool *in situ* gene expression in individual cell. Further study of other cellular skeleton and extracellular matrix components is in progress.

REFERENCES

- 1 Su CQ, Xu SF. Relationship between cytoskeleton and extracellular matrix and gastric cancer infiltration and metastasis. *Zhonghua Yixue Zazhi*, 1994;74:432-433
- 2 Capodiceci P, Magi Galluzzi C, Moreira G, Zeheb R, Loda M. Automated in situ hybridization: diagnostic and research applications. *Diagn Mol Pathol*, 1998;7:69-75
- 3 Plummer TB, Sperry AC, Xu HS, Lloyd RV. In situ hybridization detection of low copy nucleic acid sequences using catalyzed reporter deposition and its usefulness in clinical human papillomavirus typing. *Diagn Mol Pathol*, 1998;7:76-84
- 4 Obara T, Baba M, Yamaguchi Y, Fuchs E, Resau JH, Trump BF, Klein Szanto AJP. Localization of keratin mRNA in human tracheobronchial epithelium and bronchogenic carcinomas by *in situ* hybridization. *Am J Pathol*, 1988;131:519-529
- 5 Shi QH, Shan XN, Zhang JX, Zhang XR, Chen YF, Deng XZ, Huang HJ, Yu L, Zhao SY, Zheng QP, Adler ID. A DNA probe suitable for the detection of chromosome 21 copy number in human interphase nuclei by fluorescence in situ hybridization. *Zhonghua Yixue Yichuanxue Zazhi*, 1999;16:36-40
- 6 Mandry P, Murray AB, Rieke L, Becke H, Hfler H. Postembedding ultrastructural in situ hybridization on ultrathin cryosections and LR white resin sections. *Ultrastruct Pathol*, 1993;17:185-194
- 7 Wang YJ, Yang LS, Dai YM. Expression of collagen $\alpha 1$ gene in human primary carcinoma. *Linchuang & Shiyan Binglixue Zazhi*, 1993;9:167-169
- 8 Bu W, Tang ZY, Ye SL, Liu KD, Huang XW, Gao DM. Relationship between type IV collagenase and the invasion and metastasis of hepatocellular carcinoma. *Zhonghua Xiaohua Zazhi*, 1999;19:13-15

Edited by WANG Xian-Lin
Proofread by MA Jing-Yun

***In situ* detection of Epstein Barr virus in gastric carcinoma tissue in China highrisk area**

WAN Rong, GAO Mei-Qin, GAO Ling-Yun, CHEN Bi-Feng and CAI Qian-Kun

Subject headings stomach neoplasms; Epstein-Barr virus; *In situ* hybridization; LMP-1 protein

INTRODUCTION

Epstein-Barr virus (EBV), a gammaherpesvirus, has been strongly associated with African Burkitt's lymphoma and nasopharyngeal carcinoma. Recently it has been identified in lymphoepithelioma-like carcinoma of thymus, tonsil, lung and in some gastric carcinoma^[1-4]. The development of very sensitive methods for detection of EBV infection in archival pathologic tumor sections has allowed us to study the association of EBV with gastric adenocarcinomas by using *In situ* hybridization with EBER-1 oligoprobes and immunohistochemistry with anti-LMP1 antibodies.

MATERIALS AND METHODS

Materials

Cases were selected from a series of primary gastric carcinomas collected at the Department of Pathology, Fujian Medical University, Fuzhou, Fujian. The specimens included 58 primary gastric carcinomas, 5 chronic peptic ulcer and 10 additional specimens of normal gastric mucosa obtained from postmortem patients without gastrointestinal disease. Formalin-fixed, paraffin-embedded tissues were prepared for light microscopic examination.

Method

***In situ* hybridization** The EBV sequence, EBER-1, was detected with a complementary digoxigeninlabeled 30 -base oligomer using a procedure previously described^[5]. A blue-brown or brown color within

the nucleus over background levels was considered positive. In each case, hybridization was applied to section that contained both neoplastic and adjacent non-neoplastic mucosa.

A known EBV-positive nasopharyngeal carcinoma served as positive control and *In situ* hybridization without EBER probe was taken as negative control.

Immunohistology

Paraffin-embedded sections were stained with monoclonal antibodies (CS1-4, DAKO) to evaluate the expression of LMP-1. Immunostaining was performed with the avidin-biotin complex (ABC) method as previously described. For these antibodies, the method of antigen retrieval was used by microwave oven pretreatment in place of proteolytic digestion before immunostaining. LMP-1 positive nasopharyngeal carcinomas were used as positive controls.

RESULTS

Clinical data and histological subtype

The age range of patients was 37-74 years, with a median age of 54.5 years. Fifty patients were males and 8 were females, the ratio of males to females being 6.3:1. Among the 58 gastric adenocarcinomas, 22 were poorly-differentiated, 18 tubular, 10 mucinous, 7 signet-ring cell carcinoma, 1 papillary adenocarcinoma.

EBV gene expression

EBER-1 expression *In situ* hybridization, signals were strong and limited to the nucleus of carcinoma cell (Figure 1). A blue-brown or brown color was considered a positive signal. Six cases (10.3%) showed EBER-1 expression, including 5-poorly-differentiated and 1 papillary adenocarcinoma. In positive cases, virtually all malignant cells were strongly labeled with EBER probes, while the infiltrating lymphocytes, blood vessels and smooth muscle were EBER-1 negative. No EBER-1 signals were observed in adjacent non-neoplastic epithelial cells, dysplastic epithelial cells and normal gastric mucosa.

LMP-1 expression No expression of LMP-1 was seen in both EBER-1 positive and negative cases.

Department of Pathology, Fujian Medical University, Fuzhou 350004, Fujian Province, China

WAN Rong, female, born in 1965-03-23 in Fuzhou, Fujian Province, Han nationality, graduated from Fujian Medical University as a postgraduate in 1993, specialized in research of gastroenteric tumors, having 5 papers published.

Correspondence to: WAN Rong, Department of Pathology, Fujian Medical University, 88 Jiaotong Road, Fuzhou 350004, Fujian Province, China

Tel. +86-591-3314484, Fax. +86-591-3351345

Email: guhuang@pub3.fj.cn

Received 1999-06-30 **Accepted** 1999-09-15

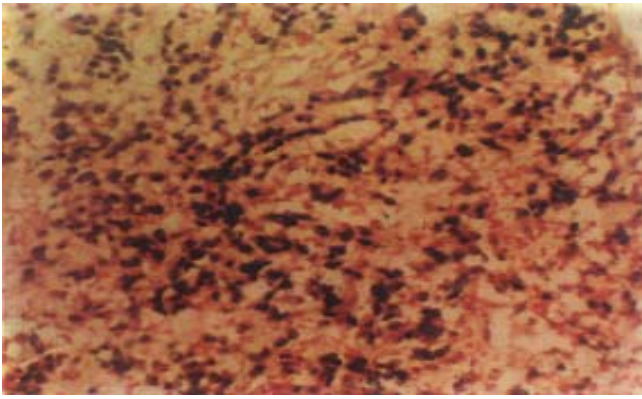


Figure 1 EBER-1 expression in nuclei of essentially all gastric malignant cells. $\times 200$

DISCUSSION

EBER-1 is EBV encoded small RNA, of which high levels expression can be up to 10^6 - 10^7 copies per cell exceeding DNA in EBV-infected cell. EBER oligoprobe may combine with EBER-1 enabling for detecting EBV on paraffin-embedded tissues using non-isotopic labeling and *In situ* hybridization technique which are now considered the most sensitive methods.

EBV is an oncogenic virus which has neoplastic transforming properties. The incidence of EBV infection is high in Chinese population especially in east and south China. In the current study, we had demonstrated the presence of viral RNA in 10.3% of our cases of gastric carcinomas by this method. The frequency of EBV gene expression in gastric malignant epithelium in Fuzhou was higher than that (1.6% to 6.1%) reported in Changsha and Shenyang^[6]. Our study suggested that the frequency of EBV infection was different in different regions of China.

The presence of EBV in neoplasms seemed to be related to the histological subtype of neoplasms. Raab-Traub *et al*^[7], found EBV in undifferentiated and poorly differentiated nasopharyngeal carcinomas, which generally contained a relatively large number of EBV genome equivalents. In Hodgkin's disease, presence of EBV was often in mixed cellularity (HD-MC, 91%) and nodular sclerosis (HD-NS, 43%) subtypes^[8]. In our study, most of the EBV-positive cases were poorly

differentiated gastric carcinomas. The relation between EBV infection and poorly differentiated carcinomas is unknown. Many believed that EBV virus might multiply easier in the poorly differentiated carcinoma, EBV genome amplification favored growth of malignant cells, promote infiltration and metastasis^[7]. We failed to detect LMP-1 expression in this tumor due to the methylation of coding and regulatory regions of this protein^[9].

Shibata *et al*^[10] and Gulley *et al*^[11], found that the EBER-1 was present in dysplastic epithelium of gastric mucosa before malignancy transformation. But our result showed no EBER-1 expression in the adjacent non-neoplastic epithelium, dysplastic cells and normal gastric mucosa. Finally low frequency of Epstein-Barr virus in gastric carcinoma suggests that EBV does not play any important role in the pathogenesis of gastric carcinoma.

REFERENCES

- Dimery IW, Lee JS, Blick M, Pearson G, Spitzer G, Hong WK. Association of the Epstein Barr virus with lymphoepithelioma of the thymus. *Cancer*, 1988;61:2475-2480
- Brich ek B, Hirsch I, "bl O, Viiksov E, Vonka V. Presence of Epstein Barr virus DNA in carcinomas of the palatine tonsil. *JNCI*, 1984;72:809-815
- Kasai K, Sato Y, Kameya T, Inoue H, Yoshimura H, Kon S, Kikuchi K. Incidence of latent infection of Epstein-Barr virus in lung cancers: an analysis of EBER-1 expression in lung cancers by *in situ* hybridization. *J Pathol*, 1994;174:257-265
- Shibata D, Tokunaga M, Uemura Y, Sato E, Tanaka S, Weiss LM. Association of Epstein Barr virus with undifferentiated gastric carcinomas with intense lymphoid infiltration (lymphoepithelioma-like carcinoma). *Am J Pathol*, 1991;139:469-474
- Hamilton Dutoit SJ, Raphael M, Audouin J, Diebold J, Lisse I, Pedersen C, Oksenhendler E, Marelle L, Pallesen G. *In situ* demonstration of Epstein-Barr virus small RNAs (EBER-1) in acquired immunodeficiency syndrome-related lymphomas: correlation with tumor morphology and primary site. *Blood*, 1993;82:619-624
- Wang M, Tokunaga M, Jia XS, Ding JY, Hou ZJ. Observations on the relation of gastric carcinoma to Epstein Barr virus. *Zhonghua Binglixue Zazhi*, 1994;23:285-287
- Raab Traub N, Flynn K, Pearson G, Huang A, Levine P, Lanier A, Pagano J. The differentiation form of nasopharyngeal carcinoma contains Epstein Barr virus DNA. *Int J Cancer*, 1987;39:25-29
- Zhou XG, Hamilton Dutoit SJ, Yan QH, Pallesen G. High frequency of Epstein Barr virus in Chinese peripheral T-cell lymphoma. *Histopathology*, 1994;24:115-122
- Imai S, Koizumi S, Sugiura M, Tokunaga M, Uemura Y, Yamamoto N, Tanaka S, Sato E, Osato T. Gastric carcinoma: monoclonal epithelia malignant cells expression Epstein Barr virus latent infection protein. *Proc Natl Acad Sci USA*, 1994;91:9131-9135
- Shibata D, Weiss LM. Epstein Barr virus associated gastric adenocarcinoma. *Am J Pathol*, 1992;140:769-774
- Gulley ML, Pulitzer DR, Eagan PA, Schneider BG. Epstein-Barr virus infection is an early event in gastric carcinogenesis and is independent of bcl-2 expression and p53 accumulation. *Hum Pathol*, 1996;27:20-27

Edited by WU Xie-Ning

Proofread by MIAO Qi-Hong

Comparison of gene expression between normal colon mucosa and colon carcinoma by means of messenger RNA differential display

WANG Li¹, LU Wei¹, CHEN Yuan-Gen¹, ZHOU Xiao-Mei² and GU Jian-Ren²

Subject headings colonic mucosa; colonic neoplasms; RNA, messenger; gene expression

INTRODUCTION

Messenger RNA differential display technique, developed by Dr. Liang in 1992^[1], is a powerful new tool for identifying and cloning differentially expressed genes in a certain type of cell line, tissue or a special developing stage. Using this method, large amounts of molecular biological information can be obtained easily and quickly. In our study, this technique was used to compare genes expressed differentially between normal colon mucosa and colon carcinomas, in order to understand the molecular biological basis of colon cancer.

MATERIALS AND METHODS

Samples

Fifteen samples of colon carcinoma were obtained from radical colectomy, samples of normal colon mucosa were obtained 8 cm - 10 cm apart from colon carcinoma.

Reagents

Guanidine thiocyanate and β -mercaptoethanol were purchased from BRL (America); T₁₂MN primer and AP primer were presented by the National Laboratory for Oncogene and Related Genes, Shanghai Cancer Institute.

Experimental procedures

RNA preparation Total RNA was isolated from

normal colon mucosa and colon carcinoma using single-step method of guanidine thiocyanate described by Chomczynski^[2,3], some steps had been modified.

Reverse transcription DNA-free RNA was reversely transcribed using the oligo-dT primer T₁₂MN in the presence of [γ -³²P]dATP.

PCR amplification Using cDNA products as templates, PCR reactions were performed in the presence of [γ -³⁵S] dATP, the primer combination was T₁₂MN and AP. Following denaturation for 30 seconds at 94 °C, the PCR steps consisted of 30 seconds at 94 °C, 2 minutes at 40 °C, 30 seconds at 72 °C for 40 cycles, followed by 5 minutes at 72 °C. Amplified PCR products from normal colon mucosa and colon carcinomas were separated side by side on a 7.5 M urea/6% polyacrylamide gel.

Recovery of differentially expressed bands After autoradiography, the cDNA bands representing differentially expressed mRNAs were excised from the gel. For each band, extracted cDNA was reamplified for 30 cycles with the same primers and the same PCR conditions used in the initial PCR, except that no radioactive dNTP was included. After PCR, the product was run on 1.5% low melt agarose gel and stained with ethidium bromide.

Northern blot analysis PCR bands of the expected size were cut from the gel, purified and used as probes. DNA probes were radio-labeled by the random prime labeling method, hybridized with RNA from pre samples and other RNA samples respectively.

RESULTS

Total RNAs from normal colon mucosa and colon carcinomas were isolated using single-step method of guanidine thiocyanate, then reversely transcribed into first string of cDNA, T₁₂MA, T₁₂MC, T₁₂MT and T₁₂MG were used as oligo-dT primer individually. The result of alkaline denatured electrophoresis indicated that cDNA molecules were in the range of 0.5kb-5kb. cDNAs were amplified

¹Department of Gastroenterology, Huashan Hospital, Shanghai Medical University, Shanghai 200040, China

²National Laboratory for Oncogene and Related Genes, Shanghai Cancer Institute, Shanghai 200032, China

Dr. WANG Li, female, born on 1996-11-24 in Jingjiang, Jiangsu Province, Han nationality, graduated from Shanghai Medical University as a Ph.D. fellow in 1999, attending doctor of gastroenterology, majoring in molecular biology research of gastroenterology, having 12 papers published.

Supported by the National Natural Science Foundation of China, No. 39470329.

Correspondence to: Dr. WANG Li, Department of Gastroenterology, Huashan Hospital, 12 Wu Lu Mu Qi Zhong Road, Shanghai 200040, China

Tel. +86-21-62489999 Ext.274

Email: Wangli@shtel.net.cn

Received 1999-04-08

by PCR reaction using the primer combination. T₁₂ MN and AP₂, AP₄, PCR products were separated by 6% polyacrylamide gel electrophoresis. Fourteen bands were obtained which were differentially displayed between normal colon mucosa and colon carcinoma. Eight bands (T₁-T₈) were highly expressed in carcinomas, and the other 6 bands were expressed only in normal tissues. T₁ band was verified to be highly expressed in tumor, but had no expression in normal tissues by Northern blot. This cDNA band would be used for cloning and sequencing.

DISCUSSION

The technique of mRNA differential display, by means of combining T₁₂MN and arbitrary primer AP, can detect all expressed genes in mammalian cells and recover their molecular biological information. These cDNA fragments can be used as probes to isolate target genes from genomic DNA or cDNA library for intensive molecular biological identification. The technique has several advantages over other methods, such as simplicity, sensitivity, reproducibility, versatility and speed, so that it has been used in researches of many diseases, especially

in molecular biological study of malignant tumors. We screened 14 cDNA fragments by means of mRNA DD, one of these bands (T₁) was highly expressed in the colon carcinoma which was used for differential display. Using T₁ band as probe, we found that it was also highly expressed in many other colon carcinomas (12/15). In the further study, this DNA fragment can be used for cloning and sequencing. Checking the database of Genbank, if the sequence of this cDNA band has no homology to the sequences of other nucleic acids, it can be considered as partial cDNA fragment of a new colon carcinoma-related gene. By screening the genomic DNA or a certain cDNA library, the full-length cDNA can be cloned, which may be helpful in the study of the molecular biology of colon carcinoma.

REFERENCES

- 1 Liang P, Pardee AB. Differential display of eukaryotic mRNAs by means of the polymerase chain reaction. *Science*, 1992;257:967-971
- 2 Chomczynski P, Sacchi N. Single-step method of RNA isolation by acid guanidinium thiocyanate phenol chloroform extraction. *Anal Biochem*, 1987;162:156-159
- 3 Sibert PD, Chenchik A. Modified and guanidinium thiocyanate phenol chloroform RNA extraction method which greatly reduced DNA contamination. *Nucleic Acid Res*, 1993;21:2019-2020

Edited by WANG Xian-Lin
Proofread by MA Jing-Yun

An improvement method for the detection of *in situ* telomerase activity: *in situ* telomerase activity labeling

FENG De-Yun, ZHENG Hui, FU Chun-Yan and CHENG Rui-Xue

Subject headings methodology; telomerase; *in situ* labeling; polymerase chain reaction

INTRODUCTION

Telomerase is a special reverse transcriptase which consists of a template RNA and protein, and uses the RNA template to catalyze the addition of telomeric DNA to chromosome ends^[1-5]. The enzyme is active in adult male germ-line cells, embryonic cells and hemopoietic stems, but is undetectable in normal somatic cells except for proliferative cells of renewal tissue, e.g., activated lymphocytes, basal cells of the epidermis and intestinal crypt cells, whereas in almost all malignant tumor cells and immortal cell lines, telomerase activity has been measured. Thus, it is believed that activation of telomerase is closely associated with genesis and development of malignant tumors. Most studies to date have measured telomerase activity by telomeric repeat amplification protocol (TRAP) in heterogeneous tissue extracts^[1,3-5]. With the introduction of sensitive TRAP, telomerase has been reported to be detectable in small tissue samples from almost all tumors and tumors-derived cell lines. It is not known if all cells within a tumor have telomerase activity or if only a subset does. It is necessary to develop an *in situ* assay for detecting telomerase activity levels in cytological and tissue samples. Ohyashiki^[2] reported an *in situ* assay for telomerase activity by *in situ* PCR with fluorescence TS and CX telomerase primers to detect telomerase activity of cultured cells and free cells, but the attempts to use *in situ* PCR telomerase assay on frozen sections of pathological materials were unsuccessful. Now we report an improved *in situ* telomerase activity

assay on the basis of TRAP, which is very easy to be performed. A stable result can be gained on frozen sections of tumor tissue.

MATERIALS AND METHODS

Samples and reagents

Twenty-four hepatocellular carcinoma (HCC), 20 colorectal carcinoma (CRC) and 18 nasopharyngeal carcinoma (NPC) tissues were obtained from patients in Xiangya Hospital and the Second Affiliated Hospital of Hunan Medical University, Changsha, People's Republic of China. Each tissue was divided into 2 pieces. One piece was fixed in 100 mL/L formalin and embedded in paraffin for pathological diagnosis, the other was soaked in liquid nitrogen, and preserved at -76 °C.

In situ TRAP kit was purchased from Department of Pathology, Beijing Medical University (P.R.China). SP detection kit and development kit were from Maixing Comp (Fuzhou, P.R.China). RNase was the product of Sino-American Ltd (Shanghai, P.R.China).

Methods-In situ telomerase activity labeling

Six frozen tissue sections were cut by freezing microtome (Leica, Germany) and the slides treated by poly-lysine were mounted, and detected for *in situ* telomerase activity. Briefly, each section was added 20 µL telomerase reaction mixture containing up-stream primer TS (5'-AATCCGTCGAGCA-GAGTT-3') 0.5 µL, down-stream primer CX (5'-CCCTTACCCTT ACCCTTACCCTTA-3') 0.5 µL, 2 mM biotin-dNTP 2 µL, 2×buffer A 5 µL, 10×buffer B µL and H₂O 11 µL, coverslips were sealed. They were then incubated at 30 °C for 60 min, rinsed with 0.01 M PBS for 3 min, fixed by 40 g/L paraformaldehyde for 15 min, rinsed with 0.01 M PBS for 2×3 min, submerged into 800 mL/L ethanol for 2 min and dried, dealt with 2% H₂O₂ for 20 min to block endoperoxidase, rinsed with 0.01 M PBS for 2×3 min, blocked by normal goat serum for 60 min, incubated by peroxidase-streptavidin at 37 °C for 60 min, rinsed with 0.01 M PBS for 3×5 min, developed with DAB, and then counterstained with hematoxylin.

Department of Pathology, Hunan Medical University, Changsha, 410078, Hunan Province, China

Dr. FENG De-Yun, male, born in 1964 in Hunan Province, graduated from Hunan Medical University in 1991, Master degree of Pathology.

Project supported by the Health Ministry Science Fund of China, No. 98-1-110

Correspondence to: Dr. FENG De-Yun, Department of Pathology, Hunan Medical University, Changsha 410078, Hunan Province, China
Tel. +86-731-4475356

Email: fdyh@public.cs.hn.cn

Received 1999-04-08

In situ TRAP

In situ telomerase activity was also detected by *in situ* TRAP. The procedure was as follows: 6 μ m frozen sections were dripped with 20 μ L mixture (primer TS 0.5 μ L, 2 \times buffer A 5 μ L, H₂O 14.5 μ L), incubated at 30 $^{\circ}$ C for 60 min, rinsed with 0.01 M PBS for 3 min, fixed by 40 g/L paraformaldehyde for 10 min, rinsed with 0.01 M PBS for 3 min, digested with 25 mg/L proteinase K at 37 $^{\circ}$ C for 10 min, washed with 0.01 M PBS for 2 \times 3 min, soaked in 800 mL/L ethanol for 2 min and dried, dripped with PCR mixture (primer TS and CX 0.5 μ L respectively, 2 mM biotin-dNTPs 2 μ L, 10 \times buffer B 1 μ L, Taq polymerase 2 U and H₂O 15 μ L), added coverglasses and sealed with liquid paraffin, and amplified by PCR (PCR conditions were 35 cycles at 95 $^{\circ}$ C for 1min, at 50 $^{\circ}$ C for 1min, at 72 $^{\circ}$ C for 1 min) on Ericomp Thermocycler (Ericomp Ltd Comp. America), washed by chloroform and absolute ethanol for 5min respectively to scavenge the liquid paraffin and the coverglasses, washed with 0.01 M PBS for 4 \times 5 min, blocked by normal goat serum at 37 $^{\circ}$ C for 60 min, dripped with ABC reagent and incubated at 37 $^{\circ}$ C for 1h, rinsed with 0.01 M PBS for 3 \times 5 min, developed by DAB, and counterstained with hematoxylin.

Negative control

Distilled water replaced primer TS and CX in reaction mixture or biotin-dNTPs in PCR mixture. The sections were digested by RNase at 37 $^{\circ}$ C for 60 min to remove telomerase RNA templates. The sections were heated at 95 $^{\circ}$ C for 10min to inactivate telomerase.

Positive control

Positive sections in the kit were used for positive control.

RESULTS

Detection of telomerase activity in HCC, CRC and NPC tissues

We first tested *in situ* labeling to detect telomerase activity in HCC, CRC and NPC tissues. Cancer cells contained detectable levels of telomerase activity. Positive signals of telomerase activity in HCC were almost in nuclei (Figure 1), a few in cytoplasm. Distributions of the positive cells were clustered or diffused in HCC. Weaker telomerase activity was also detected in cytoplasm and nuclei in liver tissues surrounding HCC, and mainly localized in nuclei of hepatocytes near cancer tissues, and positive cells were small patchy or clustered (Figure 2). In CRC, positive signals of telomerase activity were principally localized in nuclei, and much weaker in cytoplasm. In NPC, the telomerase activity was detected in nuclei (Figure 3). Distributions of

positive cells were small nested or patchy in shape.

Positive results for telomerase activity were obtained from positive control group, and negative results from negative control groups.

Comparison of results obtained by two methods

When our improved method was used to detect *in situ* telomerase activity, its positive signal localization, intensity and character, and distribution of positive cells were very similar to the results by *in situ* PCR-TRAP with much better morphology preservation and background of tissues.

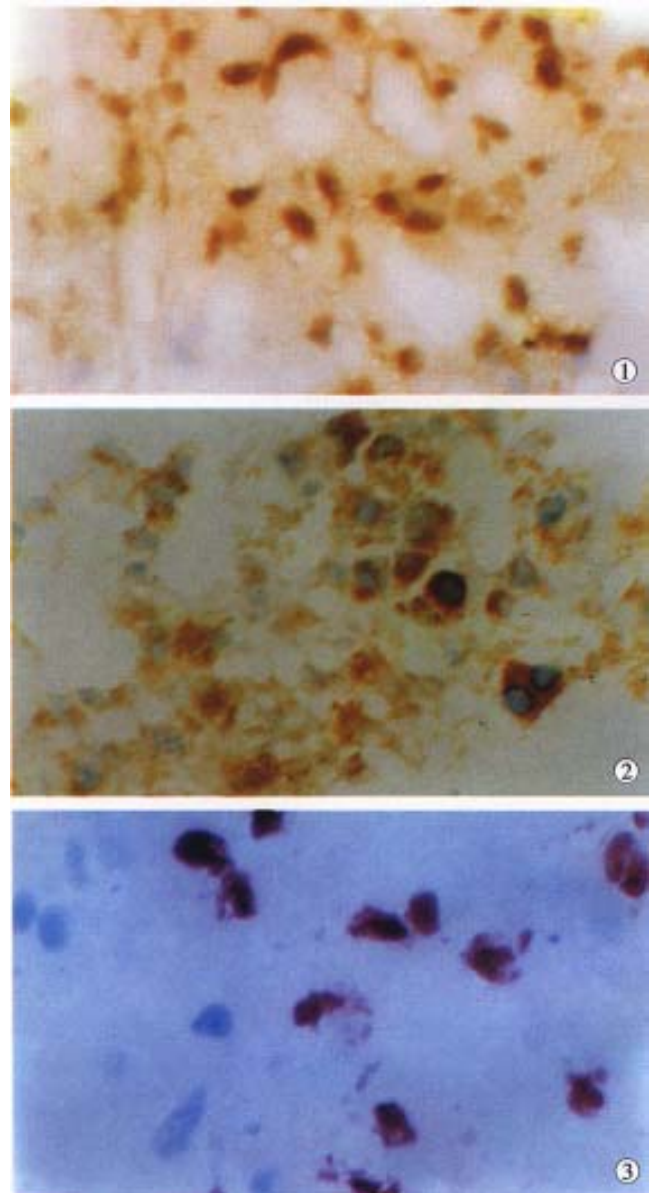


Figure 1 Positive signal of telomerase activity localized in nuclei of HCC. *In situ* labeling, $\times 400$

Figure 2 Weak positive signal of telomerase activity in liver tissue surrounding HCC in nuclei and cytoplasm of hepatocytes. *In situ* labeling, $\times 400$

Figure 3 Nuclear positive signal of telomerase activity in NPC. *In situ* labeling, $\times 400$

DISCUSSION

Telomerase is a specific reverse transcriptase which utilizes its own RNA as a template to catalyze synthesis of telomere^[1-5]. According to molecular biological theory, if the telomerase is active, it can synthesize cDNA by adding the primers and dNTPs under suitable condition. Because dNTPs used to synthesize cDNA are labeled with biotin which has an affinity for streptavidin-peroxidase, and when developed by DAB, the telomerase activity can be detected. Affinity reaction of streptavidin with biotin can amplify positive signals, therefore PCR amplification procedure may be omitted for *in situ* detection of telomerase activity. Thus, the method for *in situ* detection of telomerase activity is very simple and particularly successful on frozen sections of pathological materials. Morphological preservation and background of tissue sections are much better.

According to the data, in order to achieve satisfactory results during experiment. The following points are worth notice: ① Coverglasses, tips, forceps and distilled water must be sterilized by high temperature; ② After sections were

incubated with reaction mixture, the sections should not be rinsed too long, and intensity should not be too strong, otherwise, synthetic cDNA by reverse transcription is easy to be washed away, resulting in false negative, because cDNA is not fixed and fast adhered to the sections; ③ The slides must be treated with poly-lysine to avoid separation of the sections from slides.

REFERENCES

- 1 Nakayama J, Tahara H, Tahara E, Toyama K, Ebihara Y, Kato H, Wright WE, Shay JW. Telomerase activation by hTERT in human normal fibroblast and hepatocellular carcinomas. *Nat Genet*, 1998; 18:65-68
- 2 Ohyashiki K, Ohyashiki JH, Nishimaki J, Toyama K, Ebihara Y, Kato H, Wright WE, Shay JW. Cytological detection of telomerase activity using an *in situ* telomeric repeat amplification protocol assay. *Cancer Res*, 1997;57:2100-2103
- 3 Nouse K, Urabe Y, Higashi T, Nakatsukasa H, Hino N, Ashida K, Kinugasa N, Yoshida K, Uematsu S, Tsuji T. Telomerase as a tool for the differential diagnosis of human hepatocellular carcinoma. *Cancer*, 1996;78:232-236
- 4 Miura N, Horikawa I, Nishimoto A, Ohmura H, Ito H, Hirohashi S, Shay JW, Oshimura M. Progressive telomere shortening and telomerase reactivity during hepatocellular carcinogenesis. *Cancer Genet Cytogenet*, 1997;93:56-62
- 5 Wu S, Liew CT, Li XM, Lau WY, Leow CK, Wu BQ, Li CJ. Study on telomerase activity in hepatocellular carcinoma and chronic hepatic disease. *Zhonghua Binglixue Zazhi*, 1998;27:91-93

Edited by WANG Xian-Lin

Proofread by MA Jing-Yun

Clinicopathologic study of primary intestinal B cell malignant lymphoma

ZHOU Qin, XU Tian-Rong, FAN Qin-He and ZHEN Zou-Xung

Subject lymphoma/pathology;
headings intestinal neoplasms/pathology;
neoplasms/diagnosis

INTRODUCTION

Primary intestinal B cell lymphoma is one of the most common extra-nodal lymphomas, which includes two types: intestinal mucosa-associated lymphoid tissue lymphoma (IMALToma) and lymphomatous polyposis (LP). Both have characteristic pathologic features, immunophenotypes and biological behaviors. In this article, twenty-five cases were retrospectively analyzed with regard to criteria of diagnosis and clinicopathologic characteristics.

MATERIALS AND METHODS

Methods

All 25 tissue specimens obtained from surgical operation, were embedded in paraffin, sectioned and stained by haematoxylin-eosin and immunohistochemical stains (ABC method). The first antibody (CD₂₀, CD₄₅, CD_{45RO}, CD₆₈, CD₃₀, K, λ , IgG, IgM, IgA, IgD and bcl-2), second antibody and ABC Kit were produced by Dako and Vector Co. PBS buffer solution was substituted for the first antibodies as the negative control, whereas the lymphoma cases were used for positive control.

Clinical data

There were 21 cases of IMALToma, in which 16 were males and 5 females, age ranged 9-70 years, mean age 39.6 years. Location of tumors, 10 were situated in ileum, 2 at jejunum, 6 in colon, 1 at rectum and 2 in both ileum and colon; there were 4-cases of LP, 3 men and 1 woman, age 30-47

(average 38.8) years, all were located at the terminal ileum. Clinical manifestations of IMALToma were similar to LP with abdominal pain and mass, melena and mucous stool, intestinal intussusception and intestinal obstruction, fever, loose bowel movement.

Pathological data

Macroscopically, the IMALToma could be categorized into mushroom, constrictive and ulcerative types; the size of tumor varied from 2 cm \times 1 cm \times 1 cm to 20 cm \times 10 cm \times 3.5 cm. Sixteen cases had single nodule, five were multiple. The lymphomatous cells infiltrated in the mucosa, submucosa and muscular layer diffusely or focally. Lymphoid follicles were seen in 7 cases. In 9 cases, the germinal centers were partly or entirely replaced by lymphoma cells. Dendritic cells and macrophages with chromophilic bodies disappeared. This phenomenon is called follicular colonization (FC). 9 cases showed lymphoepithelial lesion (LEL) in which there were clusters of lymphomatous cells infiltrated focally at the surface epithelium and/or glands (Figure 1). The glandular epithelia were destroyed. The neoplastic cells presented a serial cell lineage of small lymphocyte, centrocyte-like cell (CCL), monocyte-like B cell (MCB) and lymphoplasma cell (LPC), and also centroblast like cells (CBL). All these cells, several kinds were in a mixed distribution, but usually one kind was predominant. IMALToma was divided into following subtypes:

① CCL subtype seen in 11 cases. The tumor cells were medium and small in size, with less cytoplasm, irregular and angular nuclei of dark staining, which looked like centrocytes.

② MCB subtype seen in 4 cases. The tumor cells were of medium size, their cytoplasm was abundant, lightly stained and clear. The nuclei were round, with visible nuclear membrane, fine chromatin and small nucleoli.

③ LPC subtype seen in 2 cases. The cytoplasm tumor cells looked like plasma cells and nuclei like small lymphocytes. The cytoplasm was abundant and stained red, in some, the cytoplasm contained immunoglobulin inclusions. The nuclei of tumor cells were round, dark stained, similar to small lymphocyte.

④ CBL subtype: CBL cells were more than 50% in four cases, medium size with light stained

Department of Pathology, the First Affiliated Hospital of Nanjing Medical University, Nanjing 210029, Jiangsu Province, China
Dr. ZHOU Qin, female, born in 1960-07-29 in Xuzhou, Jiangsu Province, graduated from the Shanghai Second Medical University with Master degree in 1990, associate chief, Department of Pathology, with twenty-three papers published.
Supported by the Natural Science Foundation of Jiangsu Province Education Commission, No.(Educ.)94051.

Correspondence to: ZHOU Qin, Department of Pathology, the First Affiliated Hospital of Nanjing Medical University, 300 Kuangzhou Road, Nanjing, 210029, China
Tel. +86-25-3718836 Ext. 6445, Fax. +86-25-3724440
Email: Pathojph@jlonline.com

Received 1999-05-25 **Accepted** 1999-09-13

cytoplasm and round vacuolated nuclei, and 1-3 basophilic nucleoli nearby the nuclear membrane. CBL cells were focally distributed with a few CCL cells scattering or clustering around the CBL cells. Transition could be shown between CBL and CCL cells. Mitoses were easily found, especially the pathologic mitoses.

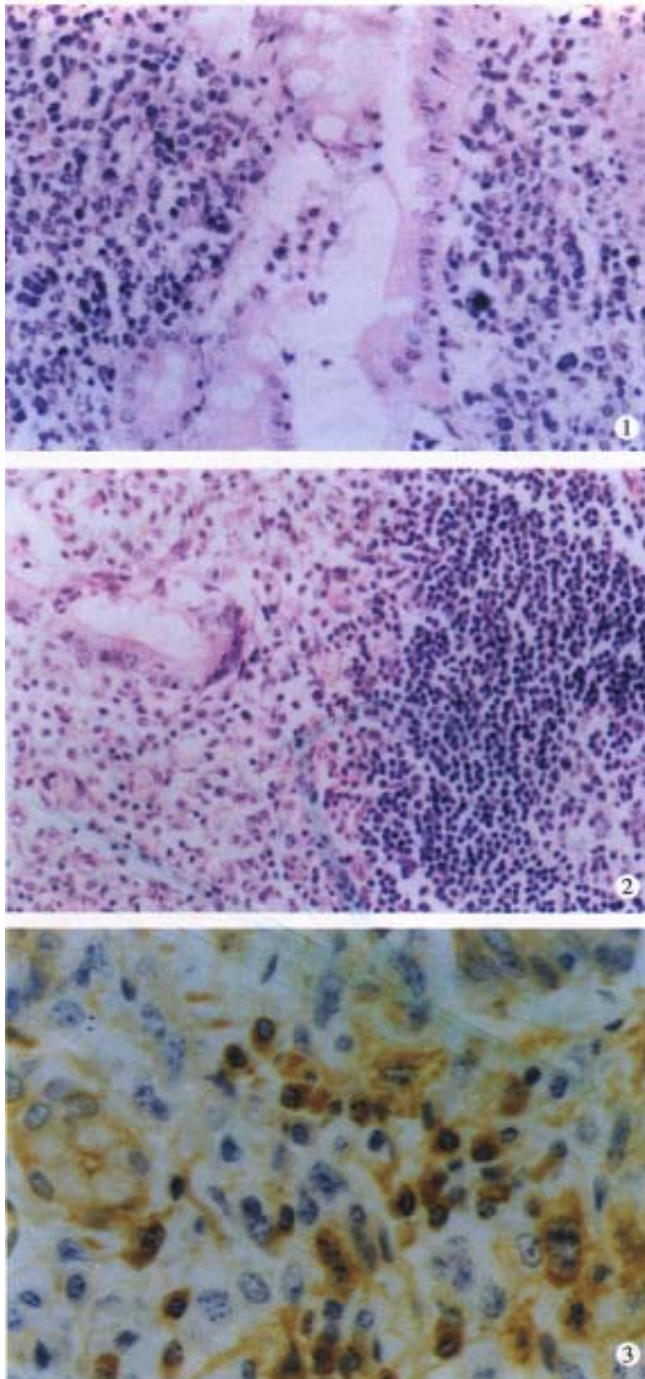


Figure 1 In IMALToma CCL cell infiltrated and destroyed glands forming the lymphoepithelial lesion, HE stains. $\times 100$

Figure 2 In LP, mantle cells increased in layers and infiltrated into germinal centers, dendritic cells and the macrophages with chromophilic bodies were replayed entirely.

Figure 3 In IMALToma, lymphoplasmatic cells infiltrated mucosa membrane, in which the CD₂₀ was positive, ABC method. $\times 100$

In the above 3 subtypes, 14 with few or none of CBL cells were low-grade malignant. Another 2 of CCL type and 1 MCB type was low-grade malignant but with high-grade malignant component, of which the proportion of CBL cells was more than 25%. Four CBL types having more than 50% CBL cells were highly malignant. Lymph node metastases were seen in 3 of 14 cases of low grade malignancy, 2 low grade malignancy with high-grade malignant component and 4 high grade malignant IMALToma.

Four cases of LP were located at terminal ileum within the range of 20cm-40cm. They were hundreds stalkless polyps, varied from millet to broad bean. Three-fourth were mushroom-like or narrow masses, which were 1 cm \times 1 cm \times 1 cm-6 cm \times 4 cm \times 2.5 cm in size; with ulceration on the surface. Histologically, the lymph follicles were surrounded by numerous layers of lymphomatous lymphocytes, infiltrating into the germinal centers. The dendritic cells and macrophages with chromophilic bodies decreased and even disappeared. Neoplastic cells infiltrated diffusely, forming nodular and mantle-like growth pattern. The nuclei of the lymphomatous cells were round or irregularly angular with thick nuclear membrane and condensed chromatin (Figure 2). One case showed blast cell transformation.

RESULT

Immunohistochemically, twenty one cases of IMALToma and four cases of LP were CD₄₅ and CD₂₀ positive (Figure 3). The reactive lymph follicles were polyclonal, while LEL and FC were monoclonal; one case of CBL lymphoma was negative for bcl-2. Ten cases and 5 cases were positive in CD₆₈ and CD_{45RO}, in reactive histocytes and small lymphocytes, respectively.

DISCUSSION

The significance of the LEL and FC pathological diagnosis of IMALToma.

LEL is considered a characteristic feature of IMALToma^[1]. In our data, less than 50% (9/21) had LEL. The nest formation could also be found in the inflammatory and reactive status, it might be difficult to distinguish them from the real LEL, in such case, immunohistochemistry may be helpful. The former is several leukocytes with poly-clone and the latter is the lymphocytes with mono-clone. FC, appeared in 9 cases, is easy to misjudge as reactive follicles. The following morphological characteristics and immuno-phenotype may be helpful for the differentiation: ① FC has no dendritic cells or macrophages with chromophilic bodies. ② CCL cell is the immunophenotype of B

cells in the marginal area, rather than at the germinal center^[2].

Both LEL and FC were characteristic features for diagnosis^[3], but they could only be seen in some of the cases, then, immunohistochemistry and molecular biology technique should be done.

The diagnostic criteria and correlations of clinico-pathologic features of low and high-grade malignant IMALToma

Fourteen were of low-grade malignancy, including CCL, MCB and LPC subtypes. The proportion of CBL cells was more than 25% in two CCL lymphoma and one MCB lymphoma, one should pay attention to transformation from low-to high-grade malignancy. Four CBL lymphomas were of high-grade malignancy, in which the CBL cells were > 50%, distributing around the FC in fused clusters or trabeculae, and Ig might be positive and *bcl-2* negative^[4,5]. The rates of metastasis of the above three types of lymphoma were 28.5%, 66.7% and 100%, respectively, which proved that histological grading and the clinical staging were intimately related to prognosis.

The origination of LP

The lymphomatous polyps were first described, and named LP by Corn in 1961. The origination of LP was argued for a long time. Only recently, LP could be defined as originating from both mantle cells and the centrocytes, which were similar in morphology^[6]. The former was positive in IgD,

CD₅ and cyclin D₁ without blastocyte transformation, while the latter was positive in IgM and CD₁₀ with blastocyte transformation^[7,8]. In our group, three cases had the morphologic feature of mantle cells, one was originated from germinal center, which was transformed from centrocytes to centroblastocytes. Thus the term LP could not reflect the origination and the nature. LP has two patterns, showing similar macroscopic and histologic features here we suggest a better terms for LP: mucosal mantle cell lymphoma and mucosal follicular lymphoma.

REFERENCES

- 1 Isaacson PG, Frcpath D. Gastrointestinal lymphoma. *Hum Pathol*, 1994;25:1020-1029
- 2 Isaacson PG. Malignant lymphomas with a follicular growth pattern. *Histopathology*, 1996;28:487-495
- 3 Montalban C, Manzanal A, Castrillo JM, Escribano L, Bellas C. Low grade B cell MALT lymphoma progressing into high grade lymphoma. Clonal identity of the two stages of the tumour, unusual bone involvement and leukaemic dissemination. *Histopathology*, 1995;27:89-91
- 4 Navratil E, Gaulard P, Kanavaros P, Audouin J, Bougaran J, Martin N, Diebold J, Mason DY. Expression of the *bcl-2* protein B cell lymphomas arising from mucosa associated lymphoid tissue. *J Clin Pathol*, 1995;48:18-21
- 5 Ashton Key M, Biddolph SC, Stein H, Gatter KC, Mason DY. Heterogeneity of *bcl-2* expression in MALT lymphoma. *Histopathology*, 1995;26:75-78
- 6 Moynihan MJ, Bast MA, Chan WC, Delabie J, Wickert RS, Wu GQ, Weisenburger MD. Lymphomatous polyposis: a neoplasm of either follicular mantle or germinal center cell origin. *Am J Surg Pathol*, 1996;20:442-452
- 7 Fraga M, Lloret E, Sanchez-Verde L, Orradre JL, Campo E, Bosch F, Piris MA. Mucosal mantle cell (centrocytic) lymphomas. *Histopathology*, 1995;26:413-422
- 8 Robert ME, Kuo FC, Longtine JA, Sklar JL, Schrock T, Weidner N. Diffuse colonic mantle cell lymphoma in a patient with presumed ulcerative colitis. *Am J Surg Pathol*, 1996;20:1024-1031

Edited by WU Xie-Ning
Proofread by MIAO Qi-Hong

VIP immunoreactive nerves and somatostatin and serotonin containing cells in Crohn's disease

LU Shi-Jun¹, LIU Yu-Qing¹, LIN Jian-Shao², WU Hong-Juan¹, SUN Yong-Hong¹ and TAN Yu-Bin²

Subject headings vasoactive intestinal peptide; somatostatin; serotonin; Crohn's disease; immunohistochemistry; histomorphometry

INTRODUCTION

With the progress of the studies on neuroendocrine and immunology in the gastrointestinal tract, it has been recognized that the intestinal neuroendocrine system and the immune system can influence and modulate each other and a neuroendocrine immunomodulation network in the intestine has been established^[1]. Neuropeptides, such as vasoactive intestinal peptide (VIP), substance P (SP), somatostatin (SS) etc. are widely distributed in the gastrointestinal tract and they play an important role in the immunomodulation of the intestinal mucosa.

MATERIALS AND METHODS

Tissue specimens

Surgical specimens were obtained from ileum of 25 cases of CD (25 ileum) and 10 normal subjects (from sudden death and who received surgery for intestinal neoplasm). The specimens were fixed in 10% formalin and embedded in paraffin. Sections with thickness of 4μm were made continuously.

Staining method

Immunohistochemical staining was carried out by ABC method. Antibodies included rabbit polyclonal antibodies to VIP (1:400), NSE (1:200), S-100 protein (1:400), SS (1:200), serotonin (1:600) (Dako Co.) and ABC Kit.

Histomorphometric analysis

Olympus CH light microscopy with ocular linear micrometer and double quadrat grid test system C64 (from the Academy of Military Medical Sciences) were used to measure immunoreactive neurons and nerve fibers in 10×40 high power field. The point count method was used^[2]. Fifteen neuron cells (with nucleus) were examined at random, the maximal diameter of each was measured and the values were averaged. The total length of all immunoreactive nerve fibers was measured separately in the mucosa and the length was estimated per unit area (μm/μm) which was expressed as linear density (Lv%). In the submucosa and the muscle layers, the total volume of the immunoreactive neurons together with the nerve fibers was measured and the volume was estimated per unit which was expressed as volume density (Vv%). The numbers of SS, serotonin immunoreactive cells and a neurophil cells in the mucosa were counted at random in 10 high power fields of each case. The results averaged.

Statistical analysis

Results were analysed by *t* and *t'* test.

RESULTS

Immunohistochemistry of neurons and nerve fibers

In CD, the VIP-IR and NSE-IR nerve fibers in the mucosa of ileum were markedly increased. They were deeply stained, coarse, irregular (Figure 1) and the linear densities were significantly raised ($P < 0.01$, $P < 0.01$, respectively, Table 1). In the submucosa, the VIP-IR neurons were hypertrophied ($P < 0.01$, Figure 2). VIP-IR, S-100 protein IR and NSE-IR nerve fibers were all remarkably increased. They were coarse, thickened and irregular (Figure 3). The neuron and nerve fiber volume density of each immunoreactive type stated above was significantly increased ($P < 0.01$, respectively). In the muscle layers the volume density of neurons and nerve fibers containing NSE or S-100 protein was also significantly increased ($P < 0.01$, respectively, Figure 4), but the changes in VIP-IR neurons and nerve fibers were unremarkable.

¹Department of Pathology, Weifang Medical College, Weifang 261042, Shandong Province, China

²Department of Pathology, Tianjin Medical University, Tianjin 300070, Tianjin, China

Dr. LU Shi-Jun, male, born in 1961-11-03, in Linqu, Shandong Province, graduated from Tianjin Medical University with Master degree in 1991, now associate professor in pathology, majoring gastroenterologic neuroendocrine immunopathology and having more than 20 papers published.

Supported by the National Natural Science Foundation of China No. 39170334

Correspondence to: Dr. LU Shi-Jun, Department of Pathology, Weifang Medical College, Weifang 261042, China
Tel. +86-536-8210220

Received 1999-07-11 **Accepted** 1999-09-22

Immunoreactive cells of somatostatin and serotonin

In CD, argyrophil and serotonin-IR cells in the ileal mucosa around the lesions were significantly reduced ($P<0.01$, respectively, Figure 5). SS-IR cells were decreased ($P<0.01$, Figure 6), Table 2

DISCUSSION

In CD, there had been several reports about the morphological alterations in the enteric nervous system. Dvorak *et al*^[3] described the changes in enteric nervous system in the surgical specimens from patients with CD including proliferation and focal necrosis of nerve fibers and hypertrophy of neurons in the myenteric plexus. Bishop *et al*^[4] and Sj-lund *et al*^[5] assessed the alterations of VIP-IR enteric nerve fibers in CD observation and counting. In the study, we used the histomorphometric analysis to obtain objective information about the changes in the immunoreactive enteric nervous system in CD. We found that in the submucosal plexus the VIP containing neurons were markedly hypertrophied, the linear density of VIP-IR nerve fibers in the mucosa and the VIP-IR neuron nerve fiber volume density in submucosa were significantly increased. The results were consistent with that of Bishop *et al* and O'Morain *et al*^[6] who measured by

immunohistochemistry and radioimmuno assay, but different from that by Sj-lund *et al* and Koch. By immunohistochemistry, Sj-lund *et al* found that in unaffected muscle layer of the ileum and the affected muscle layer of colon, the VIP-IR nerve fibers were reduced. The coarse VIP-IR nerve fibers were more frequently observed in the affected mucosa of ileum and in the affected muscle layers of the colon than those in the control. El-Sathy *et al*^[7] reported that the areas of the argyrophil cells as well as those immunoreactive to chromogranin A and serotonin were significantly increased in both patients with UC and CD, compared with those in the controls. In patients with CD, the areas of polypeptide YY (PYY) and pancreatic polypeptide (PP) immunoreactive cells were significantly reduced. In this study, we also found that SS and serotonin containing cells and argyrophil ones were reduced in CD. These diversities among different investigators may be due to the various locations selected the difference in degree of activity and the methods used.

This paper shows that VIP immunoreactive neurons and nerve fibers are increased whereas the immunoreactive cells containing somatostatin and serotonin are reduced, suggesting that there be abnormalities in neuroendocrine system in CD which may play an important role in the pathogenesis of CD.

Table 1 Lv and Vv of immunoreactive nerve fibers and neurons for VIP, S-100 protein and NSE in Crohn's disease

Item	CD		Control		P
	n	$\bar{x}\pm s$	n	$\bar{x}\pm s$	
VIP					
Mucosa Lv	25	3.6 \pm 1.2	10	2.0 \pm 0.8	<0.01
Submucosa Vv	25	2.0 \pm 1.1	10	0.9 \pm 0.8	<0.01
Submucosal neuron (diameter, μ m)	25	21.1 \pm 5.6	10	13.1 \pm 2.0	<0.01
Myenteric plexus Vv	25	3.2 \pm 1.8	10	2.6 \pm 1.4	<0.01
NSE					
Mucosa Lv	25	3.4 \pm 0.7	10	1.9 \pm 1.4	<0.01
Submucosa Vv	25	5.1 \pm 2.2	10	1.3 \pm 0.5	<0.01
Myenteric plexus Vv	25	11.1 \pm 2.6	10	5.1 \pm 1.2	<0.01
S-100 protein					
Submucosa Vv	25	3.9 \pm 1.0	10	2.3 \pm 0.4	<0.01
Myenteric plexus Vv	25	9.4 \pm 2.3	10	5.7 \pm 1.0	<0.01

Table 2 Density of serotonin, SS containing cells and argyrophil cells in Crohn's disease

Group	Serotonin containing cell		SS containing cell		Argyrophil cell	
	n	$\bar{x}\pm s$	n	$\bar{x}\pm s$	n	$\bar{x}\pm s$
CD	25	4.2 \pm 1.7 ^b	25	1.0 \pm 0.6 ^b	25	3.2 \pm 1.5 ^b
Control	10	8.9 \pm 2.9	10	2.0 \pm 1.2	10	7.7 \pm 2.5

^b $P<0.01$, vs normal control.

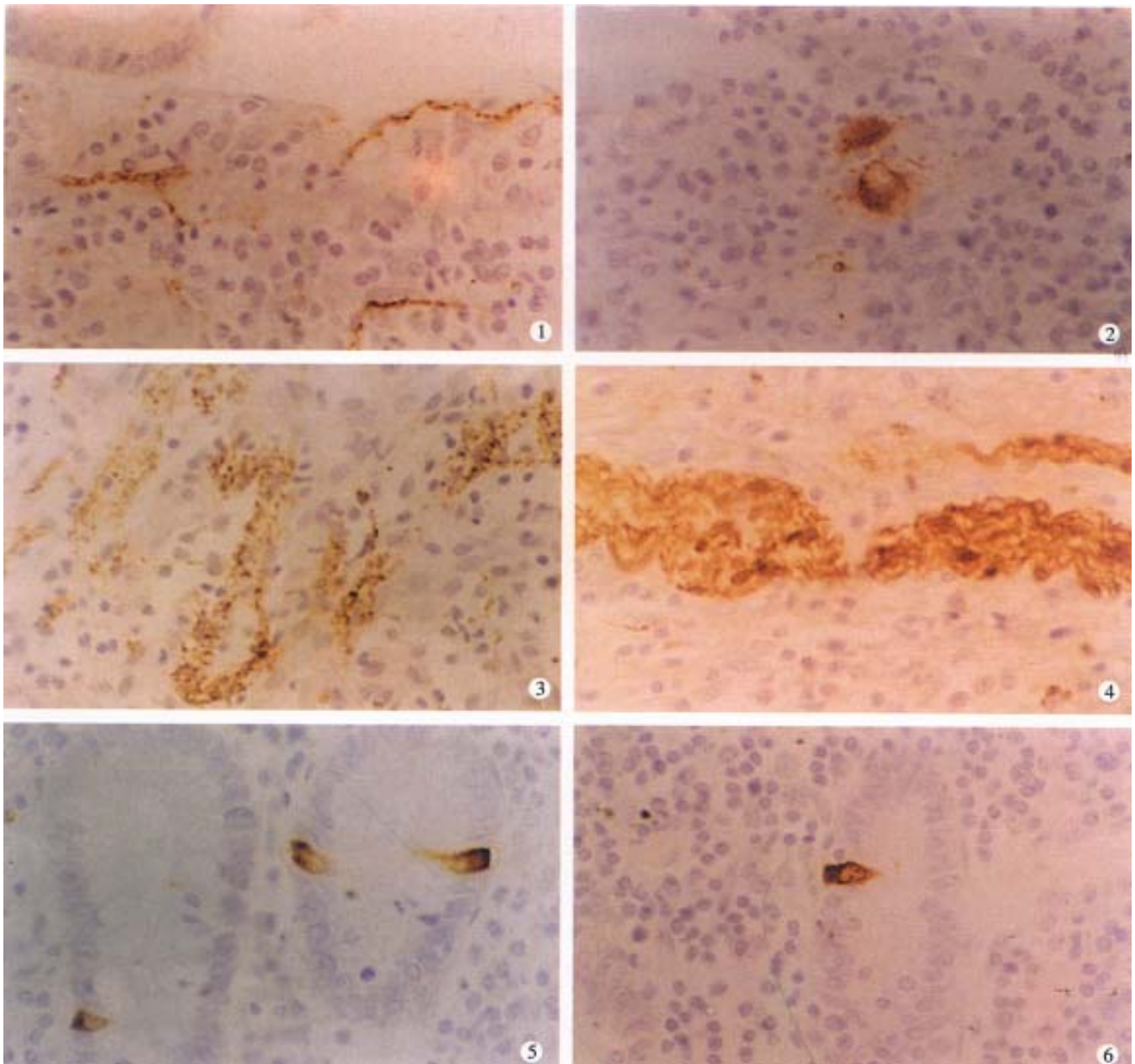


Figure 1 VIP immunoreactive nerve fibers were coarse in mucosa of CD. ABC method $\times 400$

Figure 2 VIP immunoreactive neurons were hypertrophic in submucosa of CD. ABC method $\times 400$

Figure 3 VIP immunoreactive nerve fibers were irregularly thickened in submucosa of CD. ABC method $\times 400$

Figure 4 S-100 protein immunoreactive nerve fibers were increased in myenteric plexus of CD. ABC method $\times 400$

Figure 5 Serotonin immunoreactive cells in mucosa of CD. ABC method $\times 400$

Figure 6 Somatostatin immunoreactive cells in mucosa of CD. ABC method $\times 400$

REFERENCES

- Shanahan F, Anton P. Neuroendocrine modulation of the immune system. Possible implications for inflammatory bowel disease. *Dig Dis Sci*, 1988;33:41s-49s
- Zheng F. Stereocytomorphometry. 1st Ed. Beijing: Beijing Medical University and Union Medical College United Press, 1990:18-20, 146-147
- Dvorak AM, Osage JE, Monahan RA, Dickersin GR. Crohn's disease: transmission electron microscopic studies. III. Target tissues. Proliferation of and injury to smooth muscle and the autonomic nervous system. *Human Pathol*, 1980;11:620-634
- Bishop AE, Polak JM, Bryant MG, Bloom SR, Hamilton S. Abnormalities of vasoactive intestinal polypeptide-containing nerves in Crohn's disease. *Gastroenterology*, 1980;79:853-860
- Sjölund K, Muckadell OBSD, Fahrenkrug J, Håkanson R, Peterson BG, Sundler F. Peptide containing nerve fibres in the gut wall in Crohn's disease. *Gut*, 1983;24:724-733
- O'Morain C, Bishop AE, McGregor GP, Levi AJ, Bloom SR, Polak JM, Peters TJ. Vasoactive intestinal peptide concentrations and immunohistochemical studies in rectal biopsies from patients with inflammatory bowel disease. *Gut*, 1984;25:57-61
- El-Sathy M, Danielsson A, Stenling R, Grimelius L. Colonic endocrine cells in inflammatory bowel disease. *J Intern Med*, 1997;242:413-419

Study on incisional implantation of tumor cells by carbon dioxide pneumoperitoneum in gastric cancer of a murine model

WANG Hao, ZHENG Min-Hua, ZHANG Hao-Bo, ZHU Jian, HE Jian-Rong, LU Ai-Guo, JI Yu-Bao, ZHANG Min-Jun, JIANG Yu, YU Bao-Ming and LI Hong-Wei

Subject headings stomach neoplasms; colonic neoplasms; cell movement; carbon dioxide pneumoperitoneum; murine model

INTRODUCTION

Port-site recurrence after laparoscopic tumor surgery is a frequent complication in cancer operations, such as gallbladder, stomach, ovary and colon^[1-5]. The incidence of port-site recurrence after laparoscopic colectomy ranged from 1.1% to 6.3%, in contrast to a 0.68% tumor wound recurrence rate in patients undergoing curative open colectomy^[6-8]. The possible mechanisms proposed were: ① contaminated laparoscopic instruments passing in and out of the port frequently; ② increased exfoliated cancer cells from laparoscopic manipulation; ③ adhered tumor cells by pneumoperitoneum^[9-12]. Some experiment reported that desufflation related to seeding of port wounds via a stable suspension of tumor cells in CO₂ gas was an unlikely cause of port tumors, some supported a direct intraperitoneal seeding of exfoliated tumor cells as its etiology and the instruments passing in and out of the port may play an important role in local recurrence^[13-15]. The colon tumor cells were more common since laparoscopic colectomy was widely performed.

The purpose of this study was to determine whether CO₂ pneumoperitoneum could increase tumor implants in the port site.

MATERIALS AND METHODS

Materials

A 5mm laparoscopic port (5 mm trocar) was inserted in the left iliac fossa and Veress needle was placed in the right iliac fossa, below which was the injection site of malignant cells. Then the right iliac fossa port was used for insufflation, and another was used for desufflation, through the same collection device. Laparoflator was made in Germany (laparoflator electronic 3509 WEST GmbH).

Colon cancer cell line LoVo and gastric cancer cell line SGC-7901 (from Shanghai Institute of Digestive Surgery) were suspended in liquid culture media and divided into 2 groups: ① the liquid tumor cell suspension contained 1 million cells in 1mL volume (10⁹ cells/L); ② the liquid tumor cell suspension contained 10 thousand cells in 1mL volume (10⁷ cells/L). The concentration of cells was calculated with a hemocytometer (Fischer Scientific, Pittsburg, PA) and then appropriately diluted to achieve the final concentration. Liquid culture media were RPMI 1640 containing 10 percent fetal bovine serum. Cell viability control culture and cell viability of each tumor cell preparation were determined to be greater than 95 percent by trypan blue exclusion. Continuous flow of CO₂ was allowed by leaving the outflow port opened during insufflation, intraperitoneal pressure was maintained at the desired level via constant insufflation during continuous flow studies.

Methods

Male Sprague-Dawley rats (250 g-350 g, from Shanghai Experimental Animal Center) were anesthetized with 25 g/L sodium barbitone (1 µL/g). Abdomens were shaved and prepared with bromo-geramine. Animals then received a right lower quadrant intraperitoneal injection of 1 mL of a suspension of SGC-7901 gastric cancer cells or LoVo colon cancer cells (10⁷/L, 10⁹/L), respectively. Veress needle and 5mm trocar were placed in the abdomen and served as port sites. There were 4 pairs of groups for LoVo or SGC-7901 (4 rats for each group): ① continuous pneumo of

Department of Surgery, Ruijin Hospital of Shanghai Second Medical University, Shanghai 200025, China Shanghai Institute of Digestive Surgery, Shanghai 200025, China

Dr. WANG Hao, male, born in 1972-09 in Nanyang, Henan Province, Han nationality, graduated from Shanghai Second Medical University as a postgraduate in 1998, majoring in colorectal oncology and laparoscopy, having 20 papers published.

Supported by the Shanghai Technological Development Funds, No. 98QMB1405

Correspondence to: Dr. WANG Hao, Department of Surgery, Ruijin Hospital of Shanghai Second Medical University, 197 Ruijin Er Road, Shanghai 200025, China

Tel. +86-21-64370045, Fax. +86-21-64333548

Email: wanghaosh@hotmail.com

Received 1999-07-18 **Accepted** 1999-09-18

2 kPa (5 min) at gas flow of 5 L/min for 5 min with (10⁷/L, 10⁹ /L) cells injected; ② continuous flow (5 L/min) of CO₂ with (10⁷/L, 10⁹/L) cells injected, maintaining a pressure of 4 kPa for 5 min inside the peritoneal cavity; ③ continuous flow (5 L/min) of CO₂ with (10⁷/L, 10⁹/L) cells injected, maintaining a pressure of 2 kPa inside the peritoneal cavity for 60 min; and ④ continuous flow (5 L/min) of CO₂ with (10⁷/L, 10⁹/L) cells injected, maintaining a pressure of 4 kPa for 60 min inside the peritoneal cavity. At the end of the experiments, a peritoneal washing sample was cultured as a cell viability control. All collection dishes were incubated at 37 °C and 50 mL/L CO₂ concentration for one week, then detected under microscopy to demonstrate whether tumor cells existed or not.

RESULTS

Continuous CO₂ pneumoperitoneum with different number of cell injection in LoVo & SGC-7901 cell line were shown in Table 1 and Table 2, respectively. After one week of incubation, in the group of 5 L/min, continuous CO₂ flow of 4 kPa for 60 min with 10⁹/L SGC-7901 cell injected, it demonstrated tumor growth in 3 of 4 dishes when compared with the same experimental condition in LoVo cell. All 4 peritoneal washing samples also showed tumor growth, whereas other dishes showed none.

Table 1 Results in continuous flow pneumo with LoVo cell injection

Cell number	No. of rats	Pressure (kPa)	Duration (min)	Tumor growth
10 ⁹ /L	4	2	5	0/4
10 ⁷ /L	4	2	5	0/4
10 ⁹ /L	4	4	5	0/4
10 ⁷ /L	4	4	5	0/4
10 ⁹ /L	4	2	60	0/4
10 ⁷ /L	4	2	60	0/4
10 ⁹ /L	4	4	60	0/4
10 ⁷ /L	4	4	60	0/4
Control	2			2/2

Table 2 Results in continuous flow pneumo with SGC7901 cell injection

Cell number	No. of rats	Pressure (kPa)	Duration (min)	Tumor growth
10 ⁹ /L	4	2	5	0/4
10 ⁷ /L	4	2	5	0/4
10 ⁹ /L	4	4	5	0/4
10 ⁷ /L	4	4	5	0/4
10 ⁹ /L	4	2	60	0/4
10 ⁷ /L	4	2	60	0/4
10 ⁹ /L	4	4	60	3/4
10 ⁷ /L	4	4	60	0/4
Control	2			2/2

DISCUSSION

Laparoscopic surgery has been carried out nationwide in patients with cancer of the gastrointestinal tract despite relatively high incidence of port site recurrence after curative resection^[1,7]. Several clinical reports have proposed that recurrence may be caused by direct implantation of the tumor cells, whereas the proof is still uncertain. Many experimental studies of colon carried out more than those in gastric cancer^[16].

Our design was to evaluate and compare the incidence of port site recurrence by direct seeding of either colon or gastric cancer cells. We injected LoVo cells into the mice and found none of the 32 mice had tumor growth in the dishes, but when injected SGC-7901 cells into the mice with 10⁹/L SGC901 cells and pneumoperitoneum pressure 4 kPa for 60 min, 3 out of 4 dishes showed tumor cells growth. The gastric cancer cell line SGC-7901 was more likely to cause port-site recurrence than colon cancer LoVo cell line. This may partly be due to the difference of tumor metastatic behavior. It had been reported that the capacity of gastric cancer cell implantation in the peritoneum was much easier than that of the colon cancer cells^[18,19]. Our finding corroborated the above conclusion. The pneumoperitoneum pressure in the abdominal cavity and its duration played an important role in the development of port-site recurrence of gastric cancer cells.

The mechanism for tumor cell port-site implantation may be explained as follow: ① tumor cell exfoliation by surgical manipulation of the tumor; ② contaminated laparoscopic instruments frequently passing in and out of the ports; ③ tumor cell viability, number of cells, duration, pneumoperitoneum pressure and the metastatic nature of tumor cells; ④ surgery induced immuno-suppression facilitating tumor growth at the port-site wounds^[13,20]. Thus significant effort should be strived for to prevent tumor growth in the port wound. It has been suggested that all instruments should be routinely wiped on withdrawal from a port with a cytotoxic agent (povidone-iodine) and a similar agent flushing the laparoscopic port before withdrawal. The external aspect of the port should be sprayed and wound liberally irrigated with a cytotoxic agent^[17].

REFERENCES

- Alexander RJ, Jaques BC, Mitchell KG. Laparoscopically assisted colectomy and wound recurrence. *Lancet*, 1993;341:249-250
- Drouard F, Delamarre J, Capron JP. Cutaneous seeding of gallbladder cancer after laparoscopic cholecystectomy. *N Engl J Med*, 1991;325:1316

- 3 Cava A, Roman J, Gonzalez QA, Quintela A, Martin F, Aramburo P. Subcutaneous metastasis following laparoscopy in gastric adenocarcinoma. *Eur J Surg Oncol*, 1990;16:63-67
- 4 Clair DG, Lautz DB, Brooks DC. Rapid development of umbilical metastases after laparoscopic cholecystectomy for unsuspected gallbladder carcinoma. *Surgery*, 1993;113:355-358
- 5 Gleeson NC, Nicosia SV, Mark JE, Hoffman MS, Cavanagh D. Abdominal wall metastases from ovarian cancer after laparoscopy. *Am J Obstet Gynecol*, 1993;169:522-523
- 6 Ramos JM, Gupta S, Anthone GJ, Ortega AE, Simons AJ, Beart RW Jr. Laparoscopy and colon cancer. Is the port site at risk. A preliminary report. *Arch Surg*, 1994;129:897-900
- 7 Vukasin P, Ortega AE, Greene FL, Steele GD, Simons AJ, Anthone GJ, Weston LA, Beart RW Jr. Wound recurrence following laparoscopic colon cancer resection. *Dis Colon Rectum*, 1996;39: S20-S23
- 8 Hughes ES, McDermott FT, Polglase AL, Johnson WR. Tumor recurrence in the abdominal wall scar tissue after large bowel cancer surgery. *Dis Colon Rectum*, 1983;26:571-572
- 9 Nduka CC, Monson JR, Menzies Gow N, Darzi A. Abdominal wall metastases following laparoscopy. *Br J Surg*, 1994;81:648-652
- 10 Fusco MA, Paluzzi MW. Abdominal wall recurrence after laparoscopic assisted colectomy for adenocarcinoma of the colon: report of a case. *Dis Colon Rectum*, 1993;36:858-861
- 11 Cirocco WC, Schwartzman A, Golub RW. Abdominal wall recurrence after laparoscopic colectomy for colon cancer. *Surgery*, 1994;116:842-846
- 12 Umpleby HC, Fermor B, Symes MD, Williamson RC. Viability of exfoliated colorectal carcinoma cells. *Br J Surg*, 1982;71:659-663
- 13 Iwanaka T, Arya G, Ziegler MM. Mechanism and prevention of port site tumor recurrence after laparoscopy in a murine model. *J Pediatr Surg*, 1998;33:457-461
- 14 Whelan RL, Sellers GJ, Allendorf JD, Laird D, Bessler MD, Nowygrod R, Treat MR. Trocar site recurrence is unlikely to result from aerosolization of tumor cells. *Dis Colon Rectum*, 1996;39: S7-S15
- 15 Allardyce R, Morreau P, Bagshaw P. Tumor cell distribution following laparoscopic colectomy in a porcine model. *Dis Colon Rectum*, 1996;39:S47-S52
- 16 Hubens G, Pauwels M, Hubens A, Vermeulen P, Van-Marck E, Eyskens E. The influence of a pneumoperitoneum on the peritoneal implantation of free intraperitoneal colon cancer cells. *Surg Endosc*, 1996;10:809-812
- 17 Hewett PJ, Thomas WM, King G, Eaton M. Intraperitoneal cell movement during abdominal carbon dioxide insufflation and laparoscopy. *Dis Colon Rectum*, 1996;39:S62-S66
- 18 Asao T, Nagamachi Y, Morinaga N, Shitara Y, Takenoshita S, Yazawa S. Fucosyltransferase of the peritoneum contributed to the adhesion of cancer cells to the mesothelium. *Cancer*, 1995;75 (6 Suppl):1539-1544
- 19 Asao T, Yazawa S, Kudo S, Takenoshita S, Nagamachi Y. A novel ex vivo method for assaying adhesion of cancer cells to the peritoneum. *Cancer Lett*, 1994;78:57-62
- 20 Murthy SM, Goldschmidt RA, Rao LN, Ammirati M, Buchmann T, Scanlon EF. The influence of surgical trauma on experimental metastasis. *Cancer*, 1989;64:2035-2044

Edited by WU Xie-Ning
Proofread by MIAO Qi-Hong

HCV genotypes in hepatitis C patients and their clinical significances

HUANG Fen, ZHAO Gui-Zhen and LI Yeng

Subject headings hepatitis C; hepatitis C virus; genotyping

INTRODUCTION

It has been discovered that hepatitis C virus (HCV) presents considerable nucleotide variation and has many genotypes. At least twelve, 5 of which prevalent, i.e.: I/1a, II/1b, III/2a, IV/2b, and V/3a types. The different genotypes of HCV may possess some relationship with regional distribution, clinical manifestation, response to treatment and prognosis of HCV infection, thus to study the genotypes of HCV further in different areas is of practical value. We detected HCV genotypes in 94 patients with hepatitis C and in 6 patients with primary hepatocarcinoma by PCR assay with four kinds of type-specific primers with a view to study the distribution of HCV genotypes in hepatitis C in Shenyang area and their clinical significances.

MATERIALS AND METHODS

Patients

One hundred serum samples with positive anti-HCV and HCV RNA were received from patients who were in clinic or in ward of our department from July 1993- June 1 1996. Among the 94 patients with hepatitis C, there were 9 acute hepatitis, 73 chronic hepatitis (50 mild degree, 14 moderate and 9 severe ones), 12 active posthepatic cirrhosis. Mean age 38.8 years \pm 15.6 years, male 77 and female 17. Forty-nine of them (52.1%) had history of blood or blood product transfusion. Superinfection or coinfection with B hepatitis was excluded, 2 cirrhosis were confirmed pathologically after operation. Six patients with primary hepatocarcinoma were diagnosed by serum AFP, B-ultrasound, CT and MRI. One had surgical biopsy.

The Department of Infectious Diseases, The Second Affiliated Hospital of China Medical University, Shenyang 110003, Liaoning Province, China

Dr HUANG Fen, female, born in 1962-10-06 in Shenyang, Liaoning Province, Han nationality, graduated from China Medical University in 1985 and got master degree from CMU in 1991, now Associated Professor, majoring in pathogenesis and therapy of viral hepatitis, having 20 papers published.

Correspondence to: Dr. HUANG Fen, Department of Infectious Diseases, The Second Affiliated Hospital of China Medical University, 36 block 1, San Hao Street, He-Ping District, Shenyang, Liaoning, 110003, China

Tel. +86-24-23893501-961, Fax. +86-24-23892617

Received 1999-07-03 Accepted 1999-09-18

HCV genotyping primers

HCV genotyping primers in core region were synthesized by the Bioengineering Research Center in Shanghai of Chinese Academy of Sciences. The nucleotide sequences of primers were as follows: universal primers: P₁ sense 5' CGCGCGACTAG-GAAGACTTC 3' (nt 139-158); P₂ antisense 5' ATGTACCCCATGAGGTCGCT 3' (nt 391-410), type specific primers: P₃ sense 5' AGGAA-GACTTCCGAGCGGTC 3' (nt 148-167); P₄ antisense 5' TGCCTTGGGGATAGGCTGAC 3' (nt 185-204) (HCV-I); P₅ antisense 5' GAGCCATCCT-GCCCCACCCA 3' (nt 272-291) (HCV-II); P₆ antisense 5' CCAAGAGGGACGGGAACCTC 3' (nt 302-321) (HCV-III); P₇ antisense 5' ACC-CTCGTTTCCGTACAGAG 3' (nt 251 - 270) (HCV-IV).

Methods

Serum HCV RNA was extracted using one-step method of guanidinium thiocyanate. For detecting HCV genotypes, Okamoto's^[1] method was used but modified. Major procedures were: ① reverse transcription and first PCR amplification: in extracted RNA, we added 5 units of avian myeloblastosis virus reverse transcriptase (AMV-RT) (Promega), 20 units of inhibitor of RNAase (RNasin) (Promega), 2 U *Taq* enzyme (Promega), 2 mM dNTP 3 μ L, 10 \times AMV-RT buffer 3 μ L and universal primers (P₁, P₂) 0.8 μ mol/L. Total volume was 30 μ L. After reverse transcription at 42 $^{\circ}$ C for 20 min, first PCR was performed for 35 cycles. Each cycle included denaturation at 94 $^{\circ}$ C for 1 min, annealing at 55 $^{\circ}$ C for 1.5 min and extension at 72 $^{\circ}$ C for 2 min. ② The second PCR amplification: in 5 μ L products of the first PCR, we added 3 μ L 10 \times AMV-RT buffer, 2 mM dNTP 3 μ L, 2 U *Taq* enzyme and 0.8 μ mol/L of type-specific primers (P₃, P_{4,5,6,7}). Total volume was 30 μ L. PCR conditions were: denaturation at 94 $^{\circ}$ C for 1 min, annealing at 60 $^{\circ}$ C for 1 min, extension at 72 $^{\circ}$ C 1.5 min, for 30 cycles, then another extension at 72 $^{\circ}$ C for 5 min. In every amplification, positive control of HCV RNA serum and negative control of normal blood sample were provided. ③ Ten microliters products of the second PCR were subjected to electrophoresis on 6% polyacrylamide gel, stained with ethidium bromide, and observed under ultraviolet ray. Each HCV genotype was characterized by different nucleotide lengths: 57 bp

for type I, 144 bp for type II, 174 bp for type III and 1.23 bp for type IV.

RESULTS

One hundred serum samples were genetically classified into 3 types: type II in 58 samples (58%), type III in 27 (27%) and mixed type (II/III) in 14 (14%), only 1 sample (1%) remained unclassified (Figure 1).

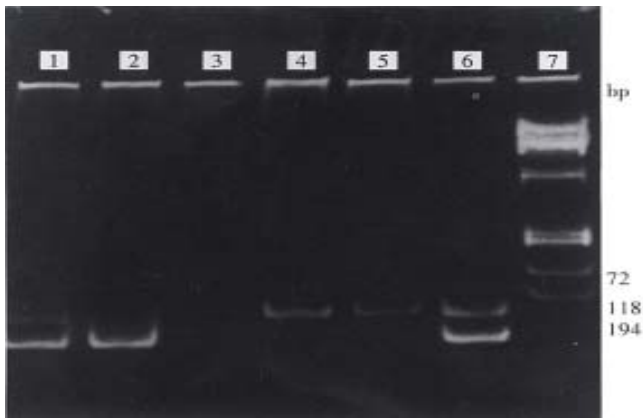


Figure 1 The results in HCV genotyping.

1, 6: II/III mixed type. 2: HCV-II genotype. 3: Negative control. 4, 5: HCV-III genotype. 7: Φ x 174 DNA / Hae III marker.

In 94 patients with hepatitis C, the distribution of HCV genotypes in patients with hepatitis C was not identical. The data were analyzed with R×C Table test, $\chi^2=28.9$, $P<0.01$. In acute hepatitis, in mild, moderate and severe chronic hepatitis, cirrhosis, the infectious rates of type II were 55.6%, 36.0%, 71.4%, 88.9% and 91.7%, respectively, but those of type III were 22.2%, 46.0%, 7.14%, 0% and 8.3%, respectively. In moderate and severe chronic hepatitis and cirrhosis, the proportion of type II was significantly elevated in comparison with that in mild chronic hepatitis

($P<0.05$ or $P<0.01$), but the proportion of type III was significantly lower than that in mild ones ($P<0.05$). Six patients with hepatocarcinoma were all infected by genotype II HCV (Table 1). The genotype distribution of HCV in post-transfusional and sporadic hepatitis C was identical. The results were analyzed with R×C Table χ^2 test, $\chi^2=3.74$, $P>0.05$ (Table 2).

DISCUSSION

There are some differences in distribution of HCV genotypes in different regions. In America, infection of HCV-I genotype is predominated, but in China and Japan, HCV-II genotype is dominant over HCV-III genotype. Du *et al*^[2] reported that infection by type II was predominant in Beijing, Wuhan, Guangzhou, Xi'an, Chongqing, Guangxi areas. Among these areas the highest infection rate of type III was in Beijing (19%), the infection rates of mixed type II/III were the highest in Guangzhou (9%). Our study showed in Shenyang that the infection rate of type II (58%) > type III (27%) and mixed type II/III (14%), the latter two were higher in Shenyang than those in other parts of China. Therefore, future prevention and treatment strategy should be directed towards type II HCV mainly, but not neglecting type III and type II/III. In our study, no HCV-I and HCV-IV were found. One serum sample was positive for HCV RNA by repeated PCR assay, but it could not be classified after the two tests, indicating there might be other HCV genotype in our area.

Clinical manifestations of hepatitis C infected by HCV type II are usually more severe, those of HCV type III are milder. The HCV genotypes seem to be closely related to the clinical condition and degree of severity of hepatitis C. All our 6 patients with hepatocarcinoma were found to carry HCV type II which indicated that infection of type II may be related to occurrence of hepatocarcinoma^[3].

Table 1 HCV genotypes of hepatitis C and hepatocarcinoma

Clinical status	Cases	HCV II		HCV III		Mixed (II/III)		Unknown	
		Cases	(%)	Cases	(%)	Cases	(%)	Cases	(%)
Acute hepatitis	9	5	(55.6)	2	(22.2)	2	(22.2)		
Chronic hepatitis									
Mild degree	50	18	(36.0)	23	(46.0)	9	(18.0)		
Moderate degree	14	10	(71.4) ^a	1	(7.14) ^a	2	(14.3)	1	(7.14)
Severe degree	9	8	(88.9) ^b			1	(11.1)		
Cirrhosis of liver	12	11	(91.7) ^b	1	(8.3)				
Hepatocarcinoma	6	6	(100.0) ^a						
Total	100	58	(58)	27	(27)	14	(14)	1	(1)

^a $P<0.05$, ^b $P<0.01$, compared with mild chronic hepatitis, by χ^2 test.

Table 2 HCV genotypes of post-transfusional and sporadic hepatitis C

Groups	Cases	HCV II		HCV III		Mixed (II/III)		Unknown	
		Cases	(%)	Cases	(%)	Cases	(%)	Cases	(%)
Post-transfusional hepatitis	49	26	(53.1)	12	(24.5)	10	(20.4)	1	(2.0)
Sporadic hepatitis	45	26	(57.8)	15	(33.3)	4	(8.9)		

No significant difference was found in the distribution of HCV genotypes in post-transfusional and sporadic hepatitis C, showing HCV genotypes may be not related to routes of infection. The infection rate (20.9%) of mixed type (II/III) in post-transfusional hepatitis was higher than that in sporadic hepatitis (9.8%), indicating repeated blood or blood product transfusion may be contributory.

REFERENCES

- 1 Okamoto H, Sugiyama Y, Okada S, Kurai K, Akahane Y, Sugai Y, Tanaka T, Sato K, Tsuda F, Miyakawa Y, Mayumi M. Typing hepatitis C virus by polymerase chain reaction with type specific primers: application to clinical surveys and tracing infectious sources. *J Gen Virol*, 1992;73:673-679
- 2 Du SC, Tao QM, Zhu L, Liu JX, Wang H, Sun Y. Genotyping study of hepatitis C virus by restriction fragment length polymorphism in its 5'NC region. *Zhonghua Yixue Zazhi*, 1993;1:7-9
- 3 Yang JM, Liu WW, Luo YH. Genotypic investigation of hepatitis C virus in patient with primary hepatic carcinoma, liver cirrhosis and hepatitis. *Zhonghua Chuanranbing Zazhi*, 1995;1:1-3

Edited by WU Xie-Ning
Proofread by MIAO Qi-Hong

Establishment and preliminary use of hepatitis B virus preS1/2 antigen assay

CHEN Kun, HAN Bao-Guang, MA Xian-Kai, ZHANG He-Qiu, MENG Li, WANG Guo-Hua, XIA Fang, SONG Xiao-Guo and LING Shi-Gan

Subject headings hepatitis B virus; PreS1/S2 antigen; ELISA; hepatitis B; E antigen/analysis

INTRODUCTION

Hepatitis B virus (HBV) is a DNA virus with an envelope, its membrane protein gene preS/S have three parts-preS1, preS2 and S, there is a translation initiation codon ATG in each of them. By different ATG, the membrane protein gene can be translated into three kinds of products, i.e. the large protein (preS1 + preS2 + S), medium (preS2 + S) and small (S) (also called primary protein). In patients with acute hepatitis B, PreS antigen occurred together with other HBV markers and parallels the level of HBV DNA. Disappearance of PreS antigen predicts a benign outcome^[1]. Its presence in chronic hepatitis B is somewhat correlated with HBsAg, the ratio of PreS1/HBsAg antigen titers can reflect the level of DNA replication^[2]. Meanwhile, the PreS domain in the membrane protein include the binding sites for hepatocyte receptor and a number of epitopes of B cells and T cells. The PreS domain possesses very strong immunogenicity in mouse and man. In mice with consanguinity, the PreS domain can induce broad-spectrum protective antibodies and overcome their nonresponsiveness to protein S. In human body, it has been proved the PreS domain is an effective immunogen at both B and T cell levels. The antibodies directing against synthetic peptides (PreS: 21 - 47) mimicking receptor-binding sites can protect chimpanzee from HBV infection^[3]. During the disease course appearance of antibody against PreS1 is considered an early marker for elimination of HBV infection^[4,5]. Therefore PreS antigen/antibody is a pair of important indexes for diagnosis of hepatitis B. As one part of a research project granted by the EC Foundation, we have

prepared a recombinant PreS protein with high purity, a polyclonal anti-PreS antibody and established the ELISA method for detection of PreS antigen, preliminary clinical studies had been carried out.

MATERIALS AND METHODS

Immunologic reagents

HRP-conjugated murine anti-human IgG was provided by Department of Molecular Immunology, Institute of Basic Medical Sciences, Academy of Military Medical Sciences; HRP-conjugated murine anti-human HBs were provided by the Department of Immunology, No.302 Hospital of PLA; and HRP-conjugated sheep anti-rabbit IgG was provided by the Department of Molecular Biology, No.307 Hospital of PLA.

Blood specimens

They were provided by the Central Blood Bank of PLA units under Beijing Command and No.301, 302 Hospitals of PLA.

Preparation of PreS antigen

The engineered *E. coli* for hepatitis B viral PreS/2 recombinant antigen was provided by Department of Virology, Max-Planck Institute of Biochemistry, Germany. The PreS1/2 recombinant antigen containing PreS1:10-108PreS2: 1-55/S1-22 (ayw subtype) was expressed by using pQe8 (Quiagen) expression vector and six histidin residuals were fused to the N-terminal of the product, which was purified by affinity chromatography using Ni-NTA agarose column (Quiagen) to a purity above 95%. The purified protein was stored at -20°C for use.

Preparation of recombinant antigen-directed immune sera

New Zealand large-ear white rabbits were immunized by four injections of renatured PreS recombinant antigen, once each on the wk 0, wk 2, wk 7 and wk 11. One hundred micrograms of the antigen were injected subcutaneously on multiple sites at one time. In the first injection, Freund's complete adjuvant was used, while Freund's incomplete adjuvant was used in the latter three injections. Blood samples were obtained before each booster injection for determination of serum antibody titer. Serum was separated from blood

Institute of Basic Medical Sciences, Academy of Military Medical Sciences, Beijing 100850, China

CHEN Kun, female, born in 1964-02-28 in Beijing, graduated from Department of Medical Laboratory Science, High Medical College, in 1992, Technician, majoring in molecular biology of viral hepatitis, having 6 papers published.

Supported by joint research with EC (CI1-CT94-0023).

Correspondence to: Institute of Basic Medical Sciences, Academy of Military Medical Sciences, Beijing 100850, China

Tel. +86-10-68285463, Fax. +86-10-68285463

Email.lingsg@nic.bmi.ac.cn

Received 1999-07-11 **Accepted** 1999-09-05

samples. The anti-PreS sera were purified using Protein A Sepharose 4B Fast Flow affinity adsorption column and was stored at -20°C for later use.

Preparation of ELISA plate for detection of PreS antigen

The ELISA plate was coated with purified rabbit anti-PreS polyclonal antibody at a concentration of 10 mg/L at 4°C stored overnight. After blockage with 1% BSA and dilution, the plate was vacuum-dried, then it was stored at 4°C for later use. When it is used, test blood sample (50 μL) was added and incubated at 37°C for 30 min. After washing, the enzyme-labelled anti-HBs monoclonal antibody was added and incubated at 37°C for 30 min after washing, OPD color developer was added to develop the color by protecting from light at 37°C for 10 min, then 2 mol/L H_2SO_4 was added to terminate the reaction. The 492 value was determined using DG3022 Enzyme Labelling Instrument. When the D value of the test sample was \geq the average positive value $\times 0.08$, it was taken as positive, otherwise, as negative.

Competitive inhibition test

The PreS-positive sera were diluted with serum-diluting solution containing purified rabbit anti-PreS antigen polyclonal antibody (20 mg/L). After incubation at 37°C for 1 h, the diluted sera were placed at 4°C overnight. The 100 μL of the sera were taken out and were added to the ELISA plate coated with rabbit anti-PreS1 antibody. After that the plate was incubated at 37°C for 30 min. The rest steps were carried out by following the routine. The neutralizing inhibition rate $\geq 50\%$ was taken as positive.

$$\text{Competitive inhibition rate} = \frac{\text{Average non-competitive D value minus Average competitive D value}}{\text{Average non-competitive D value}} \times 100\%$$

RESULTS

Purification of recombinant antigen

Using pQe8 expression vector, the vector pQePreS1/2 expressing HBV ayw subtype including PreS1 and PreS2 gene fragments was constructed. After incubation, PreS1/2 protein with the relative molecular mass of 22000 (including three parts-PreS1:10-108/preS2:1-55/S1-22) was expressed. There were six histidine residues binding to the N-terminal of the product, the quantity of the recombinant protein expressed amounted to about 10% of the whole *bacteria*. The PreS1/2 existed mainly in inclusion bodies. The inclusion bodies were dissolved by denaturant and were purified on Ni-NTA agarose column. A purity over 95% was achieved. From 1 L cultured bacteria, 10 mg

purified prote in could be obtained. Then the denaturant was removed from the purified protein in the course of renaturation.

Results

Using routine methods, rabbits were immunized with renatured recombinant PreS1/2 antigen and the titers of their immune sera against the recombinant prote in were determined by ELISA. Rabbit sera of blood samples taken before immunization served as the negative control (D value < 0.01). The titer of antibody directing against PreS1/2 antigen in rabbit sera reached 1:128 000, 1:512000, respectively on 40 d, 60 d after first immunization. In order to identify the immunogenicity of different components of the recombinant PreS1/2 antigen, recombinant PreS2 (PreS2: 1-55/S:1-9) and PreS121-47 synthetic polypeptides were also used in determination of the serum titer on d40 (Figure 1), and the result indicated in the immune sera the titers of antibodies directing against PreS1 polypeptide and PreS2 antigen were similar.

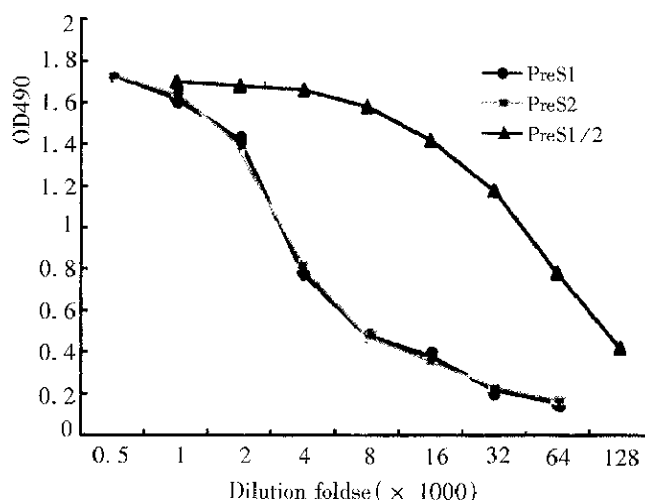


Figure1 The immunogenicity of different components of the recombinant PreS1/2 antigen

Establishment of a detection method for PreS antigen and determination of its sensitivity, specificity and preciseness

Using purified anti-PreS1/2 polyclonal antibody a double antibody sandwich ELISA method for detecting PreS1/2 antigen was established. The anti-sera of rabbits immunized with PreS1/2 were purified by using Protein A Sepharose 4B Fast Flow affinity adsorption gel column. Then 10 mg/L of the purified antibody was used to coat ELISA plate to adsorb HBV viral particles present in the sera and PreS1/2 antigen on the subunit particles. The specifically absorbed particles were detected with enzyme labeled anti-HBs antibody. This method was used in determination of purified Dane particle

sera. Along with multiple proportional dilution, the D values of reaction wells decreased successively and the dilution titer of the sera could be up to 1:2048, corresponding to detection of 5000 HBV viral particles per mL. Purified Dane particle sera and 99 hepatitis C patients' positive sera were detected and the result of the former was positive, whereas that of the latter was negative. Neutralization of PreS antigen-positive patients' sera with purified rabbit anti-PreS antibody resulted in competitive inhibition all rates reached over 80%.

Judged by intra-and inter-assay coefficients of variation, the precision of the detection method for PreS/2 antigen was evaluated. The intra-assay coefficient of variation was revealed by choosing PreS antigen-positive sera with high, medium and low values one each and by paralleled determination of 10 wells simultaneously each. The inter-assay coefficient of variation was demonstrated by determination of the above three sera for 10 times each at different time. The intra-assay coefficients of variation of the high, medium, low PreS antigen-positive sera were 3.8%, 4.5% and 13.3%, respectively; while the inter-assay coefficients of variation were 2.56%, 3.17% and 10.5%, respectively. These results indicate that precision has reached the requirement of Ministry of Public Health of China for intra and inter-assay coefficients of variation for diagnostic reagents (the national standard is $\leq 15\%$). Detection rates of PreS1/2 antigen in various populations of people, in sera of 200 normal blood donors, PreS1/2 was not positively detected. The detection rates of PreS1/2 antigen in sera of patients at different phases of HBV infection were listed in Table 1.

Table 1 Positive rates in sera at different phases of HBV infection

Phase of infection	Number of cases			Positive rate(%)
	Negative PreS1/2	Positive PreS1/2	Total	
HBsAg(+)HBeAg(+)Anti-HBc(+)	40	260	300	87
HBsAg(+)Anti-HBe(+)Anti-HBc(+)	50	142	192	74
Anti-HBs(+)	24	0	24	0

DISCUSSION

The PreS domain of HBV protein locates on the

surface of HBV particle and can induce protective antibody in human body and in mouse. In the literature it is reported that the elimination of PreS antigen from serum patients with acute hepatitis B can foresee the disappearance of clinical symptoms. For patients with chronic hepatitis B, persistent existence of PreS in serum indicates progression of the disease course. In the meantime, monitoring PreS1/2 antigen has also important significance for evaluation of curative effect of antiviral therapy in the se patients.

Most investigators have established detection methods for PreS antigen by using anti-PreS monoclonal antibody. This study used highly expressed in *Escherichia coli* and purified HBV PreS antigens, which cover the whole PreS2 domain and the most parts of PreS1 domain. Three experimental results indicate that the recombinant PreS antigen is also a good immunogen in rabbit. In rabbit anti-PreS sera, the titer of antibody directing against PreS1:21-47 basically equal to the of antibody directing against PreS2: 1 - 55. A method of detecting PreS antigen established by using purified rabbit polyclonal antibody is predicted to be able to determine simultaneously PreS1 and PreS2 antigens in serum of patient. By using this method, we have detected preliminarily PreS antigen in HBeAg positive and anti-HBeAg positive and the results show that the detection frequency of PreS antigen is relatively high in both situations. Statistical analysis indicates that the presence of PreS antigen in serum is independent of the existence of HBeAg ($\chi^2 = 12.59, P < 0.01$).

REFERENCES

- 1 Delfini C, Colloca S, Taliani G, Mazzotta F, D'Agata A, Buonamici C, Stroffolini T, Carloni G. Clearance of hepatitis B virus DNA and pre S surface antigen in patients with markers of acute viral replication. *J Med Virol*, 1989;28:169-175
- 2 Petit MA, Zoulim F, Capel F, Dubanchet S, Daugute C, Trepo C. Variable expression of preS1 antigen in serum during chronic hepatitis B virus infection: an accurate marker for the level of hepatitis B virus replication. *Hepatology*, 1990;11:809-814
- 3 Neurath AR, Seto B, Strick N. Antibodies to synthetic peptides from the preS1 region of the hepatitis B virus (HBV) envelope (env) protein are virus-neutralizing and protective. *Vaccine*, 1989;7:234-236
- 4 Galn MI, Toms J, Bernal MC, Salmeron FJ, Maroto MC. Evaluation of the pre-S (preS(1)Ag/preS(2)Ab) system in hepatitis B virus infection. *J Clin Pathol*, 1991;44:25-28
- 5 Coursaget P, Buisson Y, Bourdil C, Yvonnet B, Molinie C, Diop MT, Chiron JP, Bao O, Diop Mar I. Hepatitis B virus induced liver disease and after immunization. *Res Virol*, 1990;141:563-570

Edited by WU Xie-Ning
Proofread by MIAO Qi-Hong